Fall 12-9-2014

Pseudomonas syringae type III effectors: Targets and roles in plant immunity

Tania Y. Toruño
University of Nebraska-Lincoln, ttoruno2@unl.edu

PSEUDOMONAS SYRINGAE TYPE III EFFECTORS: TARGETS AND ROLES IN PLANT IMMUNITY

By

Tania Yaoska Toruño Calero

A DISSERTATION

Presented to the Faculty of

The Graduate College at the University of Nebraska

In Partial Fulfillment of Requirements

For the Degree of Doctor of Philosophy

Major: Biological Sciences

(Plant Pathology)

Under the Supervision of Professor James R. Alfano

Lincoln, Nebraska

December 2014

PSEUDOMONAS SYRINGAE TYPE III EFFECTORS:

TARGETS AND ROLES IN PLANT IMMUNITY

Tania Yaoska Toruño Calero, Ph.D.

University of Nebraska, 2014

Adviser: James R. Alfano

Pseudomonas syringae is a Gram-negative bacterial pathogen that infects many crops. A central virulence strategy *P. syringae* uses to successfully infect plants is the injection of type III effector proteins (T3Es) into plant cells through a type IIII protein secretion system (T3SS). The T3SS is a molecular syringe found in many Gram-negative bacterial pathogens of plants and animals that transport T3Es from the bacterial cytosol into eukaryotic cells. T3Es disrupt host processes in the plant immune system required to restrict pathogen ingress. The plant innate immune system is divided in two branches, pathogen-associated molecular patterns (PAMP)-triggered immunity (PTI) and effector-triggered immunity (ETI). The first branch recognizes conserved molecules found in microbes, known as PAMPs, and the second has the capacity to recognize injected T3Es. T3Es can suppress both PTI and ETI allowing *P. syringae* to circumvent the plant immune system and multiply in plant tissue. The majority of T3Es plant targets, their enzymatic activity and the mechanism of suppression of plant immunity are not known. *P. syringae* pv. *tomato* (*Pto*) DC3000 injects about 35 T3Es into plant cells.

In this study I characterized two T3Es from *Pto* DC3000. Firstly, I focused on the T3E HopD1. HopD1 suppresses plant immunity associated with ETI but not

PTI, suggesting that HopD1 was acquired later in the co-evolution of the pathogen and plant. HopD1 is targeted to the endoplasmic reticulum of plant cells where it interacts with the Arabidopsis NAC transcription factor NTL9. HopD1's function in virulence involves the inhibition of NTL9-regulated genes during ETI. Secondly, I focused on the T3E HopA1. This T3E exists in two classes, which I found are recognized differently in plants. HopA1 suppresses PTI and its structure resembles phosphothreonine lyases form animal pathogens. The putative active site of HopA1 was identified and I found that site-directed mutations in the active site abrogated HopA1-dependent phenotypes. HopA1 localizes mainly to plasma membrane of plant cells where it interacts with the Arabidopsis type 2C phosphatases PLL4 and PLL5. These phosphatases play roles in plant immunity as negative regulators and HopA1 likely prevents their deregulation preventing induction of the plant immune system.

Acknowledgements

I would like to thank my advisor, Dr. Jim Alfano, for giving me the opportunity to be part of this research group, for constantly contributing to my professional growth as a scientist and for his guidance through my Ph.D. program. I would like to thank my dissertation committee members Drs. Tom Clemente, Richard Wilson, Gilles Basset and Etsuko Moriyama for their valuable advice during our committee meetings.

I would like to thank all members of the Alfano research group, present and past members, for their help with molecular techniques, for always being available to give feedback on my projects, and for making my life in the lab and office very pleasant. I want to give special thanks to Ming Guo and Anna Block for their contribution to the research presented in this dissertation; also Anna Joe for her friendship and great traveling companion to many local and international meetings.

Many thanks to my parents Mayra Calero and Pablo Toruño, and my brother Carlos Cerna for always being there in the good and the not so good moments, for believing in me, and for their endless love. Thanks to my extended family Calero Silva and Calero Bellorín for their positives thoughts and good vibes. Special thanks to my friends from my beloved Nicaragua for always being there for me, for making me laugh despite the distance and for always giving me a warm welcome when returning home. Thanks to my friends from Lincoln and around the world for their friendship and love.

Table of Contents

List of Figures and Tables

Chapter 4

CHAPTER 1

BACKGROUND

This chapter provides a literature review on the plant innate immune system and strategies used by plants to counteract microbial infections. In addition, it describes the bacterial plant pathogen *Pseudomonas syringae* and mechanisms of pathogenicity that rely on the type III protein secretion system and type III effector proteins (T3Es). Targets of T3Es in plants are detailed to understand the sophisticated ways used by pathogens to suppress the plant immune system.

Plant immunity

Eukaryotic and bacterial pathogens infect a plethora of plant species causing devastating diseases that have caused significant yield and quality loss to crops. To counteract microbial infections plants have evolved two immune systems: pathogen associated-molecular pattern (PAMP)-triggered immunity (PTI) and effector-triggered immunity (ETI) (90). Plants likely first evolved PTI mediated by extracellular immune receptors to detect the presence of microbes, and then ETI mediated by intracellular immune receptors that recognize the presence of, in the case of bacterial pathogens, bacterial virulence proteins injected into plant cells. Therefore, the activation of these immunity pathways depends on the type of pathogen-specific molecules recognized by plants. Altogether, these pathways are responsible for resistance to pathogens and are described below.

a. PAMP-triggered immunity

The first layer of immunity mounted by plants is PTI. PAMPs are highly conserved molecules found in microbes, both pathogenic and nonpathogenic strains (90). Examples of PAMPs include bacterial flagellin and elongation factor

EF-Tu; components of the outer membranes and cells walls of microbes such as lipopolysaccharide and peptidoglycan of bacteria and fungal chitin (122). Plants possess extracellular receptor kinases known as pattern recognition receptors (PRRs) that perceive PAMPs and activate several immune responses. PRRs are plasma membrane-localized leucine-rich repeat receptor kinases (LRR-RKs) with an extracellular LRR domain and a cytoplasmic serine/threonine protein kinase domain (27). PAMPs are perceived by the LRR domain of PRRs and the signal is transferred to the cytoplasmic kinase domain through phosphorylation. Animals and insects possess similar proteins involved in innate immunity (145). PAMP recognition induces several immune responses including stomatal closure, oxidative burst, cell wall fortification, and hormone signaling (185). Plant immunity activates signal transduction pathways through mitogen-activated protein kinases (MAPKs) and calcium-dependent kinases (CDPKs), which results in transcriptional reprogramming of immunity-related genes.

The most studied example of PTI is the one activated by the Arabidopsis flagellin-sensing 2 (FLS2), an extracellular receptor kinase that senses bacterial flagellin (Fig. 1). A 22-amino acid peptide (flg22) from the N-terminus of bacterial flagellin is sufficient to trigger PTI (200). Upon flg22 recognition, FLS2 forms a complex with the LRR-RK BAK1 and the receptor-like cytoplasmic kinase BIK1 inducing transphosphorylation and immune signaling events (35, 74, 119, 192). After flg22 recognition, FLS2 undergoes endocytosis and subsequent degradation (20, 118, 158). In agreement with PRRs being at the front line of

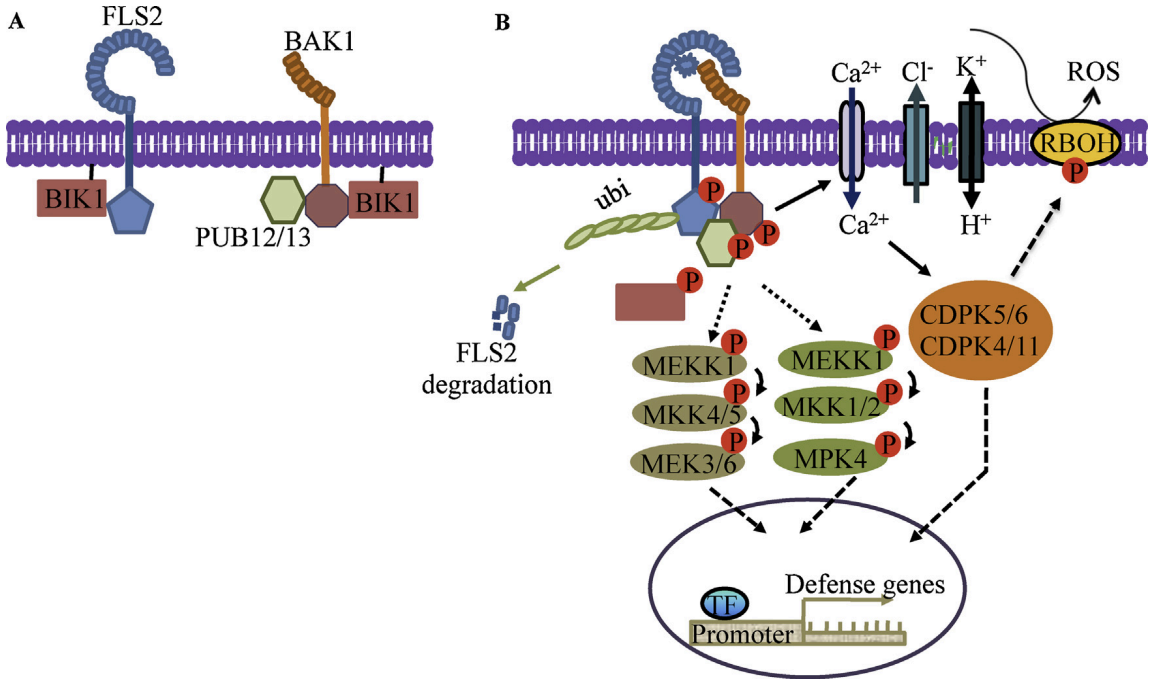

Fig. 1. A model for flg22-triggered immune responses and signal transduction pathways. (A) The resting state of FLS2 and BAK1 at the plasma membrane without microbial infection. In the absence of microbial elicitor flagellin, FLS2 and BAK1 may not form a stable complex. BAK1 is associated with BIK1 and PUB12/13 and FLS2 is also associated with BIK1. (B) Flg22-triggered immune responses and signal transduction pathways. Flg22 perception induces FLS2 and BAK1 association and phosphorylation. Activated BAK1 phosphorylates BIK1, which in turn transphosphorylates the FLS2/BAK1 complex. Phosphorylated BIK1 is released from the FLS2/BAK1complex. FLS2 and BAK1 association also recruits PUB12/13 into the receptor complex. BAK1 directly phosphorylates PUB12/13, which in turn ubiquitinates FLS2 leading to FLS2 degradation and downregulation of FLS2 signaling. Activation of the receptor complex leads to the activation of Ca^{2+} flux through Ca^{2+} channel, Cl^{-} efflux and H^{+}/K^{+} movement across the plasma membrane. MAPK and CDPK cascades are initiated downstream of the activated receptor complex and further mediate the immunity gene expression. This figure is from Wu *et al.* (185).

immunity, FLS2 is expressed in plant tissues vulnerable to bacterial invasion, such as stomata, hydathodes and lateral roots in response biotic stresses (19).

Another example of PAMP recognition is when the bacterial elongation factor EF-Tu is recognized by the LRR-RK EF-Tu receptor (EFR). EFR recognizes the N-terminus of EF-Tu comprising the first 18 amino acids (elf18), inducing similar immune responses to flg22 recognition (97). BAK1 and BIK1 also form complexes with EFR and other PRRs following PAMP perception (119, 153, 162, 168, 192). Therefore, BAK1 and BIK1 are positive regulators of PTI that act downstream of PRRs to activate plant immunity. Recognition of EF-Tu by EFR seems to be restricted to the *Brassicaceae* family, as EFR is not found in other plant families (97, 199).

Plants also perceive fungal pathogens. The component of fungal cell walls, chitin, is a PAMP recognized by chitin elicitor receptor kinase 1 (CERK1) also known as lysine motif receptor-like kinase (LysM RLK1) (133, 177). CERK1 has an extracellular LysM instead of a LRR domain. CERK1, as well as two other LysM proteins (LYM1, LYM3) also recognize the bacterial PAMP peptidoglycan (181). Several other microbial PAMPs have been characterized but their corresponding PRRs remain to be identified (27).

b. Effector-triggered immunity

The second way plant immunity can be induced is by the recognition of pathogen virulence factors. Plant intracellular receptors known as resistance (R)-proteins can recognize bacterial proteins that are delivered into plant cells to suppress PTI. In the case of the bacterial plant pathogen *P. syringae*, it injects effector

proteins through a molecular syringe known as the type III protein secretion system (T3SS). Therefore, these virulence proteins are termed type III effector proteins. The specific recognition of an effector protein by an R protein is historically known as the gene-for-gene hypothesis and recognized effectors were historically known as avirulence (Avr) proteins (55).

There are at least five classes of R proteins. The largest class of R proteins are composed of three domains, a central nucleotide binding (NB) domain, a C-terminal LRR domain and an N-terminal that can either be a coiled coil (CC) or toll-interleukin 1-receptor (TIR) domain (51). The N-terminal domain of NB-LRR proteins dictates the requirement for downstream signaling components. While the resistance regulator Enhanced Disease Susceptibility 1 (EDS1) is required by TIR-NB-LRRs to activate immune responses, Non-race specific Disease Resistance 1 (NDR1) is required for CC-NB-LRRs-mediated resistance (1). In Arabidopsis there are 159 members of the NB-LRR R protein family (71).

The majority of R proteins do not directly recognize T3Es; instead they recognize a host protein modified by a T3E. The guard hypothesis explains this indirect recognition, in which modification of a host protein (the guardee) by a T3E is guarded by an R protein (90). A variation of the guard hypothesis is the decoy model (175). This model states that plants have evolved host proteins that mimic bona fide T3E targets to function as decoys for the presence and/or activity of T3Es. These decoy proteins are thought to have arose as gene duplications or splice variants of T3E targets, and have no other function in plant cells other than to attract effectors to induce ETI.

Similar immune responses are activated by both PTI and ETI, with different amplitude and timing, whereas ETI elicits a more prolonged and robust immune response (90). ETI is usually associated with the hypersensitive response (HR), a programmed cell death response. The HR, a necrotic lesion at the site of infection, prevents the spread of the pathogen. While PTI is effective against a broad range of pathogens, ETI is specific and requires recognition of a particular effector by the corresponding R protein. Immune responses induced during plant immunity are described below.

Plant immune responses

a. Ion fluxes

Immune responses include changes in ion fluxes across the plasma membrane, including H^+, K^+, Cl_2 and Ca^{2+}. Ca^{2+} influx has been observed as an early PTI response (157). Ca^{2+} amplitude and duration differ between PAMP treatments, with flg22 inducing the highest Ca^{2+} amplitude. Increased Ca^{2+} influx from the apoplast to the cytoplasm is perceived by calcium binding sensors like calmodulin (CAM), calcineurin B-like proteins and CDPKs. These Ca^{2+} sensors activate downstream immunity signal transduction pathways (101). Four CDPKs (CDPK4, 5, 6, and 11) belong to a CDPK sub-clade that are global regulators of immunity-related genes required for flg22-induced responses (28). In addition, CDPK28 interacts with PRR complexes to regulate immune responses (135). These data indicate the importance of CDPKs in PTI signaling. Ca^{2+} signals also activate biosynthesis of the hormone salicylic acid (SA) through transcriptional

activation of *ICS1*/*SID2* by the CAM-binding transcription factor CBP60g. *ICS1*/*SID2* encodes the isochorismate synthase I, an enzyme required for SA biosynthesis (178, 192).

b. Oxidative burst

PTI and ETI induce the production of reactive oxygen species (ROS) within few minutes. ROS act as antimicrobial agents, strengthen cell walls and induce immune responses by transcriptional reprogramming (11). ROS include superoxide anion (O_2^-) and hydrogen peroxide (H_2O_2) that are produced primarily by plasma membrane NADPH oxidases encoded by *RBOH* genes (173). Additionally, ROS is also produced in other subcellular compartments. For example it is also produced by cell wall peroxidases. CDPKs also play an important role in inducing the oxidative burst by activation of RBOH through phosphorylation (50, 96).

c. MAPK activation

Immune responses also include activation of MAPK signal transduction pathways. There are two distinct MAPK cascades, one that positively regulates immunity (MEKK1/MKKs-MKK4/5-MPK3/6) and one that negatively regulates immunity (MEKK1-MKK1/2-MPK4) (61, 151, 156). MAPK signaling activates WKRY transcription factors and expression of immunity-related genes (172).

d. Transcriptional reprogramming

Activation of plant immunity induces expression of immunity-related genes. A similar set of genes is activated by several PAMPs indicating that immune signaling converges at the transcriptional level. Families of transcription factors

that are global regulators of immune signaling include bZIP (basic leucine zipper motif), AP2/ERF (APETALA2/ETHYLENE-RESPONSIVE ELEMENT BINDING FACTORS), MYB (myelobastosis related), MYC (myelocytomatosis related), NAC (no apical meristem (NAM) Arabidopsis transcription activation factor (ATAF) and cup-shaped cotyledon (CUC)), and WRKY (amino acid sequence WRKYGQK) (8). WRKY transcription factors are regulated by MAPKs and CDPKs. Some examples of the involvement of WRKYs in immunity include the following: (i) WRKY33 is phosphorylated by MPK3/6 inducing immunity responses against the necrotrophic fungi *Botrytis cinerea* (126), (ii) WRKY22/29 are also activated by MPK3/6 (13), (iii) MPK4 phosphorylates MKS1 and this leads to activation of WRKY33/25 (10, 156), and (iv) CDPK4/5/6/11 activate a group of WRKYs including WRKY8/28/48/46 (62). These data indicate that MAPKs and CDPKs synergistically activate WRKY transcription factors to induce expression of immunity-related genes.

e. Cell wall fortification

Callose deposition represents a late PTI response. Upon PAMP perception, plants deposit callose (β-1,3-glucan) in cell wall appositions called papillae to create a physical barrier against pathogens invasion (176). Callose is produced at the cell wall by the callose synthase Powdery Mildew Resistant 4, also known as glucan synthase-like 5. Antimicrobial compounds such as phenolic compounds, lignin, ROS, peroxidases and thionins can also be deposited in the callose matrix to create a physical barrier against pathogens (176).

f. Hormone signaling

Phytohormones contribute to the immune signaling response. SA and jasmonic acid (JA) are the main hormones involved in immunity, although ethylene (ET), absicic acid (ABA), auxin and cytokinin play also important roles. While SA is associated with resistance to biotroph and hemibiotroph pathogens, JA and ET are associated with resistance against necotrophs and herbivorous insects (150). Perception of pathogens by plants induces SA biosynthesis, which signals through the Nonexpressor of pathogenesis related genes 1 (NPR1). NPR1 then induces the expression of several immunity-related genes. Activation of the SA pathway at the site of infection leads to a similar response in distal plant parts to protect the entire plant from subsequent pathogen invasion; this phenomenon is known as systemic acquired resistance (186). Disruption of SA signaling affects many immunity-related genes and plants are more susceptible to different pathogens.

g. Stomatal closure

Stomata, pores in the epidermis of aerial plant organs, represent an important entry point for pathogens. PAMP treatments induce stomatal closure to restrict pathogenic invasion. However, pathogens have evolved strategies to open stomata to gain access to the plant apoplast. For example, *P. syringae* secretes the bacterial toxin coronatine, a jasmonate-isoleucine (JA-Ile) mimic, to reopen stomata upon PAMP perception (130).

h. Gene silencing

RNA silencing also plays a role in immunity. MicroRNAs (miRNAs) and small interfering RNAs (siRNAs) are involved in plant resistance to bacterial pathogens.

For example, flg22 treatment downregulates auxin responses by upregulating *miRNA393* that reduces levels of the auxin receptors TIR1, AFB2, and AFB3 (138). Repression of auxin signaling results in restriction of *P. syringae* multiplication. The RNA silencing factor RNA-dependent RNA polymerase 6 (RDR6) and *miR472* target mRNAs of members of the CC-NB-LRRs family of R proteins. RDR6 and *miR472* are negative regulators of immunity since CC-NB-LRR *R* genes are induced in the *rdr6* and *miR472* mutants and plants are more resistant to *P. syringae* pv. *tomato* DC3000 (*Pto* DC3000) and the *Pto* DC3000 strain expressing the T3E AvrPphB, which induces ETI in Arabidopsis. These data indicate that both *miR472*- and RDR6-mediated signaling pathways modulate disease resistance genes post-transcriptionally to regulate PTI and ETI responses (26). In addition, proteins required for small RNA biogenesis have been implicated in resistance to pathogens. Two proteins required for biosynthesis of miRNAs and long siRNAs, Dicer-like 1 and Hua enhancer1, are required for PTI responses (139). The miRNA effector protein Argonaute 1 is required for flg22-induced callose deposition, gene expression, and seedling growth inhibition (113).

Pseudomonas syringae

P. syringae is a Gram-negative plant pathogenic bacterium that infects a wide variety of economically important plant species. It belongs to the *Pseudomonadaceae* family, *Pseudomonadales* order and *Gammaproteobacteria* class (147, 183). This aerobic bacterium has rod shape with four polar flagella for

motility. It has a characteristic yellow fluorescent color when grown in the iron-deficient medium King's B due to the production of the siderophore pyoverdin (63). Siderophores are iron-binding molecules produced by pathogenic bacteria and are responsible for iron acquisition in iron-limited environments (38).

P. syringae lives as an epiphyte on aerial parts of the plant (78). It becomes pathogenic when it enters the plant apoplast through wounds or natural openings like stomata, where it multiplies. Disease symptoms start to develop about 5 to 7 days after initial infection. Typical disease symptoms include necrotic spots surrounded by chlorosis margins (129). Bacteria can be dispersed to other plants through wind, rain, or insects.

Individual strains of *P. syringae* are capable of infecting a wide variety of plant species. It is classified into 50 pathovars based on the plant species they infect and then into races based on the ability among strains of a pathovars to cause disease on a host plant (4, 146). Therefore, *P. syringae* is a host-specific pathogen. To become a pathogen in a particular host, *P. syringae* relies on several virulence factors for pathogenicity, including T3Es and phytotoxins. These virulence factors sabotage the plant immune system to favor infection.

In non-host plants, *P. syringae* is not able to cause disease or is recognized by an R protein eliciting the HR. The HR is generally associated with an ETI response. The majority of *P. syringae* strains are pathogenic, although some evidence indicates that few strains cannot cause disease (78). Some of the nonpathogenic strains lack a functional T3SS, which highlights the importance of the T3SS for *P. syringae* pathogenicity (37, 134).

Among *P. syringae* pathovars, *Pto* DC3000 causes bacterial speck on tomato (*Solanum lycopersicum*), which results in necrotic lesions on leaves and fruits (89). The genome of *Pto* DC3000 was the first *P. syringae* genome to be sequenced (31). Its genome (6.5 megabases) consists of a circular chromosome and two plasmids and encodes 5,763 open reading frames. *Pto* DC3000 is also pathogenic on the model plant Arabidopsis, which was the first plant genome to be sequenced (81). Arabidopsis has one of the smallest plant genomes (157 megabases) arranged in five linear chromosomes. Arabidopsis is a great model system because it has a small genome and is a relatively small plant with a rapid lifecycle, produces abundant seeds, and can be easily manipulated in the laboratory. Therefore, the *Pto* DC3000-Arabidopsis pathosystem represents a great model system to study plant-microbe interactions at the molecular level (92). Research using this pathosystem has led to the identification of key *P. syringae* virulence factors and important components of plant immunity.

Phytotoxins

Phytotoxins and T3Es are the main virulence factors used by *P. syringae* to suppress plant immune responses and successfully infect its host. Coronatine is a major toxin produced by several *P. syringae* strains (21). It is a non-host-specific polyketide that structurally mimics the jasmonate-isoleucine (JA-Ile), a JA derivative involved in JA signaling in plants. Coronatine has two moieties, the polyketide coronafacic acid and the ethylcyclopropyl amino acid coronamic acid. Coronatine has different roles in *P. syringae* virulence. It has been implicated in

the development of disease symptoms as a *Pto* DC3000 coronatine-deficient mutant has reduced chlorosis and necrosis, typical disease symptoms caused by *P. syringae* infections (30). Another role of coronatine is in systemic induced susceptibility (SIS), an enhanced secondary bacterial growth in uninfected leaves, since SIS is not induced in a coronatine-deficient mutant and is induced after treatment with purified coronatine (45). Coronatine also contributes to pathogenicity by inducing the opening of stomata during bacterial infection (130). This allows *P. syringae* to access the plant apoplast where it multiplies and causes disease. Coronatine induces stomatal opening by promoting interaction between COI1 (coronatine-insensitive 1; an F-box subunit of the SCF^{COI1} ubiquitin ligase involved in 26S proteasome-mediated degradation) and JAZ repressors (jasmonate zim domain proteins; transcriptional repressors in JA signaling) (190). Coronatine binding to the COI1-JAZ complex leads to ubiquitination and degradation of JAZ repressors by the 26S proteasome and activation of JA-responsive genes.

Another group of toxins, syringomycin and syringopeptin, makes pores in host membranes that induce electrolyte leakage leading to plant necrosis (21). The phytotoxin syringolin A (SylA), a product of nonribosomal peptide and polyketide synthetase, is a proteasome inhibitor (69). A *SylA*-negative mutant has decreased disease symptoms and thus acts as a virulence factor. SylA is a type member of a new class of proteasome inhibitor toxins known as syrbactins. SylA is taken up in plants by Yellow stripe like 7 (YSL7) and YSL8 transporters (167). SylA suppresses stomatal immunity and inhibits SA-dependent immune

responses through proteasome inhibition of NPR1 degradation (167). Another function of SylA is to help *P. syringae* escape primary infection sites and colonize adjacent regions along the vascular tissue by suppressing SA-dependent resistance in those distal regions (132).

Phaseolotoxin and tabtoxin are present in certain *P. syringae* strains. Phaseolotoxin is a sulfodiaminophosphinyl peptide that inhibits enzymes in the ornithine metabolism important for cell cycle control and senescence (16). In general, most *P. syringae* phytotoxins lack host-specificity, are not required for pathogenicity but are important virulence factors and influence disease symptom development. Toxins inducing chlorosis are coronatine, phaseolotoxin and tabtoxin, and toxins inducing necrosis are syringomycin and syringopeptin (21).

Type III secretion system

P. syringae and other Gram-negative bacterial pathogens utilize a molecular syringe to translocate T3Es into plant cells to suppress immune responses. This molecular syringe is known as the type III secretion system and is the most important virulence determinant of many plant and animal Gram-negative bacterial pathogens (59). Because of similarities in the secretion of T3Es and flagella, which is also secreted by a type III system, the virulence-associated T3SS is sometimes referred to as an injectisome or non-flagellar type III system (41, 52).

The T3SS is encoded by the *hypersensitive response and pathogenicity* (*hrp*) and *hrp conserved* (*hrc*) gene cluster (5). These genes actually encode the type

III secretion apparatus and some secreted proteins that function in the translocation of T3Es into plant cells. For example, *Pto* DC3000 strain with a mutation in the *hrcC* gene, which is within the *hrp/hrc* cluster, is defective in type III secretion and cannot inject any T3Es (191). The *Pto* DC3000 *hrcC* mutant strain is widely used as a nonpathogenic strain as well as a PTI-inducing strain since it cannot inject any T3Es and plants can sense bacterial PAMPs from this strain. The *hrp/hrc* genes are within the Hrp pathogenicity island flanked by two gene clusters that carry T3E genes: the conserved effector locus (CEL) and the exchangeable effector locus (EEL) (3, 40). The genes within the EEL are variable in different *P. syringae* strains and the genes within the CEL are conserved in all *P. syringae* strains and encode T3Es important for virulence. Deletion of the CEL in *Pto* DC3000 (encoding T3E genes *hopN1*, *hopAA1-1*, *hopM1*, and *avrE*) impairs growth in host plants.

The type III system is not constitutively expressed in bacteria and is induced only when the pathogen gains access to the plant apoplast. The alternative sigma factor HrpL drives the expression of genes encoding the T3SS and T3Es by binding to sequences in the promoter region of these genes (54, 189). These promoter sequences are known as *hrp* boxes and are highly conserved (GGAACC-N_{16}-CCACNNA) (56). Therefore, the consensus sequence of *hrp* boxes was used and is still used to identify T3Es genes from sequenced *P. syringae* genomes (114, 165). Recently, chromatin immunoprecipitation and mRNA sequencing techniques (ChIP-Seq and RNA-Seq) were used to identify additional HrpL-binding sites (99, 137). Twenty new *hrp* promoters have been

identified and are upstream of a diverse set of genes coding for regulators, enzymes, and hypothetical proteins. Interestingly, these new HrpL-regulated genes do not appear to encode T3Es. It remains to be elucidated if these non-T3Es play a role in bacterial virulence.

Induction of *HrpL* depends on transcriptional activators *hrpS* and *hrpR* (80, 189). HrpS and HrpR belong to the NtrC family of two-component regulator proteins and form heterodimers before activation of *hrpL*. The pilus forming protein HrpA1 is a positive regulator that activates HrpL upstream of HrpS and HrpR, while HrpV is a negative regulator (154, 180). Deletion of *hrpA1* or overexpression of *hrpV* suppresses the HrpS-HrpR-HrpL cascade activation. HrpG acts further upstream as anti-anti-activator by suppressing HrpV, thus activating HrpS and HrpL (180).

The assembly of the T3SS apparatus is a highly regulated process and requires specific interactions among genes encoding the T3SS (5, 40). The T3SS has three components. First, the basal body is constructed, which spans inner and outer bacterial membranes. HrcJ is a constituent protein of the inner membrane and HrcC is in the outer membrane and belongs to the secretin family of proteins (47). Second, the pilus or needle-like syringe is assembled. HrpA1 is secreted through the basal body and polymerizes to form the Hrp pilus (88, 108). Third, translocator proteins are secreted through the T3SS to create pores or channels at the host plasma membrane to allow injection of T3Es into plant cells (128). Harpin proteins are also implicated in translocation of T3Es. Harpins elicit an HR and immune responses in plants. *Pto* DC3000 encodes four harpins

(HrpZ1, HrpW1, HopAK1 and HopP1) and the translocator HrpK1 (98, 149). HrpJ is important for pathogenicity as the *Pto* DC3000 *hrpJ* mutant strain has reduced disease symptoms in Arabidopsis and reduced HR in tobacco (42, 57). HrpJ is also important for translocation since the *hrpJ* mutant strain cannot secrete HrpW1, HrpZ1, and HopAK1. This suggests that HrpJ is a multifunctional regulator for the T3SS.

Pto DC3000 perceives signals from host plants to induce T3SS genes and initiate infection. Metabolomics analyses by gas chromatography-mass spectrometry (GC-MS) identified pyroglutamic, citric, shikimic, 4-hydroxybenzoic, and aspartic acids as type III-inducing plant-derived metabolites (9). These metabolites have been implicated in regulating different aspect of *Pto* DC3000 virulence, like chemotaxis and production of the phytotoxin coronatine.

Type III effectors

T3Es are secreted into plant cells through the T3SS. Inside plant cells, T3Es interfere with various cellular pathways associated with immunity to promote pathogen multiplication and development of disease. Based on a comparative genomic analysis of 19 *P. syringae* strains, there are 58 families of T3Es in *P. syringae* (18). The T3E repertoire among *P. syringae* genomes ranges from a minimum of 9 T3Es in *P. syringae* pv. *japonica* to a maximum of 39 T3Es in *Pto* DC3000.

P. syringae T3Es share three common features in their N-terminal region: (i) enrichment of polar amino acids, more than 10% serine in the first 50 amino

acids, (ii) aliphatic amino acid or proline at position 3 or 4, and (iii) lack of acidic amino acids in the first 12 amino acids (72, 148). These features provided bioinformatic tools for the identification of candidate T3E genes from sequenced genomes.

T3Es likely first evolved to suppress immune responses activated by PRRs after PAMP recognition (i.e., PTI) and then to suppress immunity induced by the recognition of specific T3Es by R proteins (i.e., ETI). As a way to classify *Pto* DC3000 T3Es based on their ability to suppress PTI, a functional screen was performed to identify T3Es able to suppress the flg22-mediated induction of the Arabidopsis *NHO1* gene (112). *NHO1* is required for resistance to nonhost *P. syringae* strains but is ineffective against pathogenic *Pto* DC3000, and is strongly induced by flg22. T3Es with PTI suppression abilities were HopS1, HopAI1, HopAF1, HopT1-1, HopT1-2, HopAA1-1, HopF2, HopC1, and AvrPto (112). In addition, *Pto* DC3000 T3Es have been classified based on their ability to suppress the HR elicited in tobacco by the T3E HopA1 (6). There are four classes of ETI suppressors, with AvrPtoB, HopD1, HopE1, HopF2, HopK1, HopS2, HopX1, and HopAM1 belonging to class I, which consists of effectors that displayed the most robust suppression of ETI (70, 82).

Type III effector targets

T3Es evolved to suppress plant innate immunity and allow *P. syringae* strains to multiply and cause diseases in their host plants. T3Es function in different ways inside plant cells. They have diverse host targets, disrupt signal transduction

pathways, and localize to different organelles to perform their virulence function. However, the majority of T3E enzymatic activities and plant targets are not known and this represents an important area of research. Activities and targets of *P. syringae* T3Es are described below and summarized in figure 2 and table 1. Unless specified, the majority of *P. syringae* T3E targets haven been identified in Arabidopsis.

a. PAMP-receptor kinases complexes

PAMP recognition is the first layer of immunity mediated by PRRs at the plasma membrane of plant cells. Several T3Es have been identified to target PRRs to suppress downstream signaling events associated with PTI.

Two T3Es, AvrPto and AvrPtoB, target the cytoplasmic kinase domain of PRRs. AvrPtoB (also known as HopAB2) is an E3 ubiquitin ligase that promotes degradation of PRRs FLS2, EFR and CERK1 in a proteasome-dependent manner by ubiquitinating these PRRs (65, 68). The N-terminus of AvrPtoB interacts with the cytoplasmic kinase domains of FLS2, EFR, CERK1 and its C-terminus carries an ubiquitin E3 ligase domain that mediates degradation of its targets. AvrPto targets FLS2 and EFR to inhibit their kinase activities (188).

AvrPto and AvrPtoB also target the FLS2 co-receptor BAK1 and interfere with the BAK1-FLS2 association activated by flg22 (168, 198). The plasma membrane localization of AvrPto is required to dissociate the BAK1-FLS2 complex since an AvrPto derivative with a mutation (G2A) in the AvrPto myristoylation site no longer interferes with this complex (168, 169). The N-terminal 387 amino acids of AvrPtoB are required for the disruption of the BAK1-FLS2 complex. The crystal

structure of the AvrPtoB$_{250-359}$-BAK1 complex was determined and shows that amino acids 250-359 of AvrPtoB define the minimal BAK1-interacting domain as shown by Isothermal titration calorimetry (33). These reports show that AvrPto targets BAK1. However, there is conflicting evidence for this interaction (187). Therefore it is unclear whether BAK1 and/or PRRs are the true virulence targets of AvrPto.

HopF2 is a T3E that targets multiple components of PTI and localizes to the plasma membrane of plants (159). It was first shown that HopF2 blocks flg22-induced BIK1 phosphorylation (184). The myristoylation site of HopF2, responsible for its plasma membrane localization, is required for HopF2 suppression of BIK1 phosphorylation. However, HopF2 does not directly interact with BIK1 and does not inhibit BIK1 kinase activity, likely targeting components upstream of BIK1 in the FLS2/BAK1 complex. HopF2 also inhibits flg22-induced phosphorylation of PBL1, a BIK1 homolog (198). It was recently shown that HopF2 interacts with BAK1, a PTI component upstream of BIK1 (198). HopF2 interacts with BAK1 in the *fls2* mutant, indicating that this interaction is independent of FLS2.

HopAO1 is a protein-tyrosine phosphatase (53) that targets EFR (121). Phosphorylation of the EFR tyrosine residue Y836 upon elf18 binding is required for EFR activation and subsequent immune responses. HopAO1 dephosphorylates EFR upon elf18 treatment, therefore suppressing PTI responses. Although FLS2 tyrosine phosphorylation could not be evaluated, HopAO1 interacts with FLS2 and inhibits flg22-induced immune responses.

b. MAPK pathways

Mitogen-activated protein kinases act downstream of PAMP recognition to initiate a cascade of immunity-associated signaling events. Therefore, MAPK pathways are important hubs targeted by T3Es.

Besides targeting PRR complexes, HopF2 blocks multiple MAPKs. HopF2 inhibits flg22-activation of the MAPK kinase 5 (MKK5), which acts upstream of MPK3 and MPK6 in the MEKK1/MKKs-MKK4/5-MPK3/6 cascade (179). Therefore, HopF2 inhibits MPK3 and MPK6 phosphorylation and suppresses PTI. HopF2 interacts with several other MKKs, including MKK3, MKK4, MKK6 and MKK10; however, MKK4 and MKK5 appear to be the main HopF2 targets. HopF2 has ADP-ribosyltransferase activity and ADP-ribosylates the amino acid residue Arg-313 and possible other residues in the C-terminal 38 amino acids of MKK5 to block its kinase activity (179). HopF2 also inhibits flg22-activation of MPK4 by suppression of BIK1 phosphorylation (198).

HopAI1 is a phosphotreonine lyase that irreversibly inactivates MPK3 and MPK6 by dephosphorylation of a phosphotreonine residue in MPK3 and MPK6 upon flg22 treatment (193). HopAI1 therefore blocks MAPK signaling upon PAMP activation. HopAI1 also targets MPK4 to inhibit its kinase activity (195).

c. R-protein receptor complexes

To overcome PTI suppression, plants evolved a second pathway to detect the presence of the pathogen. That is, by recognizing the presence of a T3E inside plant cells. The result is the induction of an immunity pathway referred to as ETI. ETI is a more robust and prolonged response compared to PTI. However, *P.*

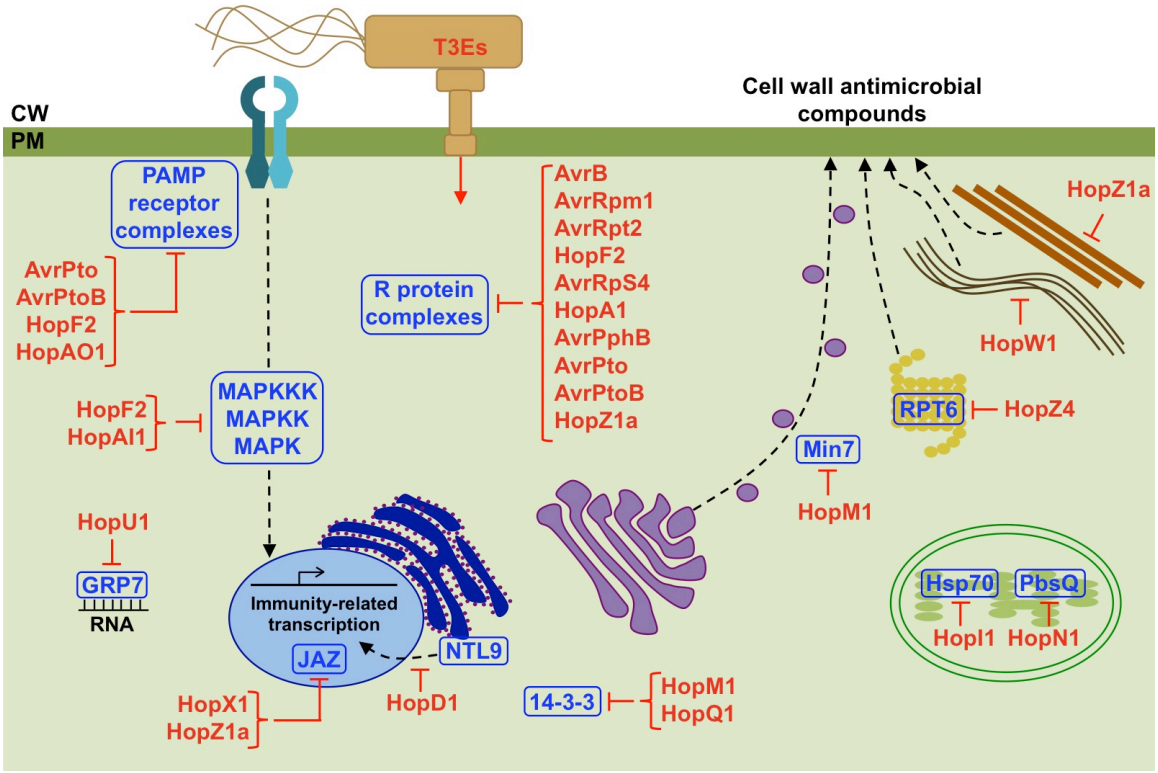

Fig. 2. Host targets of *Pseudomonas syringae* type III effectors. Type III effectors (TE3s) (red text) are injected into the host cytoplasm through the type III secretion system. T3Es target host proteins (blue text) to suppress plant innate immunity at different levels. Some T3Es block PAMP-receptor complexes to suppress the PAMP-triggered immunity (PTI) pathway. PTI activates MAPK signaling cascades to induced transcriptional reprogramming. MAPK cascades and transcription of immunity-related genes are also inactivated by several T3ES. One T3E is known to act postranscriptionally to block RNA binding proteins to bind to their target RNAs. Another important component of the innate immune system is the effector-triggered immunity (ETI) pathway mediated by R protein complexes. This immunity pathway is targeted by a large group of T3Es. Few effectors are targeted to organelles like mitochondria and chloroplast to suppress immune responses. T3Es also interfere with vesicle trafficking and the cytoskeleton (microtubules and actin) to suppress cell wall mediated immune responses.

syringae evolved or acquired new T3Es that have the ability to suppress R protein complexes to inactive ETI.

RPM1-interacting protein (RIN4) is a negative regulator of plant immunity that is localized to the plasma membrane and is targeted by several T3Es. Perturbations on RIN4 by T3Es are perceived by R proteins inducing ETI. AvrRpm1 and AvrB are two T3Es with N-terminal myristoylation sites that mediate plasma membrane localization in plant cells (141). AvrRpm1 and AvrB induce RIN4 phosphorylation to enhance the negative regulatory function of RIN4 and to suppress immunity (125). However, RIN4 phosphorylation is perceived by the R protein RPM1 activating immune responses. AvrB- and to a lesser extend AvrRpm1-mediated RIN4 phosphorylation at threonine residue T166 is critical for RPM1 activation (36). RIN4-interacting receptor-like protein kinase (RIPK) directly phosphorylates RIN4 induced by AvrRpm1 and AvrB (115). RIPK phosphorylates RIN4 specifically at amino acid residues T21, S160 and T166. AvrRpm1 has a fold related to the catalytic domain of poly(ADP-ribosyl) polymerase-1 (34). Mutations on the putative catalytic triad of AvrRpm1 abolish activation of RPM1 immunity but interestingly activate RPS2-mediated immunity. Two other T3Es target RIN4, AvrRpt2 and HopF2. AvrRpt2 is a cysteine protease that cleaves RIN4, which is perceived by the R protein RPS2 inducing ETI (14, 15). AvrRpt2 mutant alleles that are not recognized by RPS2 fail to eliminate RIN4, suggesting that RPS2 initiates immune responses after AvrRpt2-mediated degradation of RIN4. HopF2 ADP-ribosylates RIN4 to block AvrRpt2-induced RIN4 degradation, suppressing RPS2-dependent ETI (182). Unlike AvrRpm1,

AvrB, and AvrRpt2, modification of RIN4 by HopF2 is not recognized by an R protein in Arabidopsis. Therefore, HopF2 does not induce ETI and promotes bacterial growth.

Another R protein complex hub is EDS1, a resistance regulator required for immunity mediated by TIR-NB-LRR R proteins (2). The TIR-NB-LRR R proteins RPS4 and RPS6 recognize AvrRps4 and HopA1, respectively, inducing ETI (77, 94). EDS1 directly interacts with RPS4 and RPS6 but this R protein complex is disrupted by AvrRps4 and HopA1 (23, 75).

AvrPphB, also known as HopAR1, is a cysteine protease that localizes to the plasma membrane through acylation-dependent mechanism (49). AvrPphB cleaves the receptor-like cytoplasmic kinase PBS1, which is recognized by the CC-NB-LRR R protein RPS5 inducing ETI (2, 170, 192). PBS1 cleavage products but not its kinase activity are required for RPS5 activation, suggesting that RPS5 is activated by conformational changes in PBS1 (48). The plasma membrane localization of PBS1 mediated by S-acylation at its N-terminus is required for RPS5 activation (155). PBS1 carries the AvrPphB cleavage site in its N-terminus while the amino acid sequence (SEMPH) in its C-terminus is responsible for specific interaction with RPS5. The SEMPH motif represents the RPS5 recognition motif and is unique to PBS1. A new model suggests that RPS5 detects modification of the SEMPH motif in PBS1 caused by AvrPphB, instead of its proteolytic cleavage (155). Actin depolymerizing factor 4 (ADF4) is required for expression of RPS5 and resistance to AvrPphB since expression of RPS5 is reduced in an *adf4* mutant (152).

AvrPto and AvrPtoB are recognized in tomato by the Pto kinase leading to ETI (95). The N-terminal 387 amino acids of AvrPtoB is recognized by the Pto homologue, the Fen kinase, inducing immune responses (161). However, the C-terminus of AvrPtoB carries the E3 ubiquitin ligase domain that ubiquitinates Fen, which results in the degradation of Fen by the 26S proteasome and suppression of Fen-dependent ETI. Pto escapes AvrPtoB-mediated ubiquitination and activates ETI by phosphorylating the E3 ligase domain of AvrPtoB (144). However, it was recently shown that Pto binds to an AvrPtoB N-terminal domain, distal to the E3 ligase domain, to avoid ubiquitination and activation of ETI (127). Both Pto- and Fen-mediated resistance require Prf, a CC-NB-LRR R protein (136). This is an example of the guard model, in which Prf perceives modifications on Pto and Fen induced by AvrPtoB to activate ETI responses.

The HopZ family belongs to the YopJ super family of T3E with acetyl transferase and cysteine protease enzymatic activities (104). HopZ members have N-terminal myristoylation sites that mediate plasma membrane localization (103, 197). The Arabidopsis CC-NB-LRR R protein HopZ-activated resistance 1 (ZAR1) recognizes HopZ1a (107). The CC domain of ZAR1 is evolutionary distinct from other CC-NB-LRR proteins and ZAR1 activates immunity independent of *NDR1*, a gene required for CC-NB-LRR R protein signaling. The pseudokinase HopZ-ETI-deficient 1 (ZED1) is required for ZAR1-mediated immunity, as the *zed1* mutant cannot recognize HopZ1a (105). ZED1 interacts with HopZ1a and ZAR1 and HopZ1a acetylates ZED1 at residues T125 and

T177 activating ZAR1 immunity. It is still not clear whether ZED1 acts as a guardee or decoy mediating ZAR1 immunity.

HopAI1 inactivates MPK4 to suppress PTI (195). However, HopAI1 mediated inactivation of MPK4 results in activation of SUMM2-mediated immune responses Thus, it is likely that the R protein SUMM2 evolved to sense bacterial perturbations to the MAPK signaling cascade.

d. Transcription factors

Chapter 2 of this thesis describes that HopD1 interacts with the membrane-tethered transcription factor NTL9 at the plasma membrane to inhibit induction of NTL9-regulated genes (25). HopD1 suppresses immune responses associated with ETI but not PTI. NTL9-regulated genes are induced in an ETI-dependent manner and HopD1 blocks their induction.

HopZ1a targets the JA pathway by degrading jasmonate ZIM-domain (JAZ) proteins (87). JAZ proteins are transcriptional repressors of the JA signaling pathway. The acetyltransferase activity of HopZ1a is required to acetylate and degrade JAZ proteins. Degradation of JAZ proteins by HopZ1a induces expression of JA-responsive genes. Therefore, HopZ1a activates JA signaling to promote bacterial infection. HopX1 is another T3E interfering with the JA pathway, in a similar manner as HopZ1a. HopX1 is a cysteine protease that degrades JAZ proteins, leading to activation of JA-induced immune responses and downregulation of SA responses (64).

e. Post-transcriptional targets

HopU1 is a mono-ADP-ribosyltransferase that targets RNA-binding proteins including the glycine-rich RNA-binding proteins GRP7 and GRP8 (58). These RNA-binding proteins possess RNA-recognition motifs (RRMs). The arginine residue R49 in the GRP7 RRM is ADP-ribosylated by HopU1, and this modification blocks the ability of GRP7 to bind target RNAs (58, 86). GRP7 interacts with translational components suggesting that it may function by modifying translation. GRP7 likely interacts with many immunity-related RNAs. However, the only published RNA interactors are the RNAs encoding the PRRs FLS2 and EFR (140). HopU1 inhibits binding of GRP7 to FLS2 and EFR transcripts and likely other immunity-related RNAs, thereby suppressing PTI.

f. Vesicle trafficking

HopM1 degrades AtMIN7 (*A. thaliana* HopM1 interactor 7) via the 26S proteasome (142). AtMIN7 is an ADP-ribosylation factor guanine nucleotide exchange factor that regulates vesicle trafficking. HopM1 blocks vesicle trafficking to suppress PTI and SA-regulated immunity, highlighting the importance of AtMIN7 for plant immunity. HopM1 and AtMIN7 localize to the *trans*-Golgi network/early endosome (TGN/EE) (143). This suggests that the TGN/EE is an important subcellular compartment mediating immunity.

HopZ4 interacts with RPT6, a 26S proteasomal subunit, to inhibit proteasome activity (174). HopZ4 belongs to the YopJ family of T3Es. The conserved catalytic triad (H133, E152, and C194) and consensus myristoylation site characteristic of YopJ-like effector proteins are required for the HopZ4 inhibitory

effect on the proteasome. By inhibiting the proteasome, HopZ4 interferes with the secretory pathway.

g. Cytoskeleton

HopZ1a binds tubulin and microtubules, major constituents of the plant cytoskeleton (102). HopZ1a is an acetyltransferase activated by the co-factor phytic acid that acetylates itself and tubulin. A lysine in position 289 of HopZ1a is the putative autoacetylated site, and is important for HopZ1's acetyltransferase activity. Tubulin acetylation by HopZ1a disrupts tubulin networks, inhibits protein secretion, and suppresses cell wall-mediated immunity.

HopW1 disrupts the actin cytoskeleton by reducing filamentous actin (F-actin) networks (91). This modification inhibits endocytosis and trafficking of proteins to the ER and/or vacuoles, two actin-dependent processes. AvrPphB potentially targets the actin cytoskeleton by altering ADF4 phosphorylation (152). ADF4 is important in actin turnover mechanisms (76).

h. Plant organelles

At least four *P. syringae* T3Es are targeted to plant chloroplast to suppress immunity: HopI1, HopN1, HopK1 and AvrRps4. HopI1 is a T3E specifically targeted to the chloroplast through a N-terminal chloroplast targeting sequence (85). HopI1 has a J domain on its C-terminus that mediates activation of the 70 kDa heat shock proteins (Hsp70). J domains with a conserved HPD loop are found in Hsp70 cochaperones and these proteins activate the ATPase activity and folding of Hsp70 (93). Once inside the chloroplast, HopI1 remodels chloroplast thylakoid structure and reduces SA levels, which is produced in

chloroplasts during plant immune responses (84, 85). The J domain activity of HopI1 is required to alter chloroplast morphology. In this manner, HopI1 suppresses SA-mediated immunity. HopN1 is a cysteine protease that targets the tomato PsbQ, a chloroplast protein member of the oxygen-evolving complex of photosystem II (160). HopN1 degrades PsbQ to inhibit photosystem II activity and block ROS production. The catalytic triad (C1272, H283, D299) characteristic of cysteine proteases from the YopT/AvrPphB effector family is essential for the activity of HopN1 (116, 160). HopK1 and AvrRps4 are targeted to the chloroplast through an N-terminal cleavable chloroplast transit peptide to suppress PTI responses (109). Chloroplast localization of these T3Es is required for suppression of PTI-induced immune responses.

HopG1 is a T3E that localizes to the mitochondria to disrupt its function (24). HopG1 does not have an obvious mitochondrial target peptide but its N-terminal 263 amino acids are required for mitochondrial-localization. Inside mitochondria, HopG1 reduces respiration rates and increases ROS production. In addition, HopG1 alters plant morphology as transgenic plants overexpressing HopG1 show dwarfism, increased branching and infertility.

i. Hormones

Several virulence targets have been identified for HopZ1a. In addition to disrupting tubulin networks and JAZ proteins, HopZ1a targets 2-hydroxyisoflavone dehydratase (HID1), an enzyme involved in isoflavone biosynthesis in soybeans (196). Both HopZ1a and HopZ1b degrade HID1 to inhibit production of daidzein, major soybean isoflavone. Degradation of HID1 is

dependent on the acetyltransferase activity of HopZ1. Silencing *HID1* in soybeans results in increased susceptibility to *P. syringae* infection, suggesting a role for isoflavone in plant immunity.

AvrB also disrupts hormone signaling. As described earlier in this chapter, AvrB phosphorylates RIN4 to suppress immunity (125). AvrB interacts with RAR1, an important component required for ETI that functions as the HSP90 co-chaperone (44). The AvrB-RAR1 interaction enables AvrB to associate with HSP90 and MPK4 and results in the phosphorylation of RIN4 by MPK4. *In planta* expression of AvrB results in increased expression of JA-responsive genes, which is dependent on the RAR1-HSP90-MPK4 complex. Ultimately this leads to the activation of JA signaling and disease susceptibility.

HopQ1 activates cytokinin (CK) signaling (73). A characteristic aspartate motif in a putative hydrolase nucleoside domain present in HopQ1 suggests a nucleoside hydrolase activity (110). HopQ1 mimics the phosphoribohydrolase activity of LOG enzymes, which hydrolyze the CK precursor iPRMP to convert inactive CK nucleotides to active CK forms (73). HopQ1 hydrolyzes iPRMP to activate CK pathway and to upregulate CK-responsive genes. Induction of the CK pathway by HopQ1 attenuates FLS2 expression, which leads to suppression of PTI responses.

AvrRpt2 is recognized by the R protein RPS2 (22, 131). In the *rps2* mutant, AvrRpt2 increases levels of free indole acetic acid (IAA), a product of an auxin-response gene (32). In this manner, *P. syringae* delivers AvRrpt2 to modulate auxin physiology to promote disease susceptibility. Recent data indicate that

AvrRpt2 stimulates the turnover of Aux/IAA proteins, transcriptional repressors of auxin signaling stimulating auxin signaling (43). In addition, HopM1 degrades AtMin7 (142), a protein involved in vesicle trafficking and recycling of the auxin efflux carrier PIN1 (100). This suggests that HopM1 alters auxin efflux.

Several *P. syringae* T3Es disrupt the ABA, ET and SA signaling pathways. AvrPtoB induces expression of *NCED3*, which encodes a key enzyme of ABA biosynthesis, facilitating bacterial growth (46). Expression of HopAM1 *in planta* enhances ABA responses and suppresses immune responses (67). AvrPtoB and AvrPto induce expression of two tomato genes involved in ethylene production, *LeACO1* and *LeACO2*, enhancing disease development (39). HopI1 is targeted to chloroplasts to block SA biosynthesis (85).

j. 14-3-3 proteins

14-3-3 proteins are eukaryotic phosphopeptide-binding proteins that bind client proteins involved in different cellular processes. 14-3-3 proteins serve as scaffold proteins to regulate client stability, conformation, localization and/or protein-protein interactions (29). In addition to activating CK signaling, HopQ1 interacts with several 14-3-3 proteins, including TFT1 and TFT5, in a phosphorylation dependent manner (66). The N-terminus of HopQ1 possesses a 14-3-3 binding site (RSXpSXP). Phosphorylation of the HopQ1 residue serine 51 in the 14-3-3 binding site is required for binding to TFT1 and TFT5 to promote bacterial virulence *in planta* (66, 111). A second HopM1 target is AtMIN10, the 14-3-3 protein GRF8 (142). GRF8 interacts with BZR1, a transcription factor in the brassinosteroid signaling, and GRF8 interferes with accumulation of BZR1 in the

nucleus (60, 163). *In planta* expression of HopM1 leads to nuclear accumulation of BZR1 (117). This indicates that HopM1 mimics the effect of disrupting the function of 14-3-3 proteins. HopM1 degrades GRF8 to disrupt interaction with its client proteins; therefore it suppresses PTI-induced ROS production and stomatal immunity. Until now it is not clear if 14-3-3 proteins are co-factors or direct targets of HopQ1 and HopM1.

k. RNA silencing

New evidence has shown that T3Es suppress host RNA silencing pathways in order to cause disease. Components of the small RNA pathway are induced by bacterial infections. For example, the microRNA miR393 is induced after PAMP-perception and contributes to resistance against virulent *Pto* DC3000 by repressing auxin signaling (138). To counteract this pathogen restriction, *P. syringae* uses AvrPtoB, AvrPto, and HopT1-1 to suppress PAMP-induced miRNAs, including miR393a and miR393b (139). These T3Es suppress miRNAs transcriptional activation, biogenesis, stability or their activity. In addition, HopAB1, HopX1, and HopF2 have been shown to enhance gene silencing (164). However, the mechanism by which all of these T3Es manipulate host RNA silencing to suppress immunity remains to be elucidated.

In summary, T3Es interfere with several immunity-associated complexes and organelles to hijack the plant innate immune system and allow bacterial multiplication. The diversity of T3E targets illustrates sophisticated mechanisms to suppress immunity to favor pathogenicity.

Table 1. *P. syringae* type III effector's activity, plant targets and localization

Effector	Enzymatic activity	Target	Subcellular localization	Reference
AvrB	Unknown	RAR1/Hsp90/MPK4/ RIN4	Plasma membrane	(36, 44, 115, 125, 141)
AvrPphB (HopAR1)	Cysteine protease	PBS1 and PBS1-like proteins (BIK1, PBL1, PBL2)	Plasma membrane	(2, 49, 170, 194)
AvrPto	Kinase inhibitor	FLS2, EFR, BAK1, Pto, miRNA pathway	Plasma membrane	(120, 139, 168, 169, 188)
AvrPtoB (HopAB2)	E3 ubiquitin ligase	FLS2, EFR, CERK1, BAK1, Pto, Fen, miRNA pathway	Unknown	(65, 68, 83, 127, 139, 161, 168)
AvrRpm1	Unknown	RIN4	Plasma membrane	(36, 115, 125, 141)
AvrRps4	Unknown	EDS1	Nucleus and chloroplast	(23, 75, 109)
AvrRpt2	Cysteine protease	RIN4	Plasma membrane	(14, 15, 124)
HopA1	Unknown	EDS1	Nucleus and cytoplasm	(23, 75)
HopAI1	Phosphothreonine lyase	MPK3, MPK6, MPK4	Unknown	(193, 195)
HopAO1	Tyrosine phosphatase	EFR, FLS2	Unknown	(53, 121)
HopC1	Cysteine protease	Unknown	Plasma membrane	(49)
HopD1	Unknown	NTL9	Endoplasmic reticulum	(25)
HopF2	Mono-ADP-ribosyltransferase	BAK1, RIN4, MKK5	Plasma membrane	(159, 179, 182, 198)
HopG1	Unknown	Unknown	Mitochondria	(24)
HopI1	J-domain protein	Hsp70	Chloroplast	(84, 85)
HopK1	Unknown	Unknown	Chloroplast	(109)
HopM1	Unknown	AtMin7 (ARF-GEFP), AtMin10/GRF8 (14-3-3 protein)	*trans*-Golgi network/early endosome (TGN/EE)	(117, 142, 143)
HopN1	Cysteine protease	Tomato PbsQ	Chloroplast	(116, 160)
HopQ1	Nucleoside hydrolase	14-3-3 proteins (TFT1 and TFT5), iPRMP (cytokinin precursor)	Nucleus and cytoplasm	(66, 73, 111)
HopT1-1	Unknown	miRNA pathway	Unknown	(139)
HopU1	Mono-ADP-ribosyltransferase	GRP7 and RNA-binding proteins	Unknown	(58)
HopW1	Unknown	Actin cytoskeleton	Unknown	(91)
HopX1	Cysteine protease	JAZ	Nucleus and cytoplasm	(64)
HopZ1a	Acetyl transferase/cysteine protease	ZED1, tubulin, GmHID1, JAZ	Plasma membrane	(87, 102, 103, 105, 196, 197)
HopZ1b	Acetyl transferase	GmHID1	Plasma membrane	(103, 196, 197)
HopZ1c	Unknown	Unknown	Plasma membrane	(103)
HopZ2	Cysteine protease	MLO2	Plasma membrane	(103, 106)

The zigzag model of the plant immune system

The zigzag model first introduced by Jones and Dangl (90) explains the evolution of the plant innate immune system (Fig. 3). When pathogens first infected plants, it was likely that the host plant was capable of recognizing PAMPs with PRRs inducing PTI. The next likely step in the evolutionary process was that the pathogens needed to acquire a virulence factor or factors to suppress PTI. In this manner, effector genes were acquired by the pathogens to suppress PTI and allowed pathogens to grow on plants inducing effector-triggered susceptibility (ETS). However, plants also acquired R genes to encode immune receptors that recognized these effectors. These R proteins resulted in the activation of ETI and inhibiting the ability of pathogens to grow in plants. Then natural selection drove pathogens to diversify/mutate the genes that encoded recognized effectors or acquire additional effector genes to encode novel effectors to again suppress ETI, resulting again in ETS. Finally plants acquired new R proteins that could recognize the new effectors, inducing ETI again. This coevolutionary arms race between plants and pathogens results in highly virulent pathogen isolates and plants more resistant to pathogen invasion.

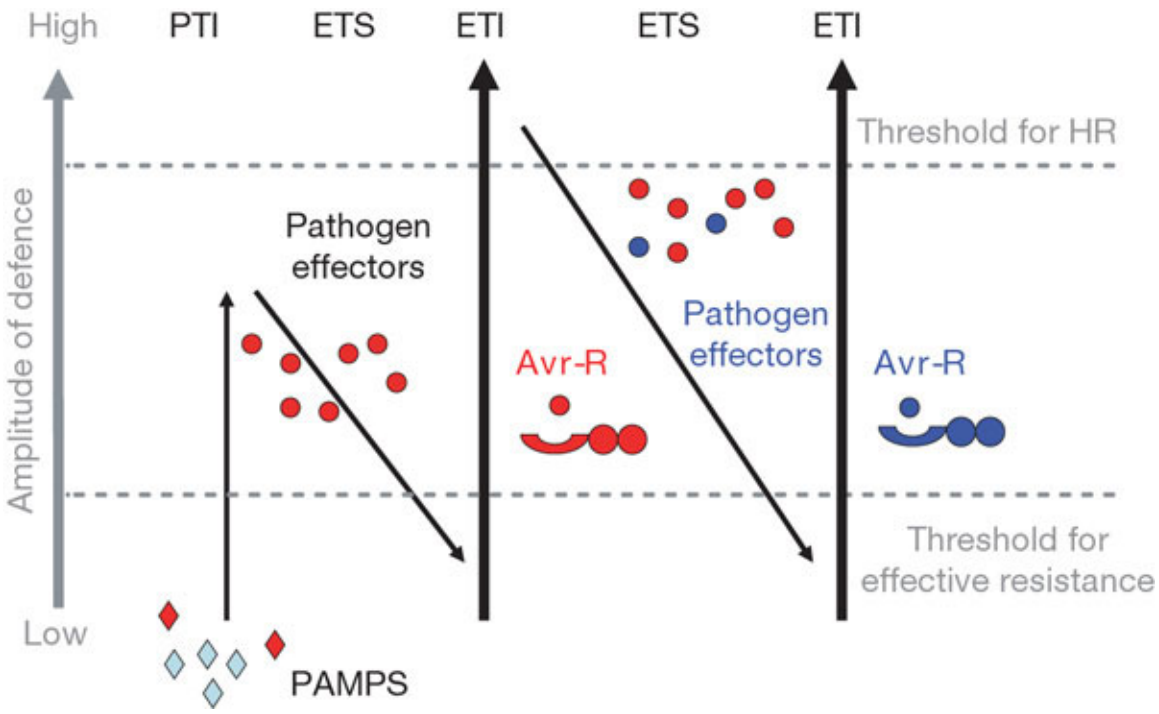

Fig. 3. A zigzag model illustrates the quantitative output of the plant immune system. Plants detect pathogen-associated molecular patterns (PAMPs, red diamonds) via pattern recognition receptors (PRRs) to induce PAMP-triggered immunity (PTI). Successful pathogens deliver effectors (red circles) that interfere with PTI, or enable pathogen nutrition and/or dispersal, resulting in effector-triggered susceptibility (ETS). When one effector is recognized by an R protein (red arc), effector-triggered immunity (ETI) is activated. ETI often passes a threshold for induction of the hypersensitive response (HR). Pathogen isolates are selected that have lost the gene that encoded the recognized effector or gained new effector genes through horizontal gene transfer that encode novel effectors (blue circles) to help pathogens suppress ETI. Selection favors new plant *R* genes (blue arc) that encode immune receptors that can recognize the newly acquired effectors, resulting again in ETI. This figure is from Jones and Dangl (90).

Evolution of type III effector inventory in *Pseudomonas syringae* strains

T3Es are key determinants in virulence and host-specificity of *P. syringae* strains. Genome comparisons in regards to the inventory of T3Es have contributed to understand the molecular basis for host range evolution of *P. syringae* pathovars. Genome sequencing and comparative genomic analyses of 19 diverse *P. syringae* strains revealed five T3E families conserved across all strains (18). The core families of T3Es include HopAA, AvrE, HopM, HopI and HopAH. In addition, nine new families of T3Es were identified: HopAY1, HopAZ1, HopBA1, HopBB1, HopBC1, HopBD1, HopBE1, HopBF1 and HopBG1. Most recently, genome-wide transcriptional analyses have identified HopBH1 and HopBI1 as two new T3E families from *P. syringae* pv. *oryzae* 1_6 and the HopBM1 family from *Pto* DC3000 (137).

The T3E repertoire between *P. syringae* strains is highly divergent, most likely as a result of selective pressures to suppress PTI and avoid host immune recognition. The most diverse T3E families identified by pairwise amino acid diversity are HopW, HopZ, AvrB, HopAO, HopT, HopAB and HopF (18). Phytotoxins (coronatine, tabtoxin, syringolin, syringopeptin, syringomycin, phaseolotoxin) are also important virulence factors influencing *P. syringae* host range. T3Es and phytotoxins content among *P. syringae* isolates representing multilocus sequence typing (MLST) groups is evolutionary dynamic. In particular, isolates from MLST group II contain fewer T3Es that are compensated by having more genes involved in phytotoxin biosynthesis. In agreement, the recently

sequenced *P. syringae* CC1557 strain contains the lowest number of T3Es but have acquired genes required for biosynthesis of the phytotoxin syringomycin (79). A new T3E, HopBJ1, with similarity to the *Escherichia coli* CNF1 toxin has been acquired by *P. syringae* CC1557 and is important for pathogenicity in *N. benthamiana*. This suggests a negative correlation between size of T3E repertoire and presence of toxins like syringomycin, syringopeptin and syringolin A.

P. syringae pv. *tomato* T1 (*Pto* T1) causes bacterial speck disease in tomato (*Solanum lycopersicum*) but is nonpathogenic in Arabidopsis. Comparison of virulence genes in *Pto* T1 and its closely related strain *Pto* DC3000, which is pathogenic on Arabidopsis, revealed that the phytotoxin coronatine and a set of T3Es are missing from *Pto* T1 (7). *Pto* T1 deploys AvrRpt2, which is recognized in Arabidopsis by the R protein RPS2. While *Pto* T1 elicits an HR in wild type Arabidopsis but not in a mutant lacking functional RPS2 (*rps2-101c*), bacterial growth in the *rps2-101c* mutant is similar to that in wild type Arabidopsis. Thus, AvrRpt2 triggers an HR in Arabidopsis but is not responsible for resistance to *Pto* T1. This suggests that other *Pto* T1 T3Es induce ETI in Arabidopsis. HopAS1 has been identified as a second T3E in *Pto* T1 that is recognized in Arabidopsis (171). Interestingly, *hopAS1* is truncated in *P. syringae* strains that are pathogenic in Arabidopsis.

In legumes, *P. syringae* pv. *phaseolicola* (*Pph*) and *P. syringae* pv. *glycinea* (*Pgy*) cause diseases in beans and soybeans, respectively. Genome-wide comparison of T3Es from *Pgy* R4 and *Pph* 1448a identified two effector genes

present in *Pgy* R4 but absent in *Pph* 1448a (17). HopC1 and HopM1 from the soybean pathogen *Pgy* R4 trigger avirulence responses in beans and thus contribute to host differentiation between *glycinea* and *phaseolicola* pathovars. This is consistent with HopC1 from *P. syringae* pv. *pisi* being an Avr protein in several French bean cultivars (12). *Pph* 1448a has a core set of six effectors (AvrB2, HopAB1/AvrPtoB, HopI1, HopR1, HopAS1 and HopAU1) that contribute to virulence in beans (123).

In order to more fully understand *P. syringae* T3Es, characterization of two T3Es was the primary focus for the research presented in this dissertation. Chapters 2-4 describe the TE3s HopD1 and HopA1 in regards to their activity, localization and targets in host cells. Chapter 5 summarizes the main discoveries of this dissertation and identifies questions that remain to be explored in our understanding of the molecular interactions of *P. syringae* with its host plant.

References

1. **Aarts, N., M. Metz, E. Holub, B. J. Staskawicz, M. J. Daniels, and J. E. Parker.** 1998. Different requirements for *EDS1* and *NDR1* by disease resistance genes define at least two *R* gene-mediated signaling pathways in Arabidopsis. Proc. Natl. Acad. Sci. USA **95:**10306-10311.
2. **Ade, J., B. J. Deyoung, C. Golstein, and R. W. Innes.** 2007. Indirect activation of a plant nucleotide binding site-leucine-rich repeat protein by a bacterial protease. Proc. Natl. Acad. Sci. USA **104:**2531-2536.
3. **Alfano, J. R., A. O. Charkowski, W. Deng, J. L. Badel, T. Petnicki-Ocwieja, K. van Dijk, and A. Collmer.** 2000. The *Pseudomonas syringae* Hrp pathogenicity island has a tripartite mosaic structure composed of a cluster of type III secretion genes bounded by exchangeable effector and conserved effector loci that contribute to parasitic fitness and pathogenicity in plants. Proc. Natl. Acad. Sci. USA **97:**4856-4861.
4. **Alfano, J. R., and A. Collmer.** 1996. Bacterial pathogens in plants: life up against the wall. Plant Cell **8:**1683-1698.
5. **Alfano, J. R., and A. Collmer.** 1997. The type III (Hrp) secretion pathway of plant pathogenic bacteria: trafficking harpins, Avr proteins, and death. J. Bacteriol. **179:**5655-5662.
6. **Alfano, J. R., H. Kim, T. P. Delaney, and A. Collmer.** 1997. Evidence that the *Pseudomonas syringae* pv. *syringae hrp*-linked *hrmA* gene encodes an Avr-like protein that acts in an *hrp*-dependent manner within tobacco cells. Mol. Plant Microbe Interact. **10:**580-588.
7. **Almeida, N. F., S. Yan, M. Lindeberg, D. J. Studholme, D. J. Schneider, B. Condon, H. Liu, C. J. Viana, A. Warren, C. Evans, E. Kemen, D. MacLean, A. Angot, G. B. Martin, J. D. Jones, A. Collmer, J. C. Setubal, and B. A. Vinatzer.** 2009. A draft genome sequence of *Pseudomonas syringae* pv. *tomato* T1 reveals a type III effector repertoire significantly divergent from that of P*seudomonas syringae* pv. *tomato* DC3000. Mol. Plant Microbe Interact. **22:**52-62.
8. **Alves, M. S., S. P. Dadalto, A. B. Gonçalves, G. B. de Souza, V. A. Barros, and L. G. Fietto.** 2014. Transcription factor functional protein-protein interactions in plant defense responses. Proteomes **2:**85-106.
9. **Anderson, J. C., Y. Wan, Y. Kim, L. Pasa-Tolic, T. O. Metz, and S. C. Peck.** 2014. Decreased abundance of type III secretion system inducing signals in Arabidopsis *mkp1* enhances resistance against *Pseudomonas syringae*. Proc. Natl. Acad. Sci. USA **111:**6846-6851.
10. **Andreasson, E., T. Jenkins, P. Brodersen, S. Thorgrimsen, N. H. Petersen, S. Zhu, J. L. Qiu, P. Micheelsen, A. Rocher, M. Petersen, M. A. Newman, H. Bjorn Nielsen, H. Hirt, I. Somssich, O. Mattsson, and J. Mundy.** 2005. The MAP kinase substrate MKS1 is a regulator of plant defense responses. EMBO J. **24:**2579-2589.
11. **Apel, K., and H. Hirt.** 2004. Reactive oxygen species: metabolism, oxidative stress, and signal transduction. Annu. Rev. Plant Biol. **55:**373-399.

12. **Arnold, D. L., R. W. Jackson, A. J. Fillinhham, S. C. Goss, J. D. Taylor, J. W. Mansfield, and A. Vivian.** 2001. Highly conserved sequences flank avirulence genes: isolation of novel avirulence genes from *Pseudomonas syringae* pv. *pisi*. Microbiology **147:**1171-1182.
13. **Asai, T., G. Tena, J. Plotnikova, M. R. Willmann, W. Chiu, L. Gomez-Gomez, T. Boller, F. M. Ausubel, and J. Sheen.** 2002. MAP kinase signalling cascade in Arabidopsis innate immunity. Nature **415:**977-983.
14. **Axtell, M. J., S. T. Chisholm, D. Dahlbeck, and B. J. Staskawicz.** 2003. Genetic and molecular evidence that the *Pseudomonas syringae* type III effector protein AvrRpt2 is a cysteine protease. Mol. Microbiol. **49:**1537-1546.
15. **Axtell, M. J., and B. J. Staskawicz.** 2003. Initiation of *RPS2*-specified disease resistance in Arabidopsis is coupled to the AvrRpt2-directed elimination of RIN4. Cell **112:**369-377.
16. **Bachmann, A. S., P. Matile, and A. J. Slusarenko.** 1998. Inhibition of ornithine decarboxylase activity by phaseolotoxin: implications for symptom production in halo blight of French bean. Physiol. Mol. Plant Pathol. **53:**287-299.
17. **Baltrus, D. A., M. T. Nishimura, K. M. Dougherty, S. Biswas, M. S. Mukhtar, J. Vicente, E. B. Holub, and J. L. Dangl.** 2012. The molecular basis of host specialization in bean pathovars of *Pseudomonas syringae*. Mol. Plant Microbe Interact. **25:**877-888.
18. **Baltrus, D. A., M. T. Nishimura, A. Romanchuk, J. H. Chang, M. S. Mukhtar, K. Cherkis, J. Roach, S. R. Grant, C. D. Jones, and J. L. Dangl.** 2011. Dynamic evolution of pathogenicity revealed by sequencing and comparative genomics of 19 *Pseudomonas syringae* isolates. PLOS Path. **7:**e1002132.
19. **Beck, M., I. Wyrsch, J. Strutt, R. Wimalasekera, A. Webb, T. Boller, and S. Robatzek.** 2014. Expression patterns of *FLAGELLIN SENSING 2* map to bacterial entry sites in plant shoots and roots. J. Exp. Bot. **65:**6487-6698.
20. **Beck, M., J. Zhou, C. Faulkner, D. MacLean, and S. Robatzek.** 2012. Spatio-temporal cellular dynamics of the Arabidopsis flagellin receptor reveal activation status-dependent endosomal sorting. Plant Cell **24:**4205-4219.
21. **Bender, C. L., F. Alarcón-Chaidez, and D. C. Gross.** 1999. *Pseudomonas syringae* phytotoxins: mode of action, regulation and biosynthesis by peptide and polyketide synthetases. Microbiol. Mol. Biol. Rev. **63:**266-292.
22. **Bent, A. F., B. N. Kunkel, D. Dahlbeck, K. L. Brown, R. Schmidt, J. Giraudat, J. Leung, and B. Staskawicz.** 1994. RPS2 of *Arabidopsis thaliana*: a leucine-rich repeat class of plant disease resistance genes. Science **265:**1856-1860.
23. **Bhattacharjee, S., M. K. Halane, S. H. Kim, and W. Gassmann.** 2011. Pathogen Effectors Target Arabidopsis EDS1 and Alter Its Interactions with Immune Regulators. Science **334:**1405-1408.

24. **Block, A., M. Guo, G. Y. Li, C. Elowsky, T. E. Clemente, and J. R. Alfano.** 2010. The *Pseudomonas syringae* type III effector HopG1 targets mitochondria, alters plant development and suppresses plant innate immunity. Cell. Microbiol. **12:**318-330.
25. **Block, A., T. Y. Toruño, C. G. Elowsky, C. Zhang, J. Steinbrenner, J. Beynon, and J. R. Alfano.** 2013. The *Pseudomonas syringae* type III effector HopD1 suppresses effector-triggered immunity, localizes to the endoplasmic reticulum, and targets the Arabidopsis transcription factor NTL9. New Phytol. **201:**1358-1370.
26. **Boccara, M., A. Sarazin, O. Thiebeauld, F. Jay, O. Voinnet, L. Navarro, and V. Colot.** 2014. The Arabidopsis *miR472-RDR6* silencing pathway modulates PAMP- and effector-triggered immunity through the post-transcriptional control of disease resistance genes. PLOS Path. **10:**e1003883.
27. **Boller, T., and G. Felix.** 2009. A renaissance of elicitors: perception of microbe-associated molecular patterns and danger signals by pattern-recognition receptors. Annu. Rev. Plant Biol. **60:**379-406.
28. **Boudsocq, M., M. R. Willmann, M. McCormack, H. Lee, L. Shan, P. He, J. Bush, S. Cheng, and J. Sheen.** 2010. Differential innate immune signalling via Ca^{2+} sensor protein kinases. Nature **464:**418-423.
29. **Bridges, D., and G. B. Moorhead.** 2005. 14-3-3 proteins: a number of functions for a numbered protein. Science Signaling **296:**re10.
30. **Brooks, D. M., G. Hernández-Guzmán, A. P. Kloek, F. Alarcón-Chaidez, A. Sreedharan, V. Rangaswamy, A. Peñazola-Vázquez, C. L. Bender, and B. N. Kunkel.** 2004. Identification and characterization of a well-defined series of coronatine biosynthetic mutants of *Pseudomonas syringae* pv. *tomato* DC3000. Mol. Plant Microbe Interact. **17:**162-174.
31. **Buell, C. R., V. Joardar, M. Lindeberg, J. Selengut, I. T. Paulsen, M. L. Gwinn, R. J. Dodson, R. T. Deboy, A. S. Durkin, J. F. Kolonay, R. Madupu, S. Daugherty, L. Brinkac, M. J. Beanan, D. H. Haft, W. C. Nelson, T. Davidsen, N. Zafar, L. Zhou, J. Liu, Q. Yuan, H. Khouri, N. Fedorova, B. Tran, D. Russell, K. Berry, T. Utterback, S. E. Van Aken, T. V. Feldblyum, M. D'Ascenzo, W. Deng, A. R. Ramos, J. R. Alfano, S. Cartinhour, A. K. Chatterjee, T. P. Delaney, S. G. Lazarowitz, G. B. Martin, D. J. Schneider, X. Tang, C. L. Bender, O. White, C. M. Fraser, and A. Collmer.** 2003. The complete genome sequence of the Arabidopsis and tomato pathogen *Pseudomonas syringae* pv. *tomato* DC3000. Proc. Natl. Acad. Sci. USA **100:**10181-10186.
32. **Chen, Z., J. L. Agnew, J. D. Cohen, P. He, L. Shan, J. Sheen, and B. N. Kunkel.** 2007. *Pseudomonas syringae* type III effector AvrRpt2 alters *Arabidopsis thaliana* auxin physiology. Proc. Natl. Acad. Sci. USA **104:**20131-20136.
33. **Cheng, W., K. R. Munkvold, H. Gao, J. Mathieu, S. Schwizer, S. Wang, Y. Yan, J. Wang, G. B. Martin, and J. Chai.** 2011. Structural analysis of *Pseudomonas syringae* AvrPtoB bound to host BAK1 reveals two similar

kinase-interacting domains in a type III effector. Cell Host Microbe **10:**616-626.

34. **Cherkis, K. A., B. R. S. Temple, E. Chung, J. Sondek, and J. L. Dangl.** 2012. AvrRpm1 missense mutations weakly activate RPS2-mediated immune response in *Arabidopsis thaliana*. PLOS One **7:**e42633.
35. **Chinchilla, D., C. Zipfel, S. Robatzek, B. Kemmerling, T. Nurmberger, J. D. Jones, G. Felix, and T. Boller.** 2007. A flagellin-induced complex of the receptor FLS2 and BAK1 initiates plant defence. Nature **448:**497-500.
36. **Chung, E., L. da Cunha, A. Wu, Z. Gao, K. Cherkis, A. J. Afzal, D. Mackey, and J. L. Dangl.** 2011. Specific threonine phosphorylation of a host target by two unrelated type III effectors activates a host innate immune receptor in plants. Cell Host Microbe **9:**125-136.
37. **Clarke, C. R., R. Cai, D. J. Studholme, D. S. Guttman, and B. A. Vinatzer.** 2010. *Pseudomonas syringae* strains naturally lacking the classical *P. syringae hrp/hrc* locus are common leaf colonizers equipped with an atypical type III secretion system. Mol. Plant Microbe Interact. **23:**198-210.
38. **Cody, Y. S., and D. C. Gross.** 1987. Characterization of Pyoverdin$_{pss}$, the fluorescent siderophore produced by *Pseudomonas syringae* pv. *syringae*. Appl. Environ. Microbiol. **53:**928-934.
39. **Cohn, J. R., and G. B. Martin.** 2005. *Pseudomonas syringae* pv. *tomato* type III effectors AvrPto and AvrPtoB promote ethylene dependent cell death in tomato. Plant J. **44:**139-154.
40. **Collmer, A., J. L. Badel, A. O. Charkowski, W. Deng, D. E. Fouts, A. R. Ramos, A. H. Rehm, D. M. Anderson, O. Schneewind, K. van Dijk, and J. R. Alfano.** 2000. *Pseudomonas syringae* Hrp type III secretion system and effector proteins. Proc. Natl. Acad. Sci. USA **97:**8770-8777.
41. **Cornelis, G. R.** 2006. The type III secretion injectisome. Nat. Rev. Microbiol. **4:**811-825.
42. **Crabill, E., A. Karpisek, and J. R. Alfano.** 2012. The *Pseudomonas syringae* HrpJ protein controls the secretion of type III translocator proteins and has a virulence role inside plant cells. Mol. Microbiol. **85:**225-238.
43. **Cui, F., S. Wu, W. Sun, G. Coaker, B. Kunkel, P. He, and L. Shan.** 2013. The *Pseudomonas syringae* type III effector AvrRpt2 promotes pathogen virulence via stimulating Arabidopsis auxin/indole acetic acid protein turnover. Plant Physiol. **162:**1018-1029.
44. **Cui, H., Y. Wang, L. Xue, J. Chu, C. Yan, J. Fu, M. Chen, R. W. Innes, and J. M. Zhou.** 2010. *Pseudomonas syringae* effector protein AvrB perturbs Arabidopsis hormone signaling by activating MAP Kinase 4. Cell Host Microbe **7:**164-175.
45. **Cui, J., A. K. Bahrami, E. G. Pringle, G. Hernández-Guzmán, C. L. Bender, N. E. Pierce, and F. M. Ausubel.** 2005. *Pseudomonas syringae* manipulates systemic plant defenses against pathogens and herbivores. Proc. Natl. Acad. Sci. USA **102:**1791-1796.

46. **de Torres-Zabala, M., W. Truman, M. H. Bennett, G. Lafforgue, J. W. Mansfield, P. Rodriguez Egea, L. Bogre, and M. Grant.** 2007. *Pseudomonas syringae* pv. *tomato* hijacks the Arabidopsis abscisic acid signalling pathway to cause disease. EMBO J. **26:**1434-1443.
47. **Deng, W. L., and H. C. Huang.** 1999. Cellular locations of *Pseudomonas syringae* pv. *syringae* HrcC and HrcJ proteins, required for harpin secretion via the type III pathway. J. Bacteriol. **181:**2298-2301.
48. **DeYoung, B. J., D. Qi, S. Kim, T. P. Burke, and R. W. Innes.** 2012. Activation of a plant nucleotide binding-leucine rich repeat disease resistance protein by a modified self protein. Cell. Microbiol. **14:**1071-1084.
49. **Dowen, R. H., J. L. Engel, F. Shao, J. R. Ecker, and J. E. Dixon.** 2009. A family of bacterial cysteine protease type III effectors utilizes acylation-dependent and -independent strategies to localize to plasma membranes. J. Biol. Chem. **284:**15867-15879.
50. **Dubiella, U., H. Seybold, G. Durian, E. Komander, R. Lassig, C. P. Witte, W. X. Schulze, and T. Romeis.** 2013. Calcium-dependent protein kinase/NADPH oxidase activation circuit is required for rapid defense signal propagation. Proc. Natl. Acad. Sci. USA **110:**8744-8749.
51. **Elmore, J. M., Z. D. Lin, and G. Coaker.** 2011. Plant NB-LRR signaling: upstreams and downstreams. Curr. Opin. Plant Biol. **14:**365-371.
52. **Erhardt, M., K. Namba, and H. K. T.** 2010. Bacterial nanomachines: the flagellum and type III injectisome. Cold Spring Harb. Perspect. Biol. **2:**a000299.
53. **Espinosa, A., M. Guo, V. C. Tam, Z. Q. Fu, and J. R. Alfano.** 2003. The *Pseudomonas syringae* type III-secreted protein HopPtoD2 possesses protein tyrosine phosphatase activity and suppresses programmed cell death in plants. Mol. Microbiol. **49:**377-387.
54. **Ferreira, A. O., C. R. Myers, J. S. Gordon, G. B. Martin, M. Vencato, A. Collmer, M. D. Wehling, J. R. Alfano, G. Moreno-Hagelsieb, W. F. Lamboy, G. DeClerck, D. J. Schneider, and S. W. Cartinhour.** 2006. Whole-genome expression profiling defines the HrpL regulon of *Pseudomonas syringae* pv. *tomato* DC3000, allows *de novo* reconstruction of the Hrp *cis* element, and identifies novel coregulated genes. Mol. Plant Microbe Interact. **19:**1167-1179.
55. **Flor, H. H.** 1971. Current status of the gene-for-gene concept. Annu. Rev. Phytopathol. **9:**275-296.
56. **Fouts, D. E., R. B. Abramovitch, J. R. Alfano, A. M. Baldo, C. R. Buell, S. Cartinhour, A. K. Chatterjee, M. D'Ascenzo, M. L. Gwinn, S. G. Lazarowitz, N. Lin, G. B. Martin, A. H. Rehm, D. J. Schneider, K. van Dijk, X. Tang, and A. Collmer.** 2002. Genome wide identification of *Pseudomonas syringae* pv. *tomato* DC3000 promoters controlled by the HrpL alternative sigma factor. Proc. Natl. Acad. Sci. USA **99:**2275-2280.
57. **Fu, Z. Q., M. Guo, and J. R. Alfano.** 2006. *Pseudomonas syringae* HrpJ is a type III secreted protein that is required for plant pathogenesis, injection of effectors, and secretion of the HrpZ1 harpin. J. Bacteriol. **188:**6060-6069.

58. **Fu, Z. Q., M. Guo, B. Jeong, F. Tian, T. E. Elthon, R. L. Cerny, D. Staiger, and J. R. Alfano.** 2007. A type III effector ADP-ribosylates RNA-binding proteins and quells plant immunity. Nature **447:**284-289.
59. **Galan, J. E., and A. Collmer.** 1999. Type III secretion machines: bacterial devices for protein delivery into host cells. Science **284:**1322-1328.
60. **Gampala, S. S., T. W. Kim, J. X. He, W. Tang, Z. Deng, M. Y. Bai, S. Guan, S. Lalonde, Y. Sun, J. M. Gendron, H. Chen, N. Shibagaki, R. J. Ferl, D. Ehrhardt, K. Chong, A. L. Burlingame, and Z. Y. Wang.** 2007. An essential role for 14-3-3 proteins in brassinosteroid signal transduction in Arabidopsis. Dev. Cell **13:**177-189.
61. **Gao, M., J. Liu, D. Bi, Z. Zhang, F. Cheng, S. Chen, and Y. Zhang.** 2008. MEKK1, MKK1/MKK2 and MPK4 function together in a mitogen-activated protein kinase cascade to regulate innate immunity in plants. Cell Res. **18:**1190-1198.
62. **Gao, X., X. Chen, W. Lin, S. Chen, D. Lu, Y. Niu, L. Li, C. Cheng, M. McCormack, J. Sheen, L. Shan, and P. He.** 2013. Bifurcation of Arabidopsis NLR immune signaling via Ca^{2+}-dependent protein kinases. PLOS Path. **9:**e1003127.
63. **Garrity, G. M., D. J. Brenner, N. R. Krieg, and J. R. Staley.** 2005. Bergey's Manual of Systematic Bacteriology, Volume Two: The Proteobacteria, Parts A-C.
64. **Gimenez-Ibanez, S., M. Boter, G. Fernández-Barbero, A. Chini, J. P. Rathjen, and R. Solano.** 2014. The bacterial effector HopX1 targets JAZ transcriptional repressors to activate jasmonate signaling and promote infection in Arabidopsis. PLOS Biol. **12:**e1001792.
65. **Gimenez-Ibanez, S., D. R. Hann, V. Ntoukakis, E. Petutschnig, V. Lipka, and J. P. Rathjen.** 2009. AvrPtoB targets the LysM receptor kinase CERK1 to promote bacterial virulence on plants. Curr. Biol. **19:**1-7.
66. **Giska, F., M. Lichocka, M. Piechocki, M. Dadlez, E. Schmelzer, J. Hennig, and M. Krzymowska.** 2013. Phosphorylation of HopQ1, a type III effector from *Pseudomonas syringae*, creates a binding site for host 14-3-3 proteins. Plant Physiol. **161:**2049-2061.
67. **Goel, A. K., D. Lundberg, M. A. Torres, R. Matthews, C. Akimoto-Tomiyama, L. Farmer, J. L. Dangl, and S. R. Grant.** 2008. The *Pseudomonas syringae* type III effector HopAM1 enhances virulence on water-stressed plants. Mol. Plant Microbe Interact. **21:**361-370.
68. **Gohre, V., T. Spallek, H. Haweker, S. Mersmann, T. Mentzel, T. Boller, M. de Torres, J. W. Mansfield, and S. Robatzek.** 2008. Plant pattern-recognition receptor FLS2 is directed for degradation by the bacterial ubiquitin ligase AvrPtoB. Curr. Biol. **18:**1824-1832.
69. **Groll, M., B. Schellenberg, A. Bachmann, C. Archer, R. Huber, T. K. Poweel, S. Lindow, M. Kaiser, and R. Dudler.** 2008. A plant pathogen virulence factor inhibits the eukaryotic proteasome by a novel mechanism. Nature **452:**755-759.
70. **Guo, M., F. Tian, Y. Wamboldt, and J. R. Alfano.** 2009. The majority of the type III effector inventory of *Pseudomonas syringae* pv. *tomato*

DC3000 can suppress plant immunity. Mol. Plant Microbe Interact. **22:**1069-1080.

71. **Guo, Y. L., J. Fitz, K. Schneeberger, S. Ossowski, J. Cao, and D. Weigel.** 2011. Genome-wide comparison of nucleotide-binding site-leucine-rich repeat-encoding genes in Arabidopsis. Plant Physiol. **157:**757-769.
72. **Guttman, D. S., B. A. Vinatzer, S. F. Sarkar, M. V. Ranall, G. Kettler, and J. T. Greenberg.** 2002. A functional screen for the type III (Hrp) secretome of the plant pathogen *Pseudomonas syringae*. Science **295:**1722-1726.
73. **Hann, D. R., A. Domínguez-Ferreras, V. Motyka, P. I. Dobrev, S. Schornack, A. Jehle, G. Felix, D. Chinchilla, J. P. Rathjen, and T. Boller.** 2014. The *Pseudomonas* type III effector HopQ1 activates cytokinin signaling and interferes with plant innate immunity. New Phytol. **201:**585-598.
74. **Heese, A., D. R. Hann, S. Gimenez-Ibanez, A. M. Jones, K. He, J. Li, J. I. Schroeder, S. C. Peck, and J. P. Rathjen.** 2007. The receptor-like kinase SERK3/BAK1 is a central regulator of innate immunity in plants. Proc. Natl. Acad. Sci. USA **104:**12217-12222.
75. **Heidrich, K., L. Wirthmueller, C. Tasset, C. Pouzet, L. Deslandes, and J. E. Parker.** 2011. Arabidopsis EDS1 connects pathogen effector recognition to cell compartment-specific immune responses. Science **334:**1401-1404.
76. **Henty, J. L., S. W. Bledsoe, P. Khurana, R. B. Meagher, B. Day, L. Blanchoin, and C. J. Staiger.** 2011. Arabidopsis actin depolymerizing factor4 modulates the stochastic dynamic behavior of actin filaments in the cortical array of epidermal cells. Plant Cell **23:**3711-3726.
77. **Hinsch, M., and B. Staskawicz.** 1996. Identification of a new Arabidopsis disease resistance locus, *RPS4*, and cloning of the corresponding avirulence gene, *avrRps4*, from *Pseudomonas syringae* pv. *pisi*. Mol. Plant Microbe Interact. **9:**55-61.
78. **Hirano, S. S., and C. D. Upper.** 2000. Bacteria in the leaf ecosystem with emphasis on *Pseudomonas syringae*- a pathogen, ice nucleus, and epiphyte. Microbiol. Mol. Biol. Rev. **64:**624-653.
79. **Hockett, K. L., M. Nishmura, E. Karlsrud, K. M. Dougherty, and D. A. Baltrus.** 2014. *P. syringae* CC1557: a highly virulent strain with an unusually small type III effector repertoire that includes a novel effector. Mol. Plant Microbe Interact. **27:**923-932.
80. **Hutcheson, S. W., J. Bretz, T. Sussan, S. Jin, and K. Pak.** 2001. Enhancer-binding proteins HrpR and HrpS interact to regulate *hrp*-encoded type III protein secretion in *Pseudomonas syringae* strains. J. Bacteriol. **183:**5589-5598.
81. **Initiative, A. G.** 2000. Analysis of the genome sequence of the flowering plant *Arabidopsis thaliana*. Nature **408:**796-815.
82. **Jamir, Y., M. Guo, H. Oh, T. Petnicki-Ocwieja, X. Tang, M. Dickman, A. Collmer, and J. R. Alfano.** 2004. Identification of *Pseudomonas syringae*

type III effectors that can suppress programmed cell death in plants and yeast. Plant J. **37:**554-565.

83. **Janjusevic, R., R. B. Abramovitch, G. B. Martin, and C. E. Stebbins.** 2006. A bacterial inhibitor of host programmed cell death defenses is an E3 ubiquitin ligase. Science **311:**222-226.
84. **Jelenska, J., J. A. van Hal, and J. T. Greenberg.** 2010. *Pseudomonas syringae* hijacks plant stress chaperone machinery for virulence. Proc. Natl. Acad. Sci. USA **107:**13177-13182.
85. **Jelenska, J., N. Yao, B. A. Vinatzer, C. M. Wright, J. L. Brodsky, and J. T. Greenberg.** 2007. A J-domain virulence effector of *Pseudomonas syringae* remodels host chloroplasts and suppresses defenses. Curr. Biol. **17:**499-508.
86. **Jeong, B., Y. Lin, A. Joe, M. Guo, C. Korneli, H. Yang, P. Wang, M. Yu, R. L. Cerny, D. Staiger, J. R. Alfano, and Y. Xu.** 2011. Structure function analysis of an ADP-ribosyltransferase type III effector and its RNA-binding target in plant immunity. J. Biol. Chem. **286:**43272-43281.
87. **Jiang, S., J. Yao, K. Ma, H. Zhou, J. Song, S. Y. He, and W. Ma.** 2013. Bacterial effector activates jasmonate signaling by directly targeting JAZ transcriptional repressors. PLOS Path. **9:**e1003715.
88. **Jin, Q., and S. Y. He.** 2001. Role of the Hrp Pilus in type III protein secretion in *Pseudomonas syringae*. Science **294:**2556-2558.
89. **Jones, J. B., J. P. Jones, R. E. Stall, and T. A. Zitter.** 1991. Compendium of tomato diseases. American Phytopathological Society. 100 p.
90. **Jones, J. D. G., and J. L. Dangl.** 2006. The plant immune system. Nature **444:**323-329.
91. **Kang, Y., J. Jelenska, N. M. Cecchini, Y. Li, M. W. Lee, D. R. Kovar, and J. T. Greenberg.** 2014. HopW1 from *Pseudomonas syringae* disrupts the actin cytoskeleton to promote virulence in Arabidopsis. PLOS Path. **10:**e1004232.
92. **Katagiri, F., R. Thilmony, and S. Y. He.** 2002. The *Arabidopsis thaliana*-*Pseudomonas syringae* interaction. Arabidopsis Book. American Society of Plant Biologists. 1:e0039.
93. **Kelley, W. L.** 1998. The J-domain family and the recruitment of chaperone power. Trends Biochem. Sci. **23:**222-227.
94. **Kim, S. H., S. I. Kwon, D. Saha, N. C. Anyanwu, and W. Gassmann.** 2009. Resistance to the *Pseudomonas syringae* effector HopA1 is governed by the TIR-NBS-LRR protein RPS6 and is enhanced by mutations in *SRFR1*. Plant Physiol. **150:**1723-1732.
95. **Kim, Y. J., N. C. Lin, and G. B. Martin.** 2002. Two distinct *Pseudomonas* effector proteins interact with the Pto kinase and activate plant immunity. Cell **109:**589-598.
96. **Kobayashi, M., I. Ohura, K. Kawakita, N. Yokota, M. Fujiwara, K. Shimamoto, N. Doke, and H. Yoshioka.** 2007. Calcium-dependent protein kinases regulate the production of reactive oxygen species by potato NADPH oxidase. Plant Cell **19:**1065-1080.

97. **Kunze, G., C. Zipfel, S. Robatzek, K. Niehaus, T. Boller, and G. Felix.** 2004. The N terminus of bacterial elongation factor Tu elicits innate immunity in Arabidopsis plants. Plant Cell **16:**3496-3507.
98. **Kvitko, B. H., A. R. Ramos, J. E. Morello, H. S. Oh, and A. Collmer.** 2007. Identification of harpins in *Pseudomonas syringae* pv. *tomato* DC3000, which are functionally similar to HrpK1 in promoting translocation of type III secretion system effectors. J. Bacteriol. **189:**8059-8072.
99. **Lam, H. N., S. Chakravarthy, H. L. Wei, H. BuiNguyen, P. V. Stodghill, A. Collmer, B. M. Swingle, and S. W. Cartinhour.** 2014. Global analysis of the HrpL regulon in the plant pathogen *Pseudomonas syringae* pv. *tomato* DC3000 reveals new regulon members with diverse functions. PLOS One **9:**e106115.
100. **Lawton, K. A., L. Friedrich, M. Hunt, K. Weymann, T. Delaney, H. Kessmann, T. Staub, and J. Ryals.** 1996. Benzothiadiazole induces disease resistance in Arabidopsis by activation of the systemic acquired resistance signal transduction pathway. Plant J. **10:**71-82.
101. **Lecourieux, D., R. Ranjeva, and A. Pugin.** 2006. Calcium in plant defence-signalling pathways. New Phytol. **171:**249-269.
102. **Lee, A. H., B. Hurley, C. Felsensteiner, C. Yea, W. Ckurshumova, V. Bartetzko, P. W. Wang, V. Quach, J. D. Lewis, Y. C. Liu, F. Bornke, S. Angers, A. Wilde, D. S. Guttman, and D. Desveaux.** 2012. A bacterial acetyltransferase destroys plant microtubule networks and blocks secretion. PLOS Path. **8:**e1002523.
103. **Lewis, J. D., W. Abada, W. Ma, D. S. Guttman, and D. Desveaux.** 2008. The HopZ family of *Pseudomonas syringae* type III effectors require myristoylation for virulence and avirulence functions in *Arabidopsis thaliana*. J. Bacteriol. **190:**2880-2891.
104. **Lewis, J. D., A. Lee, W. Ma, H. Zhou, D. S. Guttman, and D. Desveaux.** 2011. The YopJ superfamily in plant-associated bacteria. Mol. Plant Pathol. **12:**928-937.
105. **Lewis, J. D., A. H. Lee, J. A. Hassan, J. Wan, B. Hurley, J. R. Jhingree, P. W. Wang, T. Lo, J. Youn, D. S. Guttman, and D. Desveaux.** 2013. The Arabidopsis ZED1 pseudokinase is required for ZAR1-mediated immunity induced by the *Pseudomonas syringae* type III effector HopZ1a. Proc. Natl. Acad. Sci. USA **110:**18722-18727.
106. **Lewis, J. D., J. Wan, R. Ford, Y. Gong, P. Fung, H. Nahal, P. W. Wang, D. Desveaux, and D. S. Guttman.** 2012. Quantitative interactor screening with next-generation sequencing (QIS-Seq) identifies *Arabidopsis thaliana* MLO2 as a target of the *Pseudomonas syringae* type III effector HopZ2. BMC Genomics **13:**8.
107. **Lewis, J. D., R. Wu, D. S. Guttman, and D. Desveaux.** 2010. Allele-specific virulence attenuation of the *Pseudomonas syringae* HopZ1a type III effector via the Arabidopsis ZAR1 resistance protein. PLOS Genet. **6:**e1000894.
108. **Li, C. M., I. Brown, J. Mansfield, C. Stevens, T. Boureau, M. Romantschuk, and S. Taira.** 2002. The Hrp pilus of *Pseudomonas*

syringae elongates from its tip and acts as a conduit for translocation of the effector protein HrpZ. EMBO J. **21:**1909-1915.

109. **Li, G., J. E. Froehlich, C. Elowsky, J. Msanne, A. C. Ostosh, C. Zhang, T. Awada, and J. R. Alfano.** 2014. Distinct *Pseudomonas* type-III effectors use a cleavable transit peptide to target chloroplasts. Plant J. **77:**310-321.
110. **Li, W., Y. Chiang, and G. Coaker.** 2013. The HopQ1 effector's nucleoside hydrolase-like domain is required for bacterial virulence in Arabidopsis and tomato, but not host recognition in tobacco. PLOS One **8:**e59684.
111. **Li, W., K. A. Yadeta, J. M. Elmore, and G. Coaker.** 2013. The *Pseudomonas syringae* effector HopQ1 promotes bacterial virulence and interacts with tomato 14-3-3 proteins in a phosphorylation dependent manner. Plant Physiol. **161:**2062-2074.
112. **Li, X., H. Lin, W. Zhang, Y. Zou, J. Zhang, X. Tang, and J. Zhou.** 2005. Flagellin induces innate immunity in nonhost interactions that is suppressed by *Pseudomonas syringae* effectors. Proc. Natl. Acad. Sci. USA **102:**12990-12995.
113. **Li, Y., Q. Zhang, J. Zhang, L. Wu, Y. Qi, and J. Zhou.** 2010. Identification of microRNAs involved in pathogen-associated molecular pattern-triggered plant innate immunity. Plant Physiol. **152:**2222-2231.
114. **Lindeberg, M., S. Cartinhour, C. R. Myers, L. M. Schechter, D. J. Schneider, and A. Collmer.** 2006. Closing the circle on the discovery of genes encoding Hrp regulon members and type III secretion system effectors in the genomes of three model *Pseudomonas syringae* strains. Mol. Plant Microbe Interact. **11:**1151-1158.
115. **Liu, J., J. M. Elmore, Z. D. Lin, and G. Coaker.** 2011. A receptor-like cytoplasmic kinase phosphorylates the host target RIN4, leading to the activation of a plant innate immune receptor. Cell Host Microbe **9:**137-146.
116. **Lopez-Solanilla, E., P. A. Bronstein, A. R. Schneider, and A. Collmer.** 2004. HopPtoN is a *Pseudomonas syringae* Hrp (type III secretion system) cysteine protease effector that suppresses pathogen induced necrosis associated with both compatible and incompatible plant interactions. Mol. Microbiol. **54:**353-365.
117. **Lozano-Durán, R., G. Bourdais, S. Y. He, and S. Robatzek.** 2014. The bacterial effector HopM1 suppresses PAMP-triggered oxidative burst and stomatal immunity. New Phytol. **202:**259-269.
118. **Lu, D., W. Lin, X. Gao, S. Wu, C. Cheng, J. Avila, A. Heese, T. P. Devarenne, P. He, and L. Shan.** 2011. Direct ubiquitination of pattern recognition receptor FLS2 attenuates plant innate immunity. Science **332:**1439-1442.
119. **Lu, D., S. Wu, X. Gao, Y. Zhang, L. Shan, and P. He.** 2010. A receptor-like cytoplasmic kinase, BIK1, associates with a flagellin receptor complex to initiate plant innate immunity. Proc. Natl. Acad. Sci. USA **107:**496-501.
120. **Luo, Y., K. S. Caldwell, T. Wroblewski, M. E. Wright, and R. W. Michelmore.** 2009. Proteolysis of a negative regulator of innate immunity

is dependent on resistance genes in tomato and *Nicotiana benthamiana* and induced by multiple bacterial effectors. Plant Cell **21:**2458-2472.

121. **Macho, A. P., B. Schwessinger, V. Ntoukakis, A. Brutus, C. Segonzac, S. Roy, Y. Kadota, M. Oh, J. Sklenar, P. Derbyshire, R. Lozano-Durán, F. O. Malinovsky, J. Monaghan, F. L. Menke, S. C. Huber, S. Y. He, and C. Zipfel.** 2014. A bacterial tyrosine phosphatase inhibits plant pattern recognition receptor activation. Science **343:**1509-1512.
122. **Macho, A. P., and C. Zipfel.** 2014. Plant PRRs and the activation of innate immune signaling. Mol. Cell **54:**263-272.
123. **Macho, A. P., A. Zumaquero, J. J. Gonzalez-Plaza, I. Ortiz-Martín, J. S. Rufián, and C. R. Beuzón.** 2012. Genetic analysis of the individual contribution to virulence of the type III effector inventory of *Pseudomonas syringae* pv. *phaseolicola*. PLOS One **7:**e35871.
124. **Mackey, D., y. Belkhadir, J. M. Alonso, J. R. Ecker, and J. L. Dangl.** 2003. Arabidopsis RIN4 is a target of the type III virulence effector AvrRpt2 and modulates RPS2-mediated Resistance. Cell **112:**379-389.
125. **Mackey, D., B. F. Holt III, A. Wiig, and J. L. Dangl.** 2002. RIN4 interacts with *Pseudomonas syringae* type III effector molecules and is required for RPM1-mediated resistance in Arabidopsis. Cell **108:**743-754.
126. **Mao, G., X. Meng, Y. Liu, Z. Zheng, Z. Chen, and S. Zhang.** 2011. Phosphorylation of a WRKY transcription factor by two pathogen-responsive MAPKs drives phytoalexin biosynthesis in Arabidopsis. Plant Cell **23:**1639-1653.
127. **Mathieu, J., S. Schwizer, and G. B. Martin.** 2014. Pto kinase binds two domains of AvrPtoB and its proximity to the effector E3 ligase determines if it evades degradation and activates plant immunity. PLOS Path. **10:**e1004227.
128. **Mattei, P. J., E. Faudry, V. Job, T. Izore, I. Attree, and A. Dessen.** 2011. Membrane targeting and pore formation by the type III secretion system translocon. FEBS J. **278:**414-426.
129. **Mecey, C. P., M. Hauck, N. Trapp, A. Pumplin, J. Plovanich, J. Yao, and S. Y. He.** 2011. A critical role of *STAYGREEN*/Mendel's *I* locus in controlling disease symptom development during *Pseudomonas syringae* pv *tomato* infection of Arabidopsis. Plant Physiol. **157:**1965-1974.
130. **Melotto, M., W. Underwood, J. Koczan, K. Nomura, and S. Y. He.** 2006. Plant stomata function in innate immunity against bacterial invasion. Cell **126:**969-980.
131. **Mindrinos, M., F. Katagiri, G. Yu, and F. M. Ausubel.** 1994. The *A. thaliana* disease resistance gene *RPS2* encodes a protein containing a nucleotide-binding site and leucine-rich repeats. Cell **78:**1089-1099.
132. **Misas-Villamil, J. C., I. Kolodziejek, E. Crabill, F. Kaschani, S. Niessen, T. Shindo, M. Kaiser, J. R. Alfano, and R. A. L. van der Hoorn.** 2013. *Pseudomonas syringae* pv. *syringae* uses proteasome inhibitor syringolin A to colonize from wound infection sites. PLOS Path. **9:**e1003281.
133. **Miya, A., P. Albert, T. Shinya, Y. Desaki, K. Ichimura, K. Shirasu, Y. Narusaka, N. Kawakami, H. Kaku, and N. Shibuya.** 2007. CERK1, a

LysM receptor kinase, is essential for chitin elicitor signaling in Arabidopsis. Proc. Natl. Acad. Sci. USA **104:**19613-19618.

134. **Mohr, T. J., H. Liu, S. Yan, C. E. Morris, J. A. Castillo, J. Jelenska, and B. A. Vinatzer.** 2008. Naturally occurring nonpathogenic isolates of the plant pathogen *Pseudomonas syringae* lack a type III secretion system and effector gene orthologues. J. Bacteriol. **190:**2858-2870.
135. **Monaghan, J., S. Matschi, O. Shorinola, H. Rovenich, A. Matei, C. Segonzac, F. Gro Malinovsky, J. P. Rathjen, D. MacLean, T. Romeis, and C. Zipfel.** 2014. The calcium-dependent protein kinase CPK28 buffers plant immunity and regulates BIK1 turnover. Cell Host Microbe **16:**605-615.
136. **Mucyn, T. S., A. Clemente, V. M. Andriotis, A. L. Balmuth, G. E. Oldroyd, B. J. Staskawicz, and J. P. Rathjen.** 2006. The tomato NBARC-LRR protein Prf interacts with Pto kinase *in vivo* to regulate specific plant immunity. Plant Cell **18:**2792-2806.
137. **Mucyn, T. S., S. Yourstone, A. L. Lind, S. Biswas, M. T. Nishimura, D. A. Baltrus, J. S. Cumbie, J. H. Chang, C. D. Jones, J. L. Dangl, and S. R. Grant.** 2014. Variable suites of non-effector genes are co-regulated in the type III secretion virulence regulon across the *Pseudomonas syringae* phylogeny. PLOS Path. **10:**e1003807.
138. **Navarro, L., P. Dunoyer, F. Jay, B. Arnold, N. Dharmasiri, M. Estelle, O. Voinnet, and J. D. Jones.** 2006. A plant miRNA contributes to antibacterial resistance by repressing auxin signaling. Science **312:**436-439.
139. **Navarro, L., F. Jay, K. Nomura, S. Y. He, and O. Voinnet.** 2008. Suppression of the microRNA pathway by bacterial effector proteins. Science **321:**964-967.
140. **Nicaise, V., A. Joe, B. Jeong, C. Korneli, F. Boutrot, I. Westedt, D. Staiger, J. R. Alfano, and C. Zipfel.** 2013. *Pseudomonas* HopU1 modulates plant immune receptor levels by blocking the interaction of their mRNAs with GRP7. EMBO J. **32:**701-712.
141. **Nimchuk, Z., E. Marois, S. Kjemtrup, R. T. Leister, F. Katagiri, and J. L. Dangl.** 2000. Eukaryotic fatty acylation drives plasma membrane targeting and enhances function of several type III effector proteins from *Pseudomonas syringae*. Cell **101:**353-363.
142. **Nomura, K., S. DebRoy, Y. H. Lee, N. Pumplin, J. Jones, and S. Y. He.** 2006. A bacterial virulence protein suppresses host innate immunity to cause plant disease. Science **313:**220-223.
143. **Nomura, K., C. Mecey, Y. Lee, L. A. Imboden, J. H. Chang, and S. Y. He.** 2011. Effector-triggered immunity blocks pathogen degradation of an immunity-associated vesicle traffic regulator in Arabidopsis. Proc. Natl. Acad. Sci. USA **108:**10774-10779.
144. **Ntoukakis, V., T. S. Mucyn, S. Gimenez-Ibanez, H. C. Chapman, J. R. Gutierrez, A. L. Balmuth, A. M. Jones, and J. P. Rathjen.** 2009. Host inhibition of a bacterial virulence effector triggers immunity to infection. Science **324:**784-787.

145. **Nurnberger, T., F. Brunner, B. Kemmerling, and L. Piater.** 2004. Innate immunity in plants and animals: Striking similaritiies and obvious differences. Immunol. Rev. **198:**249-266.
146. **O'Brien, H. E., S. Thakur, and D. S. Guttman.** 2011. Evolution of plant pathogenesis in *Pseudomonas syringae*: A genomics perspective. Annu. Rev. Phytopathol. **49:**269-289.
147. **Orla-Jensen, S.** 1921. The main lines of the natural bacterial system. J. Bacteriol. **6:**263-273.
148. **Petnicki-Ocwieja, T., D. J. Schneider, V. C. Tam, S. T. Chancey, L. Shan, Y. Jamir, L. M. Schechter, C. R. Buell, X. Tang, A. Collmer, and J. R. Alfano.** 2002. Genomewide identification of proteins secreted by the Hrp type III protein secretion system of *Pseudomonas syringae* pv. *tomato* DC3000. Proc. Natl. Acad. Sci. USA **99:**7652-7657.
149. **Petnicki-Ocwieja, T., K. van Dijk, and J. R. Alfano.** 2005. The *hrpK* operon of *Pseudomonas syringae* pv. *tomato* DC3000 encodes two proteins secreted by the type III (Hrp) protein secretion system: HopB1 and HrpK, a putative type III translocator. J. Bacteriol. **187:**649-663.
150. **Pieterse, C. M., D. Van der Does, C. Zamioudis, A. Leon-Reyes, and S. C. Van Wees.** 2012. Hormonal modulation of plant immunity. Annu. Rev. Cell. Dev. Biol. **28:**489-521.
151. **Pitzschke, A., A. Djamei, F. Bitton, and H. Hirt.** 2009. A major role of the MEKK1-MKK1/2 -MPK4 pathway in ROS signalling. Mol. Plant **2:**120-137.
152. **Porter, K., M. Shimono, M. Tian, and B. Day.** 2012. Arabidopsis Actin-Depolymerizing Factor-4 links pathogen perception, defense activation and transcription to cytoskeletal dynamics. PLOS Path. **8:**e1003006.
153. **Postel, S., I. Kufner, C. Beuter, S. Mazzotta, A. Schwedt, A. Borlotti, T. Halter, B. Kemmerling, and T. Nurnberger.** 2010. The multifunctional leucine-rich repeat receptor kinase BAK1 is implicated in Arabidopsis development and immunity. Eur. J. Cell Biol. **89:**169-174.
154. **Preston, G., W. L. Deng, H. C. Huang, and A. Collmer.** 1998. Negative regulation of *hrp* genes in *Pseudomonas syringae* by HrpV. J. Bacteriol. **180:**4532-4537.
155. **Qi, D., U. Dubiella, S. H. Kim, D. I. Sloss, R. H. Dowen, J. E. Dixon, and R. W. Innes.** 2014. Recognition of the protein kinase AVRPPHB SUSCEPTIBLE1 by the disease resistance protein RESISTANCE TO PSEUDOMONAS SYRINGAE5 is dependent on s-acylation and an exposed loop in AVRPPHB SUSCEPTIBLE1. Plant Physiol. **164:**340-351.
156. **Qiu, J., L. Zhou, B. Yun, H. B. Nielsen, B. K. Fiil, K. Petersen, J. MacKinlay, G. J. Loake, J. Mundy, and P. C. Morris.** 2008. Arabidopsis mitogen-activated protein kinase kinases MKK1 and MKK2 have overlapping functions in defense signaling mediated by MEKK1, MPK4, and MKS1. Plant Physiol. **148:**212-222.
157. **Ranf, S., L. Eschen-Lippold, P. Pecher, J. Lee, and D. Scheel.** 2011. Interplay between calcium signalling and early signalling elements during

defence responses to microbe- or damage-associated molecular patterns. Plant J. **68:**100-113.

158. **Robatzek, S., D. Chinchilla, and T. Boller.** 2006. Ligand-induced endocytosis of the pattern recognition receptor FLS2 in Arabidopsis. Genes Dev. **20:**537-542.
159. **Robert-Seilaniantz, A., L. Shan, J.-M. Zhou, and X. Tang.** 2006. The *Pseudomonas syringae* pv. *tomato* DC3000 type III effector HopF2 has a putative myristoylation site required for its avirulence and virulence functions. Mol. Plant Microbe Interact. **19:**130-138.
160. **Rodríguez-Herva, J. J., P. González-Melendi, R. Cuartas-Lanza, M. Antúnez-Lamas, I. Río-Alvarez, Z. Li, G. López-Torrejón, I. Díaz, J. C. del Pozo, S. Chakravarthy, A. Collmer, P. Rodríguez-Palenzuela, and E. López-Solanilla.** 2012. A bacterial cysteine protease effector protein interferes with photosynthesis to suppress plant innate immune responses. Cell. Microbiol. **14:**669-681.
161. **Rosebrock, T. R., L. Zeng, J. J. Brady, R. B. Abramovitch, F. Xiao, and G. B. Martin.** 2007. A bacterial E3 ubiquitin ligase targets a host protein kinase to disrupt plant immunity. Nature **448:**370-374.
162. **Roux, M., B. Schwessinger, C. Albrecht, D. Chinchilla, A. Jones, N. Holton, F. G. Malinovsky, M. Tor, S. de Vries, and C. Zipfel.** 2011. The Arabidopsis leucine-rich repeat receptor-like kinases BAK1/SERK3 and BKK1/SERK4 are required for innate immunity to hemibiotrophic and biotrophic pathogens. Plant Cell **23:**2440-2455.
163. **Ryu, H., K. Kim, H. Cho, J. Park, S. Choe, and I. Hwang.** 2007. Nucleocytoplasmic shuttling of BZR1 mediated by phosphorylation is essential in Arabidopsis brassinosteroid signaling. Plant Cell **19:**2749-2762.
164. **Sarris, P. F., S. Gao, K. Karademiris, H. Jin, K. Kalantidis, and N. J. Panopoulos.** 2011. Phytobacterial type III effectors HopX1, HopAB1 and HopF2 enhance sense-post-transcriptional gene silencing independently of plant *R* gene-effector recognition. Mol. Plant Microbe Interact. **24:**907-917.
165. **Schechter, L. M., M. Vencato, K. L. Jordan, S. E. Schneider, D. J. Schneider, and A. Collmer.** 2006. Multiple approaches to a complete inventory of *Pseudomonas syringae* pv. *tomato* DC3000 type III secretion system effector proteins. Mol. Plant Microbe Interact. **19:**1180-1192.
166. **Schelbert Hofstetter, S., A. Dudnik, H. Widmer, and R. Dudler.** 2013. Arabidopsis YELLOW STRIPE LIKE7 and 8 transporters mediate uptake of *Pseudomonas* virulence factor syringolin A into plant cells. Mol. Plant Microbe Interact. **26:**1302-1311.
167. **Schellenberg, B., C. Ramel, and R. Dudler.** 2010. *Pseudomonas syringae* virulence factor syringolin A counteracts stomatal immunity by proteasome inhibition. Mol. Plant Microbe Interact. **23:**1287-1293.
168. **Shan, L., P. He, J. Li, A. Heese, S. C. Peck, T. Nümberger, G. B. Martin, and J. Sheen.** 2008. Bacterial effectors target the common signaling

partner BAK1 to disrupt multiple MAMP receptor-signaling complexes and impede plant immunity. Cell Host Microbe **4:**17-27.

169. **Shan, L., V. K. Thara, G. B. Martin, J. Zhou, and X. Tang.** 2000. The *Pseudomonas* AvrPto protein is differentially recognized by tomato and tobacco and is localized to the plant plasma membrane. Plant Cell **12:**2323-2338.
170. **Shao, F., C. Golstein, J. Ade, M. Stoutemyer, J. E. Dixon, and R. W. Innes.** 2003. Cleavage of Arabidopsis PBS1 by a bacterial type III effector. Science **301:**1230-1233.
171. **Sohn, K. H., S. B. Saucet, C. R. Clarke, B. A. Vinatzer, H. E. O'Brien, D. S. Guttman, and J. D. G. Jones.** 2012. HopAS1 recognition significantly contributes to Arabidopsis nonhost resistance to *Pseudomonas syringae* pathogens. New Phytol. **193:**58-66.
172. **Tena, G., M. Boudsocq, and J. Sheen.** 2011. Protein kinase signaling networks in plant innate immunity. Curr. Opin. Plant Biol. **14:**519-529.
173. **Torres, M. A., J. D. G. Jones, and J. L. Dangl.** 2006. Reactive oxygen species signaling in response to pathogens. Plant Physiol. **141:**373-378.
174. **Üstün, S., P. König, D. S. Guttman, and F. Börnke.** 2014. HopZ4 from *Pseudomonas syringae*, a member of the HopZ type III effector family from the YopJ superfamily, inhibits the proteasome in plants. Mol. Plant Microbe Interact. **27:**611-623.
175. **Van der Hoorn, R. A. L., and S. Kamoun.** 2008. From guard to decoy: A new model for perception of plant pathogen effectors. Plant Cell **20:**2009-2017.
176. **Voigt, C. A.** 2014. Callose-mediated resistance to pathogenic intruders in plant defense-related papillae. Front. Plant Sci. **5:**168.
177. **Wan, J., X. Zhang, D. Neece, K. M. Ramonell, S. Clough, S. Kim, M. G. Stacey, and G. Stacey.** 2008. A LysM receptor-like kinase plays a critical role in chitin signaling and fungal resistance in Arabidopsis. Plant Cell **20:**471-481.
178. **Wang, L., K. Tsuda, M. Sato, J. D. Cohen, F. Katagiri, and J. Glazebrook.** 2009. Arabidopsis CaM binding protein CBP60g contributes to MAMP-induced SA accumulation and is involved in disease resistance against *Pseudomonas syringae*. PLOS Path. **5:**e1000301.
179. **Wang, Y., J. Li, S. Hou, X. Wang, Y. Li, D. Ren, S. Chen, X. Tang, and J. M. Zhou.** 2010. A *Pseudomonas syringae* ADP-ribosyltransferase inhibits Arabidopsis MAP kinase kinases. Plant Cell **22:**2033-2044.
180. **Wei, C. F., W. L. Deng, and H. C. Huang.** 2005. A chaperone-like HrpG protein acts as a suppressor of HrpV in regulation of the *Pseudomonas syringae* pv. *syringae* type III secretion system. Mol. Microbiol. **57:**520-536.
181. **Willmann, R., H. M. Lajunen, G. Erbs, M. Newman, D. Kolb, K. Tsuda, F. Katagiri, J. Fliegmann, J. Bono, and J. V. Cullimore.** 2011. Arabidopsis lysin-motif proteins LYM1 LYM3 CERK1 mediate bacterial peptidoglycan sensing and immunity to bacterial infection. Proc. Natl. Acad. Sci. USA **108:**19824-19829.

182. **Wilton, M., R. Subramaniam, J. Elmore, C. Felsensteiner, G. Coaker, and D. Desveaux.** 2010. The type III effector HopF2Pto targets Arabidopsis RIN4 protein to promote *Pseudomonas syringae* virulence. Proc. Natl. Acad. Sci. USA **107:**2349-2354.
183. **Winslow, C. E., J. Broadhurst, R. E. Buchanan, C. Krumwiede, L. A. Rogers, and S. G. H.** 1917. The families and genera of the Bacteria: Preliminary report of the committee of the Society of American Bacteriologists on characterization and classification of bacterial types. J. Bacteriol. **2:**505-566.
184. **Wu, S., D. Lu, M. Kabbage, H. Wei, B. Swingle, A. R. Records, M. Dickman, P. He, and L. Shan.** 2011. Bacterial effector HopF2 suppresses Arabidopsis innate immunity at the plasma membrane. Mol. Plant Microbe Interact. **24:**585-593.
185. **Wu, S., L. Shan, and P. He.** 2014. Microbial signature-triggered plant defense responses and early signaling mechanism. Plant Sci. **228:**118-126.
186. **Wu, Y., D. Zhang, J. Y. Chu, P. Boyle, Y. Wang, I. D. Brindle, V. De Luca, and C. Despres.** 2012. The Arabidopsis NPR1 protein is a receptor for the plant defense hormone salicylic acid. Cell Reports **1:**639-647.
187. **Xiang, T., N. Zong, J. Zhang, J. Chen, M. Chen, and J. Zhou.** 2011. BAK1 is not a target of the *Pseudomonas syringae* effector AvrPto. Mol. Plant Microbe Interact. **24:**100-107.
188. **Xiang, T., N. Zong, Y. Zou, Y. Wu, J. Zhang, W. Xing, Y. Li, X. Tang, L. Zhu, J. Chai, and J. Zhou.** 2008. *Pseudomonas syringae* effector AvrPto blocks innate immunity by targeting receptor kinases. Curr. Biol. **18:**1-7.
189. **Xiao, Y., S. Heu, J. Yi, Y. Lu, and S. W. Hutcheson.** 1994. Identification of a putative alternate sigma factor and characterization of a multicomponent regulatory cascade controlling the expression of *Pseudomonas syringae* pv. *syringae Pss*61 *hrp* and *hrmA* Genes. J. Bacteriol. **176:**1025-1036.
190. **Xin, X., and S. Y. He.** 2013. *Pseudomonas syringae* pv. *tomato* DC3000: A model pathogen for probing disease susceptibility and hormone signaling in pants. Annu. Rev. Phytopathol. **51:**473-498.
191. **Yuan, J., and S. Y. He.** 1996. The *Pseudomonas syringae* hrp regulation and secretion system controls the production and secretion of multiple extracellular proteins. J. Bacteriol. **178:**6399-6402.
192. **Zhang, J., W. Li, T. Xiang, Z. Liu, K. Laluk, X. Ding, Y. Zou, M. Gao, X. Zhang, S. Chen, T. Mengiste, Y. Zhang, and J. Zhou.** 2010. Receptor-like cytoplasmic kinases integrate signaling from multiple plant immune receptors and are targeted by a *Pseudomonas syringae* effector. Cell Host Microbe **7:**290-301.
193. **Zhang, J., F. Shao, Y. Li, H. Cui, L. Chen, H. Li, Y. Zou, C. Long, L. Lan, J. Chai, S. Chen, X. Tang, and J. Zhou.** 2007. A *Pseudomonas syringae* effector inactivates MAPKs to suppress PAMP-induced immunity in plants. Cell Host Microbe **1:**175-185.

194. **Zhang, Y., S. Xu, P. Ding, D. Wang, Y. T. Cheng, J. He, M. Gao, F. Xu, Y. Li, Z. Zhu, X. Li, and Y. Zhang.** 2010. Control of salicylic acid synthesis and systemic acquired resistance by two members of a plant-specific family of transcription factors. Proc. Natl. Acad. Sci. USA **107:**18220-18225.
195. **Zhang, Z., Y. Wu, M. Gao, J. Zhang, Q. Kong, Y. Liu, H. Ba, J. Zhou, and Y. Zhang.** 2012. Disruption of PAMP-induced MAP kinase cascade by a *Pseudomonas syringae* effector activates plant immunity mediated by the NB-LRR protein SUMM2. Cell Host Microbe **11:**253-263.
196. **Zhou, H., J. Lin, A. Johnson, R. L. Morgan, W. Zhong, and W. Ma.** 2011. *Pseudomonas syringae* type III effector HopZ1 targets a host enzyme to suppress isoflavone biosynthesis and promote infection in soybean. Cell Host Microbe **9:**177-186.
197. **Zhou, H., R. Morgan, D. S. Guttman, and W. Ma.** 2009. Allelic variants of the *Pseudomonas syringae* type III effector HopZ1 are differentially recognized by plant resistance systems. Mol. Plant Microbe Interact. **22:**176-189.
198. **Zhou, J., S. Wu, X. Chen, C. Liu, J. Sheen, L. Shan, and P. He.** 2014. The *Pseudomonas syringae* effector HopF2 suppresses Arabidopsis immunity by targeting BAK1. Plant J. **77:**235-245.
199. **Zipfel, C., G. Kunze, D. Chinchilla, A. Caniard, J. D. Jones, T. Boller, and G. Felix.** 2006. Perception of the bacterial PAMP EF-Tu by the receptor EFR restricts *Agrobacterium*-mediated transformation. Cell **125:**749-760.
200. **Zipfel, C., S. Robatzek, L. Navarro, E. J. Oakeley, J. D. G. Jones, G. Felix, and T. Boller.** 2004. Bacterial disease resistance in Arabidopsis through flagellin perception. Nature **428:**764-767.

CHAPTER 2

The *Pseudomonas syringae* type III effector HopD1 suppresses effector-triggered immunity, localizes to the endoplasmic reticulum, and targets the Arabidopsis transcription factor NTL9

ABSTRACT

Pseudomonas syringae type III effectors are known to suppress plant immunity to promote bacterial virulence. However, the activities and targets of these effectors are not well understood. We used genetic, molecular, and cell biology methods to characterize the activities, localization, and target of the HopD1 type III effector in Arabidopsis. HopD1 contributes to *P. syringae* virulence in Arabidopsis and reduces effector-triggered immunity (ETI) responses but not pathogen-associated molecular pattern-triggered immunity (PTI) responses. Plants expressing HopD1 supported increased growth of ETI-inducing *P. syringae* strains compared with wild-type Arabidopsis. We show that HopD1 interacts with the membrane-tethered Arabidopsis transcription factor NTL9 and demonstrate that this interaction occurs at the endoplasmic reticulum (ER). A *P. syringae hopD1* mutant and ETI-inducing *P. syringae* strains exhibited enhanced growth on Arabidopsis *ntl9* mutant plants. Conversely, growth of *P. syringae* strains was reduced in plants expressing a constitutively active NTL9 derivative, indicating that NTL9 is a positive regulator of plant immunity. Furthermore, HopD1 inhibited the induction of NTL9-regulated genes during ETI but not PTI. HopD1 contributes to *P. syringae* virulence in part by targeting NTL9, resulting in the suppression of ETI responses but not PTI responses and the promotion of plant pathogenicity.

Author Contributions

Anna Block[1,2*], Tania Y. Toruño[1,2*], Christian G. Elowsky[3], Chi Zhang[1,4], Jens Steinbrenner[5], Jim Beynon[5] and James R. Alfano[1,2] contributed to a paper published in New Phytologist (2013, 201:1358-1370). This paper represents Chapter 2 of this thesis.

[1]Center for Plant Science Innovation, University of Nebraska, Lincoln, NE 68588-0660, USA; [2]Department of Plant Pathology, University of Nebraska, Lincoln, NE 68588-0722, USA; [3]Center for Biotechnology, University of Nebraska, Lincoln, NE 68588-0665, USA; [4]School of Biological Sciences, University of Nebraska, Lincoln, NE, 68588-0118, USA; [5]School of Life Sciences, University of Warwick, Coventry CV4 7AL, UK.

*These authors contributed equally to this work. Tania Toruño specifically performed the experiments for figures 2A-C, 4A, and supplemental figures 2, 5 and 6. Anna Block and Tania Toruño contributed to figures 1A, 6A-B, 7A and supplemental table 1.

Introduction

The Gram-negative bacterial pathogen *Pseudomonas syringae* pv. *tomato* DC3000 is the causative agent of bacterial speck disease on tomato and pathogenic on the model plant *Arabidopsis thaliana*. One of its primary virulence factors is its ability to inject type III effector (T3E) proteins into host cells using a type III protein secretion system. Once injected, T3Es target and disrupt various host processes in order to suppress plant immunity (5, 10, 13).

Plant innate immunity can be broadly separated into two branches based on how microorganism recognition is achieved. The first of these branches involves the recognition of pathogen-associated molecular patterns (PAMPs) by extracellular pattern recognition receptors (PRRs; 23). This recognition induces multiple responses, including signaling cascades involving mitogen-activated protein kinases and calcium-dependent protein kinases. These signaling events lead to a rapid burst of reactive oxygen species (ROS) production and gene expression changes (32). Later responses include cell wall modifications such as the deposition of callose. The combined response arising from this recognition event is termed PAMP-triggered immunity (PTI; 23, 32).

Pseudomonas syringae can use several of its injected T3Es to suppress PTI and achieve high growth rates within its host plants. To combat PTI suppression by T3Es and other pathogen effectors, plants evolved a second layer of immunity based on the recognition of effectors or their activities by plant immune receptors, know as resistance (R) proteins. The response from this recognition event is termed effector-triggered immunity (ETI) and induces many

of the same responses as PTI but often with different timing and amplitude (46). ETI is usually associated with a form of programmed cell death known as the hypersensitive response (HR). Thus, in order to maintain its pathogen status, *P. syringae* probably adapted/evolved T3Es to suppress PTI and/or ETI.

If a *P. syringae* strain lacks the ability to successfully suppress ETI, bacterial growth is restricted. This is classically referred to as an incompatible interaction between an avirulent strain and a resistant plant (25). If the *P. syringae* strain can suppress PTI and ETI, or does not elicit ETI but suppresses PTI, it can be pathogenic and achieve high growth rates in plant tissue. This is classically referred to as a compatible interaction between a virulent strain and susceptible plant. Many *P. syringae* T3Es have been shown to suppress PTI responses and several suppress both PTI and ETI (7, 15, 13). However, it is less clear whether *P. syringae* T3Es have evolved to suppress ETI, but not PTI.

In a previous study we screened DC3000 T3Es for their ability to suppress ETI responses induced by the T3E HopA1 in *Nicotiana tabacum* (22, 18). One of the strong ETI suppressors identified in this screen was HopD1. HopD1 is a homolog of AvrPphD from *P. syringae* pv. *phaseolicola* race 4 strain 1302A (52). A *P. syringae* pv. *phaseolicola avrPphD* mutant showed no difference in growth in either resistant or susceptible pea cultivars, indicating that its immune suppression/induction functions are probably redundant with other T3Es in this pathogen (2). Bacterial mutants lacking HopD1 homologs have differing effects on the virulence of other bacterial pathogens (17, 41). Therefore, depending on the pathogen and its likely redundancy with other T3Es, loss of *hopD1* can

reduce the virulence of a pathogen.

HopD1 has no known mechanism of action or homology to proteins with a known enzymatic function. A recent study used a high-throughput yeast two-hybrid screen to define the interactomes of *P. syringae* T3Es and the effectors from the oomycete pathogen *Hyaloperonospora arabidopsidis* with Arabidopsis proteins (33). One potential interaction identified in this screen was that of HopD1 and the Arabidopsis NTL9 (At4g35580) protein (33). NTL9 belongs to the NAC with Transmembrane Motif 1 (NTM1)-like family of transcription factors that are tethered to intracellular membranes (29). NAC transcription factors play a wide variety of roles in developmental and stress-related signaling and can also be involved in regulating cross-talk between different stresses (38).

Here we show that HopD1 is an important DC3000 virulence factor. We show that it is a strong ETI suppressor in Arabidopsis but does not significantly suppress PTI responses. Additionally, we confirm that HopD1 interacts with NTL9 and that both HopD1 and NTL9 localize to the plant endoplasmic reticulum (ER). NTL9 is important for the Arabidopsis ETI response as *ntl9* knockout plants allow for increased growth of ETI-inducing *P. syringae* strains and rescue the growth of a DC3000 *hopD1* mutant. In addition, plants expressing constitutively active *NTL9* are more resistant to virulent and ETI-inducing *P. syringae* strains, further indicating that NTL9 is a positive regulator of plant immunity. We identify several genes whose expression is induced by active NTL9 and show that HopD1 suppresses the induction of these genes during ETI but not PTI. These data indicate that HopD1 functions as a specific suppressor of ETI, in part by

inhibiting NTL9-mediated gene expression.

Results

HopD1 contributes to *P. syringae* virulence and enhances the growth of ETI-inducing *P. syringae* strains. To determine the extent of HopD1's involvement in *P. syringae* virulence, we measured the *in planta* growth of a *P. syringae* pv. *tomato* DC3000 *hopD1* mutant (UNL104; 22) in wild-type Arabidopsis (Col-0; Fig. 1A). Bacterial growth assays showed a slight but significant reduction in the growth of the *hopD1* mutant in Arabidopsis when compared with wild-type DC3000. Wild-type growth rates were restored when *hopD1* was reintroduced into the *hopD1* mutant using a T7 expression system such that *hopD1* was expressed in single copy from a type III promoter (Fig. 1A). These data show that HopD1 is required for the full virulence of *P. syringae* on Arabidopsis.

Next we examined the ability of HopD1 to promote bacterial growth *in planta* using transgenic Arabidopsis constitutively expressing HopD1 fused to a C-terminal HA tag (HopD1-HA). These plants displayed no obvious phenotypes and we confirmed that they produced HopD1-HA (Fig. S1). Wild-type Arabidopsis and HopD1-HA expressing Arabidopsis plants were syringe inoculated with wild-type DC3000, the DC3000 *hrcC* mutant defective in type III secretion, or DC3000 strains carrying plasmids expressing the T3E genes *avrRpm1* or *avrRpt2*, which encode ETI-inducing T3Es, rendering these strains avirulent. Growth of these strains was determined at 0 and 3 d postinoculation (Fig. 1B). *In planta*

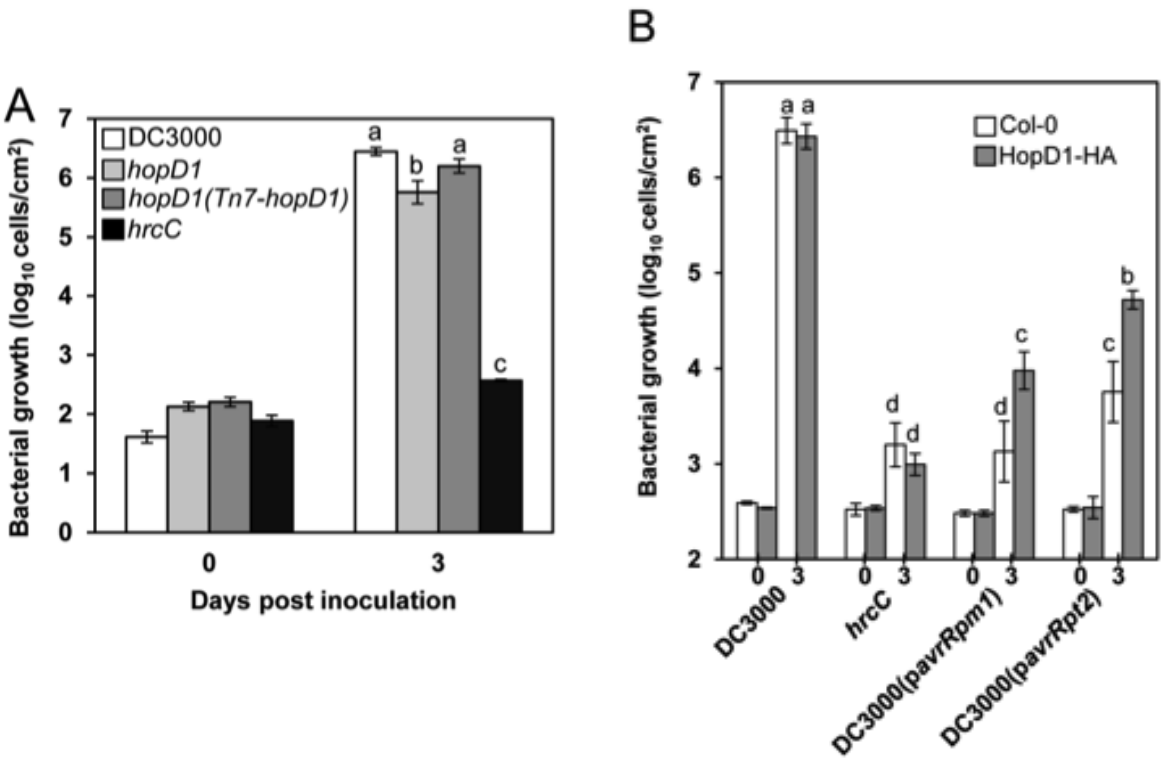

Fig. 1. HopD1 contributes to the virulence of DC3000. (a) Wild-type Arabidopsis (Col-0) plants were syringe-inoculated with 2 x 10^5 cells ml^{-1} of wild type *Pseudomonas syringae* (DC3000), the DC3000 *hopD1* mutant or the *hopD1* mutant complemented with *hopD1-flag* using the Tn7 expression system. The type III secretion defective *hrcC* mutant was included as a nonpathogenic control. Bacterial growth was determined at 0 and 3 d postinoculation (letters are significantly different, P ≤0.05). (b) Wild-type Arabidopsis (Col-0) and transgenic Arabidopsis constitutively expressing HopD1-HA were syringe-inoculated with 2 x 10^5 cells ml^{-1} of DC3000, DC3000 carrying a plasmid constitutively expressing the *avr* genes *avrRpm1* or *avrRpt2*, or the DC3000 *hrcC* mutant. Bacterial growth was measured at 0 and 3 d postinoculation (different letters indicate the values are significantly different; P ≤0.05). (a, b) Error bars, ±SE.

expression of HopD1-HA led to significantly increased growth of the two ETI-inducing avirulent strains but had no effect on the growth of wild-type DC3000 or the nonpathogenic *hrcC* mutant (Fig. 1B). These data show that HopD1 is a strong suppressor of ETI in Arabidopsis. The lack of an effect of HopD1 on the growth of the *hrcC* mutant, which cannot inject T3Es but carries PAMPs that induce PTI, suggests that HopD1 is unable to significantly suppress PTI.

Bacterially delivered HopD1 can suppress AvrRpm1-induced ETI in Arabidopsis. The increased growth of avirulent *P. syringae* strains on Arabidopsis expressing HopD1-HA indicates that HopD1 can suppress ETI induced by AvrRpm1 and AvrRpt2 in Arabidopsis. To further characterize the ability of HopD1 to suppress ETI, we used a nonpathogenic *Pf* strain carrying pLN1965, which encodes a functional *P. syringae* type III secretion system (18), and two additional plasmids expressing HopD1-FLAG and AvrRpm1. This allows the effect of HopD1 on ETI to be determined in the absence of other T3Es that may be redundant to HopD1.

To test the ability of HopD1 to suppress ETI, *Pf*(pLN1965 + p*avrRpm1*) carrying either a vector control or a plasmid constitutively expressing *hopD1-flag* were syringe-infiltrated into wild-type Arabidopsis leaves. The coexpression of *hopD1-flag* with *avrRpm1* suppressed the macroscopic HR (Fig. 2A). AvrRpm1-induced ion leakage was also measured in wild-type Col-0 infiltrated with these strains. Bacterial delivery of HopD1-FLAG suppressed ion leakage, which is correlated with cell death, to such an extent that it resembled that of leaves infiltrated with *Pf* lacking the ETI inducer AvrRpm1 (Fig. 2B). Furthermore, the

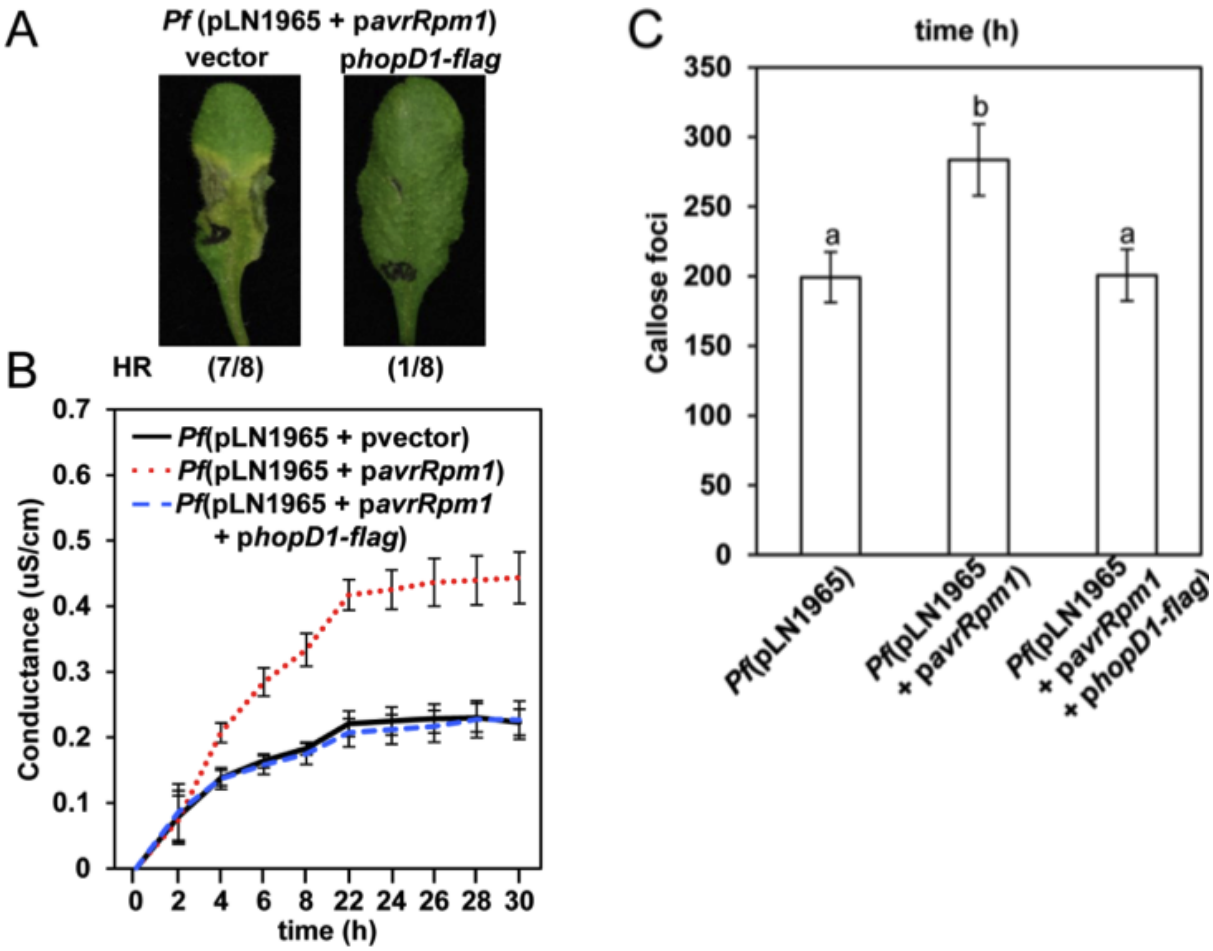

Fig. 2. HopD1 suppresses effector-triggered immunity (ETI) in Arabidopsis. Wild-type Arabidopsis (Col-0) plants were syringe-inoculated with 1 x 10^8 cells ml^{-1} of *Pseudomonas fluorescens* (*Pf*)(pLN1965), which encodes a functional type III secret ion system, and a construct carrying *avrRpm1* (*Pf*(pLN1965 + p*avrRpm1*)), carrying a vector control (*Pf*(pLN1965 + pvector)), or carrying *avrRpm1* and a plasmid constitutively expressing *hopD1-flag* (*Pf*(pLN1965 + p*avrRpm1* + p*hopD1-flag*)). (a) The hypersensitive response (HR) was scored in eight leaves per treatment at 48 h postinoculation. (b) Ion leakage was measured in leaf disks over time to quantify cell death. (c) Wild-type Arabidopsis (Col-0) leaves were syringe-inoculated with 1 x 10^6 cells ml^{-1} of *Pf*(pLN1965) or *Pf*(pLN1965) carrying *avrRpm1* with or without a plasmid constitutively expressing *hopD1-flag* and the number of callose foci were determined at 16 h postinoculation (different letters indicate that values are significantly different; P ≤0.05). Each assay was repeated at least twice with similar results. (b, c) Error bars, ±SE.

ETI-induced deposition of callose in the plant cell wall of wild-type Arabidopsis leaves infiltrated with *Pf*(pLN1965 + p*avrRpm1* + p*hopD1-flag*) was significantly lower than that in leaves infiltrated with *Pf*(pLN1965 + p*avrRpm1*; Fig. 2C). These data show that HopD1 can suppress ETI-induced HR and callose deposition.

To confirm that the HR and ion leakage suppression by HopD1 was the result of suppression of ETI, we included an Arabidopsis *rpm1* knockout line that cannot recognize AvrRpm1 and, therefore, does not exhibit AvrRpm1-induced ETI responses. Using this Arabidopsis *rpm1* mutant, there was no induction of an HR by either *Pf*(pLN1965 + p*avrRpm1*) or *Pf*(pLN1965 + p*avrRpm1* + *phopD1-flag*) and there was no difference in ion leakage (Fig. S2). Collectively, these data confirm that HopD1 can suppress AvrRpm1-induced ETI responses in Arabidopsis.

HopD1 does not suppress PAMP-induced oxidative burst or callose deposition in Arabidopsis. To determine if HopD1 could suppress PTI, we evaluated its ability to inhibit the oxidative burst that occurs within minutes of PAMP recognition (34). To do this, we measured the production of ROS in wild-type and HopD1- HA-expressing Arabidopsis after treatment with the PTI inducers flg22, elf18, and chitin. Flg22 is a 22-amino-acid peptide of the PAMP flagellin that is recognized by the plant receptor FLS2 and elf18 is an 18-amino-acid peptide of the PAMP EF-Tu that is recognized by the receptor EFR. The PAMP chitin is recognized by the receptor CERK1 (32). No difference was observed in PAMP-induced ROS production between wild-type and HopD1-HA-expressing Arabidopsis, indicating that HopD1 cannot suppress this early PTI

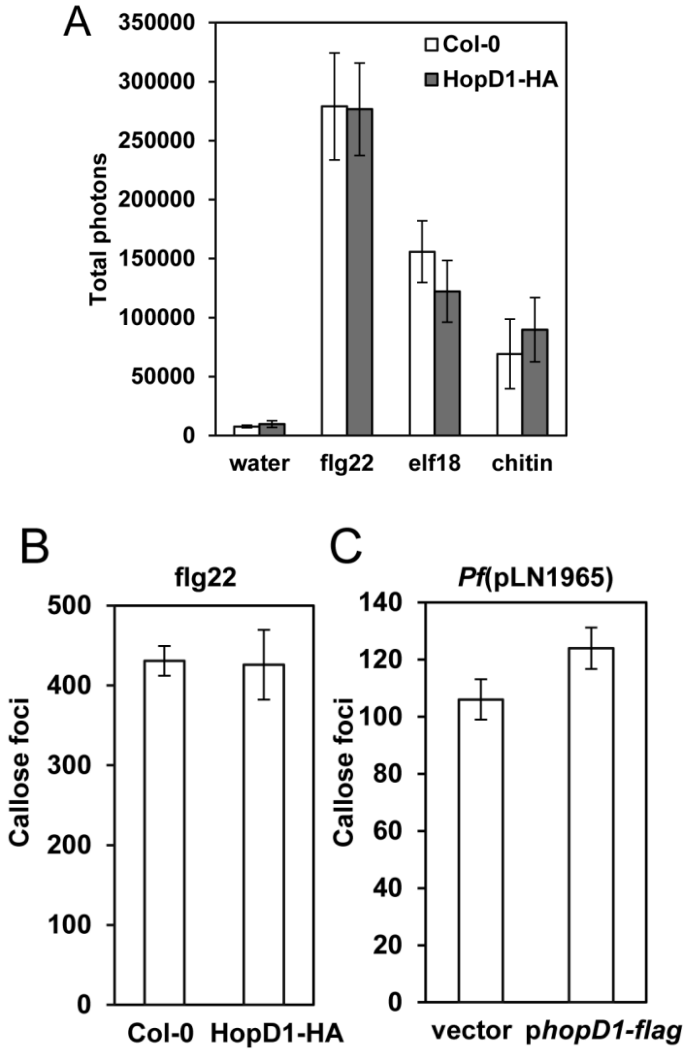

Fig. 3. HopD1 has no significant impact on pathogen-associated molecular pattern (PAMP)-induced reactive oxygen species (ROS) production or callose deposition in Arabidopsis. (a) Leaf disks were taken from wild-type Arabidopsis (Col-0; open bars) and transgenic Arabidopsis constitutively expressing HopD1-HA (closed bars) and were treated with water or the PAMPs flg22, elf18, or chitin. ROS production was measured for 30 min after treatment by quantifying luminescence of the luminol derivative L-012. (b) Callose deposition was determined in wild-type and HopD1-HA-expressing Arabidopsis in response to flg22 treatment. (c) Callose deposition was determined in wild-type Arabidopsis (Col-0) syringe-inoculated with *Pf*(pLN1965) containing either a vector control or a plasmid constitutively expressing *hopD1-flag*. Bacterial delivery of HopD1-FLAG had no effect on the production of callose in response to *Pseudomonas fluorescens* (*Pf*)(pLN1965) treatment. Each experiment was repeated at least twice with similar results and ±SE is indicated.

response (Fig. 3A).

If HopD1 targets an intermediate stage in PTI signaling, it may suppress later PTI responses without altering ROS production. Therefore, we measured the ability of HopD1 to suppress PAMP-induced callose deposition, a late PTI response (36), in wild-type and HopD1-HA expressing Arabidopsis plants treated with flg22. No difference in flg22-induced callose deposition was observed between wild-type Arabidopsis and Arabidopsis expressing HopD1-HA (Fig. 3B). To confirm this lack of PTI suppression, we measured the extent that bacterially delivered HopD1 could suppress PAMP induced callose deposition in response to recognition of *Pf* PAMPs. To do this, wild-type Arabidopsis was infiltrated with *Pf*(pLN1965) carrying a vector control or a plasmid constitutively expressing *hopD1-flag*. No difference in PAMP-induced callose deposition as a result of the bacterial delivery of HopD1 was observed (Fig. 3C). These data suggest that while HopD1 is a strong suppressor of ETI, it has no detectable effect on these PTI responses. Therefore, it is likely that HopD1 suppresses ETI-specific components of plant immunity.

HopD1 interacts with the membrane-tethered Arabidopsis transcription factor NTL9. A high-throughput yeast-two-hybrid screen that defined the *P. syringae* effector interactome with Arabidopsis proteins identified the Arabidopsis membrane tethered NAC transcription factor NTL9 as a possible interactor for HopD1 (33). Three splice variants have been identified for *NTL9* owing to differential splicing of its fourth intron. Splice variant 1 is the only one with a C terminal transmembrane domain. RT-PCR analyses with primers flanking the

fourth intron of *NTL9* were used to differentiate between splice variant 1 and splice variants 2 and 3 during biotic stress. We performed RT-PCR using these primers with RNA isolated from untreated Arabidopsis and Arabidopsis treated with *Pf*(pLN1965 + p*avrRpm1*) or *Pf*(pLN1965 + p*avrRpm1* + p*hopD1-flag*). In all treatments, splice variant 1 was the only form observed, indicating that it is the dominant form of this gene in these conditions (Fig. S3).

As the interaction between NTL9 and HopD1 was identified using a yeast two-hybrid screen, we first confirmed this interaction by cloning *hopD1* and *NTL9* into yeast two-hybrid system vectors. Yeast strains expressing both *hopD1* and *NTL9* grew on selective media while *hopD1* and *NTL9* with their respective empty vector controls did not, confirming the interaction between HopD1 and NTL9 in yeast (Fig. 4A).

The interaction of two proteins in yeast does not necessarily translate into an interaction *in planta*. To confirm their interaction *in planta*, BiFC was performed. *Nicotiana benthamiana* was co-agroinfiltrated with NTL9 fused at its N-terminus to the N-terminal half of YFP and HopD1 fused at its C-terminus to the C-terminal half of YFP. Infiltrated leaves were examined with confocal microscopy and yellow fluorescence was observed in cells of the infiltrated leaves (Fig. 4B), indicating that these proteins interacted *in planta*. The reciprocal experiment with HopD1 fused at its C-terminus to the N-terminal half of YFP and NTL9 fused at its N-terminus to the C-terminal half of YFP also produced yellow fluorescence (Fig 4B). No yellow fluorescence was observed in leaves infiltrated with BiFC HopD1 or NTL9 constructs and their corresponding nYFP or cYFP

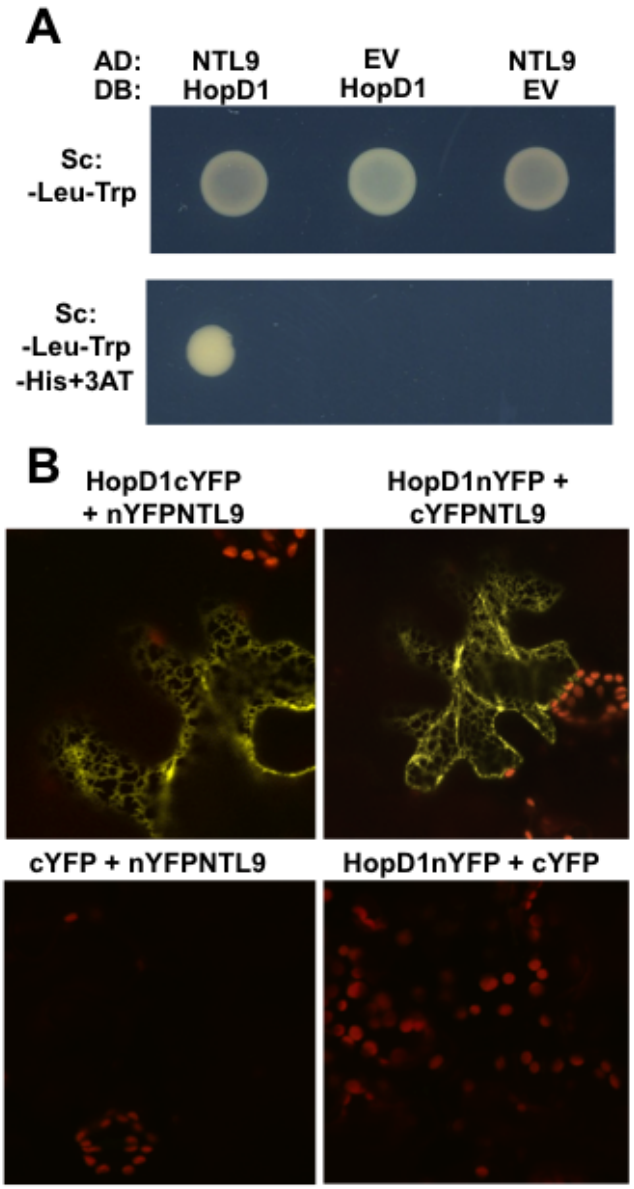

Fig. 4. HopD1 interacts with the membrane-tethered Arabidopsis transcription factor NTL9. (a) Yeast-two-hybrid analyses of HopD1 and NTL9 show growth on selective media (Sc:-Leu-Trp-His + 1mM 3AT) when both HopD1 and NTL9 are present. (b) Bimolecular fluorescence complementation (BiFC) analysis of HopD1 and NTL9 interactions in *Nicotiana benthamiana* cells. HopD1-cYFP and nYFP-NTL9 and HopD1-nYFP and cYFP-NTL9 were expressed in *N. benthamiana* using *Agrobacterium*-mediated transient expression. Yellow fluorescence indicates that yellow fluorescent protein (YFP) moieties are in close proximity to each other. Red fluorescence represents Chl autofluorescence. No YFP fluorescence was seen in coinfiltration experiments of *hopD1* and *NTL9* BiFC constructs with the respective cYFP control.

controls (Fig 4B). These data indicate that HopD1 interacts with NTL9 *in planta*.

HopD1 and NTL9 localize to the plant endoplasmic reticulum. The reticulate pattern in the cytoplasm accompanied by a distinct ring around the nucleus observed in the BiFC experiments involving HopD1 and NTL9 is characteristic of ER-localized proteins. To investigate whether HopD1 and/or NTL9 localized to the plant ER, we performed colocalization experiments with a known ER marker. DNA encoding the ER-localized RFP marker CD3-960 (35) was agroinfiltrated into *N. benthamiana* with DNA encoding either HopD1 fused at its C-terminus to GFP or NTL9 fused at its N-terminus to GFP, both under the control of a constitutive CaMV 35S promoter. Confocal microscopy revealed colocalization of HopD1-GFP with ER-RFP (Fig. 5A) and GFP-NTL9 with ER-RFP (Fig. 5B). These data indicate that both HopD1 and NTL9 are localized to the ER in *N. benthamiana*. The most likely orientation for NTL9 is with its C-terminal transmembrane domain inserted in the ER membrane with a minor portion of NTL9 in the ER lumen and the majority of the protein in the cytoplasm. Membrane-tethered transcription factors are held in a ready state in the membrane and upon activation are cleaved at the cytoplasmic side of the transmembrane domain, releasing an active transcription factor that can enter the nucleus and regulate transcription (29). The protease that performs this cleavage for NTL9 has not been identified. The localization of HopD1 and NTL9 to the ER and their interaction at this site as indicated in BiFC experiments suggests that HopD1 is targeting NTL9 while it is anchored in the ER membrane.

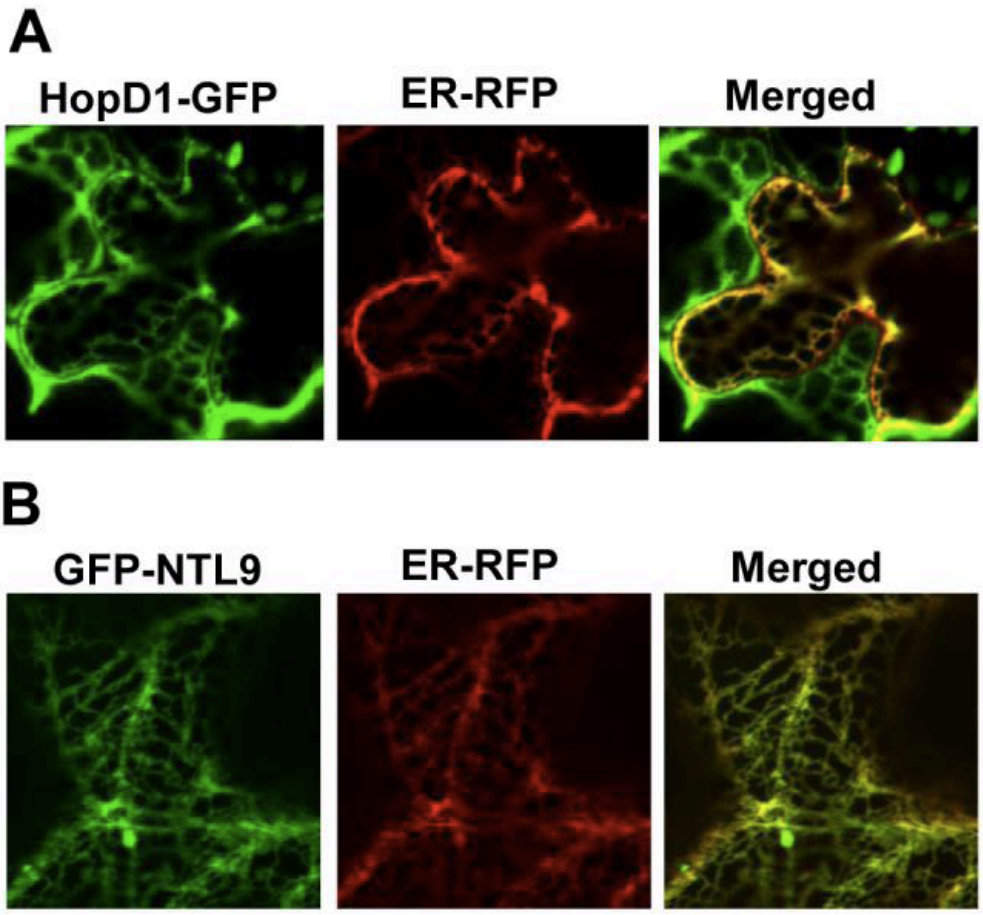

Fig. 5. HopD1 and NTL9 localize to the plant endoplasmic reticulum (ER). (a) *Agrobacterium*-mediated transient expression of a C-terminal fusion of HopD1 to green fluorescent protein (GFP) (green) (HopD1-GFP) and an ER-localized mCherry (red) fused at its N-terminus with the signal peptide from AtWAK2 and at its C-terminus with the ER retention signal (ER-RFP) in *Nicotiana benthamiana* was visualized using confocal microscopy. (b) *Agrobacterium*-mediated transient expression of NTL9 with an N-terminal GFP fusion (GFP-NTL9) and ER-localized mCherry reporter in *N. benthamiana* and visualized using confocal microscopy.

NTL9 is involved in the Arabidopsis immune response to *P. syringae*. As HopD1 is a strong suppressor of ETI, it stands to reason that if it targets NTL9, NTL9 is likely a component of plant immunity. An emerging theme for NAC transcription factors is their multiple roles in biotic and abiotic stress, as well as an ability to coordinate multiple stress responses (38). This has been seen for the membrane-tethered NAC transcription factor NTL6 that coordinates the response to cold and pathogen attack as it up-regulates pathogenesis-related genes (42). A loss-of-function line for *NTL9* (SALK-065051, *ntl9-1*) was isolated that is compromised in osmotic stress responses and has enhanced susceptibility to avirulent *Hyaloperonospora arabidopsidis* (53, 33), suggesting that NTL9 is involved in the response to both osmotic and pathogen stresses.

To investigate the role of NTL9 in the response of Arabidopsis to *P. syringae*, wild-type Arabidopsis and the Arabidopsis *ntl9-1* mutant were syringe inoculated with various *P. syringae* strains and bacterial growth was measured at 0 and 3 d postinoculation (Fig. 6A). DC3000 grew to equivalent levels in wild-type and *ntl9-1* Arabidopsis, as did the *hrcC* mutant. Interestingly, the reduced growth of the *hopD1* mutant observed in wild-type Arabidopsis plants was restored to DC3000 values in *ntl9-1* mutant plants. These data support the hypothesis that NTL9 is a target of HopD1. As expected, the DC3000 *hopD1* mutant complemented with *hopD1* showed equivalent growth to DC3000 in both wild type and *ntl9-1* mutant plants. The avirulent *P. syringae* strains DC3000(p*avrRpm1*) and DC3000(p*avrRpt2*) showed enhanced growth in Arabidopsis *ntl9-1* mutant plants compared with wild-type Arabidopsis, indicating

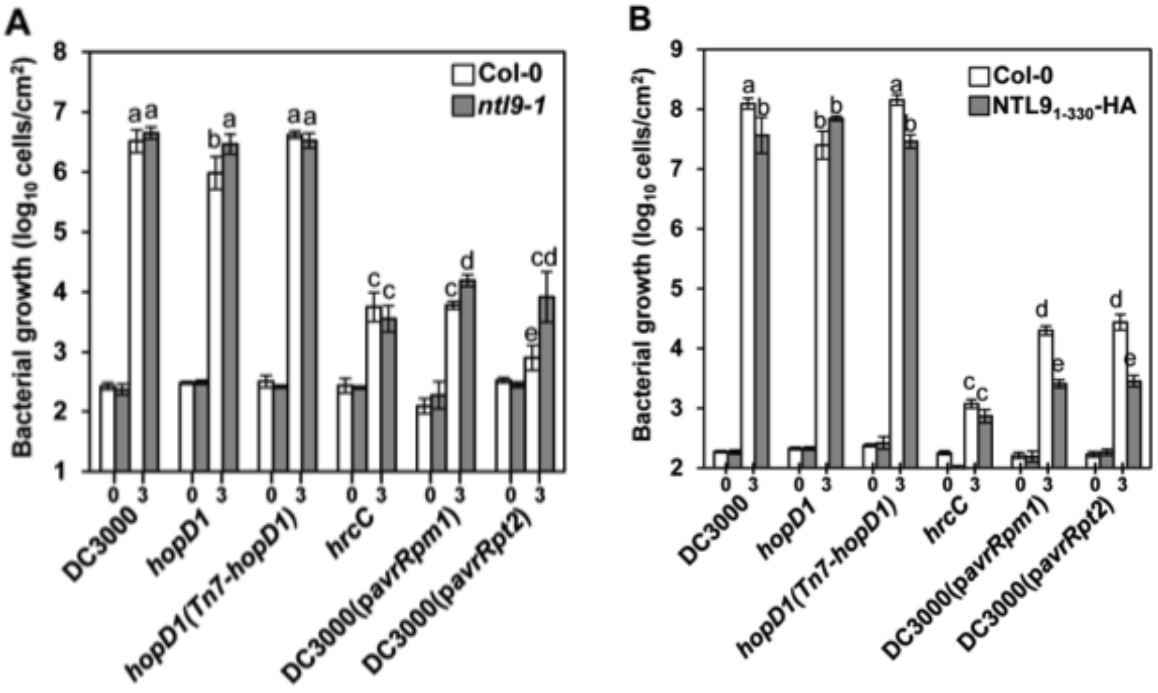

Fig. 6. NTL9 is important for the innate immune response of Arabidopsis to *Pseudomonas syringae*. (a) Wild-type Arabidopsis (Col-0) and the *ntl9* knockout mutant (*ntl9-1*) were syringe-inoculated with 2 x 10^5 cells ml^{-1} of wild-type *P. syringae* (DC3000), the *hopD1* mutant, *hopD1* complemented using the Tn7 expression system (*hopD1*(*Tn7-hopD1*)), the type III secretion defective *hrcC* mutant, and avirulent *P. syringae* strains DC3000(p*avrRpt2*) and DC3000(p*avrRpm1*). Bacterial growth was measured at 0 and 3 d postinoculation. (b) Wild-type Arabidopsis (Col-0) and transgenic plants expressing constitutively active NTL9 (*NTL9$_{1-330}$-HA*) under the control of an estradiol-inducible promoter were sprayed with 20 μM estradiol and syringe-inoculated 24 h later with 2 x 10^5 cells ml^{-1} of DC3000, *hopD1*, *hopD1*(*Tn7-hopD1*), *hrcC*, DC3000(p*avrRpt2*) or DC3000(p*avrRpm1*). Bacterial growth was measured at 0 and 3 d postinoculation. (a, b) These experiments were repeated three times with similar results (different letters indicate that the values are significantly different; P ≤0.05). Error bars, ±SE.

that NTL9 is involved in ETI. These results are consistent with our earlier results (Figs. 1B, 2), indicating that HopD1 targets components of immunity associated with ETI.

A truncated version of NTL9 that consisted of amino acids 1–330 ($NTL9_{1–330}$) is constitutively active (53). We made transgenic Arabidopsis lines expressing *NTL9*$_{1-330}$*-HA* under the control of an estradiol-inducible promoter. Wild-type and *NTL9*$_{1-330}$*-HA*-expressing Arabidopsis were sprayed with estradiol to induce transgene expression. Twenty-four hours later the plants were syringe-inoculated with 2 x 10^5 cells ml^{-1} of various *P. syringae* strains and bacterial growth was measured at 0 and 3 d postinoculation (Fig. 6B). Growth of both DC3000 and the complemented DC3000 *hopD1* mutant were reduced to that of the *hopD1* mutant in plants expressing activated *NTL9*. In addition, growth of the avirulent *P. syringae* strains was also reduced in the *NTL9*$_{1-330}$*-HA*-expressing lines. These data show that active NTL9 up-regulates plant immunity resulting in the restriction of *P. syringae* growth *in planta*.

Identification of NTL9-induced genes involved in plant immunity. If HopD1 functions by inhibiting NTL9's activity during ETI, it would be likely that HopD1 suppresses NTL9-dependent gene expression during ETI. NTL9 has been shown to regulate several genes involved in abiotic stress (53), yet its regulation of genes involved in plant immunity is not well understood. To determine if NTL9 could regulate the expression of a subset of genes associated with immunity, *FRK1*, *PAL1*, and *NHL10* expression was measured using qRT-PCR in wild-type and $NTL9_{1-330}$-HA-inducible Arabidopsis with and without estradiol treatment (Fig.

7A). The expression of all three immunity-related genes was induced exclusively in the estradiol-treated $NTL9_{1-330}$-HA plants showing that they are up-regulated either directly or indirectly by active NTL9. Because of the extensive overlap between ETI and PTI (46), we do not know if the expression of these genes represents an ETI or a PTI response in this experiment.

In a previous study, Kim *et al.* used PCR-mediated random binding site selection to identify the sequence TTGCTTANNNNNNAAG as the DNA-binding site for NTL9 (26). We used this binding site to search for additional NTL9-regulated Arabidopsis genes using RSA-tools-dna-pattern search (http://rsat.ulb.ac.be/genomescale-dna-pattern_form.cgi; 20). In all, 175 Arabidopsis genes were identified with the binding site motif in their promoter within 1 kb of their predicted translational start site. We selected 20 of these 175 genes for further analysis based on their possible role in innate immunity. Their possible involvement in immunity was established via literature searches or as a result of induction of their expression by DC3000 treatment according to the microarray database Arabidopsis eFP Browser (http://www.bar.utoronto.ca/efp/cgi-bin/efpWeb.cgi; 51).

Expression of the 20 candidate genes was measured by qRT-PCR in wild-type Arabidopsis and $NTL9_{1-330}$-HA-inducible plants with and without estradiol treatment (Table S1). Owing to the limited number of base pairs in the predicted binding site, the false positive rate was high and many of the genes tested did not show NTL9-regulated expression (Table S1). Despite this high error rate, four of the predicted genes were strongly up-regulated in estradiol-treated $NTL9_{1-330}$-

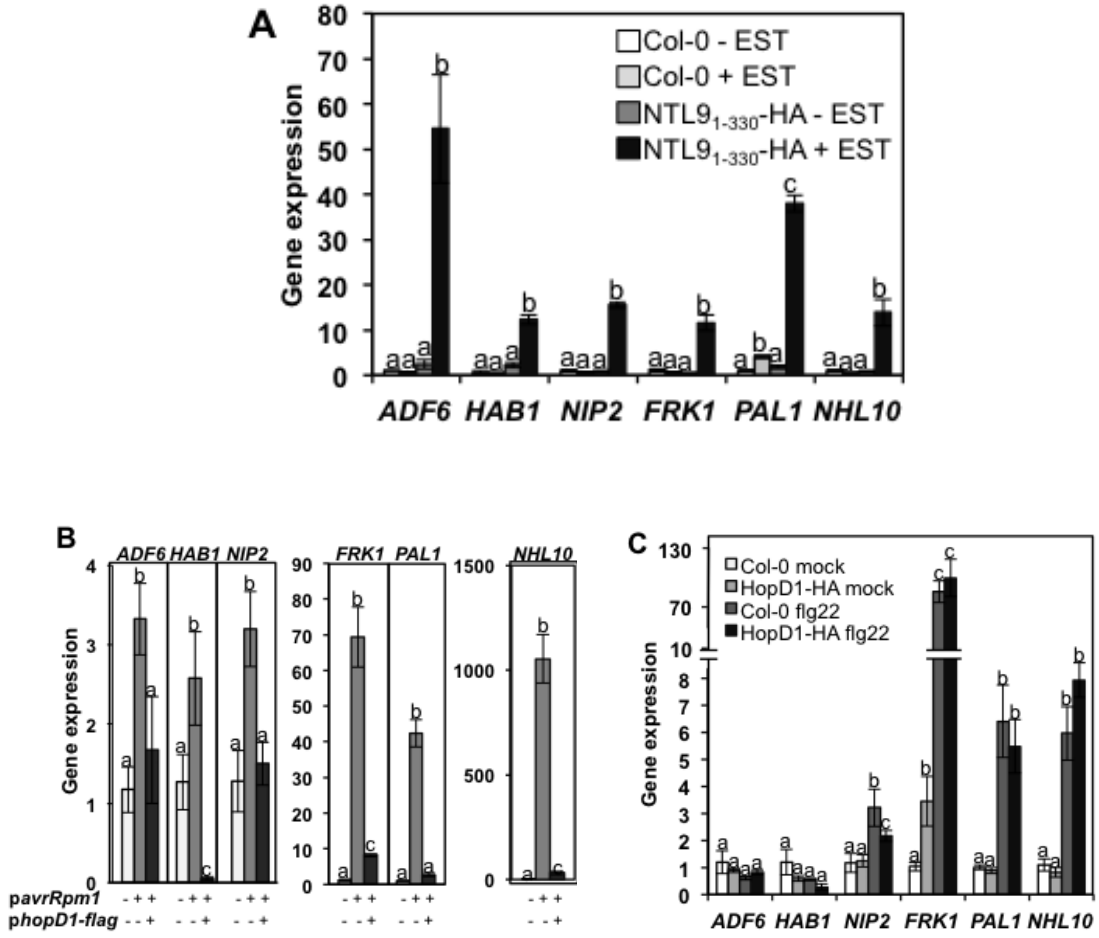

Fig. 7. HopD1 suppresses effector-triggered immunity (ETI) but not pathogen-associated molecular pattern (PAMP)-induced NTL9-regulated genes. (a) Wild-type (Col-0) and transgenic Arabidopsis expressing a constitutively active NTL9 derivative (NTL91-330-HA) under the control of an estradiol (EST)-inducible promoter were syringe-infiltrated with EST or a mock control. Leaf tissue was sampled 24 h later and gene expression was analyzed by quantitative reverse transcription polymerase chain reaction (qRT-PCR). (b) Wild-type (Col-0) Arabidopsis plants were syringe-inoculated with a mock control or 1 x 10^7 cells ml^{-1} of *Pseudomonas fluorescens* (*Pf*)(pLN1965 + p*avrRpm1*) with an empty vector control or with a plasmid constitutively expressing HopD1 FLAG. Inoculated leaves were sampled 4 h later and gene expression was measured using qRT-PCR. Expression of the genes was increased in response to the ETI-inducer AvrRpm1 only in the absence of HopD1. (c) Wild-type (Col-0) and HopD1-HA-expressing Arabidopsis were syringe-infiltrated with 1 µM flg22 or a mock control. Infiltrated leaves were sampled 4 h later and gene expression was measured using qRT-PCR. Induction of gene expression by flg22 was not significantly altered by the presence of HopD1. In all experiments, expression is relative to untreated Col-0. (a–c) Different letters indicate the values are significantly different using ANOVA (P ≤0.05); error bars, ±SE.

HA-inducible lines. These genes were *ADF6* (*At2g31200*), *NIP2* (*At2g17730*), *HAB1* (*At1g72770*) (Fig. 7A) and *BZIP9* (*At5g24800*) (Table S1).

HopD1 suppresses NTL9-regulated gene expression during ETI but not PTI. In order to investigate HopD1's ability to suppress NTL9's function in ETI, the expression of NTL9-regulated genes was measured in wild-type Arabidopsis plants infiltrated with a mock control, *Pf*(pLN1965 + p*avrRpm1*) or *Pf*(pLN1965 + p*avrRpm1* + p*hopD1-flag*). One of the genes tested (*BZIP9*) was repressed by *Pf*(pLN1965 + p*avrRpm1*) treatment (Fig. S4). The other six genes showed increased expression upon AvrRpm1-induced ETI and little if any increase in expression by AvrRpm1 in the presence of HopD1 (Fig. 7B). *FRK1* is known primarily to be associated with PTI. However, it is induced during AvrRpm1-induced ETI (Fig. 7B). These data suggest that HopD1 inhibits ETI-induction of NTL9-regulated gene expression and, therefore, it interferes with NTL9 function during ETI.

Because HopD1 specifically blocks ETI and not PTI responses, we examined the ability of HopD1 to affect the expression of the six NTL9-regulated marker genes during PTI. To accomplish this, wild-type and HopD1-HA-expressing Arabidopsis were syringe-infiltrated with flg22 or a mock control. Leaf tissue was sampled 4 h later and gene expression was measured using qRT-PCR (Fig. 7C). Three of the six genes, *FRK1*, *PAL1* and *NHL10*, showed induction in response to flg22 treatment. However, the presence of HopD1-HA had no effect on the PTI induction of these genes. Thus, taken together, these data indicate that NTL9 is specifically involved in the ETI induction of immunity-

related gene expression and the induction of a subset of these genes during PTI is probably controlled by other transcription factors.

Discussion

In this study we examined the role of the HopD1 T3E in the virulence of the bacterial pathogen *P. syringae*. Baltrus *et al*. (4) found that HopD1 was a well-distributed T3E, which was found in all sequenced strains of group I, two thirds of the sequenced group III strains, and none of the six sequenced group II strains. We found that HopD1 was necessary for the full virulence of *P. syringae* (Fig. 1A) and that it was a strong suppressor of ETI (Fig. 2), but apparently not of PTI. The extent to which transgenically expressed HopD1 was capable of PTI suppression was evaluated with three commonly used PTI assays: the *in planta* growth of a *P. syringae hrcC* mutant (Fig. 1B), defective in type III secretion, or a nonpathogenic *P. fluorescens* strain (Fig. 3C); PAMP-induced ROS production (Fig. 3A); and PAMP-induced callose deposition (Fig. 3B). However, we did not test the extent to which HopD1 allowed better *P. syringae* growth in plants pretreated with a PAMP, which would be an additional assay to evaluate PTI suppression. Nevertheless, based on these commonly used PTI assays, it seems likely that HopD1 is not an effective PTI suppressor.

We found that HopD1 interacts with the NAC transcription factor NTL9 and both localize to the ER of plants (Figs 4, 5). The growth of the *P. syringae hopD1* mutant and ETI-inducing *P. syringae* strains was enhanced in an Arabidopsis *ntl9* mutant (Fig. 6A), while expression of constitutively active NTL9 suppressed the

growth of both virulent and ETI-inducing *P. syringae* strains (Fig. 6B). This indicates that NTL9 is utilized in the Arabidopsis innate immune response to *P. syringae*. In addition, we observed that HopD1 suppressed ETI-induced but not PAMP-induced expression of NTL9-regulated genes (Fig. 7). Collectively, these data led us to conclude that HopD1 suppresses ETI and promotes virulence of *P. syringae* in part by blocking the ability of NTL9 to regulate ETI-induced gene expression.

HopD1 was shown previously to suppress the HopA1-induced HR in tobacco (22, 18). The ability of HopD1 to suppress ETI in two different systems (tobacco and Arabidopsis) and in response to multiple recognized T3Es (HopA1, AvrRpm1 and AvrRpt2) indicates that one of its primary targets is a common component of ETI. Interestingly, we did not find any evidence that HopD1 suppressed PTI. The specific effect of HopD1 on ETI suggests that the reduced virulence of the *hopD1* mutant exhibited in Arabidopsis is probably the result of an ‘unmasking’ of recognized *P. syringae* T3Es owing to the loss of HopD1’s ETI suppression activity. Earlier reports provided pioneering genetic evidence suggesting that *avr* genes, encoding recognized T3Es, can reside in virulent P. syringae strains and can be ‘unmasked’ when other T3E genes, encoding ETI suppressors, are mutated (21, 45). Moreover, Arabidopsis mutants with defective R protein complexes allow for enhanced growth of a virulent *P. syringae* strain (54), consistent with ETI playing an immunity role against virulent *P. syringae*. Our research further supports that ETI contributes to immunity against virulent *P. syringae* and that HopD1 disables ETI as a virulence strategy.

The coevolution of plants and pathogens is elegantly illustrated in the zigzag model of the plant immune system (23). In this coevolutionary model, PRRs recognize PAMPs inducing PTI. To retain pathogenicity the pathogen must acquire or evolve an effector that can suppress PTI, resulting in effector-triggered susceptibility (ETS). Therefore, the earliest T3Es used in *P. syringae* virulence are predicted to be PTI suppressors. In the next phase, the plant evolves an R protein to recognize a specific pathogen effector, thereby inducing ETI. This would put selection pressure on the pathogen to disable the gene encoding the recognized effector or acquire another effector to suppress the ETI evoked from this recognition event, allowing the return of ETS. Importantly, the ability for the pathogen to regain ETS is probably dependent on its inventory of effectors that can suppress ETI and the strength of the ETI response induced by the recognized effector. *P. syringae* T3Es have been investigated mostly for their effect on PTI (13). However, there are several examples of *P. syringae* T3Es that suppress both PTI and ETI (1, 16, 14, 49, 50). This is perhaps not surprising given the highly overlapped nature of PTI and ETI (47). What is less common are examples of *P. syringae* T3Es that suppress ETI but not PTI. These effectors would be predicted to be acquired later in the coevolution of the pathogen–plant interaction after establishment of the R protein immune receptor surveillance system. HopD1 appears to be one such effector.

We clearly show by yeast two-hybrid and BiFC assays that HopD1 interacts with NTL9. GFP fusions of both of these proteins colocalize with an ER targeted RFP fusion and BiFC assays show that HopD1 and NTL9 interact at the

ER. NTL9 was previously reported to localize to the plasma membrane and nucleus of onion cells (53). The large vacuole of onion cells that oppresses the ER against the plasma membrane, coupled with the difficulty in distinguishing nuclear and perinuclear localization with epifluorescence microscopy, may have led to these observed differences in localization.

NTL9 is one of over 110 NAC domain transcription factors in Arabidopsis (37), of which at least 13 have C-terminal transmembrane domains (28). There is precedent for pathogens to target NAC transcription factors, arguably the most well characterized of which is the capsid protein (CP) of *Turnip crinkle virus* (TCV) that interacts with the Arabidopsis NAC transcription factor TIP (39), blocking its ability to localize to the nucleus (40). We tested the extent to which HopD1 could affect the subcellular localization of NTL9 using *Agrobacterium*-mediated transient assays in *N. benthamiana* of GFP-NTL9 with or without HopD1-HA and were unable to discern any difference in GFP-NTL9 localization (Fig. S5). However, based on these results, DC3000 can induce the relocalization of NTL9-GFP to the nucleus in *N. benthamiana*. Additionally, we tested whether HopD1 was able to inhibit NTL9 transcription using a yeast one-hybrid system and were unable to detect a decrease in transcription in the presence of HopD1 (Fig. S6). Thus, HopD1 inhibits NTL9-dependent gene expression, but we do not yet know the mechanism of its inhibition.

NAC transcription factors have also been implicated in the plant immune response to bacterial pathogens. For example, the plasma membrane-bound Arabidopsis NAC transcription factor NTL6 has been implicated in the cold

induction of innate immunity as a constitutively active form of NTL6 activates the expression of the pathogenesis-related genes *PR1*, *PR2* and *PR5* (42). Arabidopsis plants constitutively expressing active NTL6 are more resistant to *P. syringae*, and NTL6 RNAi lines are more susceptible to *P. syringae* after cold pretreatment (42). Another NAC transcription factor from Arabidopsis, ATAF1, is a negative regulator of immune responses against *P. syringae* (48).

Relatively recently a report showed that *ntl9* knockout Arabidopsis plants are subtly more resistant to P. syringae (27). These data led the authors to suggest that NTL9 is a negative regulator of innate immunity. However, we did not observe any statistically significant difference in the growth of *P. syringae* in *ntl9* knockout plants compared with wild-type plants and often observed a slight increase in *P. syringae* growth (Fig. 6A), even though these experiments were repeated many times. Importantly, Arabidopsis plants expressing constitutively active *NTL9* were more resistant to *P. syringae* (Fig. 6B), which suggests that NTL9 acts as a positive regulator. We cannot account for the differences between our *P. syringae* growth phenotypes and that reported in Kim *et al.* (27). However, their subtle *P. syringae* growth data and our own data suggest that the absence of NTL9 may be compensated for by other transcription factors in plant immunity.

Our study shows that NTL9 induces the classic immune marker genes *FRK1* (19), *PAL1* (31) and *NHL10* (55), as well as at least three genes that have not been characterized as to their role in innate immunity. These genes are *HAB1*, *NIP2* and *ADF6*. NIP2 has no known role in immunity. Although no direct

role for ADF6 has been shown in the immune response to *P. syringae* infection, another actin-depolymerizing factor (ADF4) was shown to be specifically required for resistance triggered by the *P. syringae* effector AvrPphB (44). HAB1 is a negative regulator of ABA signaling. It is a 2C protein phosphatase that, in the absence of ABA, binds to SnRK2 kinases, inhibiting their activity (43). ABA has a negative role in plant immunity (8) and it would not be surprising, therefore, if the induction of a negative regulator of ABA signaling, such as HAB1, by NTL9 was important for immunity signaling. Other ETI-associated genes are also likely to be regulated by NTL9, but their identification will require extensive NTL9-dependent expression studies, which will be addressed in the future. Other future studies will examine HopD1's effect on NTL9 and other NAC transcription factors during pathogen stress, which will help to elucidate how this T3E inhibits the function of NTL9 as well as understanding the role NTL9 plays in plant immunity.

Materials and methods

Cloning and expression constructs. Genes were cloned into the Gateway entry vector pENTR-D. The pENTR-D constructs and their respective cloning primers are as follows: *hopD1* with a ribosome binding site (pLN3228) primers P0967 (5′-CACCGGGACAGCTGATAGAACAATGAATCCTCTACGCTC-3′) and P2892 (5′-GGGTGCGGGCTGCCGCGA-3′); *hopD1* (pLN5056) primers P4373 (5′-CACCATGAATCCTCTACGATCTATTCAACAC-3′) and P2892; *NTL9* (pLN5057) primers P4379 (5′-CACCATGGGTGCTGTATCGATGGAGTCG-3′) and P4393 (5′-TGAACTCACCAGTGTCCTCCACATCC-3′); and $NTL9_{1\text{-}330}$

(pLN5058) primers P4379 and P4382 (5′-GAAAGCCATGAAGTCGTTGAAAGCATCCTCTG-3′).

For the *hopD1* bimolecular fluorescence complementation (BiFC) constructs, *hopD1* with a 3′ *XhoI* restriction site was amplified with primers P4373 and P4384 (5′-GATCCTCGAGGGGTGCGGGCTG CCGCGACGTG-3′); *cyfp* with a 5′ *XhoI* restriction site was amplified with primers P4342 (5′-GATCCTCGAGATGGACAAGCAGAAGAACGGCATC-3′ – which contains an ATG start codon) and P4343 (5′-TCAGATAGATCTCTTGTACAGCTC-3′); and *nyfp* with a 5′ *XhoI* restriction site was amplified with primers P4340 (5′-GATCCTCGAGATGGTGAGCAAGGG CGAGGAG-3′) and P4341 (5′-TCAGGCCATGATATAGACGTTGTGG). The PCR products were then digested with *XhoI* and ligated. The ligation products were used as templates to clone *hopD1-cyfp* with primers P4373 and P4343 into pENTR-D, resulting in the construct pLN5066, and *hopD1-nyfp* with primers P4373 and P4341 into pENTR-D, resulting in the construct pLN5067. For the *NTL9* BiFC constructs, *NTL9* with a 5′ *XhoI* restriction site was amplified with primers P4403 (5′-GATCCTCGAGATGGTGCTGTATCGATGGAGTCG-3′) and P4393; *cyfp* with a 3′ *XhoI* restriction site was amplified with primers P4406 (5′-CACCATGGACAAGCAAGCAGAAGAACGGCATC-3′) and P4407 (5′-GATCCTCGAGGATAGATCTCTTGTACAGCTC-3′); and *nyfp* with a 3′ *XhoI* restriction site was amplified with primers P4404 (5′-CACCATGGTGAGCAAGGCGAGGAG-3′) and P4405 (5′-GATCCTCGAGGGCCTGATATAGACGTTGTGG-3′). The PCR products were

then digested with *XhoI* and ligated. The ligation products were used as templates to clone *nyfp-NTL9* with primers P4404 and P4393 into pENTR-D, resulting in the construct pLN5068, and *cyfp-NTL9* with primers P4406 and P4393 into pENTR-D, resulting in the construct pLN5069.

The BiFC clones pLN5066, pLN5067, pLN5068 and pLN5069 were placed into the plant constitutive expression vector pLN462 (22), resulting in constructs pLN5070, pLN5071, pLN5072 and pLN5073, respectively. For plant expression, *hopD1* (pLN5056) was fused to a C-terminal hemagglutinin (HA) tag by recombining into pLN462 with gateway technologies to give pLN5060 and to a C-terminal green fluorescent protein (GFP) tag by recombining into pK7FWG2 (24) to give pLN5061. For complementation of the *hopD1* mutant (UNL104), *hopD1* (pLN3228) was recombined into the Tn7 vector pLN2992 (9), resulting in construct pLN4908. This vector was then used to insert the resultant *hopD1-ha* into the chromosome of UNL104. To create an N-terminal GFP fusion to NTL9, pLN5057 was recombined with pK7WGF2 (24) to give pLN5062. To make an estradiol-inducible $NTL9_{1-330}$-HA, pLN5058 was recombined with the gateway-compatible pER8 vector pLN604 (56) to give pLN5063.

Pathogenicity assays. *Pseudomonas syringae* strains were grown overnight at 30°C on King's B (KB; 30) media with the appropriate antibiotics and resuspended to an OD_{600} of 0.2 (2×10^8 cells ml^{-1}) in 10 mM $MgCl_2$. Cells were serially diluted in 10 mM $MgCl_2$ to the appropriate cell density and infiltrated into the fully expanded leaves of 4-wk-old *Arabidopsis thaliana* Col-0 wild-type, mutant, and/or transgenic plants using a needleless syringe. Plants were kept at

100% humidity and 1 cm^2 leaf disks were sampled at the indicated times, ground in 10 mM $MgCl_2$, serially diluted and plated on KB agar plates. Plates were incubated for 48 h at 30°C and number of cells cm^{-2} was determined. Four to six leaf disks were sampled for each treatment and the statistical significance of the resulting data was analyzed by one-way ANOVA.

HR and ion leakage. *Pseudomonas fluorescens* (*Pf*)(pLN1965), *Pf*(pLN1965 + p*avrRpm1*) and *Pf*(pLN1965 + p*avrRpm1* + p*hopD1-flag*; 18) were grown overnight at 30°C in KB media with appropriate antibiotics. Bacterial strains were resuspended at 1 x 10^8 cells ml^{-1} in 5 mM 2-(4-morpholino)-ethane sulfonic acid (MES), pH 5.6. Wild-type Arabidopsis (Col-0) and *rpm1* mutant (12) leaves were infiltrated with bacterial suspensions using a needleless syringe. Nine leaf disks were harvested for each strain in each plant type using a 0.7 cm^2 cork borer. Three leaf disks were placed in each 15 ml polypropylene tube with 5 ml of water and incubated in a shaker for 30 min at room temperature. Water was removed and 5 ml of fresh water was added to each sample and tubes were placed in a shaker. Electrolyte leakage was monitored at the indicated time points using an electrical conductivity meter (Fisher Scientific, Pittsburgh, PA, USA). Conductivity was measured in µS cm^{-1}. For macroscopic HR, *Pf*(pLN1965 + p*avrRpm1*) and *Pf*(pLN1965 + p*avrRpm1* + p*hopD1-flag*) strains were infiltrated into leaves of wild-type Arabidopsis (Col-0) and the *rpm1* mutant at 1 x 10^8 cells ml^{-1} using a needleless syringe. Leaves were photographed 2 d after infiltration.

Callose assay. Wild-type (Col-0) and HopD1-HA transgenic lines were syringe-infiltrated with 10 µM flg22, or wild-type Arabidopsis leaves were syringe

inoculated with 1 x 10^6 cells ml^{-1} of *Pf*(pLN1965), *Pf*(pLN1965 + p*hopD1-flag*), *Pf*(pLN1965 + p*avrRpm1*) or *Pf*(pLN1965 + p*avrRpm1* + p*hopD1-flag*). Sixteen hours later, leaves were harvested and cleared with 100% (v/v) ethanol at 37°C for 4 h and washed twice with 70% (v/v) ethanol and three times with water. The completely cleared leaves were stained with 0.1% (w/v) aniline blue in a solution of 150 mM K_2HPO_4, pH 9.5, for 30 min and the callose deposits were enumerated as in Block *et al*. (6).

Oxidative burst measurement. Leaf disks of 0.5 cm^2 were cut from wild-type (Col-0) and HopD1-HA transgenic lines and floated on 0.1 ml of water in wells of a 96-well plate for 16 h in the dark. The water was then removed and replaced with 0.5 mM L-012 (Wako, Japan) in 10 mM MES buffer, pH 7.4. For PAMP treatment, 1 µM of flg22, elf18 or chitin was added to the buffer. The rate of ROS production was determined by counting photons from L-012-mediated chemiluminescence using a luminometer (3). The rates of ROS production were calculated as the number of photons released in 30 min after treatment with photons counted once a minute.

Yeast-two hybrid analyses. Gateway entry constructs carrying *hopD1* (pLN5056) and *NTL9* (pLN5057) were recombined by an LR reaction to the appropriate yeast two-hybrid destination vectors to generate pDEST-DB::*hopD1* (pLN4988) and pDEST-AD::*NTL9* (pLN4970). A detailed protocol for yeast two-hybrid analyses used is described in Dreze *et al*. (11). The yeast strains Y8930 (MATα) and Y8800 (MAT**a**) were transformed with expression plasmids pDEST-DB::*hopD1* and pDEST-AD::*NTL9*, respectively. Empty expression vectors (EVs)

were also transformed into the corresponding yeast strains. Yeast Y8930 (pDEST-DB::*hopD1* or EV) was mated to Y8800 (pDEST-AD::*NTL9* or EV) in a mating plate (yeast extract peptone dextrose). Growth was checked on Sc-Leu-Trp and interactions were tested by plating mated strains in Sc-Leu-Trp-His + 1 mM 3-amino-1,2,4-triazole (3AT).

Agroinfiltration and confocal microscopy. *Agrobacterium* strains were coinfiltrated into *N. benthamiana* as in Block *et al*. (6). Leaves were imaged 48 h later using a Nikon A1 confocal mounted on an Eclipse 90i Nikon compound microscope using the following excitation (ex) and emission (em) wavelengths: GFP and yellow fluorescent protein (YFP), 488 nm (ex), 500–550 nm (em); red fluorescent protein (RFP), 561.5 nm (ex) and 570–620 nm (em); Chl, 641 nm (ex) and 662–737 nm (em). Dual color image acquisition was sequential.

Semiquantitative reverse transcription polymerase chain reaction (RT-PCR). Wild-type Arabidopsis (Col-0) and pER8 $NTL9_{1-330}$-HA stable Arabidopsis lines were syringe-infiltrated with 0.2 mM estradiol or a water control. Leaf tissue was harvested for RNA extraction 24 h after treatment. Wild-type Arabidopsis (Col-0) plants were syringe-inoculated with water or 1 x 10^7 cells ml^{-1} of *Pf*(pLN1965 + p*avrRpm1*) or *Pf*(pLN1965 + p*avrRpm1* + *phopD1-flag*). Leaf tissue was harvested for RNA extraction 4 h after infiltration. Total RNA was purified using RNeasy mini Kit with on-column DNase treatment (Qiagen). The reverse transcription of RNA was carried out using RETROscript (Ambion) using oligo(dT) primers with heat denaturation of the RNA. *actin2* (*At3g18780*) was used as a reference gene with primers P3774 (5′-

GCACTTGTGTGTGACAAACTCTCTGG-3′) and P3775 (5′-GGCATCAATTCGATCACTCTAGAGC-3′). The following gene-specific primers were used to measure expression levels in quantitative (qRT-PCR): *HAB1* (*At1g72770*) P4556 (5′-GCGGTGATTCGAGGGCGGTTT-3′) and P4557 (5′-GCCACGTTTGTGTGATGTGCATT-3′); *NIP2* (*At2g17730*) P4558 (5′-TCTTCAGGATTTCCAGCTCGGTGAA-3′) and P4559 (5′-CGGGCAAGAACCGTGTCTAAGGA-3′); *ADF6* (*At2g31200*) P4560 (5′-TTGCTTGGTCTCCTTCGACCTCTGG-3′) and P4561 (5′-TCTCAGTTCGCTCGTTCGCGT-3′); *PAL1* (*At2g37040*) P3922 (5′-AGCAGCAAGAGCAGCCTACGATAA-3′) and P3923 (5′-TGTTCCAAGCTCTTCCCTCACGAA-3′); *FRK1* (*At2g19190*) P4476 (5′-ACCCCGAGTACTATTCGACTCGCCA-3′) and P4477 (5′-TGAGCTTGCAATAGCAGGTTGGCCT-3′); and *NHL10* (*At2g35980*) P4562 (5′-TCACTGTTCCTGTCCGTAACCCAA-3′) and P4563 (5′-TGGTACTAAACCGCTTTCCTCGT-3′). qRT-PCR was run using IQTM SYBR® Green supermix (BioRad) on a BioRad iCycler. Gene expression relative to Col-0 was calculated using $2^{-\Delta\Delta C}{}_{T}$ with actin2 as the reference gene and mock-treated Col-0 as the reference sample.

Supplemental figures and tables

Supplemental Table 1. Analysis of gene expression changes in Arabidopsis genes that contain a predicted NTL9 binding site in their promoters.

Gene name	Abbreviation	Predicted NTL9 binding site	Estradiol induced expression in $NTL9_{1-330}$-HA lines
At1g29330	ERD2	TTGCTTATAAAAGAAG	0.47 ± 0.04
At1g29340	PUB17	TTGCTTATAAAAGAAG	0.69 ± 0.13
At1g72770	**HAB1**	**TTGCTTAAGAACAAAG**	**22.97 ± 5.57**
At2g17730	**NIP2**	**TTGCTTAGTGGTTAAG**	**15.92 ± 3.02**
At2g22670	IAA8	TTGCTTAACAAGTAAG	1.42 ± 0.10
At2g29580	MAC5A	TTGCTTAGATCTGAAG	1.01 ± 0.02
At2g31200	**ADF6**	**TTGCTTAGTAATTAAG**	**54.60 ± 12.02**
At3g02040	SRG3	TTGCTTAAAAAAGAAG	0.95 ± 0.18
At3g04580	EIN4	TTGCTTAAGCGAAAAG	1.45 ± 0.68
At3g17880	TDX	TTGCTTAGACAAGAAG	0.96 ± 0.14
At4g20200	F1C12.120	TTGCTTAGTTAAGAAG	0.85 ± 0.59
At4g23510	F16G20.210	TTGCTTAAGAAACAAG	0.37 ± 0.04
At4g25470	CBF2	TTGCTTAAAATCGAAG	0.41± 0.08
At4g30650	F17I23.10	TTGCTTAGATGGCAAG	1.03 ± 0.84
At5g24800	**BZIP9**	**TTGCTTAGCCATTAAG**	**98.13 ± 10.79**
At5g25050	T11H3.60	TTGCTTACATCAAAAG	1.24 ± 0.18
At5g41740	MUF8.2	TTGCTTATTTTTCAAG	1.57 ± 0.15
At5g50120	MPF21.14	TTGCTTATGAAGGAAG	1.58 ± 0.03
At5g66640	DAR3	TTGCTTATATTACAAG	0.99 ± 0.25
At5g67220	K21H1.18	TTGCTTAGAAATAAAG	1.13 ± 0.11

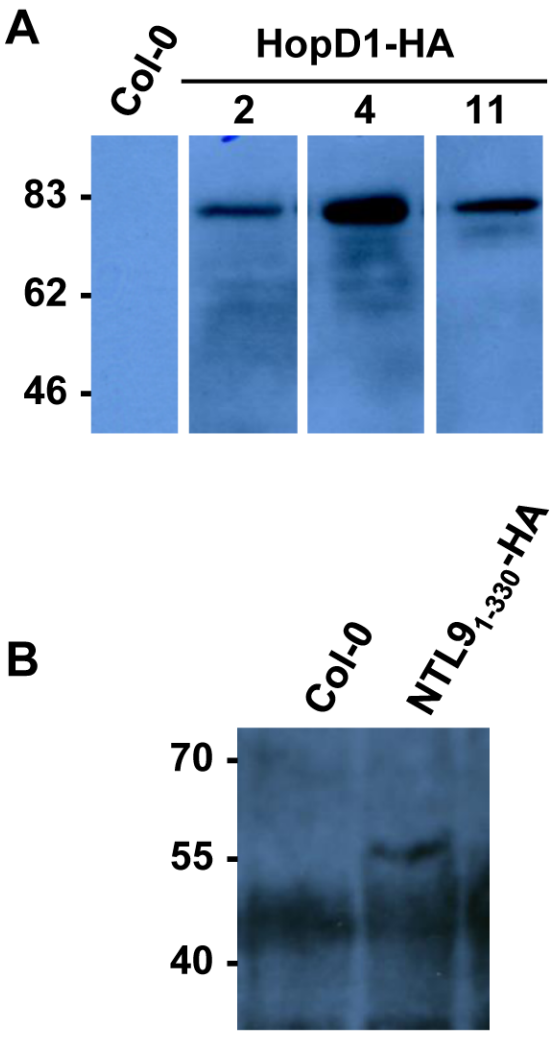

Supplemental Fig. 1. Immunoblots showing that transgenic Arabidopsis express HopD1-HA or NTL9$_{1-330}$-HA. (A) Expression of HopD1-HA in Arabidopsis was analyzed using immunoblots with anti-HA antibodies. Plants from line 2 were used in Fig. 3B, line 11 in Fig. 3A, and line 4 in Figs 1B and 7C. **(B)** Arabidopsis plants expressing the constitutively active NTL9 derivative NTL9$_{1-330}$-HA were confirmed using immunoblots with anti-HA antibodies. These plants were used in Fig. 6B and Fig. 7A.

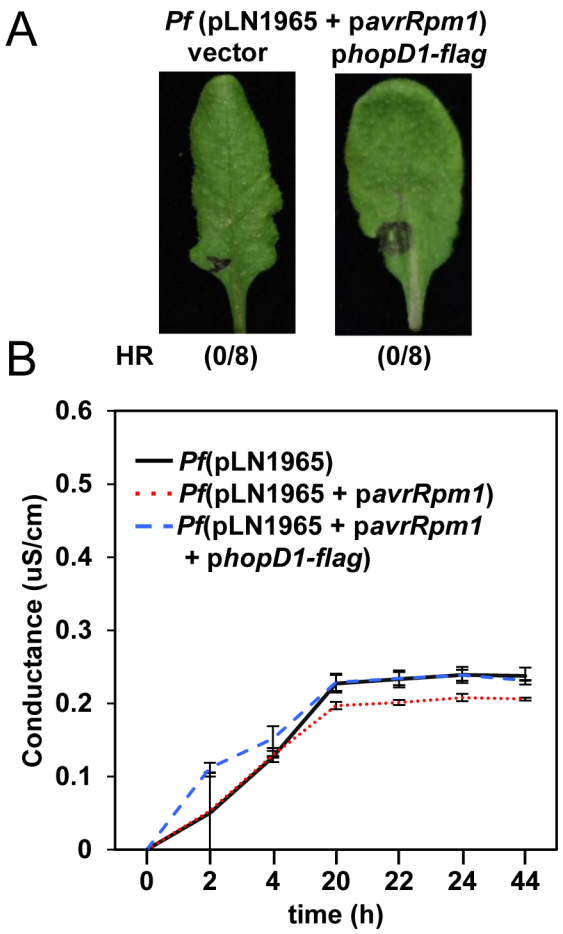

Supplemental Fig. 2. No HR or ion leakage observed in the Arabidopsis *rpm1* mutant in response to bacterial strains. Arabidopsis *rpm1* mutant plants were syringe-inoculated with 1 x 10^8 cells ml^{-1} of *Pseudomonas fluorescens(Pf)*(pLN1965 + p*avrRpm1*) carrying a vector control or a plasmid constitutively expressing *hopD1-flag*. HR was scored 48 h after infiltration (**A**) and ion leakage was measured in leaf disks over time as an indicator of cell death (**B**). No difference was observed in HR or ion leakage between *Pf*(pLN1965 + p*avrRpm1*) and *Pf*(pLN1965 +p*avrRpm1* + p*hopD1-flag*).

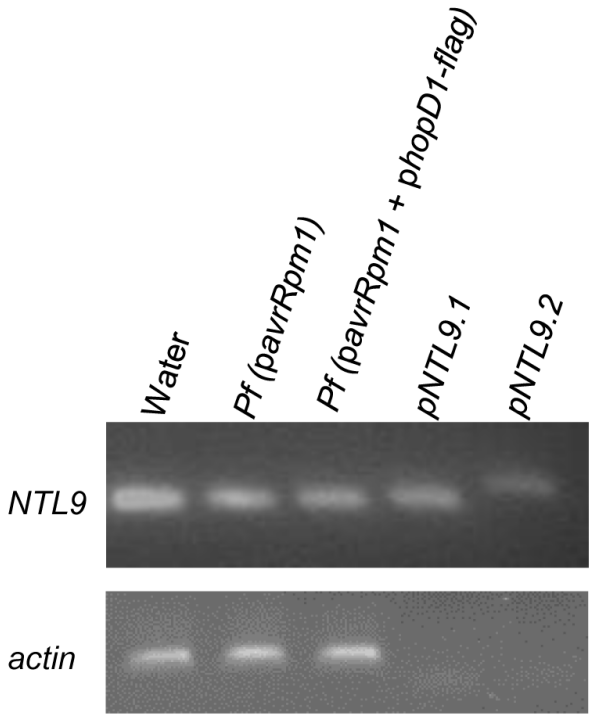

Supplemental Fig. 3. The first splice variant of *NTL9* is the dominant form in Arabidopsis. RT-PCR on Arabidopsis (Col-0) plants treated with water or syringe-inoculated with 1 x 10^7 cells ml^{-1} of *Pf*(pLN1965 + p*avrRpm1*) or *Pf*(pLN1965 + p*avrRpm1* + p*hopD1-flag*). RNA was made from tissue harvested 4 h post-infiltration. Primers 5'-ATCCGGGCTCGACAGCCTCA-3' and 5'-TAGACTCACCAGTGTCCTCCATATAC CCATCC-3' flanking the differentially spliced intron were used to distinguish between splice variants 1 and 2 of *NTL9* and compared to plasmid controls (pNTL9.1 and pNTL9.2). Splice variant *NTL9.1* was the predominant form of *NTL9* expressed under the conditions tested.

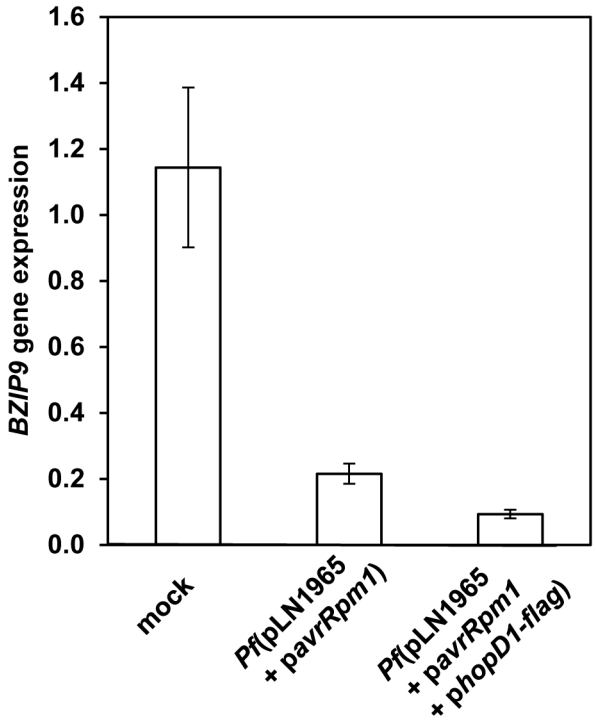

Supplemental Fig. 4. NTL9 regulated BZIP9 expression is repressed by ETI. Wild-type Arabidopsis (Col-0) plants were infiltrated with a mock control or 1 x 10^7 cells ml^{-1} of *P*f(pLN1965 + p*avrRpm1*) with an empty vector control or with a plasmid constitutively expressing *hopD1-flag*. Infiltrated leaves were sampled after 4 h and gene expression of *BZIP9* was measured using semi-qRT-PCR with primers 5'-TGCACAGTCCTCAATCTGCGAGAA-3' and 5'-TGCCCTGCTTCTGTCTCGGC-3'. Gene expression is relative to untreated Col-0.

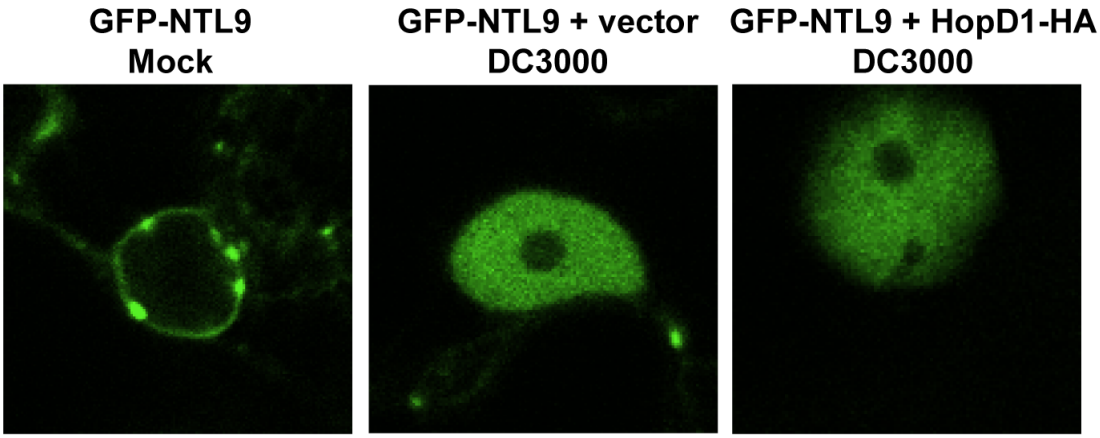

Supplemental Fig. 5. GFP-NTL9 inside plant cells is not altered by the presence of HopD1-HA. *Nicotiana benthamiana* leaves were co-infiltrated with *Agrobacterium* strains carrying GFP-NTL9 and HopD1-HA or empty vector control in the presence of the proteasome inhibitor MG132 (100 μM). After 24 h leaves were infiltrated with DC3000 (1 x 10^6 cells ml^{-1}) and visualized with confocal microscopy.

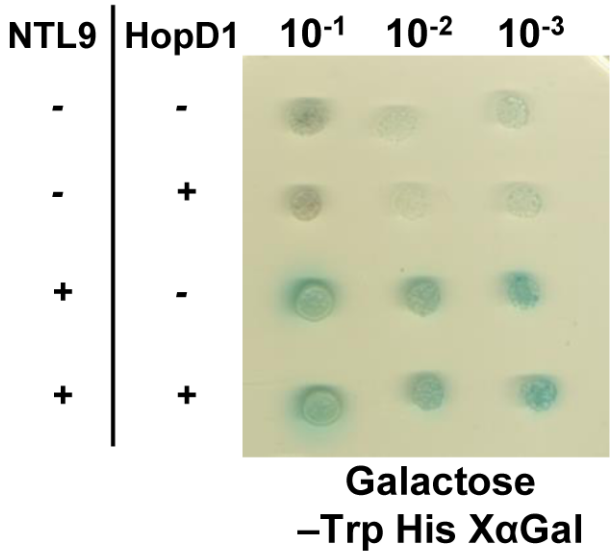

Supplemental Fig. 6. HopD1 does not alter NTL9-dependent gene expression in the yeast one-hybrid system. Yeast strain Y187 (pGBKT7 containing *NTL9* or an empty vector (EV)) mated with yeast strain AH109 (pGilda containing *hopD1* or an EV) were tested for the ability of HopD1 to block NTL9 autoactivation. Mated yeast strains were plated on Sc-Trp-His galactose plates and photographed after 2 d.

References

1. **Abramovitch R. B., Y. J. Kim, S. Chen , M. D. Dickman, and G. B. Martin.** 2003. *Pseudomonas* type III effector AvrPtoB induces plant disease susceptibility by inhibition of host programmed cell death. EMBO J. **22:**60-9.
2. **Arnold D. L., M. J. Gibbon, R. W. Jackson, J. R. Wood, J. Brown, J. W. Mansfield, J. D. Taylor, and A. Vivian.** 2001. Molecular characterization of *avrPphD*, a widely-distributed gene from *Pseudomonas syringae* pv. *phaseolicola* involved in non-host recognition by pea (*Pisum sativum*). Physiol. Mol. Plant P. **58:**55-62.
3. **Asai S., K. Ohta, and H. Yoshioka.** 2008. MAPK signaling regulates nitric oxide and NADPH oxidase-dependent oxidative bursts in *Nicotiana benthamiana*. Plant Cell **20:**1390-1406.
4. **Baltrus D. A., M. T. Nishimura, A. Romanchuk, J. H. Chang, M. S. Mukhtar, K. Cherkis, J. Roach, S. R. Grant, C. D. Jones, and J. L. Dangl.** 2011. Dynamic evolution of pathogenicity revealed by sequencing and comparative genomics of 19 *Pseudomonas syringae* isolates. PLOS Path. **7:**e1002132.
5. **Block A., and J. R. Alfano.** 2011. Plant targets for *Pseudomonas syringae* type III effectors: virulence targets or guarded decoys? Curr. Opin. Microbiol. **14:**39-46.
6. **Block A., M. Guo, G. Li, C. Elowsky, T. E. Clemente, and J. R. Alfano.** 2010. The *Pseudomonas syringae* type III effector HopG1 targets mitochondria, alters plant development and suppresses plant innate immunity. Cell. Microbiol. **12:**318-30.
7. **Block A., G. Li, Z. Q. Fu, and J. R. Alfano.** 2008. Phytopathogen type III effector weaponry and their plant targets. Curr. Opin. Plant Biol. **11:**396-403.
8. **Cao F. Y., K. Yoshioka, and D. Desveaux.** 2011. The roles of ABA in plant-pathogen interactions. J. Plant Res. **124:**489-99.
9. **Choi K. H., J. B. Gaynor, K. G. White, C. Lopez, C. M. Bosio, R. R. Karkhoff-Schweizer, and H. P. Schweizer.** 2005. A Tn7-based broad-range bacterial cloning and expression system. Nat. Methods **2:**443-8.
10. **Deslandes L., and S. Rivas.** 2012. Catch me if you can: bacterial effectors and plant targets. Trends Plant Sci. **17:**644-55.
11. **Dreze M., D. Monachello, C. Lurin, M. E. Cusick, D. E. Hill, M. Vidal, P. Braun.** 2010. High-quality binary interactome mapping. Method Enzymol. **470:**281-315.
12. **Eitas T. K., Z. L. Nimchuk, and J. L. Dangl.** 2008. Arabidopsis TAO1 is a TIR-NB-LRR protein that contributes to disease resistance induced by the *Pseudomonas syringae* effector AvrB. Proc. Natl. Acad. Sci. USA **105:**6475-80.
13. **Feng F., and J. M. Zhou.** 2012. Plant-bacterial pathogen interactions mediated by type III effectors. Curr. Opin. Plant Biol. **15:**469-76.
14. **Gimenez-Ibanez S., D. R. Hann, V. Ntoukakis, E. Petutschnig, V. Lipka,**

and J. P. Rathjen. 2009. AvrPtoB targets the LysM receptor kinase CERK1 to promote bacterial virulence on plants. Curr. Biol. **19:**423-9.

15. **Gimenez-Ibanez S., and J. P. Rathjen.** 2010. The case for the defense: plants versus *Pseudomonas syringae*. Microb. Infect. **12:**428-37.
16. **Gohre V., T. Spallek, H. Haweker, S. Mersmann, T. Mentzel, T. Boller, M. de Torres, J. W. Mansfield, and S. Robatzek.** 2008. Plant pattern-recognition receptor FLS2 is directed for degradation by the bacterial ubiquitin ligase AvrPtoB. Curr. Biol. **18:**1824-32.
17. **Guo M., S. Manulis, H. Mor, and I. Barash.** 2002. The presence of diverse IS elements and an *avrPphD* homologue that acts as a virulence factor on the pathogenicity plasmid of *Erwinia herbicola* pv. *gypsophilae*. Mol. Plant Microbe Interact. **15:**709-16.
18. **Guo M., F. Tian, Y. Wamboldt, and J. R. Alfano.** 2009. The majority of the type III effector inventory of *Pseudomonas syringae* pv. *tomato* DC3000 can suppress plant immunity. Mol. Plant Microbe Interact. **22:**1069-80.
19. **He P., L. Shan, N. C. Lin, G. M. Martin, B. Kemmerling, T. Nurnberger, and J. Sheen.** 2006. Specific bacterial suppressors of MAMP signaling upstream of MAPKKK in Arabidopsis innate immunity. Cell **125:**563-75.
20. **van Helden J., B. Andre, and J. Collado-Vides.** 2000. A web site for the computational analysis of yeast regulatory sequences. Yeast **16:**177-87.
21. **Jackson R. W., E. Athanassopoulos, G. Tsiamis, J. W. Mansfield, A. Sesma, D. L. Arnold, M. J. Gibbon, J. Murillo, J. D. Taylor, and A. Vivian.** 1999. Identification of a pathogenicity island, which contains genes for virulence and avirulence, on a large native plasmid in the bean pathogen *Pseudomonas syringae* pathovar *phaseolicola*. Proc. Natl. Acad. Sci. USA **96:**10875-80.
22. **Jamir Y., M. Guo, H. S. Oh, T. Petnicki-Ocwieja, S. Chen, X. Tang, M. B. Dickman, A. Collmer, and J. R. Alfano.** 2004. Identification of *Pseudomonas syringae* type III effectors that can suppress programmed cell death in plants and yeast. Plant J. **37:**554-65.
23. **Jones J. D., and J. L. Dangl.** 2006. The plant immune system. Nature **444:**323-9.
24. **Karimi M., D. Inze, and A. Depicker.** 2002. GATEWAY vectors for *Agrobacterium*-mediated plant transformation. Trends Plant Sci **7:**193-5.
25. **Keen N. T.** 1990. Gene-for-gene complementarity in plant-pathogen interactions. Annu. Rev. Genet. **24:**447-63.
26. **Kim H. S., B. O. Park, J. H. Yoo, M. S. Jung, S. M. Lee, H. J. Han, K. E. Kim, S. H. Kim, C. O. Lim, D. J. Yun, S. Y. Lee and W. S. Chung.** 2007a. Identification of a calmodulin-binding NAC protein as a transcriptional repressor in Arabidopsis. J. Biol. Chem. **282:**36292-302.
27. **Kim H. S., H. C. Park, K. E. Kim, M. S. Jung, H. J. Han, S. H. Kim, Y. S. Kwon, S. Bahk, J. An, D. W. Bae, D. J. Yun, S. S. Kwak, and W. S. Chung.** 2012. A NAC transcription factor and SNI1 cooperatively suppress basal pathogen resistance in *Arabidopsis thaliana*. Nucleic Acids Res. **40:**9182-92.

28. **Kim S. Y., S. G. Kim, Y. S. Kim, P. J. Seo, M. Bae, H. K. Yoon, and C. M. Park.** 2007b. Exploring membrane-associated NAC transcription factors in Arabidopsis: implications for membrane biology in genome regulation. Nucleic Acids Res. **35:**203-13.
29. **Kim Y. S., S. G. Kim, J. E. Park, H. Y. Park, M. H. Lim, N. H. Chua, and C. M. Park.** 2006. A membrane-bound NAC transcription factor regulates cell division in Arabidopsis. Plant Cell **18:**3132-44.
30. **King E. O., M. K. Ward, and D. E. Raney.** 1954. Two simple media for the demonstration of pyocyanin and fluorescin. J. Lab. Clin. Med. **44:**301-7.
31. **Mishina T. E., and J. Zeier.** 2007. Bacterial non-host resistance: interactions of Arabidopsis with non-adapted *Pseudomonas syringae* strains. Physiol. Plant. **131:**448-61.
32. **Monaghan J., and C. Zipfel.** 2012. Plant pattern recognition receptor complexes at the plasma membrane. Curr. Opin. Plant Biol. **15:**1-9.
33. **Mukhtar M. S., A. R. Carvunis, M. Dreze, P. Epple, J. Steinbrenner, J. Moore, M. Tasan, M. Galli, T. Hao, M. T. Nishimura, S. J. Pevzner, S. E. Donovan, L. Ghamsari, B. Santhanam, V. Romero, M. M. Poulin, F. Gebreab, B. J. Gutierrez, S. Tam, D. Monachello, M. Boxem, C. J. Harbort, N. McDonald, L. Gai, H. Chen, Y. He, European Union Effectoromics Consortium, J. Vandenhaute, F. P. Roth, D. E. Hill, J. R. Ecker, M. Vidal, J. Beynon, P. Braun, and J. L. Dangl.** 2011. Independently evolved virulence effectors converge onto hubs in a plant immune system network. Science **333:**596-601.
34. **Nanda A. K., E. Andrio, D. Marino, N. Pauly, and C. Dunand.** 2010. Reactive oxygen species during plant-microorganism early interactions. J. Integr. Plant Biol. **52:**195-204.
35. **Nelson B. K., X. Cai, and A. Nebenfuhr.** 2007. A multicolored set of *in vivo* organelle markers for co-localization studies in Arabidopsis and other plants. Plant J. **51:**1126-36.
36. **Nicaise V., M. Roux, and C. Zipfel.** 2009. Recent advances in PAMP-triggered immunity against bacteria: pattern recognition receptors watch over and raise the alarm. Plant Physiol. **150:**1638-47.
37. **Ooka H., K. Satoh, K. Doi, T. Nagata, Y. Otomo, K. Murakami, K. Matsubara, N. Osato, J. Kawai, P. Carninci, Y. Hayashizaki, K. Suzuki, K. Kojima, Y. Takahara, K. Yamamoto, and S. Kikuchi.** 2003. Comprehensive analysis of NAC family genes in *Oryza sativa* and *Arabidopsis thaliana*. DNA Res. **10:**239-47.
38. **Puranik S., P. P. Sahu, P. S. Srivastava, and M. Prasad.** 2012. NAC proteins: regulation and role in stress tolerance. Trends Plant Sci. **17:**369-81.
39. **Ren T., F. Qu, and T. J. Morris.** 2000. *HRT* gene function requires interaction between a NAC protein and viral capsid protein to confer resistance to *Turnip Crinkle Virus*. Plant Cell **12:**1917-25.
40. **Ren T., F. Qu, and T. J. Morris.** 2005. The nuclear localization of the Arabidopsis transcription factor TIP is blocked by its interaction with the

coat protein of *Turnip Crinkle Virus*. Virology **331:**316-24.

41. **Schulze S., S. Kay, D. Buttner, M. Egler, L. Eschen-Lippold, G. Hause, A. Kruger, J. Lee, O. Muller, D. Scheel, R. Szczesny, F. Thieme, and U. Bonas.** 2012. Analysis of new type III effectors from *Xanthomonas* uncovers XopB and XopS as suppressors of plant immunity. New Phytol. **195:**894-911.
42. **Seo P. J., M. J. Kim, J. Y. Park, S. Y. Kim, J. Jeon, Y. H. Lee, J. Kim, and C. M. Park.** 2010. Cold activation of a plasma membrane-tethered NAC transcription factor induces a pathogen resistance response in Arabidopsis. Plant J. **61:**661-71.
43. **Soon F. F., L. M. Ng, X. E. Zhou, G. M. West, A. Kovach, M. H. Tan, K. M. Suino-Powell, Y. He, Y. Xu, M. J. Chalmers, J. S. Brunzelle, H. Zhang, H. Yang, H. Jiang, J. Li, E. L. Yong, S. Cutler, J. K. Zhu, P. R. Griffin, K. Melcher, and H. E. Xu.** 2012. Molecular mimicry regulates ABA signaling by SnRK2 kinases and PP2C phosphatases. Science **335:**85-8.
44. **Tian M., F. Chaudhry, D. R. Ruzicka, R. B. Meagher, C. J. Staiger, and B. Day.** 2009. Arabidopsis actin-depolymerizing factor AtADF4 mediates defense signal transduction triggered by the *Pseudomonas syringae* effector AvrPphB. Plant Physiol. **150:**815-24.
45. **Tsiamis G., J. W. Mansfield, R. Hockenhull, R. W. Jackson, A. Sesma, E. Athanassopoulos, M. A. Bennett, C. Stevens, A. Vivian, J. D. Taylor, and J. Murillo.** 2000. Cultivar-specific avirulence and virulence functions assigned to *avrPphF* in *Pseudomonas syringae* pv. *phaseolicola*, the cause of bean halo-blight disease. EMBO J. **19:**3204-14.
46. **Tsuda K., and F. Katagiri.** 2010. Comparing signaling mechanisms engaged in pattern-triggered and effector-triggered immunity. Curr. Opin. Plant Biol. **13:**459-65.
47. **Tsuda K., M. Sato, J. Glazebrook, J. D. Cohen, and F. Katagiri.** 2008. Interplay between MAMP-triggered and SA-mediated defense responses. Plant J. **53:**763-75.
48. **Wang X., B. M. Basnayake, H. Zhang, G. Li, W. Li, N. Virk, T. Mengiste, and F. Song.** 2009. The Arabidopsis ATAF1, a NAC transcription factor, is a negative regulator of defense responses against necrotrophic fungal and bacterial pathogens. Mol. Plant Microbe Interact. **22:**1227-38.
49. **Wang Y., J. Li, S. Hou, X. Wang, Y. Li, D. Ren, S. Chen, X. Tang, and J. M. Zhou.** 2010. A *Pseudomonas syringae* ADP-ribosyltransferase inhibits Arabidopsis mitogen-activated protein kinase kinases. Plant Cell **22:**2033-44.
50. **Wilton M., R. Subramaniam, J. Elmore, C. Felsensteiner, G. Coaker, and D. Desveaux.** 2010. The type III effector HopF2Pto targets Arabidopsis RIN4 protein to promote *Pseudomonas syringae* virulence. Proc. Natl. Acad. Sci. USA **107:**2349-54.
51. **Winter D., B. Vinegar, H. Nahal, R. Ammar, G. V. Wilson, and N. J. Provart.** 2007. An “Electronic Fluorescent Pictograph” browser for exploring and analyzing large-scale biological data sets. PLOS ONE

2:e718.

52. **Wood J. R., A. Vivian, C. Jenner, J. W. Mansfield, and J. D. Taylor.** 1994. Detection of a gene in pea controlling nonhost resistance to *Pseudomonas syringae* pv. *phaseolicola*. Mol. Plant Microbe Interact. **7:**534-7.
53. **Yoon H. K., S. G. Kim, S. Y. Kim, and C. M. Park.** 2008. Regulation of leaf senescence by NTL9-mediated osmotic stress signaling in Arabidopsis. Mol. Cells **25:**438-45.
54. **Zhang J., H. Lu, X. Li, Y. Li, H. Cui, C. K. Wen, X. Tang, Z. Su, and J. M. Zhou.** 2010. Effector-triggered and pathogen-associated molecular pattern-triggered immunity differentially contribute to basal resistance to *Pseudomonas syringae*. Mol. Plant Microbe Interact. **23:**940-8.
55. **Zipfel C., S. Robatzek, L. Navarro, E. J. Oakeley, J. D. Jones, G. Felix, and T. Boller.** 2004. Bacterial disease resistance in Arabidopsis through flagellin perception. Nature **428:**764-7.
56. **Zuo J., Q. W. Niu, and N. H. Chua.** 2000. Technical advance: an estrogen receptor-based transactivator XVE mediates highly inducible gene expression in transgenic plants. Plant J. **24:**265-73.

CHAPTER 3

Structure function analysis of the *Pseudomonas syringae* type III effector HopA1 shows similarity to phosphothreonine lyases from animal pathogens

ABSTRACT

Pseudomonas syringae is a plant bacterial pathogen that injects type III effector proteins into plant cells for pathogenicity. One such effector is HopA1, which exists in two distinct classes and these classes are recognized differently by plants. HopA1 found in *P. syringae* pathovar *syringae* 61 ($HopA1_{61}$) but not HopA1 found in *P. syringae* pathovar *tomato* DC3000 ($HopA1_{DC}$) elicits a hypersensitive response in both *Nicotiana tabacum* (tobacco) and Arabidopsis. Moreover, expression of $HopA1_{61}$ but not $HopA1_{DC}$ in the virulent *P. syringae* pv. *tabaci* 11528 converts it to an avirulent strain, indicating that only $HopA1_{61}$ acts as an inducer of effector-triggered immunity in tobacco. Expression of HopA1 in yeast revealed that only $HopA1_{61}$ inhibits yeast growth, suggesting that these HopA1 classes have different virulence activities and/or targets. A DC3000 *hopA1* deletion mutant was only reduced subtly in virulence. In addition, *in planta* expression of $HopA1_{DC}$ allowed increased growth of *P. syringae* strains and inhibition of PAMP-triggered immunity responses. HopA1 shares sequence similarity with the *Photorhabdus luminescens* insecticidal toxin Mcf2. We determined the structure of $HopA1_{61}$ and $HopA1_{DC}$ proteins and both resemble phosphothreonine lyases from animal pathogens. Five conserved residues between HopA1 and Mcf2, which also correspond to solvent exposed residues in the predicted active site, were mutated to alanine. All of these residues were required for the majority of HopA1-dependent phenotypes consistent with HopA1 being an enzyme structurally related to phosphothreonine lyases.

Introduction

Pseudomonas syringae is a Gram-negative bacterial pathogen that causes diseases in a wide range of plants. *P. syringae* is classified into 50 pathovars based on host plant specificity (18). *P. syringae* pv. *tomato* (*Pto*) DC3000 causes bacterial speck on tomato and is also pathogenic on the plant model organism *Arabidopsis thaliana*. *Pto* DC3000 relies on the injection of about 35 type III effector proteins inside plant cells through a type III protein secretion system as a virulence strategy to suppress host immunity (15, 37). The type III secretion system is a nanosyringe used by Gram-negative bacterial pathogens of plants and animals to inject or translocate effectors into host cells for pathogenicity (46). In plants, immunity can be initiated in two ways. One layer of immunity is induced by recognition of pathogen-associated molecular patterns (PAMPs), highly conserved molecules found commonly in nonpathogenic and pathogenic microbes. These include bacterial flagellin, elongation factor EF-Tu, and fungal chitin. PAMPs are recognized by plant pattern-recognition receptors (PRRs) at the cell surface, leading to PAMP-triggered immunity (PTI) (9, 50). A second layer of immunity is induced by recognition of injected type III effectors, which are indirectly recognized by intracellular immune receptors known as resistance (R) proteins. This immunity pathway is known as effector-triggered immunity (ETI) (1). PTI and ETI induce similar immune responses, including oxidative burst, transcriptional reprogramming, mitogen-activated protein kinases (MAPKs) signaling cascades, and callose fortification. However, ETI actives these immune responses in a more robust and prolonged fashion than PTI and usually includes

the hypersensitive response (HR), a programmed cell death at the site of infection to prevent spread of the pathogen (1, 30).

The type III effector inventory is one of the central factors that dictate *P. syringae* host specificity. Homologs of type III effectors that are distributed across several *P. syringae* pathovars represent common effector families (47). One such effector is HopA1 (previously named HrmA or HopPsyA). HopA1 was the first *P. syringae* effector known to be active inside plant cells eliciting an HR and was first isolated from *P. syringae* pv. *syringae* 61 from cosmid pHIR11, which allowed *Escherichia coli* and other nonpathogenic bacteria to elicit an HR in plants (2, 26, 27). HopA1 is present in several *P. syringae* pathovars including *tomato*, *lachrymans* and *actinidiae* (2, 26, 40). HopA1 from *P. syringae* pv. *syringae* 61 ($HopA1_{61}$) causes an HR in *Nicotiana* species and in *A. thaliana* ecotype Ws-0, but not in Col-0 (2, 22). Interestingly, expression of $HopA1_{61}$ in *Pto* DC3000 triggers resistance in *A. thaliana* ecotypes Col-0 and Ws-0 and this resistance is dependent on enhanced disease susceptibility 1 (EDS1) (22). EDS1 is a resistance regulator required for immunity mediated by Toll/Interleukin-1 receptor (TIR) nucleotide-binding site (NBS) leucine-rich repeat (LRR) R proteins (21). The TIR-NBS-LRR R protein RPS6 in Arabidopsis recognizes $HopA1_{61}$ (32) whereas the R protein that recognizes $HopA1_{61}$ in *Nicotiana* spp. has not been identified.

The function of the majority of type III effectors to disrupt host processes and promote virulence remains to be elucidated. However, enzymatic activities of a subset of *P. syringae* type III effectors have been determined; these activities

include mono-ADP-ribosyltransferases, cysteine proteases, E3 ligases, protein tyrosine phosphatases and phosphothreonine lyases (7, 17, 20). The enzymatic activity of HopA1 is not known. Nevertheless it shares sequence similarity with the N-terminal region of the bacterial toxin makes caterpillars floppy 2 (Mcf2) first described in *Photorhabdus luminescens* (53), but also found in other *Photorhabdus*, *Vibrio* and *Providencia* species. Besides the domain with homology to HopA1, Mcf2 shares similarities with two other toxins: toxin B (CdtB) from *Clostridium difficile* and RTX-repeat containing cytotoxin from *Vibrio vulnificus* (53).

Here we show that $HopA1_{DC}$ contributes weakly to *P. syringae* virulence. Unlike $HopA1_{61}$, $HopA1_{DC}$ does not induce ETI in Arabidopsis and tobacco but suppresses PAMP-induced oxidative burst and cell wall fortification. We identified that an N-terminal portion of $HopA1_{61}$ is recognized in Arabidopsis while a C-terminal portion is recognized in tobacco. We report the structure of $HopA1_{DC}$ covering residues 122-380. The structure of HopA1 resembles phosphothreonine lyases from animal pathogens and site-directed mutations in the putative active site residues abrogate HopA1-dependent phenotypes.

Initial characterization of the T3E HopA1 was done by Dr. Ming Guo, a research assistant professor in Dr. James R. Alfano's research group at the Center for Plant Science Innovation and the Department of Plant Pathology, University of Nebraska, Lincoln, NE.

Results

HopA1$_{61}$, but not HopA1$_{DC}$, acts as an avirulence protein in tobacco and Arabidopsis. Because HopA1$_{61}$ is recognized by tobacco and Arabidopsis inducing ETI (.i.e., an avirulence protein), we wanted to determine the extent that HopA1$_{DC}$ could induce ETI. Plasmid constructs containing *hopA1$_{61}$* or *hopA1*$_{DC}$ were transformed into a nonpathogenic *P. fluorescence (Pf)* strain carrying cosmid pLN1965, which encodes a functional *P. syringae* type III secretion system (24). Tobacco and *A. thaliana* ecotype Ws-0 were syringe-infiltrated with *Pf*(pLN1965+*hopA1*$_{61}$) or *Pf*(pLN1965+*hopA1*$_{DC}$) and monitored for the development of an HR. As expected *Pf*(pLN1965+*hopA1*$_{61}$) elicited an HR in tobacco or *A. thaliana* Ws-0 within twenty-four hours (Fig. 1A). However, *Pf*(pLN1965+*hopA1*$_{DC}$) was unable to elicit an HR in tobacco or *A. thaliana* Ws-0 (Fig. 1A), suggesting that HopA1$_{DC}$ does not act as an avirulence protein in these plants. Whether a type III effector is an Avr protein can also be evaluated by transient expression *in planta* using agroinfiltrations. In contrast to *Pf*(pLN1965)-delivered HopA1$_{61}$ or HopA1$_{DC}$, we found that *Agrobacterium*-mediated transient expression of both HopA1s induced the HR in tobacco (Fig. S1). Because the *Pf(*pLN1965) delivery system resembles how type III effectors are injected into plant cells in nature, the HR elicited using agroinfiltrations of HopA1$_{DC}$ may be artefactual, possibly due to high expression levels.

To further evaluate the extent that HopA1$_{DC}$ could act as an Avr protein we heterologously expressed it in *P. syringae* pv. *tabaci* (*Pta*) 11528. This strain is virulent in tobacco and when it heterologously expresses HopA1$_{61}$ it converts this

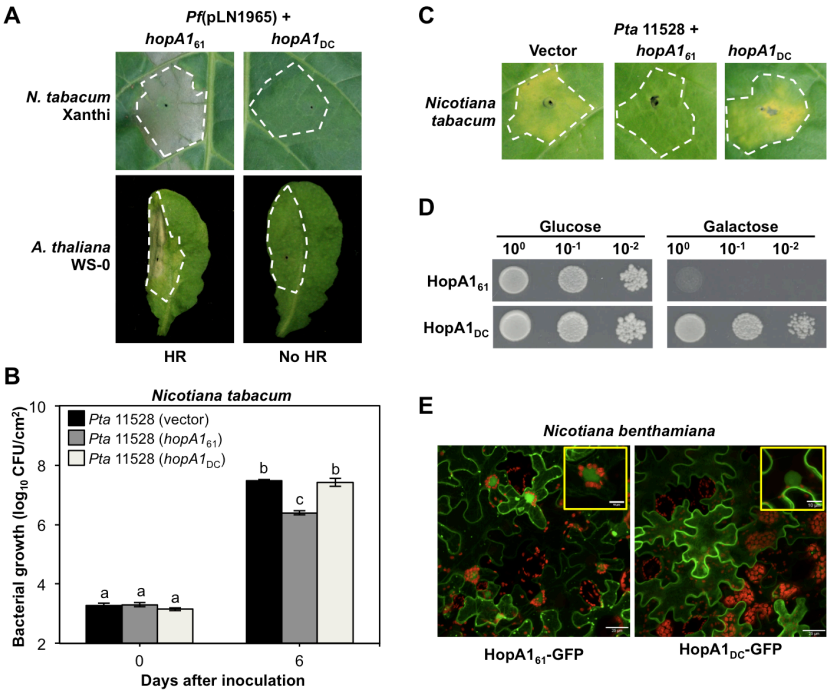

Fig. 1. HopA1 classes have different host recognition and localization, and effector activity in yeast (**A**) *Pseudomonas fluorescens Pf*(pLN1965) strain expressing a functional *P. syringae* type III secretion system and carrying *hopA1*$_{61}$ or *hopA1*$_{DC}$ was syringe-infiltrated into leaves of *Nicotiana tabacum* cultivar Xanthi (tobacco) and *Arabidopsis thaliana* ecotype Ws-0 at cell density of 1 x 10^9 cells mL^{-1}. Leaves were evaluated for the development of a hypersensitive response (HR) and were photographed 48 h after infiltration. Only HopA1$_{61}$ elicited an HR in tobacco and *A. thaliana* Ws-0. (**B**) Tobacco leaves were syringe-inoculated with 1 X 10^5 cells mL^{-1} of *P. syringae* pathovar *tabaci* (*Pta*) 11528 carrying a vector control, *hopA1*$_{61}$ or *hopA1*$_{DC}$. Bacterial growth was measured at 0 and 6 d postinoculation. Different letters indicate that values are significantly different ($p \leq 0.05$); SE bars are shown. *Pta* 11528 expressing HopA1$_{61}$ had reduced bacterial growth compared to *Pta* 11528 (vector or HopA1$_{DC}$). (**C**) Disease symptoms in tobacco infiltrated with *Pta* 11528 strains as described in B. Leaves were photographed 6 d postinoculation. Only HopA1$_{61}$ converted *Pta* 11528 to an avirulent strain in tobacco. (**D**) *Saccharomyces cerevisiae* strain BY4743 harboring the vector pGilda containing *hopA1*$_{61}$ or *hopA1*$_{DC}$ was grown overnight at 30°C in selective media. The cultures were plated on selective media containing glucose or galactose. Photographs were taken 2 d later. Only HopA1$_{61}$ inhibited yeast growth. (**E**) HopA1$_{61}$-GFP and HopA1$_{DC}$-GFP were transiently expressed in *N. benthamiana* by *Agrobacterium*-mediated transformation. GFP was visualized using a confocal microscope 2 d postinfiltration. HopA1$_{61}$-GFP and HopA1$_{DC}$-GFP localize to the plasma membrane, cytoplasm, nucleus and nucleolus of plant cells. Insets display a zoom-in area of a nucleus. Chloroplasts aggregate around the nucleus only in HopA1$_{61}$-GFP micrographs. Experiment was repeated three times with similar results.

strain to an avirulent strain (2). *Pta* 11528 was transformed with a construct carrying *hopA1*$_{61}$ or *hopA1*$_{DC}$. These strains were infiltrated into tobacco, and bacterial growth was evaluated. The growth of *Pta* 11528 expressing HopA1$_{61}$ was restricted (Fig. 1B). However, *Pta* 11528 expressing HopA1$_{DC}$ grew to similar levels as the wild type control (Fig. 1B) and produced disease symptoms on tobacco similar to the wild type control (Fig. 1C). These results are consistent with HopA1$_{61}$, but not HopA1$_{DC}$, acting as an Avr protein in tobacco.

HopA1$_{61}$, but not HopA1$_{DC}$ inhibits yeast growth. We discovered that yeast expressing HopA1$_{61}$ grew poorly in yeast two-hybrid experiments. To investigate if HopA1$_{DC}$ behaved similarly, we expressed both in *Saccharomyces cerevisiae*. We transformed strain BY4743 with constructs containing *hopA1*$_{61}$ or *hopA1*$_{DC}$. Induction of *hopA1*$_{61}$ and *hopA1*$_{DC}$ expression in galactose media showed that HopA1$_{61}$ inhibited yeast growth, but HopA1$_{DC}$ did not cause this phenotype (Fig. 1D). To determine if the phenotype caused by expression of HopA1$_{61}$ was due to growth inhibition or cell death, we used a LIVE/DEAD yeast viability assay. When *hopA1*$_{61}$ or *hopA1*$_{DC}$ were induced in yeast, they had similar number of dead cells (Fig. S2). However, induction of *hopA1*$_{61}$ resulted in fewer number of cells compared to *hopA1*$_{DC}$, indicating that HopA1$_{61}$ inhibits yeast growth.

HopA1 localizes to the plasma membrane, cytoplasm, and nucleus. To test if both HopA1 proteins localized to the same sub-cellular compartment in plants, we delivered *hopA1*$_{61}$ or *hopA1*$_{DC}$ fused at their 3' ends to DNA encoding the green fluorescence protein (GFP) into *N. benthamiana* leaves. Both HopA1$_{61}$-GFP and HopA1$_{DC}$-GFP localized to the plasma membrane, cytoplasm, and the

nucleus and nucleolus of plant cells (Fig. 1E). We noticed two differences in the micrographs of HopA1$_{61}$-GFP compared to HopA1$_{DC}$-GFP. In the HopA1$_{61}$-GFP micrographs there were punctate fluorescent spots mostly along the plasma membrane. Also, several nuclei in the HopA1$_{61}$-GFP expressing cells had chloroplasts surrounding each nucleus. Similar nuclei were observed in plant cells in the mid to late stages of programmed cell death (57).Thus, it is likely that HopA1$_{61}$-GFP is inducing programmed cell death in these cells, which is consistent with it acting as an Avr protein in tobacco, *N. benthamiana*, and Arabidopsis.

An N-terminal portion of HopA1$_{61}$ is recognized in Arabidopsis while a C-terminal portion is recognized in tobacco. We wanted to determine which regions within HopA1$_{61}$ were required for HR induction. Four constructs were made that contains different *hopA1* derivatives that corresponded to different N-terminal truncations and transformed into *Pf*(pLN1965). These strains were infiltrated into tobacco leaves. All of them, with the exception of the full-length HopA1$_{61}$, failed to elicit an HR (Fig. 2A). Interestingly, the first 122 amino acids were sufficient for the elicitation of an HR in *A. thaliana* Ws-0 (Fig. 2A). This suggests that distinct R proteins recognize HopA1$_{61}$ in tobacco and Arabidopsis. The ability of an effector protein to induce ETI results in reduced growth of the bacterial strain from which it is expressed. To confirm that the first 122 amino acids were sufficient for the recognition of HopA1$_{61}$ in Arabidopsis, we transformed *Pto* DC3000 with a plasmid expressing full-length HopA1$_{61}$ (HopA1$_{61(1-375)}$) or N-terminal truncations and determined the extent that these

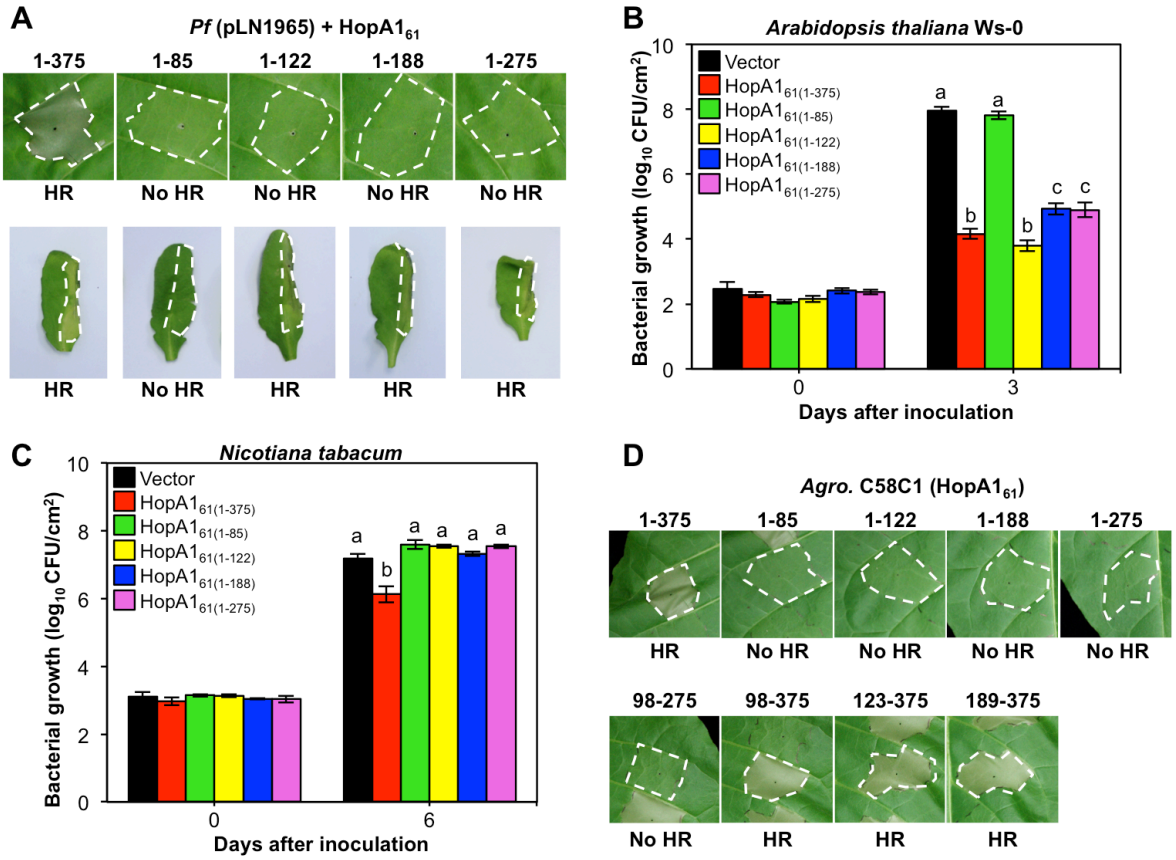

Fig. 2. Different portions of HopA1$_{61}$ are recognized in Arabidopsis and tobacco. (**A**) *Pf*(pLN1965) strains carrying full-length *hopA1*$_{61}$ or N-terminal truncations were syringe-infiltrated into leaves of tobacco and *A. thaliana* Ws-0 at cell density of 1 x 10^9 and 5 x 10^8 cells mL^{-1}, respectively. Leaves were monitored for the development of an HR 2 d postinoculation. None of the N-terminal truncations elicited an HR in tobacco whereas the first 122 amino acids were sufficient for the elicitation of an HR in *A. thaliana* Ws-0. (**B**) *P. syringae* pv. *tomato* DC3000 (*Pto*) strains expressing full-length HopA1$_{61}$ or N-terminal truncations were syringe-infiltrated into leaves of *A. thaliana* Ws-0 at 2 x 10^5 cells mL^{-1}. Bacterial growth was measured at 0 and 3 d after inoculation. Full-length HopA1$_{61}$ and N-terminal truncations that elicited an HR in *A. thaliana* Ws-0 restricted *in planta Pto* DC3000 growth. (**C**) Tobacco leaves were syringe-inoculated with 1 X 10^5 cells mL^{-1} of *Pta* 11528 strains expressing full-length HopA1$_{61}$ or N-terminal truncations. Bacterial growth was measured at 0 and 6 postinoculation. Only *Pta* 11528 expressing full-length HopA1$_{61}$ had reduced growth in tobacco. (**D**) Tobacco leaves were syringe-infiltrated with 8 x 10^8 cells mL^{-1} of *Agrobacterium* C58C1 strains carrying full-length *hopA1*$_{61}$ or truncations. Pictures of infiltrated leaves were taken 2 d postinoculation. Only full length HopA1$_{61}$ and C-terminal truncations (HopA1$_{61(98-375)}$, HopA1$_{61(123-375)}$, and HopA1$_{61(189-375)}$) elicited an HR in tobacco. Experiments repeated twice with similar results. Different letters in B and C indicate statistical differences ($p \leq 0.05$) and SE bars are shown.

strains could grow in *A. thaliana* Ws-0 leaves. As expected, DC3000 expressing full-length HopA1$_{61}$ had reduced growth compared to the DC3000 vector control (Fig. 2B). DC3000 expressing a HopA1$_{61}$ truncation corresponding to the N-terminal 85 amino acids (HopA1$_{61(1-85)}$) had similar growth to the wild type control indicating that this portion does not induce ETI. However, DC3000 strains expressing larger HopA1$_{61}$ truncations that elicited an HR in *A. thaliana* Ws-0 had similar growth to DC3000 expressing the full-length HopA1$_{61}$.

Consistent with these results, *in planta* transgenic expression of full-length HopA1$_{61}$ or the N-terminal truncation corresponding to the N-terminal 122 amino acids (HopA1$_{61(1-122)}$) induced an HR-like cell death in Arabidopsis but not in the *rps6-1* mutant (Fig. S3). This confirms that full-length HopA1$_{61}$ and HopA1$_{61(1-122)}$ are recognized in Arabidopsis in an RPS6-dependent manner. To confirm that N-terminal truncations of HopA1$_{61}$ are not recognized in tobacco, *Pta* 11528 carrying the full-length *hopA1$_{61}$* or one of the truncations were infiltrated into tobacco leaves and *in planta* bacterial growth was determined. Consistent with our earlier results, none of the N-terminal HopA1$_{61}$ truncations restricted *Pta* 11528 growth or altered disease symptom production (Fig. 2C and Fig. S4). Altogether, these data indicate that the N-terminal 122 amino acids of HopA1$_{61}$ are sufficient to induce ETI in Arabidopsis but not in tobacco.

Since N-terminal truncations of HopA1$_{61}$ are not recognized in tobacco, we made additional HopA1$_{61}$ truncation constructs in an *Agrobacterium* binary vector that corresponded to different regions of HopA1$_{61}$. These constructs were transformed into *Agrobacterium* C58C1 and HopA1 truncations were transiently

expressed in tobacco. We found that three HopA1$_{61}$ C-terminal truncations (HopA1$_{61(98-375)}$, HopA1$_{61(123-375)}$ and HopA1$_{61(189-375)}$) elicited an HR in tobacco (Fig. 2D), indicating that a C-terminal portion of HopA1$_{61}$ contained with HopA1$_{61(189-375)}$ was sufficient to elicit an HR in tobacco. To further confirm these results, transgenic *A. thaliana* Ws-0 plants expressing full-length HopA1$_{61}$, HopA1$_{61(1-122)}$, and two C-terminal truncations (HopA1$_{61(98-375)}$ and HopA1$_{61(123-375)}$) that were recognized in tobacco were made. Dexamethasone (DEX)-inducible expression of these HopA1$_{61}$ derivatives resulted in lethality only when full-length HopA1$_{61}$ and the N-terminal truncation HopA1$_{61(1-122)}$ were induced, but not with the C-terminal truncations HopA1$_{61(98-375)}$ and HopA1$_{61(123-375)}$ (Fig. S5). Collectively these data indicate that N-terminal 122 amino acids of HopA1$_{61}$ is sufficient to induce ETI in Arabidopsis whereas the C-terminal truncation HopA1$_{61(189-375)}$ was sufficient to induce ETI in tobacco.

HopA1 contributes subtly to *P. syringae* virulence. To determine the contribution that HopA1 makes to virulence, a *Pto* DC3000 *hopA1* mutant was made. We measured bacterial growth of *Pto* DC3000 and the *hopA1* mutant in *A. thaliana* Col-0. The *hopA1* mutant was slightly reduced in growth *in planta* compared to wild type *Pto* DC3000 (Fig. 3A). Introduction of wild type *hopA1* into the DC3000 *hopA1* mutant complemented the reduced growth phenotype. To determine if stably expressed HopA1$_{DC}$ allowed wild type *Pto* DC3000 or the type III defective DC3000 *hrcC* mutant to grow better we made transgenic plants expressing HopA1$_{DC}$ (HopA1$_{DC}$-HA) after induction with DEX. Wild type DC3000 and the DC3000 *hrcC* mutant both grew slightly better in transgenic plants

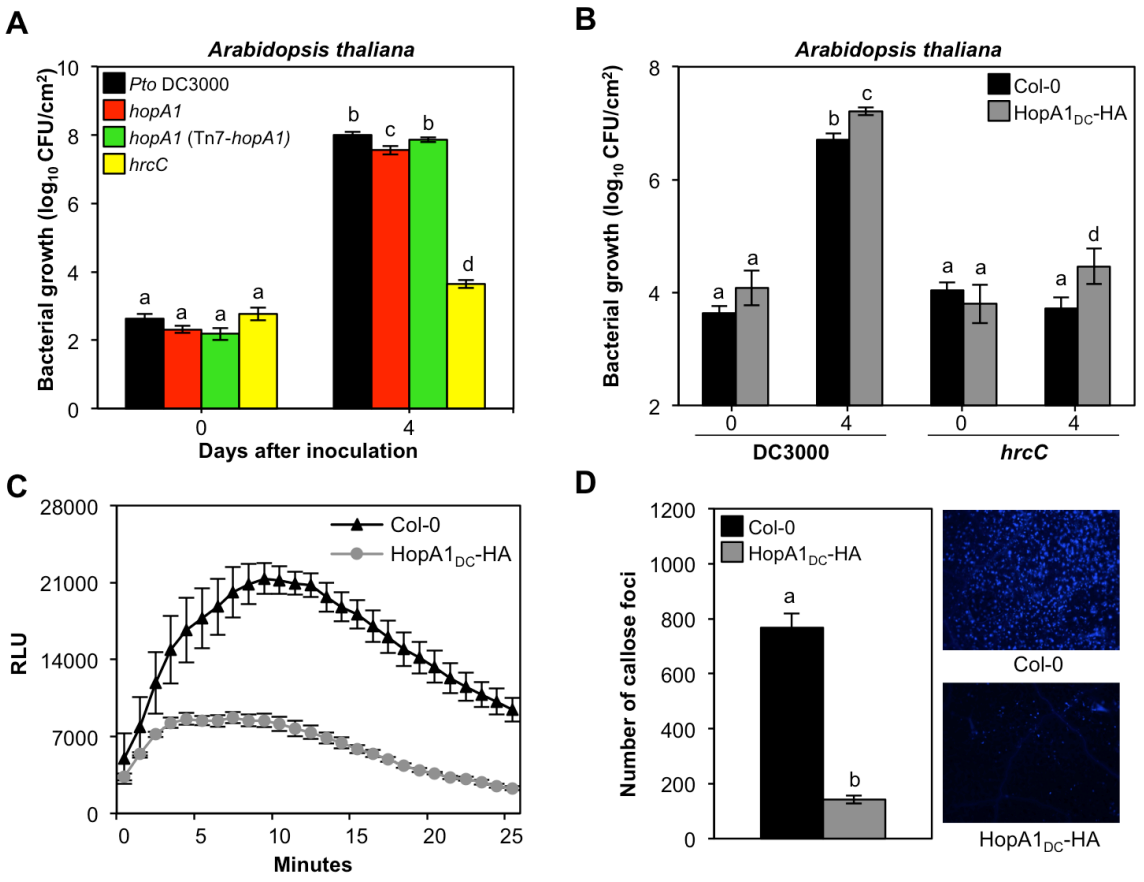

Fig. 3. HopA1 contributes subtly to *P. syringae* virulence and suppresses PTI. (**A**) *A. thaliana* Col-0 plants were syringae-inoculated with 2 X 10^5 cells mL^{-1} of *Pto* DC3000, the *hopA1* mutant, complemented *hopA1* mutant [*hopA1* (Tn7-*hopA1*)], or the type III secretion defective *hrcC* mutant. Bacterial growth was measured at 0 and 4 d postinoculation. The growth of the *hopA1* mutant was slightly reduced compared to wild type *Pto* DC3000. (**B**) Wild type Col-0 and dexamethasone (DEX)-inducible transgenic plants expressing $HopA1_{DC}$-HA were sprayed with 30 µM DEX. Twenty-four hours later plants were syringe-inoculated with 2 X 10^5 cells mL^{-1} of *Pto* DC3000 or the *hrcC* mutant. Bacterial growth numbers were counted at 0 and 4 d after inoculation. Both strains grew slightly better in transgenic plants expressing $HopA1_{DC}$-HA. Different letters indicate values that are significantly different ($p \leq 0.05$) and SE bars are shown. (**C**) Wild type Col-0 and $HopA1_{DC}$-HA expressing plants were sprayed with 30 µM DEX. Leaf disks were harvested 24 h later and the reactive oxygen species (ROS) burst (reported in relative light units, RLU) was measured for 30 min after treatment with 1 µM flg22 in the luminol derivative L-012 buffer. $HopA1_{DC}$ suppressed flg22-induced ROS production *in planta*. (**D**) Twenty-four h after 30 µM DEX treatment plants were infiltrated with 10 µM flg22. Leaves were harvested 16 h later, stained with aniline blue and callose foci were enumerated. $HopA1_{DC}$ suppressed flg22-induced callose deposition. Letters "a" and "b" are statistically different ($p \leq 0.05$). Standard error values are indicated as mean ± SE. Each experiment was repeated three times with similar results.

expressing HopA1$_{DC}$-HA than they did in wild type Col-0 plants (Fig 3B). This data indicates that HopA1$_{DC}$ contributes to the virulence of *Pto* DC3000.

HopA1 suppresses PAMP-triggered ROS production and callose deposition. To determine if HopA1$_{DC}$ was capable of suppressing Arabidopsis plant immunity, transgenic plants expressing HopA1$_{DC}$-HA were assessed for their ability to suppress two main PTI responses: ROS production and callose deposition in the cell wall. We measured ROS production in wild type Col-0 and HopA1$_{DC}$-HA expressing plants after treatment with flg22, a peptide derived from the flagellin PAMP. Transgenic plants expressing HopA1$_{DC}$-HA treated with flg22 have reduced ROS production compared to wild type Col-0 plants (Fig. 3C). Moreover, transgenic plants expressing HopA1$_{DC}$-HA treated with flg22 also exhibited reduced callose deposition compared to wild type Col-0 plants (Fig. 3D). These data indicates that HopA1$_{DC}$ suppresses PTI responses.

The structure of the HopA1 C-terminal domain has similarities to phosphothreonine lyases from animal pathogens. To gain insight into the potential function of HopA1, Alexander U. Singer and Alexei Savchenko (Department of Chemical Engineering and Applied Chemistry, University of Toronto, Toronto, Ontario, Canada) undertook its structural characterization. The recombinant expression of a HopA1$_{DC}$ fragment encompassing residues 122 to 380 (HopA1$_{DC(122-380)}$) yielded a soluble polypeptide of the correct molecular mass supporting the notion that this part of HopA1$_{DC}$ forms a distinct domain. The structure of HopA1$_{DC(122-380)}$ fragment was solved to 2.3 Å resolution by the single-wavelength anomalous dispersion (SAD) technique using a

selenomethionine-enriched protein sample. The final model contained all $HopA1_{DC}$ residues from 122 to 380, with the exception of residues 201, 202 and 380, which appear disordered. The model shows good stereochemistry, with no residues giving backbone torsion angles in the disallowed region of the Ramachandran plot (Table 3). The overall structure of $HopA1_{DC(122-380)}$ adopts a α/β fold with seven β strands (β1 – β7) forming an antiparallel β-sheet and nine α-helices (α1 – α9). The two most N-terminal and C-terminal α-helices (α1-α2 and α8-α9 respectively) form a four-helix bundle capping the central β-sheet, while the rest of the α-helices (α3- α7) shield the β-sheet from one side (Fig. 4A).

A search for structural homologues using the DALI server (25) demonstrated that the $HopA1_{DC(122-380)}$ structure shares significant similarity with the structures of the *Shigella* type III effector OspF (PDB 3I0U, Z-scores 8.5) and its homologues SpvC from *Salmonella* (PDB 2Z8M, Z-score 8.4) and VirA from *Chromobacterium violaceum* (3BO6, Z-core 8). The $HopA1_{DC(122-380)}$ and OspF structures superimpose with rms deviation of 3.2 Å over 134 Ca atoms that correspond primarily to the central β-sheet and to the helices α6 and α7 in the $HopA1_{DC(122-380)}$ structure (Fig. 4B). Interestingly, the four-helix bundle in the $HopA1_{DC(122-380)}$ structure does not have a matching partner in OspF/SpvC/VirA structures.

The OspF/SpvC/VirA family of effectors has been characterized as phosphothreonine lyases that promote the irreversible removal of the phosphate moiety from the phosphothreonine residue in the activation loop of host MAP kinases (36, 59). The active site of these proteins was located within the large

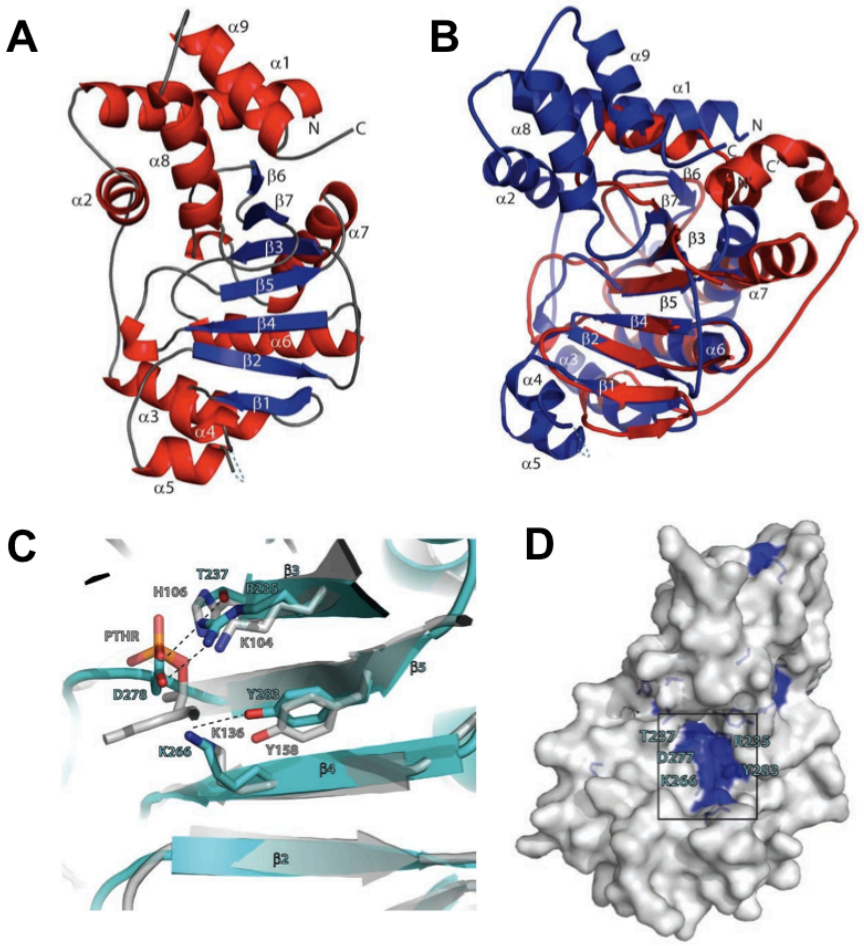

Fig. 4. Structure of HopA1$_{DC(122-380)}$ has similarity to the structure of SpvC phosphothreonine lyase. (**A**) Ribbon diagram of HopA1$_{DC(122-380)}$. Secondary elements are colored (red helices, blue beta strands and gray turns) and labeled, as well as the position of the N- and C-terminus. (**B**) Superimposition of HopA1$_{DC(122-380)}$ (blue) with *Salmonella* SpvC phosphotreonine lyase (PDB 2Z8M) (red). Similar to A, the N- and C-terminus of SpvC is denoted N' and C', respectively. (**C**) Close-up of the alignment between HopA1$_{DC(122-380)}$ and the SpvC/phosphopeptide complex (PDB code 2Q8Y) in a similar position and orientation as A. The ribbons of HopA1$_{DC}$ and SpvC are colored cyan and white, respectively, and the five residues in HopA1$_{DC(122-380)}$ targeted for mutation and their corresponding residues in SpvC are emphasized by a stick representation and labeled. The position of K136 (an Ala in PDB 2Q8Y) was modeled to the conformation present in apo-SpvC structures. (**D**) Semi-transparent surface representation of HopA1$_{DC(122-380)}$ in which five conserved residues are highlighted as sticks and shaded blue on an otherwise white surface.

open groove formed by the central β-sheet, which adapts a “cupped hand” shape (Fig. 4B). The HopA1$_{DC(122-380)}$ structure also features a large open groove in the central β-sheet formed by strands β3, β4 and β5 and by the loop between the β7 strand and the α8 helix (Figs. 4A-B). Further analysis of this groove in the HopA1$_{DC(122-380)}$ structure demonstrated that it harbors a significant number of residues conserved among HopA1 alleles (Fig. S6). Specifically, residues R235, T237, K266, D278 and Y283, are completely conserved among HopA1 homologues as well as in Mcf2 toxins, and are co-localized at the bottom of the central groove (Figs. 4C and S6). Superimposition of the HopA1$_{DC(122-380)}$ structure with the structures of the SpvC and OspF effectors demonstrated that these conserved HopA1$_{DC}$ residues correspond to the functionally important residues in the phosphothreonine lyase active site (Figure 4C). In particular R235, K266, and Y283 in HopA1$_{DC}$ correspond to SpvC K104, K136, and Y158, respectively. The HopA1$_{DC}$ T237 residue corresponds to H106 of SpvC, while the HopA1$_{DC}$ D278 residue side chain occupies the position corresponding to the phosphate group of the phosphothreonine in the SpvC-phosphopeptide complex structure. The SpvC H106, K136, Y158 and K104 residues and their analogues in OspF are directly involved in catalysis and substrate binding (59), suggesting that the corresponding HopA1 residues may be part of the catalytic and/or binding site in this protein. We also determined the structure of an analogous region of HopA1$_{61}$ and this structure looked nearly identical to HopA1$_{DC(122-380)}$ (Fig. S11).

Taken together our structural analysis demonstrated that the HopA1$_{DC(122-380)}$ fragment represents a distinct domain with a general fold similar to that of OspF and SpvC type III effectors. The similarity between HopA1 and OspF/SpvC structures extends into the arrangement of specific residues co-localized in the open groove formed by the central β-sheet in each of these protein structures. Considering the critical role of conserved residues for the OspF/SpvC phosphothreonine lyase activity and that the five HopA1$_{DC}$ residues are also solvent exposed (Fig. 4D), we speculate that these residues in HopA1$_{DC}$ form part of this protein active site.

Residues in the putative active site of HopA1 are required for HopA1-dependent phenotypes. The structural analysis presented above suggested that the HopA1$_{DC(122-380)}$ domain may possess enzymatic activity similar to the phosphothreonine lyase activity of OspF and SpvC effectors. General *in vitro* enzymatic assays using a library of phosphopeptide substrates did not reveal any significant phosphothreonine lyase activity for the full-length HopA1$_{DC}$ and HopA1$_{DC(122-380)}$ fragment (not shown). Individual alanine substitutions of active site residues in OspF or SpvC effectors abrogated their activity *in vivo* (59). Thus, we sought to test the effect of site-directed mutations in the putative HopA1 active site. Accordingly, HopA1$_{DC}$ residues R235, T237, K266, D278 and Y283 and HopA1$_{61}$ residues R231, T233, K262, D274, and Y279 were individually substituted to alanine by site-directed mutagenesis. First we tested the extent that the HopA1$_{61}$ site-directed mutation derivatives could elicit an HR in tobacco and inhibit yeast growth. The five HopA1$_{61}$ site-directed mutation derivatives

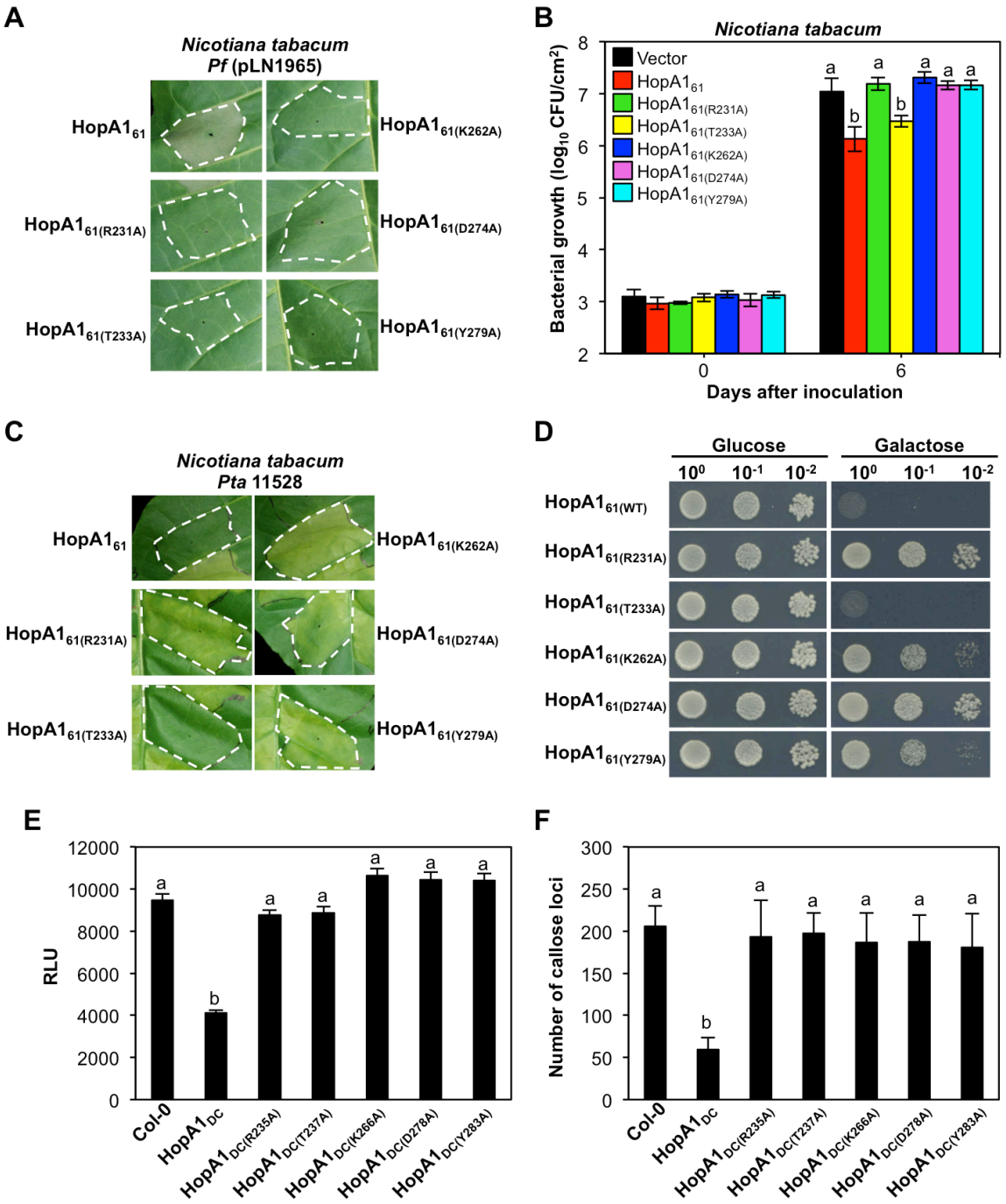

Fig. 5. Solvent exposed residues in the putative active site of HopA1 are required for the HopA1-dependent phenotypes (**A**) *Pf*(pLN1965) strain carrying wild type *hopA1*$_{61}$ or site-directed mutants were syringe-infiltrated into tobacco leaves at cell density of 1 x 10^9 cells mL^{-1}. Leaves were evaluated for the development of an HR and photographed 48 hours after infiltration. All five HopA1$_{61}$ residues were required for the elicitation of an HR in tobacco. (**B**) Tobacco leaves were syringe-infiltrated with 1 X 10^5 cells mL^{-1} of *Pta* 11528

strains expressing HopA1$_{61}$ or site-directed mutation derivatives and bacterial growth was monitored at 0 and 6 d after inoculation. All five HopA1$_{61}$ residues, except T233, were required to convert *Pta* 11528 to an avirulent strain. (**C**) Disease symptoms in tobacco infiltrated with *Pta* 11528 strains described in B. Leaves were photographed 6 d postinoculation. The residue T233 was not required for the avirulence function of HopA1$_{61}$. (**D**) Yeast strain BY4743 expressing wild type *hopA1*$_{61}$ or site-directed mutants was grown overnight at 30°C in selective media. The cultures were plated in selective media containing glucose or galactose. Photographs were taken 2 days later. All but one HopA1$_{61}$ residues were required to inhibit yeast growth. (**E**) The ROS production was assessed in wild type Col-0 and transgenic plants expressing wild type HopA1$_{DC}$ or site-directed mutants after treatment with 1 µM flg22. All five HopA1$_{DC}$ residues were required for the suppression of flg22-induced ROS production. (**F**) Wild type Col-0 and transgenic plants expressing wild type HopA1$_{DC}$ or site-directed mutants were infiltrated with 10 µM flg22. The plant tissue was harvested 16 h later, stained with aniline blue and callose foci were enumerated using Image J software. All five HopA1$_{DC}$ residues were required for the suppression of flg22-induced callose deposition.

were transformed into *Pf*(pLN1965) strain and infiltrated into tobacco leaves. All five HopA1$_{61}$ site-directed mutants were unable to elicit an HR (Fig. 5A). *Pta* 11528 was also transformed with constructs containing genes corresponding to the wild type HopA1$_{61}$ and each site-directed mutant and these strains were infiltrated into tobacco to determine how well they grew in tobacco. We found that strains expressing all of the site-directed mutants, with the exception of HopA1$_{61(T233A)}$, grew and produced wildfire disease symptoms similar to the wild type *Pta* 11528 control (Figs. 5B-C). We observed similar results when the HopA1$_{61}$ site-directed mutants were expressed in yeasts to evaluate the extent that these residues were required for the HopA1$_{61}$-dependent growth restriction phenotype. All HopA1$_{61}$ site-directed mutants, except HopA1$_{61(T233A)}$, failed to exhibit the growth restriction phenotype (Fig. 5D). Therefore, these conserved solvent exposed residues were all required for the elicitation of the HR in tobacco and, with the exception of residue T233, were required for HopA1$_{61}$-dependent yeast growth inhibition and converting *Pta* 11528-tobacco interaction to an incompatible interaction.

Next we evaluated the extent that these solvent exposed residues were required for HopA1$_{DC}$'s ability to suppress flg22-induced ROS production and callose deposition. Transgenic Arabidopsis plants expressing HopA1$_{DC}$ derivatives with alanine substitution mutations in residues R235, T237, K266, D278, and Y283 lost their ability to suppress flg22-induced ROS production (Fig. 5E) and callose deposition in Arabidopsis (Fig. 5F). Therefore, all of these residues were required for HopA1$_{DC}$'s ability to suppress PTI. We also wanted to

evaluate the requirement of the HopA1$_{DC}$ solvent exposed residues to the virulence of *Pto* DC3000. However, the *hopA1* mutant had a weak virulence phenotype (Fig. 3A) and complementation of the *hopA1* mutant with site directed mutation derivatives would have not been robust enough to evaluate the contribution of these HopA1$_{DC}$ residues to the virulence of *Pto* DC3000.

Discussion

In this study we characterized two classes of the *P. syringae* type III effector HopA1. We found that in contrast to HopA1$_{61}$, HopA1$_{DC}$ does not act as an avirulence protein in tobacco and Arabidopsis (Fig. 1). HopA1 is among the most diverse type III effector families based on its pairwise amino acid diversity and high pairwise nucleotide diversity value (π) compared to π values for housekeeping genes (4). The high degree of diversification in the HopA1 family suggests that HopA1$_{61}$ and HopA1$_{DC}$ have undergone different evolutionary pressures that likely altered their specificity.

The *P. syringae* type III effector family HopZ1 provides an example of how allelic diversification is the result of selective pressures imposed by plant immunity. Members of the HopZ1 family have diversified into three functional allelic variants (HopZ1a, HopZ1b and HopZ1c) and two degenerate alleles (ψHopZ1a and ψHopZ1b) via pathoadaptation in response to plant immunity *(35, 39, 58)*. In this sense, we speculate that HopA1$_{DC}$ has diversified from HopA1$_{61}$ to avoid recognition by host resistance proteins, which further suggests that the HopA1$_{61}$ class of HopA1 is more ancient than the HopA1$_{DC}$ class.

In addition, expression of $HopA1_{DC}$ in yeast does not inhibit growth of yeast cells as $HopA1_{61}$ does (Fig. 1D). In plants we observed that $HopA1_{61}$ elicits an HR as a result of an R protein-mediated recognition and in yeast it inhibits cell growth. Since yeasts lack *R* genes, it is likely that the virulence activity of HopA1 is responsible for the growth inhibition phenotype. The fact that $HopA1_{DC}$ did not inhibit yeast growth suggests that its virulence activity has also diversified from $HopA1_{61}$. The virulence target of $HopA1_{61}$ in yeast and the mechanism of growth inhibition remain to be elucidated.

$HopA1_{61}$ and $HopA1_{DC}$ localized predominately to the plasma membrane. However, significant amounts also were found in the nucleus and nucleolus of plant cells (Fig. 1E). Our data is in agreement with two previous reports that show nuclear localization in mammalian cells of the N-terminal region of the insecticidal toxin Mcf2 that has homology to HopA1 (53) and plasma membrane localization of HopA1 in tomato epidermal cells and yeast cells (48).

We observed that chloroplasts aggregated around the nucleus only when $HopA1_{61}$ was transiently expressed into *N. benthamiana* cells. Mitochondria and chloroplasts have been reported to move on transvacuolar strands to form a ring structure around the nucleus during late stages of programmed cell death (38, 54, 57). Thus, the phenomenon we observed is the result of the $HopA1_{61}$-dependent elicitation of a hypersensitive response, a localized programmed cell death response in plants.

We determined the structure of the C-terminal regions of $HopA1_{DC}$ and $HopA1_{61}$ (Fig. 4A). They share structural similarity to phosphothreonine lyases

from animal pathogens, including *Shigella* OspF, *Salmonella* SpvC and *Chromobacterium* VirA (Fig. 4B). Phosphothreonine lyases irreversibly remove the phosphate from the threonine residue on the activation loop of host MAP kinases, thus rendering the MAPK inactive (36). This post-translational modification is referred as Eliminylation (10). We identified five solvent exposed conserved residues that reside within regions structurally related to the active site of the SpvC and OspF phosphothreonine lyases (Fig. 4C-D) (11, 43, 52). Site-directed mutagenesis of these residues in $HopA1_{DC}$ blocked the ability of $HopA1_{DC}$ to suppress flg22-induced callose deposition and ROS production (Fig. 5E-F). Moreover, site-directed mutagenesis of these residues in $HopA1_{61}$ abrogated the HR production in tobacco (Fig. 5A), the ETI-induced restricted growth of *Pta* 11528 in tobacco, and the yeast growth inhibition phenotype (with the exception of $HopA1_{61(T233A)}$) (Fig. 5B-D). The conservation of the putative active site of $HopA1_{DC}$ and $HopA1_{61}$ and their requirement for HopA1-dependent phenotypes *in planta* and yeast, are consistent with HopA1 being a phosphothreonine lyase or a related enzyme.

It has been reported that HopA1 targets the immunity regulator EDS1 (6). However we did not find any interaction of HopA1 with EDS1 in a yeast two-hybrid assay (Fig. S10). Even though EDS1 could be a potential target of HopA1, is not known to be a phosphorylated protein. We therefore could not directly test the phosphothreonine lyase enzymatic activity of HopA1 using EDS1 as a substrate.

The fact that HopA1$_{61}$ elicits an HR in tobacco and *A. thaliana* Ws-0 prompted us to identify the avirulence portion of HopA1$_{61}$. We found that the C-terminus of HopA1$_{61}$ elicited an HR in tobacco (Fig. 2), indicating that the virulence domain of HopA1$_{61}$ resides in its C-terminus. This agrees with the fact that the virulence domain of type III effectors usually resides in their C-terminal region, after the secretion signal domain and/or type III chaperone-binding domain. However, we found that the N-terminus of HopA1$_{61}$ was recognized in *A. thaliana* Ws-0, and to our surprise, the first 122 amino acids were sufficient to elicit an HR (Fig. 2A). The type III secretion signal resides in the N-termini of type III effectors (13, 45). The structure of the HopA1$_{DC}$ secretion signal and chaperone-binding site bound to its type III chaperone has been elucidated and correspond to the N-terminus 102 amino acids (29). Since the majority of the N-terminal 122 amino acids contain the type III secretion signal and chaperone-binding site, it is not likely that the virulence domain resides in this region. This suggests that instead HopA1$_{61}$ is directly recognized by the R protein RPS6 in *A. thaliana* Ws-0. Direct recognition of HopA1$_{61}$ in Arabidopsis is unusual because the majority of type III effectors are indirectly recognized by R proteins as explained in the guard model (16). This model states that R proteins monitor modifications executed by type III effectors on their target proteins. Therefore, R proteins indirectly recognized virulence activities of type III effectors to initiate effector-triggered immunity. We concluded that while HopA1$_{61}$ is indirectly recognized in tobacco, is recognition in Arabidopsis is direct.

Materials and methods

DNA manipulation. Plasmids used in this work and primers used for cloning are listed in tables 1 and 2. For cloning of entry vectors we used Gateway technology (Invitrogen). *Pf*(pLN1965), *Pto* DC3000 or *Pta* 11528 strains were transformed with pLN615 derivatives; *Agrobacterium* C58C1 was transformed with pLN462, pK7FWG2, or pTA7002 derivatives; and *S. cerevisiae* strains were transformed with pGilda, pGBKT7 or pGADT7 derivatives. A DC3000 *hopA1* mutant was generated using the pKnockout-Ω suicide vector pLN23. For the complementation of the *hopA1* mutant, pLN1028 was recombined into the Tn7 vector pLN2992. The resulting Tn7 construct was integrated into the chromosome of the *hopA1* mutant strain. $HopA1_{DC}$ and $HopA1_{61}$ site-directed mutations were generated following the QuikChange® site-directed mutagenesis instructions (Stratagene).

Plant assays. For pathogenicity assays, *P. syringae* strains were grown overnight at 30°C on King's B (KB) plates with appropriate antibiotics and resuspended in 5 mM MES (morpholinoethanesulfonic acid, pH 5.6). Bacterial suspensions of 1 X 10^5 and 2 X 10^5 cells ml^{-1} were syringe-infiltrated into leaves of tobacco and Arabidopsis, respectively. Four leaf discs of 0.8-cm^2 were excised for each infiltrated *P. syringae* strain at the indicated time points. Samples were ground in 250 µL of sterile water, 10-fold serially diluted, and plated on KB agar plates with appropriate antibiotics. Bacterial numbers were counted 2 days later. Statistical differences were calculated using one-way ANOVA.

For HR assays, Pf(pLN1965) strains were grown overnight in KB medium at 30°C. Cells were resuspended in 5 mM MES and bacterial suspensions of 1 x 10^9 and 5 x 10^8 cells ml^{-1} were infiltrated into leaves of tobacco and *A. thaliana* Ws-0, respectively. The development of the HR was monitored and infiltrated leaves were photographed after 2 days.

ROS and callose assays were done as described before (8). The ROS burst was determined by counting photons from L-012-mediated chemiluminescence using a Synergy 2 luminometer. Luminescence was recorded every minute for 30 minutes. Callose stained leaves were analyzed under a Zeiss Axionplan 2 imaging microscope. The number of callose deposits were counted using ImageJ software.

Generation of transgenic Arabidopsis plants. To make DEX-inducible transgenic plants, *A. thaliana* Col-0 plants were transformed with *Agrobacterium* C58C1 strains carrying pTA7002 derivatives using the floral dip method (5). Transgene expression was confirmed with immunoblots using anti-HA primary antibodies (Roche, Basal, Switzerland) and anti-rat immunoglobulin G alkaline-phosphatase conjugates as secondary antibodies (Sigma Chemical Co., St. Louis, U.S.A.). Proteins on immunoblots were visualized using the CDP-Star chemiluminescence detection kit (Tropix, Bedford, MA, U.S.A.) followed by autoradiography. For plant assays with DEX-inducible transgenic Arabidopsis lines, plants were sprayed a day before with 30 μM DEX.

Yeast assays. The pGILDA derivatives were transformed into *S. cerevisiae* using the lithium acetate transformation method (23). Yeast strains were grown

overnight at 30°C in SD (-His) glucose non-inducing liquid culture. Yeast cultures were normalized at OD_{600} of 0.1 and 10-fold serially diluted. Five microliters of each dilution were dropped onto SD (-His/Glucose) or SD (-His/Galactose) plates. Cells were incubated at 30°C for 2 days and photographed.

For yeast viability assay, yeast strain EGY48 harboring the vector pGilda containing *hopA1*$_{DC}$, *hopA1*$_{61}$ or vector control was grown overnight at 30°C in SD (-His) glucose non-inducing liquid media. Yeast cultures were normalized to an OD_{600} of 0.2 in SD (-His) galactose-inducing media and incubated for 3 hours in a 30°C shaker. Cultures were resuspended in 1 mL of sterile water containing 2% D-(+)-glucose and 10 mM Na-HEPES (pH 7.2) and stained with 10 μM FUN® 1 and 25 μM Calcofluor™ White MR2 (LIVE/DEAD Yeast viability kit, Cat. No. L7009, Molecular Probes). Cells were incubated at 30°C in the dark for 30 minutes and visualized with a fluorescence microscope.

For yeast two-hybrid analyses, strain Y187 carrying pGBKT7:*eds1* was mated to strain AH109 carrying pGADT7:*hopA1* in a mating plate (yeast extract peptone dextrose, YPD). To test interaction of target proteins mated yeast strains were grown in SD (-Trp-Leu) media overnight. Cells were plated in quadruple dropout (QDO) selective media. Cells were photographed 2 days later.

Confocal microscopy. *Agrobacterium* strains were transiently expressed in leaves of *N. benthamiana* as described previously (28). Infiltrated leaves were visualized 45 hours later using a Nikon A1 confocal mounted on a Nikon 90i compound microscope with sequential imaging at 488 nm excitation and 500-550

nm emission wavelengths (GFP). For chloroplast autofluorescence, 640.6 nm excitation and 663-738 nm emission wavelengths were used.

Protein purification and structure determination. Fragments of *hopA1*$_{DC}$ were cloned into the expression plasmid p15TvLic, and the plasmid was transformed into *E. coli* BL21(DE3)-RIPL (Stratagene). Following determination of solubility in test expression studies, *E. coli* cells carrying a construct that contained *hopA1*$_{DC(122\text{-}380)}$ were then cultured in 1 L of Luria Broth (LB) medium at 37°C to an OD_{600} of approximately 1.2, and 0.4 mM IPTG was added to induce protein expression. After induction, cells were incubated overnight with shaking at 25°C. Cells were harvested by centrifugation, disrupted by sonication, and the insoluble material was removed by centrifugation. The HopA1$_{DC}$ C-terminal domain was purified from the supernatant using Ni-NTA affinity chromatography. Tobacco Etch Virus (TEV) protease was added to the eluted protein, and the mixture was dialyzed at 4°C overnight in a buffer with 10 mM HEPES (pH 7.5), 300 mM NaCl and 0.5 mM TCEP, concentrated to 69 mg ml^{-1} and stored at -70°C. Crystallization trials were performed using hanging-drop vapor diffusion with an optimized sparse matrix crystallization screen (33). The crystal used for data collection (see Table 3) was grown from crystallization liquor containing 0.2 N disodium tartrate, 25% PEG3350, and 0.1 M Tris (pH 8.5) and cryoprotected with N-paratone oil (Hampton Research) and flash-frozen in liquid nitrogen prior to data collection.

Data Collection, Structure Determination and Refinement. The structure of HopA1$_{DC(122\text{-}380)}$ was determined by SAD phasing using a crystal derived from

selenomethionine-enriched protein at the peak wavelength l=0.97943. Diffraction data was collected at 100°K at beamline 19-ID. Diffraction data were integrated and scaled using HKL3000 (41). Positions of heavy atoms were found using SHELXD (49), followed by solvent flattening using SHELXE (51), which was in turn used to automatically build an initial model using ArpWARP (44), which was all used within the CCP4 program suite (12). The model was then improved by alternate cycles of manual building and water-picking using COOT (19) and restrained refinement against a maximum-likelihood target with 5% of the reflections randomly excluded as an R_{free} test set. All refinement steps were performed using REFMAC (42) in the CCP4 program suite. Only three residues (residues 201, 202 and 380) of the 260-residue fragment of $HopA1_{DC}$ were omitted from the model due to poor electron density. The final model contains one molecule of $HopA1_{DC(122-380)}$ and 150 solvent molecules and was refined to an R_{work} of 16.3% and R_{free} of 22.7%, including TLS parameterization (55, 56). Data collection, phasing and structure refinement statistics are summarized in Table 3. The Ramachandran plot generated by PROCHECK (34) showed very good stereochemistry overall with 100% of the residues in the most favored and additional allowed regions (see Table 3).

Supplemental figures and tables

Supplemental Table 1. Plasmids used in this study

Plasmid	Description	Primers used	Reference
pENTR/D-TOPO	Gateway entry vector, Km^r		Invitrogen
pGilda	Yeast expression vector under a galactose-inducible promoter, Ap^r		Clontech
pK7FWG2	Gateway binary vector with a C-terminal GFP gene for fusions, Sp^r		(31)
pLN23	pKnockout-Ω derivative carrying *hopA1*$_{DC}$, Sp^r		(28)
pLN458	Entry vector carrying *hopA1*$_{61}$, Km^r		(28)
pLN462	pPZP212 derivative gateway destination binary vector containing 35S promoter and HA tag for C-terminal fusion, Sp^r		(28)
pLN474	pLN462 derivative carrying *hopA1*$_{61}$, Sp^r		This work
pLN479	pLN462 derivative carrying *hopA1*$_{DC}$, Sp^r		This work
pLN532	pGilda derivative carrying *hopA1*$_{DC}$, Ap^r	P0474, P0475	This work
pLN533	pGilda derivative carrying *hopA1*$_{61}$, Ap^r	P0963, P0964	This work
pLN615	pML123 derivative gateway destination binary vector containing an HA tag for C-terminal fusion, Gm^r		(24)
pLN666	pK7FWG2 derivative carrying *hopA1*$_{61}$, Sp^r		This work
pLN668	pK7FWG2 derivative carrying *hopA1*$_{DC}$, Sp^r		This work
pLN714	Entry vector carrying *hopA1*$_{61}$ with its cognate chaperone *shcA*$_{61}$ and a ribosome binding site, Km^r		(28)
pLN1028	Entry vector carrying *hopA1*$_{DC}$ with its cognate chaperone *shcA*$_{DC}$ and a ribosome binding site, Km^r		(24)

pLN1323	pLN615 derivative carrying *hopA1*$_{DC}$ with its cognate chaperone *shcA*$_{DC}$ and a ribosome binding site, Gm^r		(24)
pLN1658	pGADT7 derivative gateway destination vector containing GAL4 activation domain, *LEU2*, Ap^r		Tian, F (unpublished)
pLN2232	pGBKT7 derivative gateway destination vector containing GAL4 DNA binding domain, *TRP1*, Sp^r		Tian, F (unpublished)
pLN2992	pUC18T-mini-Tn7 derivative destination vector containing C-terminal HA tag and *avrPto1* promoter, Ap^r Cm^r Gm^r		(14)
pLN3203	Entry vector carrying *hopA1*$_{DC}$, Km^r	P2844, P2845	This work
pLN3207	pTA7002 derivative carrying *hopA1*$_{61}$, Km^r	P4117, P2843	This work
pLN3208	pTA7002 derivative carrying *hopA1*$_{DC}$, Km^r	P4187, P2845	This work
pLN3873	Entry vector carrying *hopA1*$_{61(1-188)}$, Km^r	P0787, P3476	This work
pLN3874	Entry vector carrying *hopA1*$_{61(189-375)}$, Km^r	P3477, P2880	This work
pLN3886	Entry vector carrying *hopA1*$_{61(R231A)}$, Km^r	P3577, P3578	This work
pLN3887	Entry vector carrying *hopA1*$_{61(K262A)}$, Km^r	P3581, P3582	This work
pLN3888	Entry vector carrying *hopA1*$_{61(D274A)}$, Km^r	P3583, P3584	This work
pLN3889	Entry vector carrying *hopA1*$_{61(Y279A)}$, Km^r	P3585, P3586	This work
pLN3936	Entry vector carrying *hopA1*$_{DC(R235A)}$, Km^r	P3564, P3565	This work
pLN3937	Entry vector carrying *hopA1*$_{DC(K266A)}$, Km^r	P3568, P3569	This work
pLN3938	Entry vector carrying *hopA1*$_{DC(D278A)}$, Km^r	P3570, P3571	This work
pLN3939	Entry vector carrying *hopA1*$_{DC(Y283A)}$, Km^r	P3572, P3573	This work
pLN3956	Entry vector carrying *hopA1*$_{DC(T237A)}$, Km^r	P3566, P3567	This work
pLN4000	Entry vector carrying *hopA1*$_{61(T233A)}$, Km^r	P3579, P3580	This work

pLN4006	pGilda derivative carrying *hopA1*$_{61(R231A)}$, Ap^r	P0963, P0964	This work
pLN4007	pGilda derivative carrying *hopA1*$_{61(T233A)}$, Ap^r	P0963, P0964	This work
pLN4008	pGilda derivative carrying *hopA1*$_{61(K262A)}$, Ap^r	P0963, P0964	This work
pLN4009	pGilda derivative carrying *hopA1*$_{61(D274A)}$, Ap^r	P0963, P0964	This work
pLN4010	pGilda derivative carrying *hopA1*$_{61(Y279A)}$, Ap^r	P0963, P0964	This work
pLN4126	Entry vector carrying *shcA*$_{61}$ *hopA1*$_{61(R231A)}$ with a ribosome binding site, Km^r	P3577, P3578	This work
pLN4127	Entry vector carrying *shcA*$_{61}$ *hopA1*$_{61(T233A)}$ with a ribosome binding site, Km^r	P3579, P3580	This work
pLN4128	Entry vector carrying *shcA*$_{61}$ *hopA1*$_{61(K262A)}$ with a ribosome binding site, Km^r	P3581, P3582	This work
pLN4129	Entry vector carrying *shcA*$_{61}$ *hopA1*$_{61(D274A)}$ with a ribosome binding site, Km^r	P3583, P3584	This work
pLN4130	Entry vector carrying *shcA*$_{61}$ *hopA1*$_{61(Y279A)}$ with a ribosome binding site, Km^r	P3585, P3586	This work
pLN4135	pLN615 derivative carrying *shcA*$_{61}$ *hopA1*$_{61(R231A)}$ with a ribosome binding site, Gm^r		This work
pLN4136	pLN615 derivative carrying *shcA*$_{61}$ *hopA1*$_{61(T233A)}$ with a ribosome binding site, Gm^r		This work
pLN4137	pLN615 derivative carrying *shcA*$_{61}$ *hopA1*$_{61(K262A)}$ with a ribosome binding site, Gm^r		This work
pLN4138	pLN615 derivative carrying *shcA*$_{61}$ *hopA1*$_{61(D274A)}$ with a ribosome binding site, Gm^r		This work
pLN4139	pLN615 derivative carrying *shcA*$_{61}$ *hopA1*$_{61(Y279A)}$ with a ribosome binding site, Gm^r		This work
pLN4186	Entry vector carrying *hopA1*$_{61(1-85)}$, Km^r	P0787, P3669	This work
pLN4186b	pLN462 derivative carrying *hopA1*$_{61(1-85)}$, Sp^r		This work
pLN4187	Entry vector carrying *hopA1*$_{61(1-122)}$, Km^r	P0787, P3670	This work

pLN4374	Entry vector carrying *shcA*$_{61}$ *hopA1*$_{61(1-85)}$ with a ribosome binding site, Km^r	P1082, P3669	This work
pLN4374b	pLN615 derivative carrying *shcA*$_{61}$ *hopA1*$_{61(1-85)}$ with a ribosome binding site, Gm^r		This work
pLN4424	pLN615 derivative carrying *hopA1*$_{61}$ with its cognate chaperone *shcA*$_{61}$ and a ribosome binding site, Gm^r		This work
pLN4437	Entry vector carrying *hopA1*$_{61(98-275)}$, Km^r	P3834, P3835	This work
pLN4437b	pLN462 derivative carrying *hopA1*$_{61(98-275)}$, Sp^r		This work
pLN4438	Entry vector carrying *hopA1*$_{61(98-375)}$, Km^r	P3834, P2880	This work
pLN4438b	pLN462 derivative carrying *hopA1*$_{61(98-375)}$, Sp^r		This work
pLN4514	Entry vector carrying *shcA*$_{61}$ *hopA1*$_{61(1-188)}$ with a ribosome binding site, Km^r	P1082, P3476	This work
pLN4515	Entry vector carrying *shcA*$_{61}$ *hopA1*$_{61(1-275)}$ with a ribosome binding site, Km^r	P1082, P3835	This work
pLN4516	pLN615 derivative carrying *shcA*$_{61}$ *hopA1*$_{61(1-188)}$ with a ribosome binding site, Gm^r		This work
pLN4517	pLN615 derivative carrying *shcA*$_{61}$ *hopA1*$_{61(1-275)}$ with a ribosome binding site, Gm^r		This work
pLN4550	pLN2992 derivative carrying *hopA1*$_{DC}$ with its cognate chaperone *shcA*$_{DC}$ and a ribosome binding site, Ap^r Gm^r		This work
pLN4642	pTA7002 derivative carrying *hopA1*$_{61(98-375)}$, Km^r	P4118, P2843	This work
pLN4644	pTA7002 derivative carrying *hopA1*$_{DC(R235A)}$, Km^r	P4187, P2845	This work
pLN4645	pTA7002 derivative carrying *hopA1*$_{DC(T237A)}$, Km^r	P4187, P2845	This work
pLN4646	pTA7002 derivative carrying *hopA1*$_{DC(K266A)}$, Km^r	P4187, P2845	This work
pLN4647	pTA7002 derivative carrying *hopA1*$_{DC(D278A)}$, Km^r	P4187, P2845	This work
pLN4648	pTA7002 derivative carrying *hopA1*$_{DC(Y283A)}$, Km^r	P4187, P2845	This work

pLN4909	Entry vector carrying *eds1*, Km^r	P4878, P5385	This work
pLN4912	Entry vector carrying $hopA1_{61(123-375)}$, Km^r	P4442, P2880	This work
pLN4914	pLN462 derivative carrying $hopA1_{61(123-375)}$, Sp^r		This work
pLN4925	pGADT7 derivative carrying $hopA1_{DC}$, Ap^r		This work
pLN4941	pGBKT7 derivative carrying *eds1*, Sp^r		This work
pLN4954	pTA7002 derivative carrying $hopA1_{61(1-122)}$, Km^r	P4117, P4443	This work
pLN4955	pTA7002 derivative carrying $hopA1_{61(123-375)}$, Km^r	P4440, P2843	This work
pLN5207	pLN462 derivative carrying $hopA1_{61(1-122)}$, Sp^r		This work
pLN5208	pLN462 derivative carrying $hopA1_{61(189-375)}$, Sp^r		This work
pLN5326	Entry vector carrying $shcA_{61}$ $hopA1_{61(1-122)}$ with a ribosome binding site, Km^r	P1082, P3670	This work
pLN5327	pLN615 derivative carrying $shcA_{61}$ $hopA1_{61(1-122)}$ with a ribosome binding site, Gm^r		This work
pLN5630	pLN462 derivative carrying $hopA1_{61(1-188)}$, Sp^r		This work
pLN5631	Entry vector carrying $hopA1_{61(1-275)}$, Km^r	P0787, P3835	This work
pLN5632	pLN462 derivative carrying $hopA1_{61(1-275)}$, Sp^r		This work
pTA7002	Binary vector for glucocorticoid-inducible expression containing a C-terminal HA tag, Km^r		(3)

Supplemental Table 2. Primers used in this study

Primer	Sequence
P0474	5’-TTGAATTCATGAACCCCATTCAGTCAC-3’
P0475	5’-TTCTCGAGTCAAGTGCGCACCTCAATGCC-3’
P0787	5’-CACCTTAGCGTAAGGAGCTAACAATGAACCC-3’
P0963	5’-TTGAATTCGGCAGACGCTTCGATCTG-3’
P0964	5'-TTCTCGAGTCAGTTTCGCGCCCTGAGC-3'
P1082	5’-CACCCACCCGACAAATCCACAG-3’
P2843	5’-GCTCACTAGTTCAAGCGTAATCTGGAACATCGTATGGGTAG TTTCGCGCCCTGAGCGCCG-3’
P2844	5’-CACCCTCGAGATGAACCCCATTCAGTCACG-3’
P2845	5’-GCTCACTAGTTCAAGCGTAATCTGGAACATCGTATGGGTAT TTCGTGTTTCGAAGGGCCG-3’
P2880	5’-GTTTCGCGCCCTGAGCGCC-3’
P3476	5’-CTGCGGGGCGTATGATAAGG-3’
P3477	5’-CACCATGATCCATGATGATCGGGAAGAG-3’
P3564	5’-CGAGAAGATAAGAATCAAGGGGCATTGACCATTGGCGTGC AACCC-3’
P3565	5’-GGGTTGCACGCCAATGGTCAATGCCCCTTGATTCTTATCTT CTCG-3’
P3566	5’-GATAAGAATCAAGGGCGATTGGCCATTGGCGTGCAACCCC AATAT-3’
P3567	5’-ATATTGGGGTTGCACGCCAATGGCCAATCGCCCTTGATTCT TATC-3’
P3568	5’-GAAAGTGCAATCACGCATGGCGCAGTAATAGGCCCCGCCT GCCAC-3’
P3569	5’-GTGGCAGGCGGGGCCTATTACTGCGCCATGCGTGATTGCA CTTTC-3’
P3570	5’-GCCTGCCACGGCCAAATGACCGCTTCGGCAGTTTTGTATAT CAAC-3’
P3571	5’-GTTGATATACAAAACTGCCGAAGCGGTCATTTGGCCGTGGC AGGC-3’
P3572	5’-ATGACCGATTCGGCAGTTTTGGCTATCAACGGTGATGTTGC AAAG-3’
P3573	5’-CTTTGCAACATCACCGTTGATAGCCAAAACTGCCGAATCGG TCAT-3’
P3577	5’-GCACCTGAGACAAACTCGGGAGCACTTACCATTGGTGTAGA ACCT-3’
P3578	5’-AGGTTCTACACCAATGGTAAGTGCTCCCGAGTTTGTCTCAG GTGC-3’
P3579	5’-GAGACAAACTCGGGACGACTTGCCATTGGTGTAGAACCTAA ATAT-3’
P3580	5’-ATATTTAGGTTCTACACCAATGGCAAGTCGTCCCGAGTTTGT CTC-3’
P3581	5’-CACAAATCTGTGACACAAGGTGCAGTCGTCGGTCCGGCAA

	AATAT-3’
P3582	5’-ATATTTTGCCGGACCGACGACTGCACCTTGTGTCACAGATT TGTG-3’
P3583	5’-GCAAAATATGGCCAGCAAACTGCCTCTGCCATTCTTTACATA AAT-3’
P3584	5’-ATTTATGTAAAGAATGGCAGAGGCAGTTTGCTGGCCATATTT TGC-3’
P3585	5’-CAAACTGACTCTGCCATTCTTGCCATAAATGGTGATCTTGCA AAA-3’
P3586	5’-TTTTGCAAGATCACCATTTATGGCAAGAATGGCAGAGTCAG TTTG-3’
P3669	5’-TTTCTCGTTGAGTACCTGGGC-3’
P3670	5’-TGTCAGTCGGCTGTCGGCAGC-3’
P3834	5’-CACCTTAGCGTAAGGAGCTAACAATGAGACGCTTCG-3’
P3835	5’-AGAGTCAGTTTGCTGGCCATA-3’
P4117	5’-ATGCCTCGAGACCATGGATGAACCCTATCCATGCACGC-3’
P4118	5’-ATGCCTCGAGACCATGGATGAGACGCTTCGATCTGGAG-3’
P4187	5’-ATGCCTCGAGACCATGGATGAACCCCATTCAGTCACG-3’
P4442	5’-CACCATGTCAAAACAGACATTTGCCAG-3’
P4443	5’-GCTCACTAGTTCAAGCGTAATCTGGAACATCGTATGGGTAT GTCAGTCGGCTGTCGGCAG-3’
P4878	5’-CACCATGGCGTTTGAAGCTCTTACC-3’
P5385	5’-GATCCTCGAGGGTATCTGTTATTTCATCCAT-3’

Supplemental Table 3. Data Collection and Refinement Statistics for

$HopA1_{DC(122-380)}$

Data collection	
Space group	$P6_5$
Cell dimensions	
a=*b*, *c* (Å)	80.6, 96.0
Wavelength (Å)	0.97943
Resolution (Å)	50-2.30(2.38-2.30)
R_{merge} (%)[a]	0.105(0.488)
$I/\sigma I$	40.07(7.6)
Completeness (%)	100.0(100.0)
Redundancy	14.7(14.8)
Refinement	
Resolution (Å)	19.78-2.30
No. reflections	15742
R_{work} (%)[b]	16.3
R_{free} (%)[c]	22.7
No. atoms	
Protein	2001
Water	150
Other	5
B-factors (Å^2)	
Overall	38.8
Protein	38.5
Water	42.7
Other	43.8
r.m.s. deviations	
Bond lengths (Å)	0.018
Bond angles (º)	1.66
Ramachandran Plot	
% in Most Favored Regions	91.4
% in Additionally Allowed Regions	8.6
% in Generously Allowed or Disallowed Regions	0

Notes:
Values in parentheses are for the highest-resolution shell.

[a] $R_{merge} = \sum_{hkl} \left| I - \langle I \rangle \right| / \sum_{hkl} I$

[b] $R_{work} = \sum \left| F_{obs} - F_{calc} \right| / \sum \left| F_{obs} \right|$, where F_{obs} and F_{calc} are the observed and the calculated structure factors, respectively.

[c] R_{free} calculated using 5% of total reflections randomly chosen and excluded from the refinement

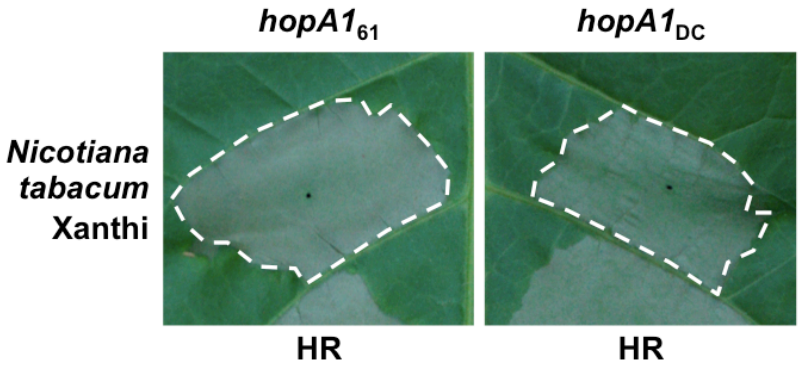

Supplemental Fig. 1. HopA1$_{61}$ and HopA1$_{DC}$ elicit an HR in tobacco when delivered by *Agrobacterium*. HopA1$_{61}$ and HopA1$_{DC}$ were transiently expressed in tobacco by *Agrobacterium*-mediated transformation. Leaves were photographed 2 d postinoculation. Both HopA1$_{61}$ and HopA1$_{DC}$ elicited an HR in tobacco.

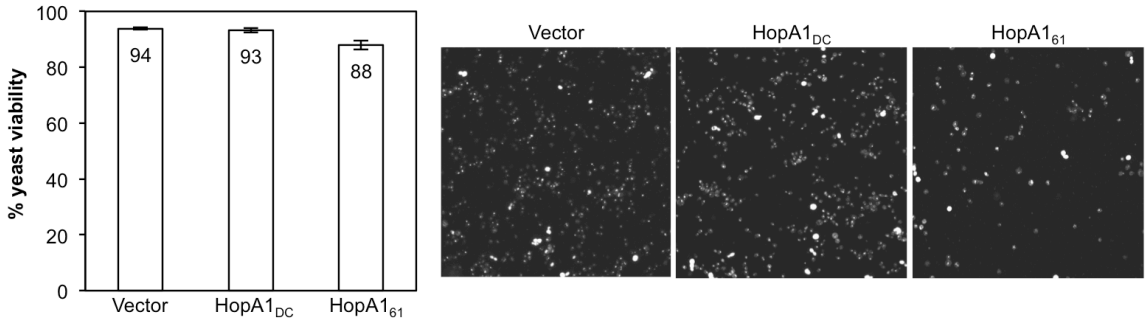

Supplemental Fig. 2. HopA1$_{61}$ inhibits yeast growth but is not lethal. Yeast strain EGY48 expressing *hopA1$_{61}$* or *hopA1$_{DC}$* was grown overnight at 30°C in selective non-inducing media. Cells were induced in galactose media for 3 hours and stained with FUN® 1 and Calcofluor™ White MR2 following the LIVE/DEAD Yeast viability kit and visualized with a fluorescence microscope. Number of dead cells (white cells) and total number of cells were counted using ImageJ software. The number of dead cells was similar when either HopA1$_{61}$ or HopA1$_{DC}$ were expressed in yeast, however there was less number of cells in HopA1$_{61}$ expressing cells. Error bars designate standard error.

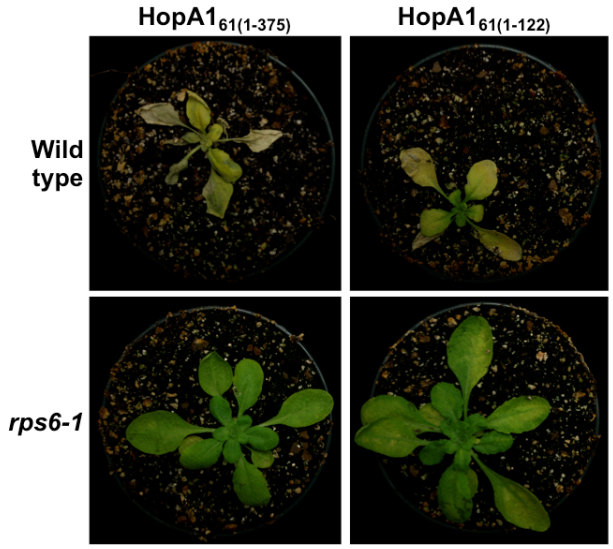

Supplemental Fig. 3. Recognition of HopA1$_{61}$ in Arabidopsis is RPS6-dependent. Wild type Arabidopsis and *rps6-1* mutant plants expressing full-length HopA1$_{61}$ or HopA1$_{61(1-122)}$ in a DEX-inducible manner, were sprayed with 30 μM DEX. Plants were photographed 3 d later. Expression of HopA1$_{61}$ was lethal in wild type Arabidopsis but not in the *rps6-1* mutant.

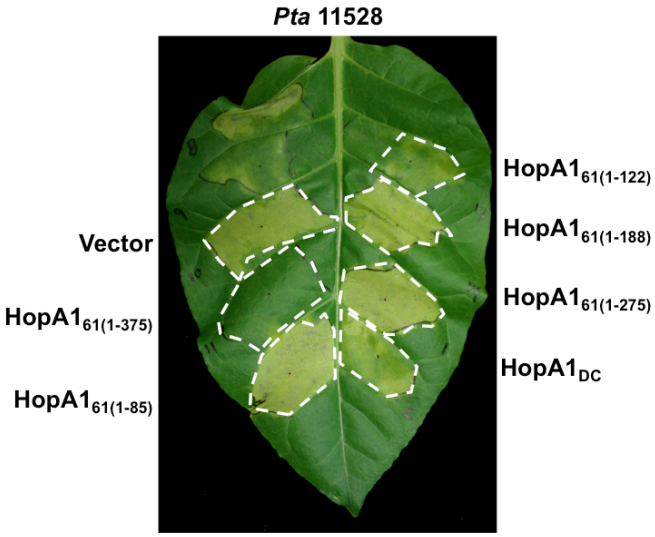

Supplemental Fig. 4. HopA1$_{61}$ converts *Pta* 11528 to an avirulent strain in tobacco. Tobacco leaves were syringe-inoculated with 1 X 10^5 cells mL^{-1} of *Pta* 11528 strains expressing HopA1$_{DC}$, full-length hopA1$_{61}$ or N-terminal truncations. Plants were monitored for the development of disease symptoms and photographed 6 d after inoculation. Only full-length HopA1$_{61}$ restricted development of disease symptoms.

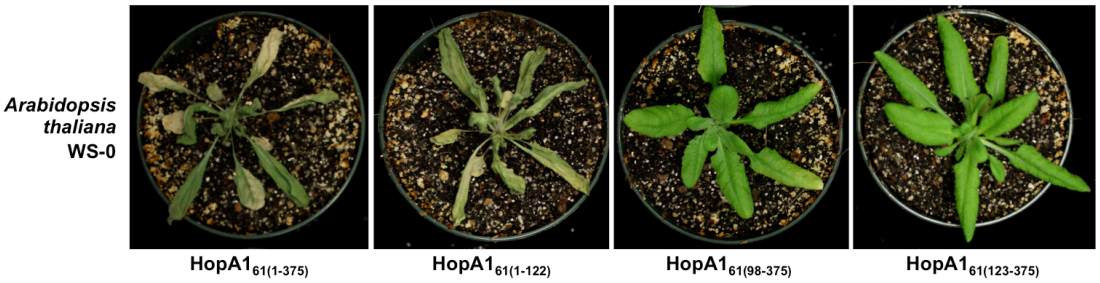

Supplemental Fig. 5. *In planta* expression of full-length HopA1$_{61}$ and an N-terminal truncation, but not C-terminal truncations, caused lethality in Arabidopsis. Transgenic *A. thaliana* Ws-0 plants expressing full-length HopA1$_{61}$, HopA1$_{61(1-122)}$, HopA1$_{61(98-375)}$ and HopA1$_{61(123-375)}$ were induced after 30 μM DEX treatment. Only expression of full-length HopA1$_{61}$ and HopA1$_{61(1-122)}$ were lethal to *A. thaliana* Ws-0.

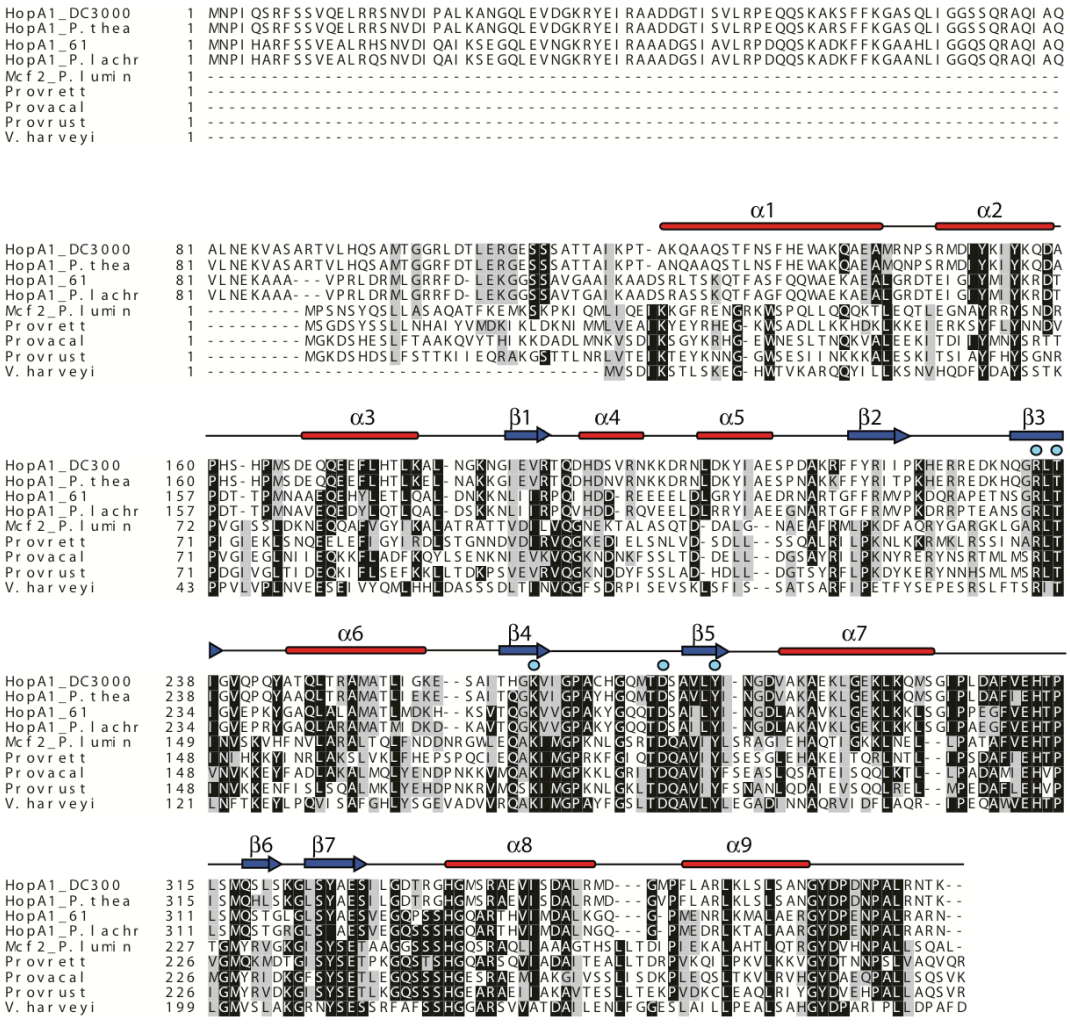

Supplemental Fig. 6. Sequence alignment of HopA1 and Mcf2 alleles. Positions of helices (red cylinders) and beta strand (blue arrows) based on the structure of $HopA1_{DC(122\text{-}380)}$ are shown above the alignment. Residues targeted for site-directed mutagenesis are indicated with cyan circles. The alignment was generated using ClustalX and plotted using BoxShade. The alignment contains the four most divergent HopA1 alleles as well as the region with homology to Mcf2 toxins.

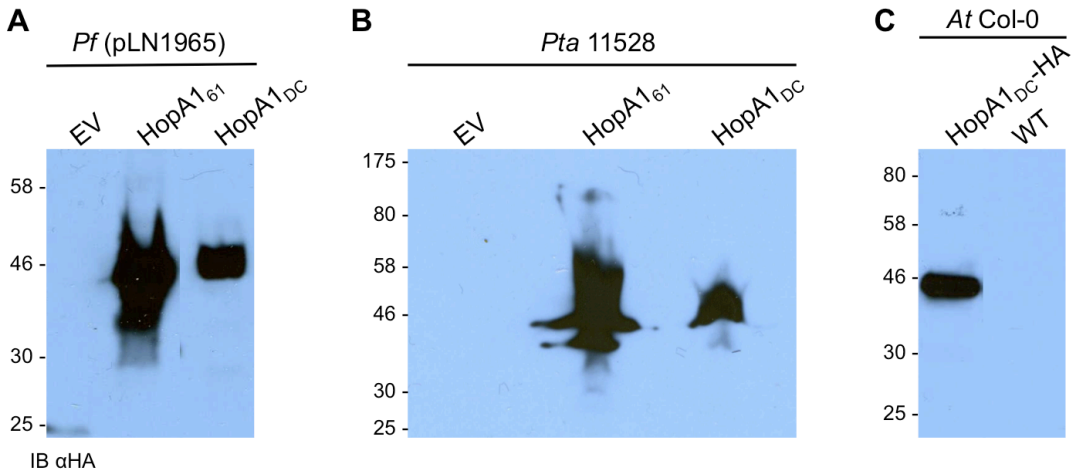

Supplemental Fig. 7. Immunoblots show expression of HopA1$_{61}$ and HopA1$_{DC}$ from bacterial strains and transgenic Arabidopsis. Expression of HopA1$_{61}$ and HopA1$_{DC}$ from *Pf*(pLN1965) (**A**), *Pta* 11528 (**B**), and transgenic Arabidopsis plants (**C**) was confirmed by immunoblots with anti-HA antibody. Expected protein size: HopA1$_{DC}$ or HopA1$_{61}$ = 42 kDa.

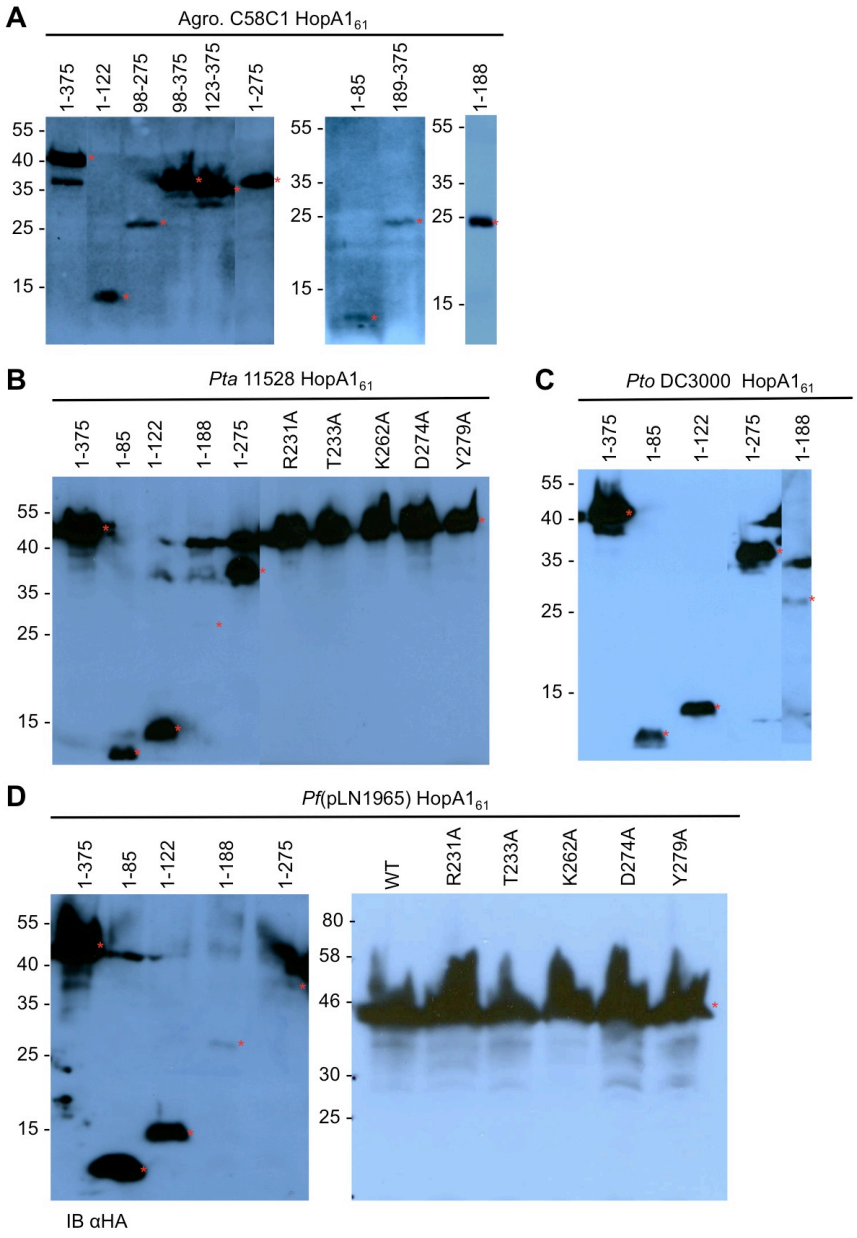

Supplemental Fig. 8. Expression of HopA1$_{61}$ truncations and site-directed mutation derivatives. Immunoblots with anti-HA antibody show expression of HopA1$_{61}$ derivatives from agroinfiltrated *N. benthamiana* leaves (**A**) and from bacterial strains *Pta* 11528 (**B**), *Pto* DC3000 (**C**), and *Pf*(pLN1965) (**D**). Asterisks indicate the expected size for each derivative. Expected protein size: full-length HopA1$_{61}$ or site-directed mutants = 42 kDa; HopA1$_{61(1-85)}$ = 10 kDa; 1 HopA1$_{61(1-122)}$ = 14 kDa; HopA1$_{61(1-188)}$ = 21 kDa; HopA1$_{61(1-275)}$ = 31 kDa; HopA1$_{61(98-275)}$ = 20 kDa; HopA1$_{61(98-375)}$ = 31 kDa; HopA1$_{61(123-375)}$ = 29 kDa; HopA1$_{61(189-375)}$ = 21 kDa.

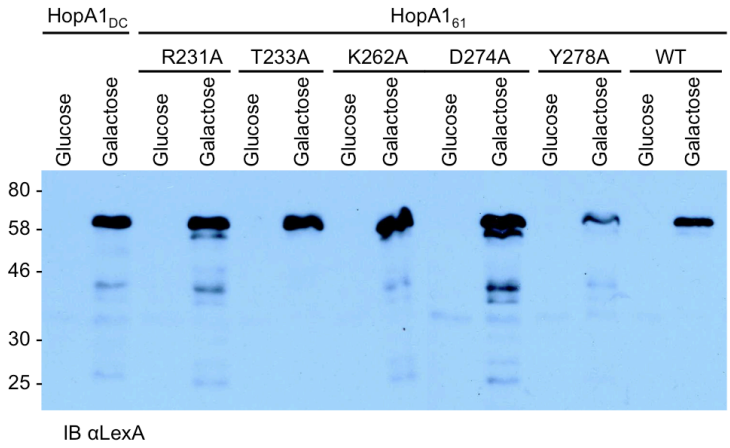

Supplemental Fig. 9. Immunoblots indicate expression of HopA1$_{61}$ site-directed mutants in yeast. Yeast strain BY4743 carrying wild type *hopA1*$_{61}$ or site-directed mutations derivatives were grown at 30°C in selective media containing either glucose or galactose. Immunoblots with anti-LexA antibody confirm expression of each derivative in inducing media.

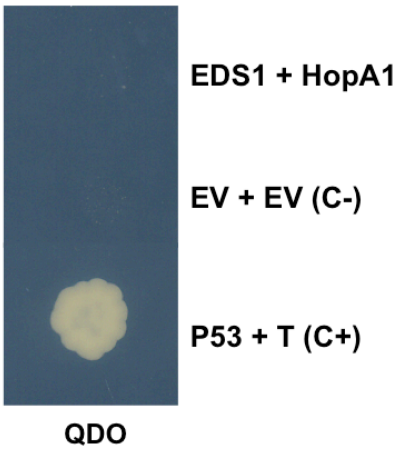

Supplemental Fig. 10. HopA1 does not interact with EDS1. Yeast two-hybrid interaction between EDS1 and $HopA1_{DC}$ did not show growth of yeast strain expressing EDS1 and HopA1 when plated in selective media (Quadruple dropout, QDO).

References

1. **Abramovitch, R. B., J. C. Anderson, and G. B. Martin.** 2006. Bacterial elicitation and evasion of plant innate immunity. Nat. Rev. Mol. Cell Biol. **7:**601-611.
2. **Alfano, J. R., H. Kim, T. P. Delaney, and A. Collmer.** 1997. Evidence that the *Pseudomonas syringae* pv. *syringae hrp*-linked *hrmA* gene encodes an Avr-like protein that acts in an *hrp*-dependent manner within tobacco cells. Mol. Plant Microbe Interact. **10:**580-588.
3. **Aoyama, T., and N. Chua.** 1997. A glucocorticoid-mediated transcriptional induction system in transgenic plants. Plant J. **11:**605-612.
4. **Baltrus, D. A., M. T. Nishimura, A. Romanchuk, J. H. Chang, M. S. Mukhtar, K. Cherkis, J. Roach, S. R. Grant, C. D. Jones, and J. L. Dangl.** 2011. Dynamic evolution of pathogenicity revealed by sequencing and comparative genomics of 19 *Pseudomonas syringae* isolates. PLOS Path. **7:**e1002132.
5. **Bechtold, N., J. Ellis, and G. Pelletier.** 1993. *In planta Agrobacterium* mediated gene transfer by infiltration of adult *Arabidopsis thaliana* plants. C R Acad Sci Paris Life Sci **316:**1194-1199.
6. **Bhattacharjee, S., M. K. Halane, S. H. Kim, and W. Gassmann.** 2011. Pathogen effectors target Arabidopsis EDS1 and alter its interactions with immune regulators. Science **334:**1405-1408.
7. **Block, A., and J. R. Alfano.** 2011. Plant targets for *Pseudomonas syringae* type III effectors: virulence targets or guarded decoys? Curr. Opin. Microbiol. **14:**39-46.
8. **Block, A., T. Y. Toruño, C. G. Elowsky, C. Zhang, J. Steinbrenner, J. Beynon, and J. R. Alfano.** 2013. The *Pseudomonas syringae* type III effector HopD1 suppresses effector-triggered immunity, localizes to the endoplasmic reticulum, and targets the Arabidopsis transcription factor NTL9. New Phytol. **201:**1358-1370.
9. **Boller, T., and G. Felix.** 2009. A renaissance of elicitors: perception of microbe-associated molecular patterns and danger signals by pattern-recognition receptors. Annu. Rev. Plant Biol. **60:**379-406.
10. **Brennan, D. F., and D. Barford.** 2009. Eliminylation: a post-translational modification catalyzed by phosphothreonine lyases. Trends Biochem. Sci. **34:**108-114.
11. **Chen, L., H. Wang, J. Zhang, L. Gu, N. Huang, J. Zhou, and J. Chai.** 2008. Structural basis for the catalytic mechanism of phosphothreonine lyase. Nat. Struct. Mol. Biol. **15:**101-102.
12. **Collaborative Computational Project, N.** 1994. The CCP4 suite: programs for protein crystallography. Acta Crystallogr D **50:**760-763.
13. **Collmer, A., M. Lindeberg, T. Petnicki-Ocwieja, D. J. Schneider, and J. R. Alfano.** 2002. Genomic mining type III secretion system effectors in *Pseudomonas syringae* yields new picks for all TTSS prospectors. Trends Microbiol. **10:**462-469.

14. **Crabill, E., A. Karpisek, and J. R. Alfano.** 2012. The *Pseudomonas syringae* HrpJ protein controls the secretion of type III translocator proteins and has a virulence role inside plant cells. Mol. Microbiol. **85:**225-238.
15. **Cunnac, S., M. Lindeberg, and A. Collmer.** 2009. *Pseudomonas syringae* type III secretion system effectors: repertoires in search of functions. Curr. Opin. Microbiol. **12:**53-60.
16. **Dangl, J. L., and J. D. G. Jones.** 2001. Plant pathogens and integrated defence responses to infection. Nature **411:**826-833.
17. **Deslandes, L., and S. Rivas.** 2012. Catch me if you can: bacterial effectors and plant targets. Trends Plant Sci. **17:**644-655.
18. **Dye, D. W., J. F. Bradbury, M. Goto, A. C. Hayward, R. A. Lelliott, and M. N. Schroth.** 1980. International standards for naming pathovars of phytopathogenic bacteria and a list of pathovar names and pathtype strains. Rev. Plant Pathol **59:**153-168.
19. **Emsley, P., and K. Cowtan.** 2004. Coot: model-building tools for molecular graphics. Acta Crystallogr D **60:**2126-2132.
20. **Feng, F., and J.-M. Zhou.** 2012. Plant-bacterial pathogen interactions mediated by type III effectors. Curr. Opin. Plant Biol. **15:**469-476.
21. **García, A. V., S. Blanvillain-Baufumé, E. P. Huibers, M. Wiermer, G. Li, E. Gobbato, S. Rietz, and J. E. Parker.** 2010. Balanced Nuclear and Cytoplasmic Activities of EDS1 Are Required for a Complete Plant Innate Immune Response. PLOS Path. **6:**e1000970.
22. **Gassmann, W.** 2005. Natural variation in the Arabidopsis response to the avirulence gene *hopPsyA* uncouples the hypersensitive response from disease resistance. Mol. Plant Microbe Interact. **18:**1054-1060.
23. **Gietz, D., A. St. Jean, R. A. Woods, and R. H. Schiestl.** 1992. Improved method for high efficiency transformation of intact yeast cells. Nucleic Acids Res. **20:**1425.
24. **Guo, M., F. Tian, Y. Wamboldt, and J. R. Alfano.** 2009. The majority of the type III effector inventory of *Pseudomonas syringae* pv. *tomato* DC3000 can suppress plant immunity. Mol. Plant Microbe Interact. **22:**1069-1080.
25. **Holm, L., and P. Rosenstrom.** 2010. Dali server: conservation mapping in 3D. Nucleic Acids Res. **38:**W545-549.
26. **Huang, H., S. W. Hutcheson, and A. Collmer.** 1991. Characterization of the hrp cluster from *Pseudomonas syringae* pv. *syringae* 61 and *TnphoA* tagging of genes encoding exported or membrane-spanning Hrp proteins. Mol. Plant Microbe Interact. **4:**469-476.
27. **Huang, H., R. Schuurink, T. P. Denny, M. M. Atkinson, C. J. Baker, I. Yucel, S. W. Hutcheson, and A. Collmer.** 1988. Molecular cloning of a *Pseudomonas syringae* pv. *syringae* gene cluster that enables *Pseudomonas fluorescens* to elicit the hypersensitive response in tobacco plants. J. Bacteriol. **170:**4748-4756.
28. **Jamir, Y., M. Guo, H. Oh, T. Petnicki-Ocwieja, X. Tang, M. Dickman, A. Collmer, and J. R. Alfano.** 2004. Identification of *Pseudomonas syringae*

type III effectors that can suppress programmed cell death in plants and yeast. Plant J. **37:**554-565.

29. **Janjusevic, R., C. M. Quezada, J. Small, and C. E. Stebbin.** 2013. Structure of the HopA1(21-102)-ShcA chaperone-effector complex of *Pseudomonas syringae* reveals conservation of a virulence factor binding motif from animal to plant pathogens. J. Bacteriol. **195:**658-664.
30. **Jones, J. D. G., and J. L. Dangl.** 2006. The plant immune system. Nature **444:**323-329.
31. **Karimi, M., D. Inzé, and A. Depicker.** 2002. GATEWAY^{TM} vectors for *Agrobacterium*-mediated plant transformation. Trends Plant Sci. **7:**193-195.
32. **Kim, S. H., S. I. Kwon, D. Saha, N. C. Anyanwu, and W. Gassmann.** 2009. Resistance to the *Pseudomonas syringae* effector HopA1 is governed by the TIR-NBS-LRR protein RPS6 and is enhanced by mutations in *SRFR1*. Plant Physiol. **150:**1723-1732.
33. **Kimber, M. S., F. Vallee, S. Houston, A. Necakov, T. Skarina, E. Evdokimova, S. Beasley, D. Christendat, A. Savchenko, C. H. Arrowsmith, M. Vedadi, M. Gerstein, and A. M. Edwards.** 2003. Data mining crystallization databases: knowledge-based approaches to optimize protein crystal screens. Proteins **51:**562-568.
34. **Laskowski, R. A., M. W. MacArthur, D. S. Moss, and J. M. Thornton.** 1993. PROCHECK: a program to check the stereochemical quality of protein structures. J Appl Crystallogr **26:**283-291.
35. **Lewis, J. D., W. Abada, W. Ma, D. S. Guttman, and D. Desveaux.** 2008. The HopZ family of *Pseudomonas syringae* type III effectors require myristoylation for virulence and avirulence functions in *Arabidopsis thaliana*. J. Bacteriol. **190:**2880-2891.
36. **Li, H., H. Xu, Y. Zhou, J. Zhang, C. Long, S. Li, S. Chen, J. M. Zhou, and F. Shao.** 2007. The phosphothreonine lyase activity of a bacterial type III effector family. Science **315:**1000-1003.
37. **Lindeberg, M., S. Cartinhour, C. R. Myers, L. M. Schechter, D. J. Schneider, and A. Collmer.** 2006. Closing the circle on the discovery of genes encoding Hrp regulon members and type III secretion system effectors in the genomes of three model *Pseudomonas syringae* strains. Mol. Plant Microbe Interact. **11:**1151-1158.
38. **Lord, C. E., J. N. Wertman, S. Lane, and A. H. Gunawardena.** 2011. Do mitochondria play a role in remodelling lace plant leaves during programmed cell death? BMC Plant Biol. **11:**102.
39. **Ma, W., F. F. T. Dong, J. Stavrinides, and D. S. Guttman.** 2006. Type III effector diversification via both pathoadaptation and horizontal transfer in response to a coevolutionary arms race. PLOS Gen. **2:**2131-2142.
40. **McCann, H. C., E. H. A. Rikkerink, F. Bertels, M. Fiers, A. Lu, J. Rees-George, M. T. Andersen, A. P. Gleave, B. Haubold, M. W. Wohlers, D. S. Guttman, P. W. Wang, C. Straub, J. Vanneste, P. B. Rainey, and M. D. Templeton.** 2013. Genomic analysis of the kiwifruit pathogen

Pseudomonas syringae pv. *actinidiae* provides insight into the origins of an emergent plant disease. PLOS Path. **9:**e1003503.

41. **Minor, W., M. Cymborowski, Z. Otwinowski, and M. Chruszcz.** 2006. HKL-3000: the integration of data reduction and structure solution - from diffraction images to an initial model in minutes. Acta Crystallogr D **62:**859-866.
42. **Murshudov, G. N., A. A. Vagin, and E. J. Dodson.** 1997. Refinement of macromolecular structures by the maximum-likelihood method. Acta Crystallogr D **53:**240-255.
43. **Pei, Q., A. Christofferson, H. Zhang, J. Chai, and N. Huang.** 2011. Computational investigation of the enzymatic mechanisms of phosphothreonine lyase. Biophys. Chem. **157:**16-23.
44. **Perrakis, A., R. Morris, and V. S. Lamzin.** 1999. Automated protein model building combined with iterative structure refinement. Nat. Struct. Biol. **6:**458-463.
45. **Petnicki-Ocwieja, T., D. J. Schneider, V. C. Tam, S. T. Chancey, L. Shan, Y. Jamir, L. M. Schechter, C. R. Buell, X. Tang, A. Collmer, and J. R. Alfano.** 2002. Genomewide identification of proteins secreted by the Hrp type III protein secretion system of *Pseudomonas syringae* pv. *tomato* DC3000. Proc. Natl. Acad. Sci. USA **99:**7652-7657.
46. **Puhar, A., and P. J. Sansonetti.** 2014. Type III secretion system. Curr. Biol. **24:**R784-R791.
47. **Rohmer, L., D. S. Guttman, and J. L. Dangl.** 2004. Diverse evolutionary mechanisms shape the type III effector virulence factor repertoire in the plant pathogen *Pseudomonas syringae*. Genetics **167:**1341-1360.
48. **Salomon, D., Y. Guo, L. N. Kinch, N. V. Grishin, K. H. Gardner, and K. Orth.** 2013. Effectors of animal and plant pathogens use a common domain to bind host phosphoinositides. Nature Communications **4:**2973.
49. **Schneider, T. R., and G. M. Sheldrick.** 2002. Substructure solution with SHELXD. Acta Crystallogr D **58:**1772-1779.
50. **Schwessinger, B., and C. Zipfel.** 2008. News from the frontline: Recent insights into PAMP-triggered immunity in plants. Curr. Opin. Plant Biol. **11:**389-395.
51. **Sheldrick, G. M.** 2008. A short history of SHELX. Acta Crystallogr A **64:**112-122.
52. **Smith, G. K., Z. Ke, A. C. Hengge, D. Xu, D. Xie, and H. Guo.** 2009. Active-site dynamics of SpvC virulence factor from *Salmonella typhimurium* and density functional theory study of phosphothreonine lyase catalysis. J. Phys. Chem. **113:**15327-15333.
53. **Waterfield, N. R., P. J. Daborn, A. J. Dowling, G. Yang, M. Hares, and R. H. ffrench-Constant.** 2003. The insecticidal toxin makes caterpillars floppy 2 (Mcf2) shows similarity to HrmA, an avirulence protein from a plant pathogen. FEMS Microbiol. Lett. **229:**265-270.
54. **Wertman, J., C. E. Lord, A. N. Dauphinee, and A. H. Gunawardena.** 2012. The pathway of cell dismantling during programmed cell death in

lace plant (*Aponogeton madagascariensis*) leaves. BMC Plant Biol. **12:**115.

55. **Winn, M. D., M. N. Isupov, and G. N. Murshudov.** 2001. Use of TLS parameters to model anisotropic displacements in macromolecular refinement. Acta Crystallogr D **57:**122-133.
56. **Winn, M. D., G. N. Murshudov, and M. Z. Papiz.** 2003. Macromolecular TLS refinement in REFMAC at moderate resolutions. Methods Enzymol. **374:**300-321
57. **Wright, H., W. G. van Doorn, and A. H. L. A. N. Gunawardena.** 2009. *In vivo* study of developmental programmed cell death using the lace plant (*Aponogeton madagascariensis*; Aponogetonaceae) leaf model system. Am. J. Bot. **96:**865-876.
58. **Zhou, H., R. Morgan, D. S. Guttman, and W. Ma.** 2009. Allelic variants of the *Pseudomonas syringae* type III effector HopZ1 are differentially recognized by plant resistance systems. Mol. Plant Microbe Interact. **22:**176-189.
59. **Zhu, Y., H. Li, C. Long, L. Hu, H. Xu, L. Liu, S. Chen, D. C. Wang, and F. Shao.** 2007. Structural insights into the enzymatic mechanism of the pathogenic MAPK phosphothreonine lyase. Mol. Cell **28:**899-913.

CHAPTER 4

The *Pseudomonas syringae* type III effector HopA1 targets Arabidopsis type 2C protein phosphatases to suppress plant immunity

ABSTRACT

The Gram-negative plant pathogenic bacterium *Pseudomonas syringae* causes diseases in many crops. For pathogenicity, *P. syringae* relies on a type III protein secretion system to inject type III effector proteins (T3Es) into plant cells. T3Es are the main virulence determinants of this pathogen and are known to hijack the plant immune system, both pathogen-associated molecular pattern-triggered immunity and effector-triggered immunity pathways. *P. syringae* pv. *tomato* DC300 (*Pto* DC3000) injects about 35 type III effectors into plants to promote bacterial virulence.

One of them is the effector HopA1 that suppresses immune responses and its structure resembles phosphothreonine lyases from animal pathogens. Here I show that HopA1 interacts with PLL4 and PLL5, two Arabidopsis type 2C protein phosphatases from clade C (PP2C-C) involved in leaf development. I demonstrate that the interaction occurs at the plasma membrane of plant cells. PLL4 and PLL5 act as negative regulators of plant immunity and they are induced after pathogen infection. While Arabidopsis plants with T-DNA insertions in *PLL4* and *PLL5* are more resistant to bacterial infections and have stronger immune responses, *in planta* expression of these phosphatases results in plants more susceptible to bacterial infections with reduced immune responses. This is the first report of members of the PP2C-C family being targeted by a pathogen effector to suppress plant immunity.

Introduction

P. syringae is a plant pathogenic Gram-negative bacterium that infects a wide range of crops. There are about 50 *P. syringe* pathovars (pv.) that are capable of infecting specific plant species, therefore *P. syringe* is a host-specific pathogen (25). *Pto* DC3000 infects tomato (*Solanum lycopersicum)* causing bacterial speck disease, and is also pathogenic on the model plant *Arabidopsis thaliana*. To become a successful pathogen, DC3000 relies on the injection of about 35 virulence proteins known as type III effector proteins into plant cells, which are injected through a type III protein secretion system (1). To counteract pathogenic infections, plants evolved two ways to trigger innate immunity. The first layer of immunity is induced after recognition of conserved microbial molecules like bacterial flagellin or fungal chitin. These molecules are known as PAMPs and are recognized by extracellular plant receptor kinases. This immunity pathway is known as PAMP-triggered immunity (PTI). The second way immunity is activated is by recognition of pathogen effectors by plant immune receptors known as resistance (R) proteins leading to effector-triggered immunity (ETI) (19). In the case of bacterial pathogens, ETI is induced by the recognition of T3Es inside plant cells by intracellular R proteins. Activation of these immunity pathways induces responses and signal transduction pathways including the mitogen-activated protein kinases (MAPKs) and Calcium-Dependent Protein Kinases signaling cascades, transcriptional reprogramming of immunity-related genes, callose deposition at the cell wall, and production of reactive oxygen species (ROS) (32). T3Es disrupt several host processes to suppress plant immunity and

favor bacterial multiplication and the development of the disease. T3Es suppress plant immunity at different levels. Some T3Es disable PAMP receptor complexes or R protein complexes, several inactivate MAPKs signaling cascades, and others act post-transcriptionally to suppress immune responses (4, 33). However, the enzymatic activity and plant targets for the majority of T3Es remain to be elucidated (5, 10).

PP2Cs have been implicated in plant stress signaling, as inhibitors of MAPK signaling pathways or co-receptors of the stress hormone abscisic acid (ABA) (27). *A. thaliana* encodes 80 PP2Cs that are classified into 11 clades (13). The most studied clade of Arabidopsis PP2Cs is clade A (PP2C-A), whose members are negative regulators of ABA signaling pathways. ABA is involved in plant development and tolerance to abiotic and biotic stresses (8). PP2C-D members regulate phosphorylation of the plasma membrane H^+-ATPase to regulate cell expansion (16, 31). Clade C of the PP2C family includes POL and PLL1-5. POL and PLL1 are two dually acetylated plasma membrane phosphatases that promote shoot and root meristem and embryo formation (14, 30). PLL4 and PLL5 regulate leaf development and the role of PLL2 and PLL3 have not been identified (30). Negative roles in plant development and abiotic/biotic stress perception have become a common theme for PP2Cs. Recently, PP2C-A members have been identified as negative regulators of plant immunity by regulating the phosphorylation status of PAMP receptor complexes (28).

In chapter three of this thesis, I showed that HopA1 suppresses PTI-induced callose deposition and ROS production, two PTI responses. I also showed that *in*

planta transgenic expression of HopA1 allowed better growth of wild type DC3000 and the type III secretion defective *hrcC* mutant compared to growth in wild type Col-0 plants. Here I report that the DC3000 type III effector HopA1 interacts at the plasma membrane of plant cells with two PP2C-C members, PLL4 and PLL5. I provide evidence that these phosphatases play roles in plant immunity as negative regulators. This is the first report of PP2Cs from clade C with roles in plant immunity.

Results

HopA1 interacts with PLL4 and PLL5, two Arabidopsis type 2C protein phosphatases. In an effort to elucidate the mechanism of PTI suppression, we searched for proteins that interacted with HopA1 in plant cells. In a yeast two-hybrid screen done by Dr. Ming Guo, a research assistant professor in Dr. Jim Alfano's research group, we identified that HopA1 interacts with two Arabidopsis PP2Cs: PLL4 (AT2G28890) and PLL5 (AT1G07630). A large interactome screen also provided preliminary evidence that these phosphatases are putative targets of HopA1 (23). First I confirmed the interaction of HopA1 with PLL4 and PLL5. Yeast two-hybrid analyses between HopA1 in the DNA-binding domain pGBKT7 vector and PLL4 or PLL5 in the activation domain pGADT7 vector resulted in a positive interaction (Fig. 1A). When PLL4 or PLL5 were mated to the empty pGBKT7 vector, no interaction was detected. To explore if HopA1 interacts with other members of this PP2C clade, I carried out yeast two-hybrid analyses with

PLL1 and PLL2. I did not find any interaction between HopA1 and PLL1 or PLL2 (Fig. S1). Therefore, HopA1 interacted specifically with PLL4 and PLL5.

To confirm the interaction of HopA1 with these phosphatases *in planta*, I performed bimolecular fluorescence complementation (BiFC) assays. *Agrobacterium*-mediated transient expression of HopA1-nYFP and PLL4-cYFP in *Nicotiana benthamiana* leaves resulted in fluorescence, indicating that HopA1 and PLL4 interacted (Fig. 1B). When *Agrobacterium* strains expressing HopA1-nYFP and PLL5-cYFP were coinfiltrated in *N. benthamiana* leaves, similar results were obtained, although it resulted in lower fluorescence compared to the HopA1-PLL4 interaction. These results suggested that HopA1 interact with PLL4 and PLL5 in plant cells and based on the location of the fluorescent reporter they may interact at the plasma membrane. To investigate if the HopA1-PLL4 and HopA1-PLL5 interactions occur at the plasma membrane, I performed plasmolysis experiments to visualize Hechtian strands connecting the plasma membrane to the cell wall. Plasmolysis of cells coinfiltrated with HopA1-nYFP and PLL4-cYFP and HopA1-nYFP and PLL5-cYFP in the presence of 5% NaCl confirmed that these interactions occurred at the plasma membrane as indicated by the presence of reconstituted YFP in Hechtian strands (Fig. 1B). To further confirm that HopA1 interacted with PLL4 and PLL5 at the plasma membrane, I did colocalization experiments with *hopA1* fused to red fluorescence protein (RFP) gene and *PLL4* or *PLL5* fused to green fluorescence protein (GFP) gene. When *Agrobacterium* strains expressing HopA1-RFP and PLL4-GFP were coinfiltrated into *N. benthamiana* leaves I found that they both localized to the

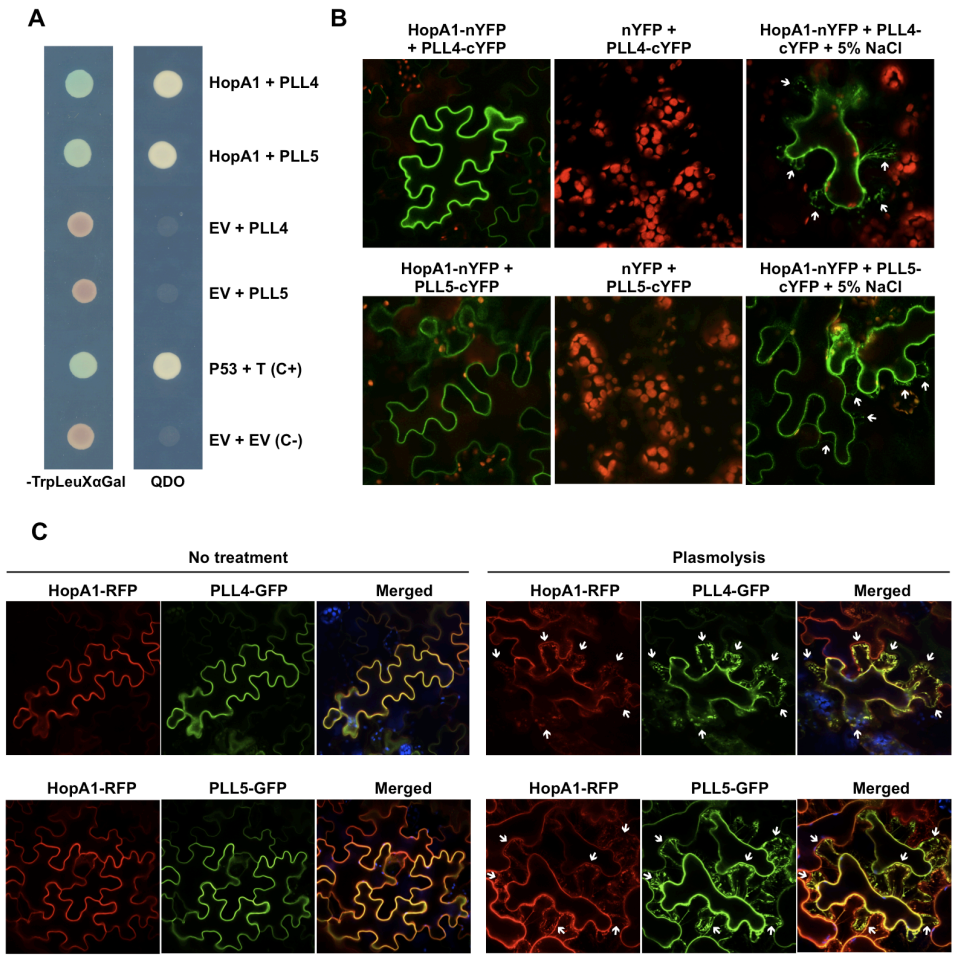

Figure 1. HopA1 interacts with the Arabidopsis type 2C protein phosphatases PLL4 and PLL5. (**A**) Yeast two-hybrid analyses show interaction when strains containing HopA1 with PLL4 or PLL5 were grown on selective media (QDO and -Trp-Leu+XαGal). No interaction was seen when strains containing PLL4 or PLL5 with the empty vector (EV) control were plated on selective media. (**B**) Bimolecular fluorescence complementation (BiFC) assays between HopA1 and PLL4 and HopA1 and PLL5. *Nicotiana benthamiana* leaves were coinfiltrated with HopA1-nYFP and PLL4-cYFP or PLL5-cYFP by *Agrobacterium*-mediated transformation. Green fluorescence indicates *in planta* interaction between HopA1 and PLL4 or PLL5. No fluorescence was observed when nYFP control was coinfiltrated with PLL4-cYFP or PLL5c-YFP. Red fluorescence represents chloroplast autofluorescence. Pictures were taken 2 days after infiltration. (**C**) HopA1-RFP and PLL4-GFP and HopA1-RFP and PLL5-GFP were transiently co-expressed in *N. benthamiana* by *Agrobacterium*-mediated transformation. HopA1-RFP colocalized with PLL4-GFP or PLL5-GFP mainly at the plasma membrane, as seen in merged pictures of the green and red channels. Chlorophyll autofluorescence appears blue in these micrographs. Infiltrated cells were photographed 2 days after infiltration. For panels B and C, plasmolysis experiments were performed in the presence of 5% NaCl for 10 m. Arrows indicate visible Hechtian strands.

plasma membrane (Fig. 1C). HopA1-RFP and PLL5-GFP coinfiltrations showed similar localization at the plasma membrane. Plasmolysis experiment confirmed colocalization of HopA1 and PLL4 and HopA1 and PLL5 in Hechtian strands (Fig. 1C). Plasma membrane localization has been described for POL and PLL1, two other members of PP2C-C (14). In addition, localization to the plasma membrane has also been reported for HopA1 (chapter 3 of this thesis and (26)). These data confirm that the interactions of HopA1 with PLL4 and HopA1 with PLL5 occur at the plasma membrane.

***PLL4 and PLL5 have roles in leaf development and are induced after pathogen infection*.** Members of the PP2C-C are regulators of meristem and organ development as abnormal leaf development was observed in T-DNA insertion mutants in each of these genes (30). Leaf phenotypes described for these T-DNA mutants were mainly in the *A. thaliana* ecotype Ler background, and it was reported that the phenotypes of *pll4-1* and *pll5-1* mutants were weaker in the *A. thaliana* Col-0 background. I acquired seeds of T-DNA insertion mutants in *PLL4* and *PLL5* in the *A. thaliana* Col-0 background. The *pll4* (SALK_206631C) and *pll5* (SALK_044162C) mutants were genotyped to confirm T-DNA insertion mutagenesis of these genes (Fig. S2). I found abnormal leaf development in *pll4* and *pll5* mutants compared to wild type Col-0 plants (Fig. 2A). Leaves were longer and more curled on the mutants than wild type Col-0. This phenotype was much more pronounced in *pll5* than in *pll4*. I crossed these mutants to generate the *pll4 pll5* double mutant. I observed that the Col-0 *pll4 pll5* double mutant carried the *pll5* phenotype. I performed qRT-PCR analysis to

determine the expression of *PLL4* and *PLL5* in the single and double mutants and confirmed that their expression was greatly reduced in mutants compared to wild type Col-0 (Fig. S3). To begin characterization of these phosphatases in regards to plant immunity, I investigated if they were previously reported to be induced during biotic stress using the eFP browser (http://bar.utoronto.ca). I found that *PLL4* and *PLL5* were induced by several biotic stresses including DC3000 *hrcC* mutant and flg22, the 22-amino acid epitope from bacterial flagellin PAMP. Next I wanted to confirm if *PLL4* and *PLL5* were induced by DC3000 infections. I measured gene expression of *PLL4* and *PLL5* in *A. thaliana* Col-0 plants infiltrated with DC3000 or mock treatments 6 hours after inoculation. Interestingly, both *PLL4* and *PLL5* were induced by DC3000 (Fig. 2B). *FRK1* and *NHL10* have been extensively used as hallmark immunity-regulated genes (6, 7, 17, 22, 28). Therefore, I also measured expression of *FRK1* and *NHL10* after DC3000 treatment as positive controls. As expected, these genes were highly induced by DC3000 (Fig. 2B). In addition, I tested induction of *PLL4* and *PLL5* by an avirulent strain DC3000(p*avrRpm1*), which produces the T3E AvrRpm1 that is recognized in *A. thaliana* Col-0 by the R protein RPM1 inducing ETI (9). *PLL4* and *PLL5* were both induced by this avirulent strain indicating that they are induced during ETI (Fig. 2C). To explore if *PLL4* and *PLL5* are induced during PTI, I infiltrated *A. thaliana* Col-0 with flg22. *PLL4* and *PLL5* were highly induced by flg22 (Fig. 2D). Altogether, these data indicate that *PLL4* and *PLL5* are induced by *P. syringae* during ETI and PTI. This suggests that PLL4 and PLL5 play roles in plant immunity.

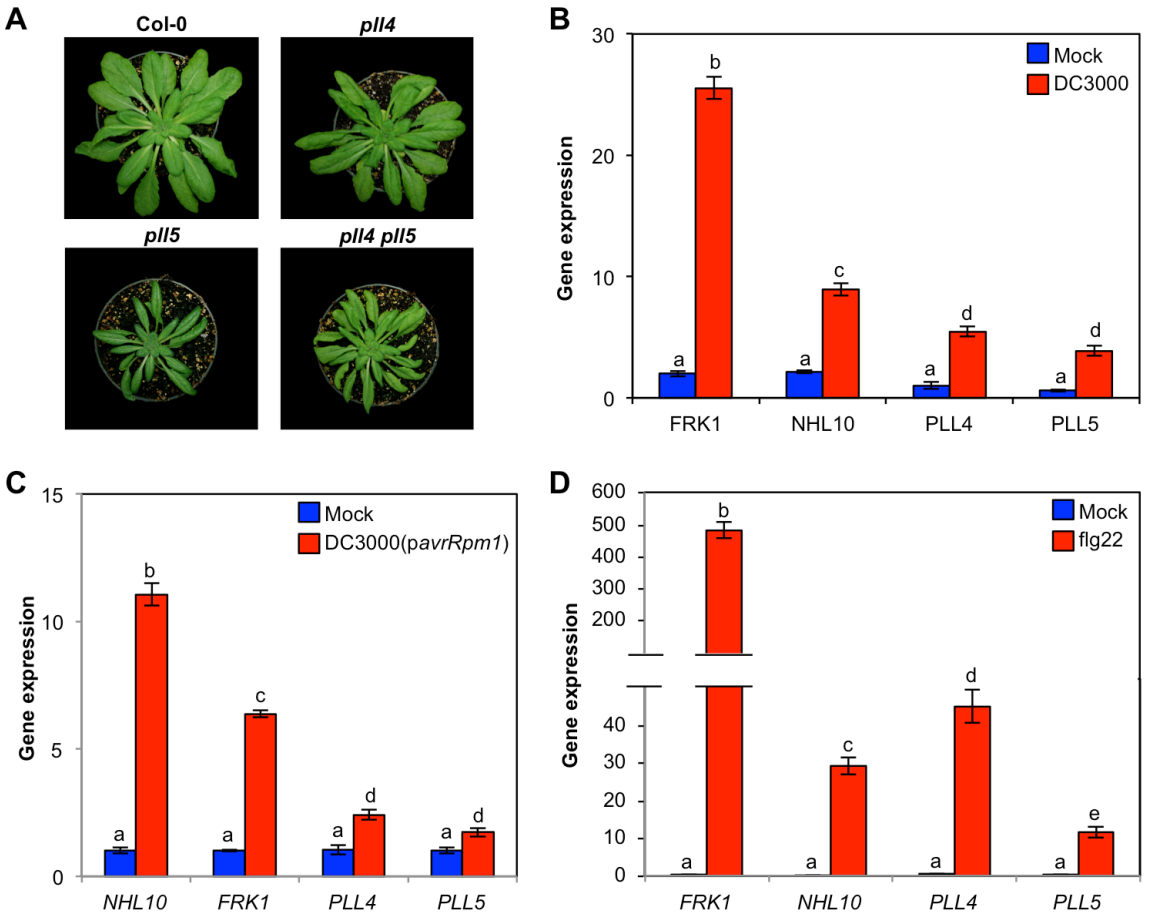

Figure 2. PLL4 and PLL5 are induced after pathogen infection. (**A**) Pictures of *A. thaliana* Col-0, *pll4* (SALK_206631C), *pll5* (SALK_044162C), and *pll4 pll5* double mutant. Mutations in *PLL4* and *PLL5* resulted in altered leaf development, even more pronounced in the *pll5* mutant. Col-0 plants were syringe-infiltrated with 1 x 10^6 cells/mL of DC3000 (**B**), DC3000(p*avrRpm1*) (**C**) or 1 µM flg22 (**D**). Infiltration with 5mM MES buffer (pH 5.6) was used as mock control for each experiment. Leaves were harvested 6 h after infiltration for RNA extraction. Expression of *PLL4* and *PLL5*, as well as the immunity-regulated genes *FRK1* and *NHL10*, was measured by qRT-PCR analyses. *PLL4 and PLL5* were induced by all treatments. Different lowercase letters in panels B, C and D indicate that the values are significantly different ($p \leq 0.05$). Standard error bars are shown.

PLL4 and PLL5 act in plant immunity as negative regulators. No role in plant immunity has been described for any members of the PP2C-C family of phosphatases including PLL4 and PLL5. I first investigated the role of these phosphatases during pathogen infection. Transgenic plants expressing PLL4 or PLL5 both fused to a hemagglutinin (HA) tag, hereinafter referred to as PLL4-OX and PLL5-OX, were generated in *A. thaliana* Col-0 using an estradiol-inducible vector. Expression of each protein was confirmed with immunoblots using anti-HA antibody (Fig. S4). Wild type Col-0, PLL4-OX, and PLL5-OX plants, as well as *pll4*, *pll5*, and *pll4 pll5* mutant plants were syringe-inoculated with 2 x 10^5 cells/mL of DC3000. I found that DC3000 grew better in plants expressing either PLL4-HA or PLL5-HA but worse in *pll4*, *pll5*, and *pll4 pll5* mutants comparing each transgenic or mutant plants to wild type Col-0 (Fig. 3A). DC3000 growth was greatly reduced in *pll4 pll5* double mutant and disease symptoms were barely visible compared to wild type Col-0 plants (Fig. 3B). To further characterize the involvement of these phosphatases in plant immunity, I analyzed how well these plants were able to induce PTI by measuring flg22-induced ROS production and flg22-induced callose deposition. Wild type Col-0, PLL4-OX , and PLL5-OX plants were treated with estradiol to induce expression of each phosphatase and 24 hours later samples were harvested for ROS assay. I found that flg22 treatment induced higher levels of ROS production in wild type Col-0 compared to PLL4-OX and PLL5-OX pretreated with estradiol (Fig. 3C). These data suggest that PLL4 and PLL5 are negative regulators of immunity since overexpression of these phosphatases resulted in plants with reduced PTI-

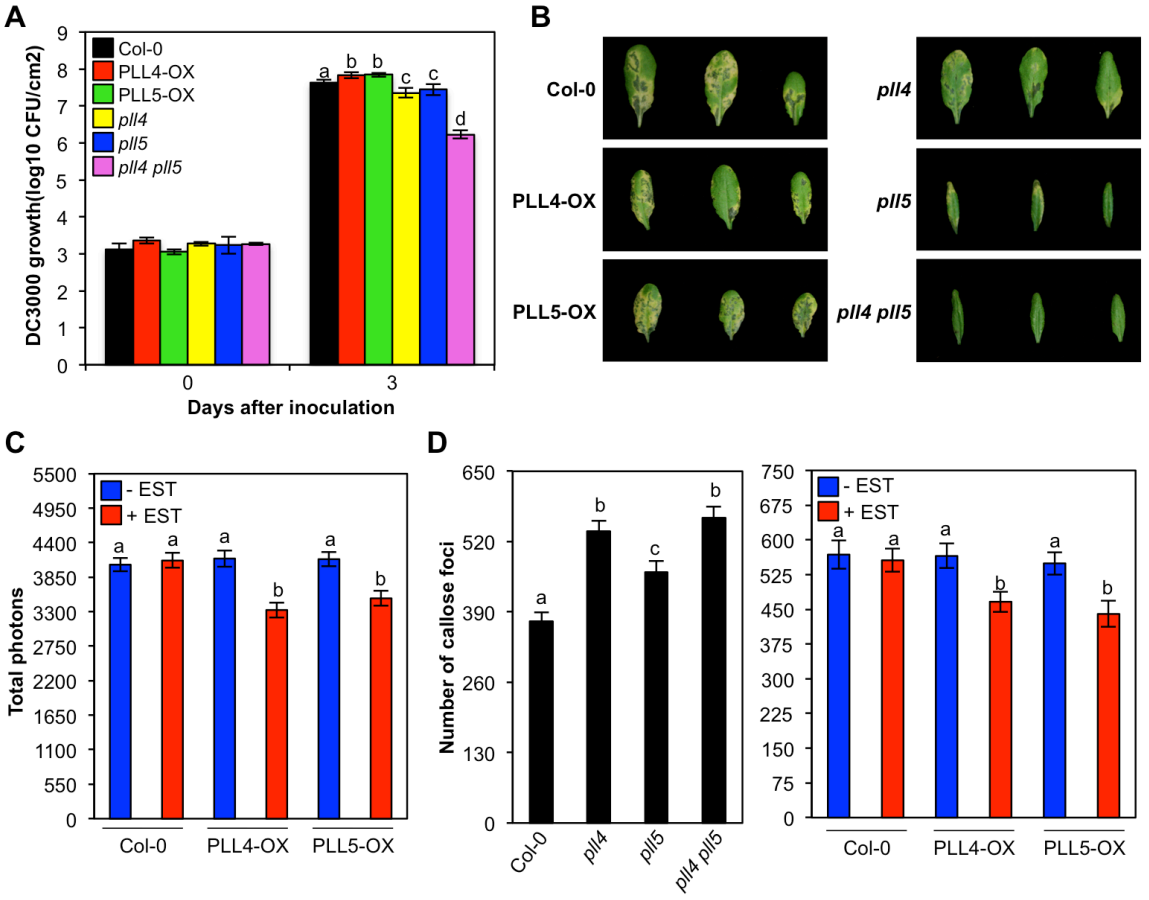

Figure 3. PLL4 and PLL5 are negative regulators of plant innate immunity. (**A**) Wild type Col-0, transgenic plants overexpressing PLL4 (PLL4-OX) and PLL5 (PLL5-OX), *pll4*, *pll5,* and *pll4 pll5* mutant plants were syringe-inoculated with 2 x 10^5 cells/mL of DC3000. Bacterial growth was counted 0 and 3 days after inoculation (dai). DC3000 grew better in PLL4-OX and PLL5-OX plants and were reduced in growth in *pll4* and *pll5* mutants (**B**) Disease symptoms of plants inoculated with DC3000 as described in A. Pictures taken 4 dai. (**C**). Wild type Col-0 and estradiol inducible PLL4-OX and PLL5-OX plants were infiltrated with 20 µM estradiol (+EST) or water (-EST). Twenty-four hours later, leaves were treated with 1 µM flg22 and ROS production was determined. Estradiol-inducible expression of PLL4 and PLL5 suppressed the flg22-induced ROS production. (**D**) Plants were syringe-infiltrated with 10 µM flg22 and callose deposition was determined; leaves were harvested after 16 h and callose was stained with aniline blue. Pictures were taken using a fluorescence microscope and the number of callose deposits were counted using Image J software. T-DNA mutants in *PLL4* and *PLL5* have increased flg22-induced callose deposition, while PLL4-OX and PLL5-OX lines were suppressed in this immune response. The different lowercase letters in A, C, and D indicate statistical differences ($p < 0.05$) and SE bars are shown.

related ROS production. Next I examined callose deposition in plants induced by flg22. I infiltrated wild type Col-0, *pll4*, *pll5,* and *pll4 pll5* plants with 10 µM flg22 and carried out callose deposition assays. I observed more callose deposits in the *pll4*, *pll5*, and *pll4 pll5* mutants compared to Col-0 plants (Fig. 3D). In addition, lower amounts of callose were observed in PLL4-OX and PLL5-OX plants after flg22 treatment (Fig. 3D). Collectively, these results indicate that PLL4 and PLL5 act as negative regulators of plant immunity.

To further investigate PLL4's and PLL5's effect on plant immunity, I analyzed expression of the PTI-induced genes *FRK1* and *NHL10* in *pll4*, *pll5*, and *pll4 pll5* mutants and in plants overexpressing PLL4 and PLL5. Expression of *FRK1* and *NHL10* was induced by the avirulent *P. syringae* strain DC3000(p*avrRpm1*) in Col-0 compared to a mock inoculation (Fig. 4A). Expression of these genes after DC3000(p*avrRpm1*) treatment was reduced in PLL4-OX and PLL5-OX plants but greatly enhanced in *pll4, pll5,* and *pll4 pll5* mutants. Additionally, I measured *FRK1* and *NHL10* after flg22 treatment. *FRK1* and *NHL10* expression was reduced in plants expressing PLL4 and PLL5, but enhanced in *pll4*, *pll5,* and *pll4 pll5* mutant plants (Fig. 4B). These findings confirm that PLL4 and PLL5 act as negative regulators of plant immunity. These data provide the first evidence of the involvement of PP2C-C, including PLL4 and PLL5, in plant immunity and provide the first evidence that a plant pathogen effector targets PP2C-C members.

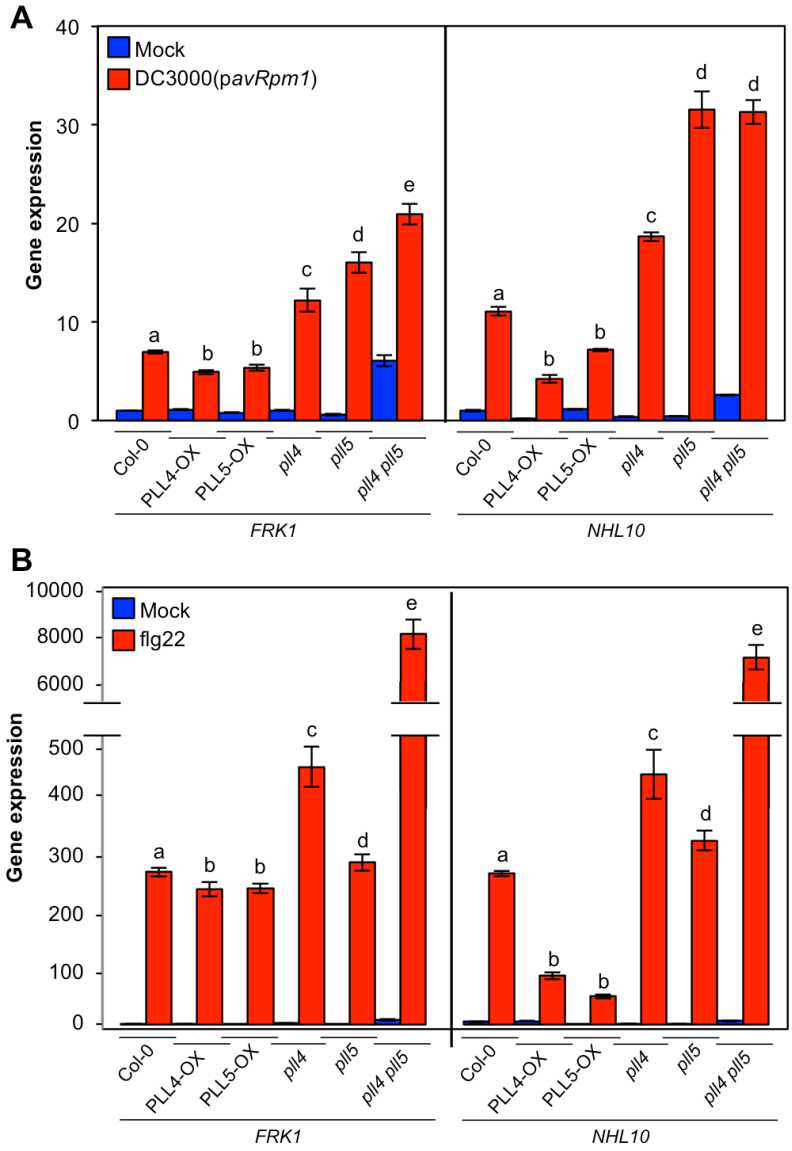

Figure 4. PLL4 and PLL5 overexpressors suppressed and *pll4* and *pll5* T-DNA mutants increased the expression of immunity-regulated genes. Expression analysis of the immunity-regulated genes *FRK1* and *NHL10* was measured by qRT-PCR after induction with 1 x 10^6 cells/mL of DC3000(p*avrRpm1*) (**A**) or 1 µM flg22 (**B**). Infiltrated leaves were harvested after 6 h for RNA extraction. Expression of *FRK1* and *NHL10* was down-regulated in PLL4-OX and PLL5-OX and up-regulated in *pll4*, *pll5,* and *pll4 pll5* mutant plants after DC3000(p*avrRpm1*) and flg22 treatments. Different letters indicate statistical differences ($p < 0.05$). Error bars represent the standard error.

Discussion

In this study I examined the role of the type III effector HopA1 from *P. syringae* pv. *tomato* DC3000. I identified the Arabidopsis targets of HopA1, which are the PP2C-C PLL4 and PLL5. I showed that HopA1 interacts with PLL4 and PLL5 using the yeast two-hybrid, BiFC and co-localization assays (Fig. 1). HopA1 interacts with PLL4 and PLL5 at the plasma membrane as plasma membrane-cell wall connections known as Hechtian strands were observed if the tissue was subjected to plasmolysis (Fig. 1B-C). PP2C-C family members have N-terminal myristoylation and palmitoylation signal peptides that mediate their localization to the plasma membrane (14). POL and PLL1 are dual-acetylated plasma membrane proteins that require phospholipids, mainly phosphatidylinositol (4) phosphate [PI(4)P], for activation and phosphatase activity *in planta* (14). Furthermore, the rice homolog of PLL4 and PLL5, XB15, also localizes to the plasma membrane of rice protoplast cells (24).

HopA1 from *P. syringae* pv. *syringae* 61 is recognized in Arabidopsis by the R protein RPS6 (21). It was recently reported that EDS1, a positive regulator of immunity, forms complexes with the R proteins RPS6 and RPS4 and that two *P. syringae* effectors, AvrRps4 and HopA1, target EDS1 (3). In chapter three of this thesis I presented data that indicates that I could not discern any interaction of HopA1 with EDS1 in a yeast two-hybrid assay. However, I observed weak interaction between HopA1 and EDS1 in BiFC assays (Fig. S5). Since HopA1 interacts with PLL4 and PLL5 and possibly with EDS1, I investigated whether PLL4 and/or PLL5 interacted with EDS1. Preliminary results indicate that EDS1

interacts with PLL4 and PLL5 in a yeast two-hybrid assay (Fig. S6). However I could not detect any interaction *in planta* using BiFC assays (not shown). EDS1 localizes to the cytoplasm and nucleus of plant cells, and HopA1, PLL4, and PLL5 localize to the plasma membrane. Differences in their subcellular localization and the fact that I could not detect interactions in multiple assays suggest that EDS1 does not interact with HopA1, PLL4, or PLL5. This phenomenon needs to be further investigated and is outside the scope of this chapter.

Because PLL4 and PLL5 localize to the plasma membrane, it is likely that their targets are plasma membrane-localized proteins. Several examples of plasma membrane-localized targets of PP2Cs exist. For example, XB15, the rice homolog of PLL4 and PLL5, interacts and dephosphorylates the plasma membrane localized PRR XA21 leading to a negative regulation of XA21-mediated immunity (24). In addition, the Arabidopsis Kinase-Associated Protein Phosphatase interacts with several plasma membrane-localized receptor kinases including FLS2, CLV1, SERK1, BRI1, and BAK1 (11, 15, 29). My hypothesis is that PLL4 and PLL5 play roles in plant immunity as negative regulators by acting on a PRR kinase domain keeping the PRR inactive in the absence of biotic stress and that HopA1 prevents these phosphatases from becoming inactive, which prevents PTI from being induced even after PAMP detection.

The evidence that PLL4 and PLL5 act as negative regulators of plant immunity are as follows: (i) T-DNA mutants in *PLL4* or *PLL5* are more resistant to DC3000, while overexpressing lines are more susceptible (Fig. 3A-B); (ii) Plants

overexpressing PLL4 or PLL5 display reduced flg22-induced callose deposition (Fig. 3C); (iii) T-DNA mutants in *PLL4 and PLL5* have more flg22-induced ROS production, while overexpressing lines are compromised in this response (Fig. 3D); and (iv) expression of the immunity-regulated genes *FRK1* and *NHL10* is enhanced in T-DNA mutants in *PLL4* and *PLL5* and decreased in overexpressing lines after DC3000(p*avrRpm1*) and flg22 treatments (Fig. 4). Mutants defective in negative regulators of immunity would be expected to be more resistant to pathogens because their immune responses are no longer repressed. Moreover, plants overexpressing a negative regulator would be expected to be more susceptible to pathogens because their immune responses are prevented from being induced. The observations of plants affected in PLL4 and PLL5 are consistent with both proteins acting as negative regulators of immunity.

Here I propose a model for PLL4's and PLL5's role in plant immunity and why HopA1 targets these phosphatases (Fig. 5). PLL4 and PLL5 are negative regulators of plant immunity that localized at the plasma membrane of plant cells. In the absence of the pathogen, PLL4 and PLL5 keep the PTI pathway off by reducing the phosphorylation of PAMP receptor complexes. PAMP receptor complexes are the best candidates for PLL4 and PLL5 substrates since they reside at the plasma membrane and their kinase domains are activated by phosphorylation. Once *P. syringae* lands on the leaf surface and gains access to the apoplast, PLL4 and PLL5 are deregulated by an unknown mechanism. This leads to activation of PTI and the induction of immune responses including callose deposition and ROS production to restrict pathogen ingress. One way

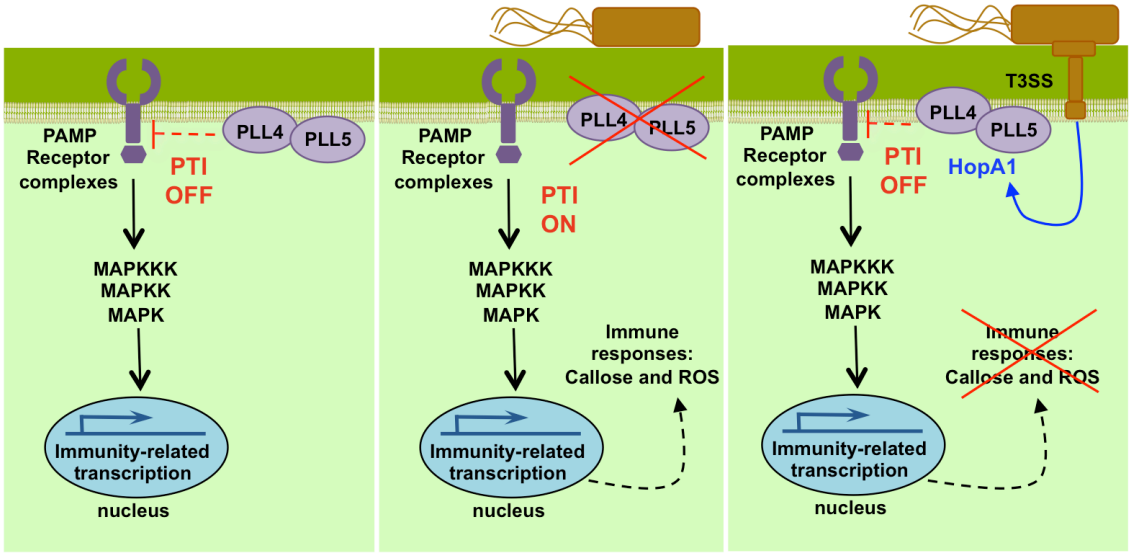

Figure 5. Model for PLL4's and PLL5's role immunity and as HopA1 targets. PLL4 and PLL5 are two negative regulators of immunity that localize to the plant plasma membrane. These phosphatases most likely inhibit the activation of PAMP receptors complexes that also reside at the plasma membrane by reducing their phosphorylation and maintaining the pathogen-associated molecular pattern-triggered immunity (PTI) pathway in an inactivate state in the absence of pathogen stress. When *P. syringae* is in contact with plant cells the phosphatase activity of PLL4 and PLL5 is normally inhibited by an unknown mechanism. This leads to activation of PTI and immune responses like callose deposition and ROS production, which restricts bacterial multiplication. However, *P. syringae* overcomes this restriction by injecting the type III effector HopA1. Inside cells, HopA1 interacts with PLL4 and PLL5 most likely inhibiting their deregulation to keep PTI off, which allows the pathogen to continue to multiply and cause disease.

that *P. syringae* overcomes plant immunity is by injecting the type III effector HopA1. HopA1 targets PLL4 and PLL5 at the plasma membrane to block their deregulation, which keeps PTI from becoming activated. This allows the pathogen to grow and ultimately to cause disease.

In summary, my work demonstrates that HopA1 interacts with the PP2Cs PLL4 and PLL5 to suppress PTI. PLL4 and PLL5 are involved in plant immunity by acting as negative regulators. Future studies for this project include the identification of PLL4 and PLL5 substrates, and determining the mechanism that HopA1 uses to inhibits PLL4 and PLL5.

Materials and methods

Cloning. The *hopA1* gene was PCR amplified from DC3000 using primers P2844 and P2845. From *A. thaliana* Col-0 the following genes were amplified with the specified primer pair: *PLL4* (*AT2G28890*) with P4580 and P4581; *PLL5* (*AT1G07630*) with P4594 and P4595; *PLL1* (*AT2G35350*) with P4896 and P4897; *PLL2* (*AT5G02400*) with P4611 and P4612; and *EDS1* (*AT3G48090*) with P4878 and P4445. The resulting PCR products were cloned into the Gateway vector pENTR-D resulting in pLN3203 (*hopA1*), pLN5173 (*PLL4*), pLN5176 (*PLL5*), pLN5463 (*PLL1*), pLN5204 (*PLL2*), and pLN4909 (*EDS1*). To generate estradiol-inducible plants expressing PLL4 or PLL5, pLN5173 (*PLL4*) and pLN5176 (*PLL5*) were separately recombined into pLN604, the gateway-compatible pER8 vector (34). For yeast two-hybrid vectors, pENTR-D constructs pLN3203 (*hopA1*) and pLN4909 (*EDS1*) were recombined into the gateway-

compatible DNA-binding domain vector pGBKT7 (pLN2232) by LR recombination reaction. The pENTR-D constructs pLN5173 (*PLL4*), pLN5176 (*PLL5*), pLN5463 (*PLL1*), and pLN5204 (*PLL2*) were recombined into the gateway-compatible activation domain vector pGADT7 (pLN1658).

For BiFC constructs, *hopA1* with a 3' *EcoRI* restriction site was amplified with primers P3560 and P4613. The portion of *YFP* corresponding to the N-terminal region (*nYFP*) with a 5' *EcoRI* restriction site was amplified with primers P4615 and P4341. The *hopA1* and *nYFP* PCR products were gel-extracted, digested with *EcoRI*, ligated, PCR-amplified with primers P3560 and P4341, and cloned into pENTR-D. *PLL4* with a 3' *EcoRV* restriction site was amplified with primers P4580 an*d* P5386; *PLL5* with a 3' *EcoRI* restriction site was amplified with primers P4594 and P4692; and EDS1 with a 3' *XhoI* restriction site was amplified with primers P4878 and P5385. The portion corresponding to C-terminal region of YFP (*cYFP*) was amplified with reverse primer P4343 and forward primers P5081 (containing a 5' *EcoRV* restriction site), P4693 (containing a 5' *EcoRI* restriction site), or P4342 (containing a 5' *XhoI* restriction site). The PCR products were gel-extracted, digested with the corresponding restriction enzymes, and ligated. From ligation products, *PLL4-cYFP* was amplified with primers P4580 and P4343, *PLL5-cYFP* with P4596 and P4343, and *EDS1-cYFP* with P4878 and P4343. These fusion PCR products were cloned into pENTR-D. All BiFC constructs were recombined by LR reaction to the gateway-compatible pPZP212 vector (pLN462 (18)).

To make C-terminal fusions to *eqFP611*, the gene encoding the RFP (12), *hopA1* and *EDS1* with a 3' *XhoI* site were amplified with primer pairs P3560/P2844 and P4878/P5385, respectively. *RFP* with a 5' *XhoI* site was amplified with primers P3388 and P3040. PCR fragments were gel-extracted, digested with *XhoI*, ligated and PCR-amplified with the corresponding primer set: P3560/P3040 for *hopA1-RFP* and P4878/P3040 for *EDS1-RFP*. The *hopA1-RFP* and *EDS1-RFP* fusions were cloned into pENTR-D and then recombined into pLN462. For C-terminal GFP fusions, pLN5173 (*PLL4*) and pLN5176 (*PLL5*) were recombined into pK7FWG2 (20).

Yeast two-hybrid analyses. *Saccharomyces cerevisiae* strain Y187 (MATα) was transformed with pGBKT7 constructs (-Trp) and strain AH109 (MATa) was transformed with pGADT7 constructs (-Leu). Yeast Y187 (pGBKT7:HopA1, EDS1 or EV) was mated to yeast AH109 (pGADT7:PLL4 or PLL5) in a mating plate (yeast extract peptone dextrose, YPD). Y187 (pGBKT7:HopA1) was also mated to AH109 (pGADT7:PLL1 or PLL2). To test interaction of target proteins mated yeast strains were plated in selective QDO and -Trp-Leu+XαGal media and photographed 2 days later.

Confocal microscopy. BiFC, RFP- and GFP-fusion constructs in the plant constitutive expression vector pLN462 were transformed into *Agrobacterium* C58C1. *Agrobacterium* strains were infiltrated into leaves of *N. benthamiana* as described previously (18) at a final absorbance (OD_{600}) of 0.4 for each strain. Infiltrated leaves were imaged in a Nikon A1 confocal mounted on an Eclipse 90i Nikon compound microscope 2 days after agroinfiltrations. The following

excitation (ex) and emission (em) wavelengths were used for colocalization experiments: GFP, 488 nm (ex) and 500-550 nm (em); and RFP, 561.4 nm (ex) and 570-620 nm (em). For BiFC assays, pictures were taken sequentially at 514.5 nm (ex) and 525-555 nm (em). Chloroplasts were imaged at 640.6 nm (ex) and 663-738 nm (em). Plasmolysis was performed in the presence of 5% NaCl for 10 m.

Genotyping of Arabidopsis T-DNA lines. T-DNA insertion lines in *PLL4* and *PLL5* were requested from the Arabidopsis Biological Resource Center. Cross-fertilization was performed using *pll5* as female plant and *pll4* as pollen donor plant. Single and double mutants were genotyped using primers P5087 (right border primer of SALK_206631), P5088 (left border primer of SALK_206631), P5082 (right border primer of SALK_044162), P5083 (left border primer of SALK_044162), and LBa1 (P2630, primer in T-DNA).

Generation of transgenic Arabidopsis plants. PLL5 and PLL4 in the estradiol-inducible pER8 vector were transformed into *Agrobacterium* C58C1. Arabidopsis Col-0 plants were transformed using the floral-dip method (2). Transgene expression was confirmed with immunoblots using anti-HA primary antibody (Roche, Basal, Switzerland) and anti-rat immunoglobulin G alkaline-phosphatase conjugates as secondary antibodies (Sigma Chemical Co., St. Louis, U.S.A.).

Plant assays. For pathogenicity assays DC3000 was grown overnight in King's B (KB) media at 30°C. Arabidopsis plants were syringe-inoculated with 2 x 10^5 cells/mL of DC3000. Samples were collected 0 and 3 days after inoculation, ground in 250 µL water, serially-diluted and plated on KB agar plates containing

25 µg/ml rifampicin. Bacterial numbers were counted after two days. For plants over-expressing PLL4 (PLL4-OX) or PLL5 (PLL5-OX) after estradiol treatment, plants were sprayed with 30 µM estradiol 1 day before DC3000 inoculations. ROS and callose assays were done as published (6) and as previously described in chapters 2 and 3 of this thesis.

qRT-PCR analysis. Total RNA was purified using RNeasy plant mini kit with on-column DNase treatment (QIAGEN). Reverse transcription was performed following RETROscript Reverse transcription kit (Ambion) using oligo(dT) primers with heat denaturation of the RNA. qRT-PCR was run using iTaq Universal SYBR green supermix (BioRad) on a BioRad iCycler. Gene expression in wild type Col-0 and each mutant was measured using primer pairs P5091/P5092 for *PLL4* and P5084/P5085 for *PLL5*. Primers to measure gene expression of *FRK1* (*AT2G19190*) and *NHL10* (*AT2G35980*) were P4476/P4477 and P4562/P4563, respectively. Gene expression relative to Col-0 was calculated using the $2^{-\Delta\Delta CT}$ method with *actin2* as the reference gene and mock treated Col-0 as the reference sample. Primers for *actin* (*AT3G18780*) were P3775 and P3776.

Supplemental figures and tables

Supplemental Table 1. Plasmids used in this study

Primer	Sequence
P2630	5’-TGGTTCACGTAGTGGGCCATCG-3’
P2844	5’-CACCCTCGAGATGAACCCCATTCAGTCACG-3’
P2845	5’-GCTCACTAGTTCAAGCGTAATCTGGAACATCGTATGGGTATTTC GTGTTTCGAAGGGCCG-3’
P3040	5’-TCAAAGACGTCCCAGTTTGG-3’
P3388	5’-AGTCCTCGAGATGAATTCACTGATCAAGG-3’
P3560	5’-CACCATGAACCCCATTCAGTCACG-3’
P3775	5’-GGCATCAATTCGATCACTCAGAGC-3’
P3776	5’-ACCTTAGAAGATGGTTGGTTGACT-3’
P4341	5’-TCAGGCCATGATATAGACGTTGTGG-3’
P4342	5’-GATCCTCGAGATGGACAAGCAGAAGAACGGCATC-3’
P4343	5’-TCAGATAGATCTCTTGTACAGCTC-3’
P4445	5’-CACAGCTCGAGTCAGGTATCTGTTATTTCATCCAT-3’
P4476	5’-ACCCCGGATACTATTCGACTCGCCA-3’
P4477	5’-TGAGCTTGCAATAGCAGGTTGGCCT-3’
P4562	5’-TCACTGTTCCTGTCCGTAACCCAA-3’
P4563	5’-TGGTACTAAACCGCTTTCCTCGT-3’
P4580	5’-CACCATGGGTAACGGAATCGGGAAG-3’
P4581	5’-TACACAAGATTTCCACATTCT-3’
P4594	5’-CACCATGGGTAACGGAGTAACAAAA-3’
P4595	5’-TACACAAGATTTCCACATTCT-3’
P4611	5’-CACCATGGGAAATGGAGTCACCACT-3’
P4612	5’-CATTGATGATCTCCATATTCT-3’
P4613	5’-GATCGAATTCTTTCGTGTTTCGAAGGGCCGG-3’
P4615	5’-GATCGAATTCATGGTGAGCAAGGGCGAGGAG-3’
P4692	5’-GATCGAATTCTACACAAGATTTCCACATTCT-3’
P4693	5’-GATCGAATTCATGGACAAGCAGAAGAACGGCATC-3’
P4878	5’-CACCATGGCGTTTGAAGCTCTTACC-3’
P4896	5’-CACCATGGGAAGTGGATTCTCCTCC-3’
P4897	5’-AAGATACTTTCCTGATGACTT-3’
P5081	5’-GATCGATATCATGGACAAGCAGAAGAACGGCATC-3’
P5082	5’-CATTCAAAGAACCAACCTTTGAC-3’
P5083	5’-ACGAGGAAACGATGATGAATG-3’
P5084	5’-ACAAGGTGAACGAAGACGGT-3’
P5085	5’-CAACATAGTACATGATTCAGAGTTGATGA-3’
P5087	5’-TCGATTACAAAGGGACGTCAC-3’
P5088	5’-AACACTTCCAACACGTATTTGC-3’
P5091	5’-ACGTCTTCCTGCGTTTTTGAG-3’
P5092	5’-AGGAAGAATGTGGAAATCTTGTGT-3’
P5385	5’-GATCCTCGAGGGTATCTGTTATTTCATCCAT-3’
P5386	5’-GATCGATATCTACACAAGATTTCCACATTCT-3’

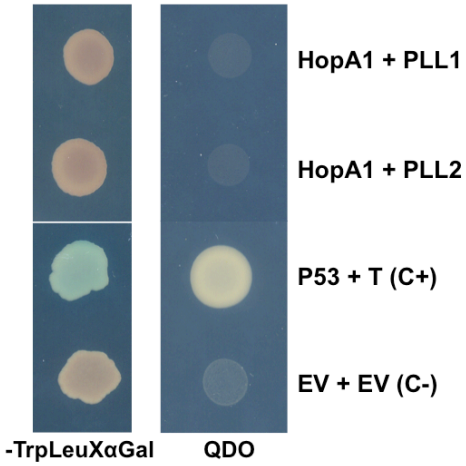

Supplemental Figure 1. HopA1 does not interact with other members of clade C of type 2C protein phosphatases. Yeast two-hybrid between HopA1 and two other members of PP2Cs clade C. HopA1 did not interact with PLL1 and PLL2 displaying similar reporter induction as the negative control when plated on selective QDO and -Trp-Leu+XαGal media.

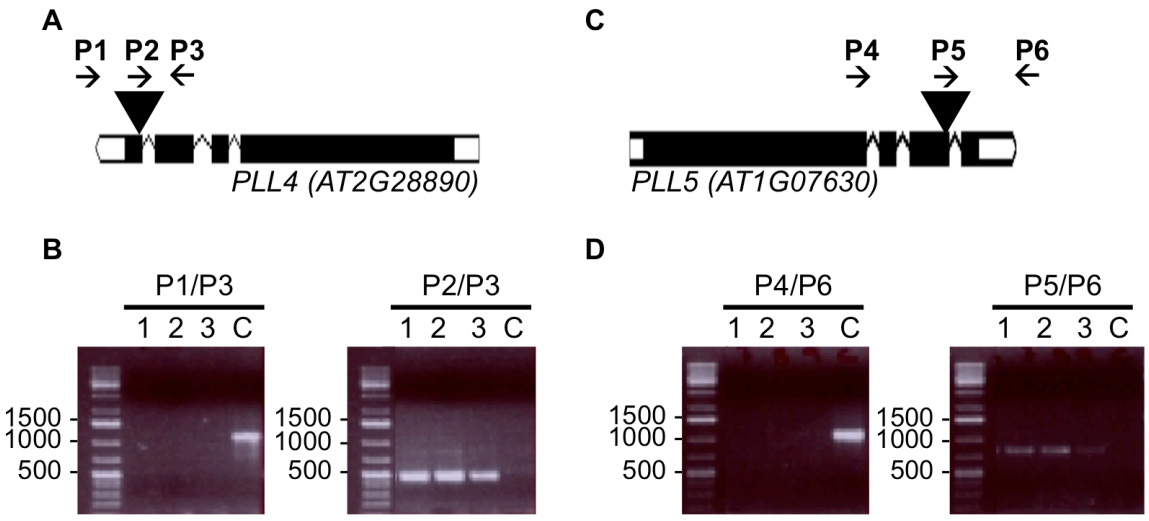

Supplemental Fig. 2. Characterization of SALK T-DNA knock-out lines in *PLL4* and *PLL5* genes. (**A**) Schematic representation of *PLL4* (*AT2G28890)* in *A. thaliana* Col-0 in relation to the SALK T-DNA insertion line SALK_206631C. T-DNA insertion (triangle) is in the fourth exon of *PLL4*. Primers used to confirm the homozygosity of the *pll4* mutant are depicted as P1 (P5088), P2 (P2630), and P3 (P5087). (**B**) PCR with primer set P1/P3 that amplifies the wild type Col-0 DNA (1136 bp) and primer set P2/P3 that amplifies the T-DNA insertion junction in the *pll4* mutant (509-809 bp). PCR confirmed that three *pll4* mutant plants are homozygous for the T-DNA insert. (**C**) Schematic representation of *PLL5* (*AT1G07630)* in *A. thaliana* Col-0 in relation to the SALK T-DNA insertion line SALK_044162C. T-DNA insertion (triangle) is in the third exon of *PLL5*. Primers used to confirm the homozygosity of the *pll5* mutant are depicted as P1 (P5083), P2 (P2630), and P3 (P5082). (**D**) PCR with primer set P4/P6 that amplifies the wild type Col-0 DNA (1053 bp) and primer set P5/P6 that amplifies the T-DNA insertion junction in the *pll4* mutant (533-833 bp). PCR confirmed that three *pll5* mutant plants are homozygous for the T-DNA insert.

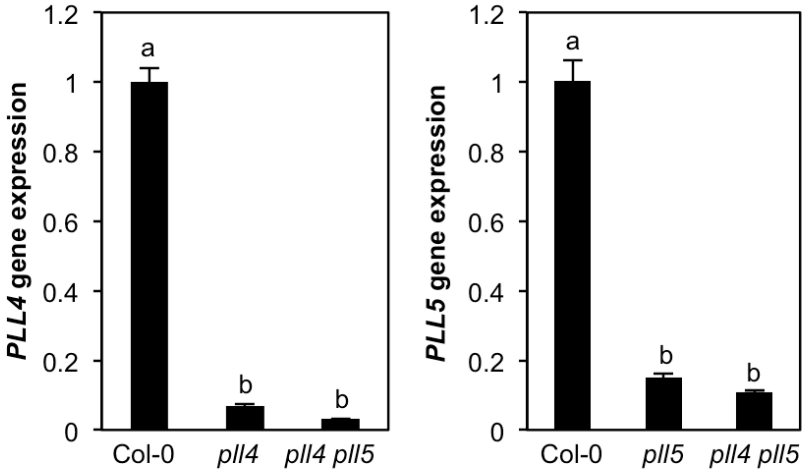

Supplemental Fig. 3. *PLL4* and *PLL5* show reduced expression in single and double mutants. Gene expression of *PLL4* and *PLL5* was analyzed by qRT-PCR analysis in the corresponding single or double mutant lines. Expression of each gene was greatly reduced in mutants compared to wild type Col-0. Letters “a” and “b” are statistically different ($p < 0.001$). Error bars designate standard error.

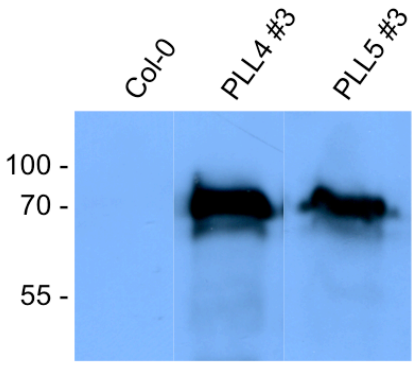

Supplemental Fig. 4. Immunoblots showing *in planta* expression of PLL4 and PLL5. *A. thaliana* Col-0 plants expressing PLL4 or PLL5 in an estradiol-inducible manner were sprayed with 30 μM estradiol to induce expression of target proteins. Leaf tissue was collected 24 hours after inoculation and performed immunoblots with anti-HA antibody. Expected protein size: PLL4= 72.48 kDa and PLL5 = 74.27 kDa.

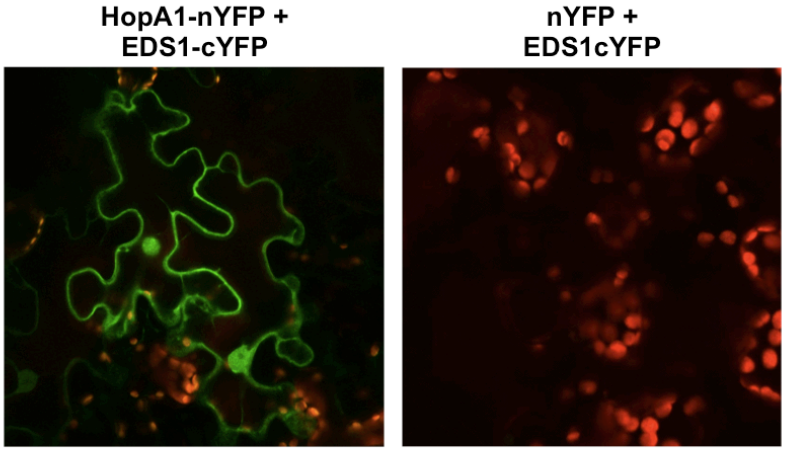

Supplemental Fig. 5. HopA1 interacts with the immunity regulator EDS1. BiFC assays show interaction between HopA1 and EDS1. HopA1-nYFP and EDS1-cYFP were coinfiltrated into *N. benthamiana* leaves, as well as EDS1-cYFP with nYFP vector control. Cells were visualized under a confocal microscope 2 days after infiltration. HopA1 and EDS1 interacted *in planta*.

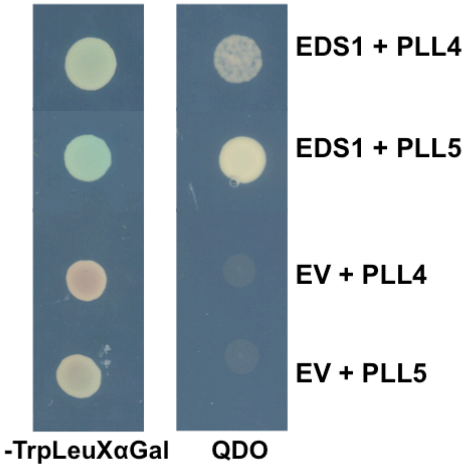

Supplemental Fig. 6. EDS1 interacts with PLL4 and PLL5. Yeast two-hybrid interactions between EDS1 and PLL4 and PLL5 show growth of yeast strain expressing EDS1-PLL4 and EDS1-PLL5 when plated on selective media. No interaction was detected when PLL4 or PLL5 and the vector control were plated on selective media.

References

1. **Alfano, J. R., and A. Collmer.** 1997. The type III (Hrp) secretion pathway of plant pathogenic bacteria: Trafficking harpins, Avr proteins, and death. J. Bacteriol. **179:**5655-5662.
2. **Bechtold, N., J. Ellis, and G. Pelletier.** 1993. In planta *Agrobacterium* mediated gene transfer by infiltration of adult *Arabidopsis thaliana* plants. Comptes Rendus de l'Académie des Sciences Paris **316:**1194-1199.
3. **Bhattacharjee, S., M. K. Halane, S. H. Kim, and W. Gassmann.** 2011. Pathogen effectors target Arabidopsis EDS1 and alter its interactions with immune regulators. Science **334:**1405-1408.
4. **Block, A., and J. R. Alfano.** 2011. Plant targets for *Pseudomonas syringae* type III effectors: virulence targets or guarded decoys? Curr. Opin. Microbiol. **14:**39-46.
5. **Block, A., G. Li, Z. Q. Fu, and J. R. Alfano.** 2008. Phytopathogen type III effector weaponry and their plant targets. Curr. Opin. Plant Biol. **11:**396-403.
6. **Block, A., T. Y. Toruño, C. G. Elowsky, C. Zhang, J. Steinbrenner, J. Beynon, and J. R. Alfano.** 2013. The *Pseudomonas syringae* type III effector HopD1 suppresses effector-triggered immunity, localizes to the endoplasmic reticulum, and targets the Arabidopsis transcription factor NTL9. New Phytol. **201:**1358-1370.
7. **Boudsocq, M., M. R. Willmann, M. McCormack, H. Lee, L. Shan, P. He, J. Bush, S. Cheng, and J. Sheen.** 2010. Differential innate immune signalling via Ca^{2+} sensor protein kinases. Nature **464:**418-423.
8. **Cutler, S. R., P. L. Rodriguez, R. R. Finkelstein, and S. R. Abrams.** 2010. Abscisic acid: Emergence of a core signaling network. Annu. Rev. Plant Biol. **61:**651-679.
9. **Dangl, J. L., C. Ritter, M. J. Gibbon, L. A. Mur, J. R. Wood, S. Goss, J. Mansfield, J. D. Taylor, and A. Vivian.** 1992. Functional homologs of the Arabidopsis *RPM1* disease resistance gene in bean and pea. Plant Cell **4:**1359-1369.
10. **Deslandes, L., and S. Rivas.** 2012. Catch me if you can: bacterial effectors and plant targets. Trends Plant Sci. **17:**644-655.
11. **Ding, Z., H. Wang, X. Liang, E. R. Morris, F. Gallazzi, S. Pandit, J. Skolnick, J. C. Walker, and S. R. Van Doren.** 2007. Phosphoprotein and phosphopeptide interactions with the FHA domain from Arabidopsis kinase-associated protein phosphatase. Biochemistry **46:**2684-2696.
12. **Forner, J., and S. Binder.** 2007. The red flurescence protein eqFP611: application in subcellular localization studies in higher plants. BMC Plant Biol. **7:**28.
13. **Fuchs, S., E. Grill, I. Meskiene, and A. Schweighofer.** 2013. Type 2C protein phosphatases in plants. FEBS J. **280:**681-693.
14. **Gagne, J. M., and S. E. Clark.** 2010. The Arabidopsis stem cell factor POLTERGEIST is membrane localized and phospholipid stimulated. Plant Cell **22:**729-743.

15. **Gómez-Gómez, L., Z. Bauer, and T. Boller.** 2001. Both the extracellular leucine-rich repeat domain and the kinase activity of FSL2 are required for flagellin binding and signaling in Arabidopsis. Plant Cell **13:**1155-1163.
16. **Hayashi, Y., K. Takahashi, S. Inoue, and T. Kinoshita.** 2014. Abscisic acid suppresses hypocotyl elongation by dephosphorylating plasma membrane H^+-ATPase in *Arabidopsis thaliana*. Plant Cell Physiol. **55:**845-853.
17. **Henty-Ridilla, J. L., J. Li, B. Day, and C. J. Staiger.** 2014. ACTIN DEPOLYMERIZING FACTOR4 regulates actin dynamics during innate immune signaling in Arabidopsis. Plant Cell **26:**340-352.
18. **Jamir, Y., M. Guo, H. Oh, T. Petnicki-Ocwieja, X. Tang, M. Dickman, A. Collmer, and J. R. Alfano.** 2004. Identification of *Pseudomonas syringae* type III effectors that can suppress programmed cell death in plants and yeast. Plant J. **37:**554-565.
19. **Jones, J. D. G., and J. L. Dangl.** 2006. The plant immune system. Nature **444:**323-329.
20. **Karimi, M., D. Inzé, and A. Depicker.** 2002. GATEWAY™ vectors for *Agrobacterium*-mediated plant transformation. Trends Plant Sci. **7:**193-195.
21. **Kim, S. H., S. I. Kwon, D. Saha, N. C. Anyanwu, and W. Gassmann.** 2009. Resistance to the *Pseudomonas syringae* effector HopA1 is governed by the TIR-NBS-LRR protein RPS6 and is enhanced by mutations in *SRFR1*. Plant Physiol. **150:**1723-1732.
22. **Macho, A. P., B. Schwessinger, V. Ntoukakis, A. Brutus, C. Segonzac, S. Roy, Y. Kadota, M. Oh, J. Sklenar, P. Derbyshire, R. Lozano-Durán, F. O. Malinovsky, J. Monaghan, F. L. Menke, S. C. Huber, S. Y. He, and C. Zipfel.** 2014. A bacterial tyrosine phosphatase inhibits plant pattern recognition receptor activation. Science **343:**1509-1512.
23. **Mukhtar, M. S., A. Carvunis, M. Dreze, P. Epple, J. Steinbrenner, J. Moore, M. Tasan, M. Galli, T. Hao, M. T. Nishimura, S. J. Pevzner, S. E. Donovan, L. Ghamsari, B. Santhanam, V. Romero, M. M. Poulin, F. Gebreab, B. J. Gutierrez, S. Tam, D. Monachello, M. Boxem, C. J. Harbort, N. McDonald, L. Gai, H. Chen, Y. He, E. U. E. Consortium, J. Vandenhaute, F. P. Roth, D. E. Hill, J. R. Ecker, M. Vidal, J. Beynon, P. Braun, and J. L. Dangl.** 2011. Independently evolved virulence effectors converge onto hubs in a plant immune system network. Science **333:**596-601.
24. **Park, C., Y. Peng, X. Chen, C. Dardick, D. Ruan, R. Bart, P. E. Canlas, and P. C. Ronald.** 2008. Rice XB15, a protein phosphatase 2C, negatively regulates cell death and XA21-mediated innate immunity. PLOS Biol. **6:**e231.
25. **Preston, G. M.** 2000. *Pseudomonas syringae* pv. *tomato*: The right pathogen, of the right plant, at the right time. Mol. Plant Microbe Interact. **1:**263-275.

26. **Salomon, D., Y. Guo, L. N. Kinch, N. V. Grishin, K. H. Gardner, and K. Orth.** 2013. Effectors of animal and plant pathogens use a common domain to bind host phosphoinositides. Nature Comm. **4:**2973.
27. **Schweighofer, A., H. Hirt, and I. Meskiene.** 2004. Plant PP2C phosphatases: emerging functions in stress signaling. Trends Plant Sci. **9:**237-243.
28. **Segonzac, C., A. P. Macho, M. Sanmartín, V. Ntoukakis, J. J. Sánchez-Serrano, and C. Zipfel.** 2014. Negative control of BAK1 by protein phosphatase 2A during plant innate immunity. EMBO J. **33:**2069-2079.
29. **Shah, K., E. Russinova, T. W. J. Gadella, J. Willemse, and S. C. De Vries.** 2002. The Arabidopsis kinase-associated protein phosphatase controls internalization of the somatic embryogenesis receptor kinase 1. Genes Dev. **16:**1707-1720.
30. **Song, S., and S. E. Clark.** 2005. POL and related phosphatases are dosage-sensitive regulators of meristem and organ development in Arabidopsis. Dev. Biol. **285:**272-284.
31. **Spartz, A. K., H. Ren, M. Y. Park, K. N. Grandt, S. H. Lee, A. S. Murphy, M. R. Sussman, P. J. Overvoorde, and W. M. Gray.** 2014. SAUR inhibition of PP2C-D phosphatases activates plasma membrane H^+-ATPases to promote cell expansion in Arabidopsis. Plant Cell **26:**2129-2142.
32. **Wu, S., L. Shan, and P. He.** 2014. Microbial signature-triggered plant defense responses and early signaling mechanism. Plant Sci. **228:**118-126.
33. **Xin, X., and S. Y. He.** 2013. *Pseudomonas syringae* pv. *tomato* DC3000: A model pathogen for probing disease susceptibility and hormone signaling in plants. Annu. Rev. Phytopathol. **51:**473-498.
34. **Zuo, J., Q. W. Niu, and N. H. Chua.** 2000. Technical advance: an estrogen receptor-based transactivator XVE mediates highly inducible gene expression in transgenic plants. Plant J. **24:**265-273.

CHAPTER 5

SUMMARY

The plant pathogenic bacteria *Pseudomonas syringae* depends on the type III protein secretion system (T3SS) for pathogenicity. Type III effectors (T3Es), virulence proteins injected into plant cells through the T3SS, are key virulence determinants of this pathogen. A casual agent of bacterial speck of tomato, *P. syringae* pv. *tomato* DC3000 (*Pto* DC3000), injects about 35 T3Es into plants to suppress plant immunity. An important topic of research in the field of molecular plant-microbe interactions has been the characterization of T3Es to understand how these virulence determinants suppress the plant immune system. Research in this field has identified the enzymatic activities and plant targets of only a subset of *P. syringae* T3Es. Thus, the majority of T3E targets and their biochemical function remain to be elucidated.

To better understand plant-microbe interactions, I fully characterized two T3Es, HopD1 and HopA1. HopA1 was first isolated from *P. syringae* pv. *syringae* 61 and was one of the first T3E known to elicit a hypersensitive response (HR) in plants after being injected into plant cells by the T3SS (1, 7). The HR is a programmed cell death response at the site of infection to restrict the spread of the pathogen. It is a characteristic response associated with effector-triggered immunity (ETI), since it is elicited after recognition of a T3E by the corresponding resistance (R) protein in plants. T3Es have been classified based on their ability to suppress the HR induced by HopA1 in plants (6, 8). Among the strongest ETI suppressors was HopD1 (6). I investigated the activities of HopD1 and HopA1 *in planta*, their subcellular localization and host targets to elucidate the host component(s) inhibited by these T3Es to hijack the plant immune system. Main

conclusions of this thesis and questions that remain to be addressed are highlighted below.

HopD1 suppresses ETI but not PAMP-triggered immunity

T3Es can suppress both branches of plant immunity: pathogen-associated molecular pattern (PAMP)-triggered immunity (PTI) and ETI. PTI likely evolved first to inhibit the growth of pathogens and nonpathogens in plant tissue because it recognizes general conserved molecules on microbes and ETI later as a stronger more prolonged immunity that is induced by pathogen effectors that were first delivered to plants to suppress PTI. In bacterial-plant interactions these effectors are all T3Es. However, our data shows that HopD1 evolved after PTI to exclusively suppress ETI responses. While this would be predicted based on evolution, HopD1 is the first published account of an effector that suppresses ETI but not PTI. Besides being one of the strongest ETI suppressors, expression of HopD1 in *Arabidopsis thaliana* allowed better growth of ETI-inducing *Pto* DC3000 strains. Pathogen strains that are recognized by R proteins and, therefore, induce ETI are historically known as avirulent strains. Two examples of *Pto* DC3000 avirulent strains are DC3000(p*avrRpm1*) and DC3000(p*avrRpt2*) that are recognized by the Arabidopsis R proteins RPM1 and RPT2, respectively (2, 4, 14). *In planta* expression of HopD1 did not allow better growth of the *Pto* DC3000 *hrcC* mutant strain. This strain is a PTI-inducer since it has a defective T3SS and cannot inject any T3Es; thus plants can sense bacterial PAMPs from this strain and the strain cannot suppress PTI. These results suggested that while HopD1 is

a strong ETI suppressor, it did not suppress PTI. Furthermore, we also showed that HopD1 could suppress the AvrRpm1-induced HR, ion leakage and callose deposition responses but not PTI-induced callose deposition and production of reactive oxygen species (ROS). Altogether, our data indicates that HopD1 is a T3E that was acquired later in the coevolution of the *Pto* DC3000-Arabidopsis interaction after establishment of the R protein immune receptor surveillance system.

HopD1 targets Arabidopsis NAC transcription factor NTL9 to inhibit expression of NTL9-regulated genes

Our characterization of HopD1 provides the first evidence of a *Pto* DC3000 T3E targeting a NAC transcription factor as a way to suppress plant immunity. We showed that HopD1 interacts with the Arabidopsis NTL9, a membrane-bound NAM, ATAF1/2, CUC2 (NAC) transcription factor. NAC transcription factors are involved in plant development, and biotic and abiotic stress regulation (20). NTL9 belongs to the NAC with transmembrane motif 1 (NTM1) family of transcription factors that are tethered to intracellular membranes (10, 11). NTL9 has been implicated in regulating osmotic stress during leaf senescence (21). HopD1 interacted with NTL9 at the endoplasmic reticulum (ER) of plant cells. As a transcription factor, NTL9 mediates activation of target genes. We identified and confirmed several genes induced by NTL9. To understand the role of NTL9 in plant immunity, we selected a subset of NTL9-regulated genes that are known to be induced during biotic stress or involved in plant immunity. These genes were

upregulated by NTL9 during ETI but not PTI, and HopD1 suppressed induction of these NTL9-regulated genes. We hypothesize that NTL9 is anchored to the endoplasmic reticulum in a ready state and upon stress perception (osmotic stress and ETI) NTL9 is cleaved from the ER and translocated to the nucleus where it regulates expression of target genes.

Recent studies have identified NAC transcription factors as cellular hubs for targets of effectors and virulence factors from several plant pathogens. The RxLR effector Pi03192 from the potato late blight pathogen *Phytophthora infestans* targets two potato membrane-bounds NAC transcription factors, NTP1 and NTP2. Pi03192 interacts with NTP1/2 at the endoplasmic reticulum and blocks NTP1/2 relocalization from the ER to the nucleus after pathogen perception (13). In addition, the capsid protein (CP) of *Turnip crinkle virus* (TCV) targets the Arabidopsis NAC transcription factor TCV-interacting protein (TIP) (16, 17). The virus CP binds to TIP to block its ability to localize to the nucleus. These data show that NAC transcription factors are important host targets for pathogens to suppress the plant immunity system.

What is the mechanism of action for the HopD1 inhibition of NTL9-regulated genes?

In an attempt to investigate the mechanism that HopD1 uses to inhibit NTL9 function, we tested the subcellular localization of NTL9 with and without HopD1 in *Nicotiana benthamiana* using *Agrobacterium*-mediated transient assays. Although we found that NTL9 relocalizes to the nucleus after *Pto* DC3000

treatment, we could not detect any inhibition of NTL9 relocalization to the nucleus by HopD1. Membrane bound NAC transcription factors are activated by proteolytic cleavage mediated by proteases or ubiquitination-dependent proteasome activities. The specific proteolytic event that mediates cleavage of NTL9 from the ER is not known and, therefore, remains to be identified. We also tested the ability of HopD1 to inhibit NTL9 transcription. We could not see a decreased in NTL9 transcription in the presence of HopD1 using a yeast one-hybrid assay. Based on these results, HopD1 most likely affects NTL9's function postranscriptionally. The precise mechanism of HopD1 inhibition of NTL9 remains an important question to be answered as well as the role of NTL9 in plant immunity.

There are 13 members of membrane-bound NAC transcription factors in Arabidopsis (10). Since HopD1 localizes to the endoplasmic reticulum, it is possible that HopD1 interacts with other membrane-bound NAC transcription factors to suppress plant defenses. That is, it is possible that NTL9 may not be the true HopD1 target and that the true target is a similar NAC transcription factor. This would explain why we were unable to see any effect on NTL9 by HopD1. If this is true, that another NAC transcription factor is the actual target of HopD1, then yeast two-hybrid and bimolecular fluorescence complementation (BiFC) assays can be performed to answer this question. If other NAC targets are identified, then similar experiments as the ones described in Chapter 2 would need to be done to determine if the new NAC targets are affected by HopD1. The best hypothesis to explain HopD1's effect on NAC transcription factors remains

that HopD1 prevents the relocalization of the NAC transcription factor to the nucleus to prevent ETI-related transcription. It seems through the course of evolution if one effector evolved to target a specific component of immunity other effectors might have also evolved to target the same protein or process. Thus, the field of *Pto* DC3000-Arabidopsis interactions will also benefit from screening the complete T3E inventory for interaction with NTL9 and any other NAC transcription factors that is shown to interact with HopD1.

Diversification of the HopA1 family of T3Es

HopA1 is present in several *P. syringae* pathovars. I characterized two HopA1 classes, one from *P. syringae* pv. *syringae* 61 ($HopA1_{61}$) and another class from *P. syringae* pv. *tomato* DC3000 ($HopA1_{DC}$). $HopA1_{61}$ is an avirulence (Avr) protein in *N. tabacum* cultivar Xanthi (tobacco) and *A. thaliana* ecotype Ws-0. However, these plants do not recognize $HopA1_{DC}$ as an Avr protein. Avr proteins are different types of proteins in different pathogens. In bacterial pathogens, all Avr proteins to date are T3Es and when Avr proteins are recognized by R proteins they induce ETI including the HR. Even though these HopA1 classes share 56% amino acid sequence similarity, $HopA1_{DC}$ was not able to elicit an HR in tobacco and *A. thaliana* Ws-0. Thus, unlike $HopA1_{61}$, $HopA1_{DC}$ is not an Avr protein in *N. tabacum* cv. Xanthi or *A. thaliana* ecotype Ws-0. I also explored the expression of HopA1 proteins in a heterologous system. When I induced expression of $HopA1_{61}$ or $HopA1_{DC}$ in the model eukaryotic yeast *Saccharomyces cerevisiae*, I discovered that $HopA1_{61}$, but not $HopA1_{DC}$,

inhibited yeast growth. Differences between HopA1$_{61}$ and HopA1$_{DC}$ were also observed when I explored their subcellular localization in *N. benthamiana* using the *Agrobacterium*-mediated transient assay. Both HopA1's localize to the plasma membrane, cytoplasm, nucleus and nucleolus of plant cells. However I observed punctate spots along the plasma membrane and aggregation of chloroplasts around the nucleus only when HopA1$_{61}$ was transiently expressed in plants. Chloroplast aggregation around the nucleus is associated with late stages of programmed cell death (PCD) in plants and, since the HR is a type of PCD, it confirms the HR-eliciting phenotype of HopA1$_{61}$. I hypothesize that at a certain point in the evolution of the HopA1 family of T3Es, HopA1$_{DC}$ diverged such that it was no longer recognized as an Avr protein most likely as a result of selective pressures imposed by the ETI.

Since HopA1$_{61}$ is recognized in tobacco (cv Xanthi) and *A. thaliana* Ws-0, I explored which portions of HopA1$_{61}$ were responsible for the elicitation of an HR in these plants. I discovered that a portion containing the C-terminal 186 amino acids of HopA1$_{61}$ was recognized in tobacco. These data indicate that the Avr domain of HopA1$_{61}$ resides in its C-terminus and is responsible for the elicitation of an HR in tobacco. However, I found that the N-terminal region of HopA1$_{61}$ was recognized in *A. thaliana* Ws-0, with the first 122 amino acids being sufficient for the elicitation of an HR. I was surprised by these results since all *P. syringae* T3Es to date have been recognized indirectly by the modifications that they carry out on their targets. The modification of the target is detected by an R protein inducing ETI as predicted by the guard hypothesis. The effector domains of T3Es

reside in their C-terminal region after the secretion signal and chaperone-binding site. In fact, the $HopA1_{DC}$ secretion signal and chaperone-binding site reside in the N-terminus 102 amino acids (9). Because of this it is not likely that the $HopA1_{61}$ portion from amino acids 1-122 has any virulence activity. These results indicate that $HopA1_{61}$ is probably directly recognized in *A. thaliana* Ws-0 by the R protein RPS6. However, the virulence domain of $HopA1_{61}$, which resides in its C-terminus, is likely indirectly recognized in tobacco by a yet unknown R protein. This agrees with the guard hypothesis that states that R proteins monitor modifications on host proteins targeted by pathogen effectors; in this manner T3Es are indirectly recognized by R proteins inducing ETI. Indirect recognition has been demonstrated for the T3Es that have been looked at in manner. Thus, the direct recognition of $HopA1_{61}$ by the RPS6 R protein in *A. thaliana* Ws-0 represents an exceptional case and warrants further study.

$HopA1_{DC}$ suppresses PTI in Arabidopsis and resemble phosphothreonine lyases from animal pathogens

To investigate the contribution of $HopA1_{DC}$ to the virulence of *Pto* DC3000, I performed pathogenicity assays in Arabidopsis. I found that the *hopA1* mutant had reduced growth compared to wild type *Pto* DC3000 and that *in planta* expression of $HopA1_{DC}$ allowed better growth of wild type *Pto* DC3000 and the type III secretion defective *hrcC* mutant. Although the contribution of $HopA1_{DC}$ to the virulence of *Pto* DC3000 was subtle, it greatly reduced PTI responses,

including callose deposition and ROS production. Thus, $HopA1_{DC}$ suppresses PTI.

The structure of $HopA1_{DC}$ encompassing residues 122 to 380 was determined and has similarity to a class of enzymes known as phosphothreonine lyases. Examples of this enzyme in animal pathogens include SpvC from *Shigella*, OspF from *Salmonella* and VirA from *Chromobacterium* (12, 22). The OspF/SpvC/VirA family of effectors with phosphothreonine lyase enzymatic activity irreversible removes the phosphate moiety from the phosphothreonine residue in the activation loop of host MAP kinases. Alignment of the structures of $HopA1_{DC}$ and SpvC identified five $HopA1_{DC}$ residues in regions with similarity to important residues in the active site of phosphothreonine lyases. These $HopA1_{DC}$ residues were also solvent exposed and I changed each of these to alanine by site-directed mutagenesis. I found that these residues were required for the ability of $HopA1_{DC}$ to suppress PTI-induced callose deposition and ROS production. I also matched these five $HopA1_{DC}$ residues to the corresponding residues in $HopA1_{61}$ and did site-directed mutagenesis. I discovered that the majority of $HopA1_{61}$ residues were required for the $HopA_{61}$-dependent phenotypes: HR elicitation in tobacco and yeast growth inhibition. I, therefore, concluded that these residues are important for the enzymatic activity of HopA1 and that HopA1 might be a phosphothreonine lyase or a related enzyme based on its similarity to this enzyme. Furthermore, the fact that the conserved residues were required for $HopA1_{DC}$ virulence activity (i.e., suppression of PTI) and $HopA1_{61}$'s Avr activity, this further suggests that $HopA1_{61}$ is recognized in tobacco indirectly by whatever

modification that it carries out on its target protein, which would be predicted to be monitored by an R protein.

HopA1 interacts with two Arabidopsis type 2C protein phosphatases involved in plant immunity

To further investigate the virulence function of HopA1 and understand the way it suppresses PTI, I explored the targets of HopA1 in Arabidopsis. I discovered that HopA1 interacts with two type 2C protein phosphatases (PP2C): PLL4 and PLL5. PLL4 and PLL5 belong to clade C of PP2C (PP2C-C) and have known roles in leaf development (19). HopA1 interacts with PLL4 and PLL5 at the plasma membrane of plant cells. I observed BiFC and colocalization of HopA1 and PLL4 and PLL5 in Hechtian strands, typical cell wall-plasma membrane connections detectable after plasmolysis. These results agree with plasma membrane localization of members of the PP2C-C family (5).

Up until now, PLL4 and PLL5 were not known to be associated with plant immunity. I explored if these phosphatases are induced during biotic stress, specifically during bacterial infections. Compared to mock inoculations in *A. thaliana* Col-0 plants, *PLL4* and *PLL5* were both induced after inoculations with virulent DC3000, avirulent DC3000(p*avrRpm1*) and flg22 (the 22 amino acid epitope of bacterial flagellin). These data indicate that PLL4 and PLL5 are involved in plant immunity. I further investigated how *pll4* and *pll5* T-DNA insertion mutants and plants overexpressing these phosphatases respond to *P. syringae* inoculations and flg22-induced defense responses. I found that *pll4* and

pll5 mutants are more resistant to *Pto* DC3000, while plants overexpressing PLL4 or PLL5 are more susceptible. Flg22-induced ROS production was suppressed in plants overexpressing PLL4 or PLL5 compared to wild type Col-0 plants. In addition, flg22-induced callose deposition was restricted in PLL4 or PLL5 overexpressing plants and enhanced in *pll4 and pll5* mutants. Lastly, DC3000(p*avrRpm1*)- and flg22-mediated induction of the immunity-regulated genes *NHL10* and *FRK1* was suppressed in PLL4 or PLL5 overexpressing plants and highly induced in *pll4 and pll5* mutants. Altogether, these data indicate that PLL4 and PLL5 are negative regulators of plant immunity. Members of the PP2C family have been described as negative regulators of immunity. For instance, clade A PP2Cs members are negative regulators of immunity by modulating the phosphorylation status of PAMP receptor complexes (18). In addition, the rice homolog of PLL4 and PLL5, XB15, interacts and dephosphorylates the plasma membrane pathogen recognition receptor XA21 leading to a negative regulation of XA21-mediated immunity (15). Therefore, negative regulation of PP2Cs in plant immunity appears to becoming a common theme for this family of phosphatases.

What are the substrates of PLL4 and PLL5?

Now that we know that PLL4 and PLL5 are involved in plant immunity as negative regulators, and since they are plasma membrane-localized proteins, it is likely that they regulate plasma membrane proteins to suppress plant immunity. PAMP receptor complexes localize to the plasma membrane and recognize

microbial PAMPs to initiate PTI. Therefore, PAMP receptor complexes are good candidates as targets of PLL4 and PLL5. I hypothesize that PLL4 and PLL5 negatively regulate these PAMP receptor complexes to keep PTI off in the absence of the pathogen. After initial *P. syringae* infection, by a yet unknown mechanism, these phosphatases are inactivated leading to activation of PTI and initiation of immune responses including ROS production and callose deposition. However, it appears that *P. syringae* evolved to inject the T3E HopA1 to target PLL4 and PLL5 at the plasma membrane to inhibit their deregulation and prevent PTI induction. I predict that PLL4 and PLL5 act on components of immunity associated with PTI, most likely PAMP receptor complexes. Yeast two-hybrid analysis between PLL4 and PLL5 and PAMP receptor complexes, as well as immunoprecipitation followed by mass spectrometry analyses need to be done to identify the substrates of PLL4 and PLL5. This will help elucidate the mechanism of negative regulation achieved by PLL4 and PLL5 as well as their roles in plant immunity.

Does HopA1 interact with EDS1?

It has been reported that HopA1 interacts with the immunity regulator EDS1 (3). That report shows that EDS1 interacts with the R proteins RPS4 and RPS6 and that HopA1 disrupts EDS1 association with R protein complexes. Because I was interested in targets of HopA1, I wanted to confirm the interaction of EDS1 with HopA1. I found that EDS1 only interacted weakly with HopA1 in BiFC assays and not at all in yeast-two-hybrid assays. Based on our structural analyses, HopA1 is

a phosphothreonine lyase or a related enzyme. Phosphothreonine lyases remove phosphates from their substrates. EDS1 is not known to be a phosphorylated protein. Therefore, if HopA1 is a phosphothreonine lyase, EDS1 does not seem to be a true target for HopA1. Unfortunately, because EDS1 is not phosphorylated, I could not test phosphothreonine lyase enzymatic activity of HopA1 using EDS1 as a substrate.

Since HopA1 interacts with PLL4 and PLL5 and EDS1 is a putative target, I wanted to investigate if PLL4 and PLL5 interact with EDS1. I found interaction between PLL4 and PLL5 with EDS1 in a yeast two-hybrid analysis, but I could not detect interaction using BiFC assays. In Chapter 4 of this thesis I confirmed interaction of HopA1 with PLL4 and PLL5 by yeast two-hybrid and BiFC assays. I also provided evidence that HopA1 and PLL4 and PLL5 colocalize at the plasma membrane of plant cells. EDS1 is not known to localize to the plasma membrane and has been shown to be a cytoplasmic and nuclear protein (3). The difference in localization and the fact that EDS1 does not interact with HopA1 and PLL4 and PLL5 by both yeast two-hybrid and BiFC assays suggest that EDS1 is not a true target of HopA1. In addition, my model for the PLL4- and PLL5-HopA1 interaction suggests that they might target components of immunity associated with PTI at the plasma membrane. The fact that EDS1 is involved in ETI and not PTI also implies that EDS1 is likely not a true HopA1 target.

References

1. **Alfano, J. R., H. Kim, T. P. Delaney, and A. Collmer.** 1997. Evidence that the *Pseudomonas syringae* pv. *syringae hrp*-linked *hrmA* gene encodes an Avr-like protein that acts in an *hrp*-dependent manner within tobacco cells. Mol. Plant Microbe Interact. **10:**580-588.
2. **Bent, A. F., B. N. Kunkel, D. Dahlbeck, K. L. Brown, R. Schmidt, J. Giraudat, J. Leung, and B. Staskawicz.** 1994. *RPS2* of *Arabidopsis thaliana*: a leucine-rich repeat class of plant disease resistance genes. Science **265:**1856-1860.
3. **Bhattacharjee, S., M. K. Halane, S. H. Kim, and W. Gassmann.** 2011. Pathogen effectors target Arabidopsis EDS1 and alter its interactions with immune regulators. Science **334:**1405-1408.
4. **Dangl, J. L., C. Ritter, M. J. Gibbon, L. A. Mur, J. R. Wood, S. Goss, J. Mansfield, J. D. Taylor, and A. Vivian.** 1992. Functional homologs of the Arabidopsis *RPM1* disease resistance gene in bean and pea. Plant Cell **4:**1359-1369.
5. **Gagne, J. M., and S. E. Clark.** 2010. The Arabidopsis stem cell factor POLTERGEIST is membrane localized and phospholipid stimulated. Plant Cell **22:**729-743.
6. **Guo, M., F. Tian, Y. Wamboldt, and J. R. Alfano.** 2009. The majority of the type III effector inventory of *Pseudomonas syringae* pv. *tomato* DC3000 can suppress plant immunity. Mol. Plant Microbe Interact. **22:**1069-1080.
7. **Huang, H., R. Schuurink, T. P. Denny, M. M. Atkinson, C. J. Baker, I. Yucel, S. W. Hutcheson, and A. Collmer.** 1988. Molecular cloning of a *Pseudomonas syringae* pv. *syringae* gene cluster that enables *Pseudomonas fluorescens* to elicit the hypersensitive response in tobacco plants. J. Bacteriol. **170:**4748-4756.
8. **Jamir, Y., M. Guo, H. Oh, T. Petnicki-Ocwieja, X. Tang, M. Dickman, A. Collmer, and J. R. Alfano.** 2004. Identification of *Pseudomonas syringae* type III effectors that can suppress programmed cell death in plants and yeast. Plant J. **37:**554-565.
9. **Janjusevic, R., C. M. Quezada, J. Small, and C. E. Stebbin.** 2013. Structure of the HopA1(21-102)-ShcA chaperone-effector complex of *Pseudomonas syringae* reveals conservation of a virulence factor binding motif from animal to plant pathogens. J. Bacteriol. **195:**658-664.
10. **Kim, S., S. Kim, Y. Kim, P. Seo, M. Bae, H. Yoon, and C. Park.** 2007. Exploring membrane-associated NAC transcription factors in Arabidopsis: Implications for membrane biology in genome regulation. Nucleic Acids Res. **35:**203-213.
11. **Kim, S., S. Lee, J. Ryu, and C. Park.** 2010. Probing protein structural requirements for activation of membrane-bound NAC transcription factors in Arabidopsis and rice. Plant Sci. **178:**239-244.

12. **Li, H., H. Xu, Y. Zhou, J. Zhang, C. Long, S. Li, S. Chen, J. Zhou, and F. Shao.** 2007. The phosphothreonine lyase activity of a bacterial type III effector family. Science **315:**1000-1003.
13. **McLellan, H., P. C. Boevink, M. R. Armstrong, L. Pritchard, S. Gomez, J. Morales, S. C. Whisson, J. L. Beynon, and P. R. J. Birch.** 2013. An RxLR effector from *Phytophthora infestans* prevents re-localisation of two plant NAC transcription factors from the endoplasmic reticulum to the nucleus. PLoS Path. **9:**e1003670.
14. **Mindrinos, M., F. Katagiri, G. Yu, and F. M. Ausubel.** 1994. The *A. thaliana* disease resistance gene *RPS2* encodes a protein containing a nucleotide-binding site and leucine-rich repeats. Cell **78:**1089-1099.
15. **Park, C., Y. Peng, X. Chen, C. Dardick, D. Ruan, R. Bart, P. E. Canlas, and P. C. Ronald.** 2008. Rice XB15, a protein phosphatase 2C, negatively regulates cell death and XA21-mediated innate immunity. PLoS Biol. **6:**e231.
16. **Ren, T., F. Qu, and T. J. Morris.** 2000. *HRT* gene function requires interaction between a NAC protein and viral capsid protein to confer resistance to *Turnip Crinkle Virus*. Plant Cell **12:**1917-1925.
17. **Ren, T., F. Qu, and T. J. Morris.** 2005. The nuclear localization of the Arabidopsis transcription factor TIP is blocked by its interaction with the coat protein of *Turnip Crinkle Virus*. Virology **331:**316-324.
18. **Segonzac, C., A. P. Macho, M. Sanmartín, V. Ntoukakis, J. J. Sánchez-Serrano, and C. Zipfel.** 2014. Negative control of BAK1 by protein phosphatase 2A during plant innate immunity. EMBO J. **33:**2069-2079.
19. **Song, S., and S. E. Clark.** 2005. POL and related phosphatases are dosage-sensitive regulators of meristem and organ development in Arabidopsis. Dev. Biol. **285:**272-284.
20. **Wang, Z., and F. Dane.** 2013. NAC (NAM/ATAF/CUC) transcription factors in different stresses and their signaling pathway. Acta Physiol. Plant. **35:**1397-1408.
21. **Yoon, H., S. Kim, S. Kim, and C. Park.** 2008. Regulation of leaf senescence by NTL9-mediated osmotic stress signaling in Arabidopsis. Mol. Cells **25:**438-445.
22. **Zhu, Y., H. Li, C. Long, L. Hu, H. Xu, L. Liu, S. Chen, D. Wang, and F. Shao.** 2007. Structural insights into the enzymatic mechanism of the pathogenic MAPK phosphothreonine lyase. Mol. Cell **28:**899-913.